School of
ENGINEERING
DUKE UNIVERSITY

Solid Mechanics Series No. 11

Index

MICROPLASTIC DEFORMATION OF FIBROUS COMPOSITES

Final Report

M.S. MADHAVA RAO and GEORGE J. DVORAK

September 1974

ARMY MATERIALS AND MECHANICS RESEARCH CENTER
Watertown, Massachusetts 02172
Contract No. DAAG 46-73-C-0228
Department of Civil Engineering
Duke University

Approved for public release; Distribution Unlimited

Solid Mechanics Series No. 11

MICROPLASTIC DEFORMATION OF FIBROUS COMPOSITES

Final Report

M. S. Madhava Rao and George J. Dvorak

September 1974

U.S. Army Materials and Mechanics Research Center

Watertown, Massachusetts 02172

Contract No. DAAG 46-73-C-0228

Department of Civil Engineering

Duke University

Durham, N. C. 27706

The findings in this report are not to be construed as an official department of the Army position, unless so designated by other authorized documents.

ABSTRACT

This is a two-part study on the plastic deformation of the fiber-reinforced metal matrix composites.

In the first part of the study, a plasticity theory is formulated to predict analytically the macroscopic and microscopic responses of the unidirectional fiber-reinforced metal matrix composites, loaded by axisymmetric composite stress states. The composites are made of isotropic, linearly elastic fibers, and elastic-plastic, nonhardening matrix of Mises type, and are assumed to be both plastically extensible and compressible. It is shown that the unidirectional composites experience kinematic hardening when loaded by axisymmetric composite stresses. The hardening and flow rules governing the kinematic hardening are formulated. The results obtained by the hardening and flow rules are compared with exact plasticity solutions based on the finite element method. A very good agreement is obtained both for proportional and general loading regimes. An approximate method for the determination of microstresses in the unidirectional composites under axisymmetric loading is described.

The plasticity theory is used to solve micromechanics problems which arise as a result of heat treatment of the composites during fabrication. The residual microstresses and the yield surfaces of several heat-treated unidirectional metal matrix composites are predicted by analytical simulation of the heat treatment sequences. The results obtained for a heat-treated tungsten-aluminum composite are compared with existing experimental work to show that the analytical predictions are very accurate. In addition, new heat treatment sequences that may improve the properties of unidirectional boron-aluminum composites are described.

The second part of the study is concerned with composite laminates. Specifically, solution procedures are described for the determination of microstresses in the laminae, and in the fiber crossover regions at the interfaces between the laminae. Particular solutions are presented for the 0-90 deg. B-Aℓ laminates. The local microstresses, and the initial yield surfaces of the laminates are found for the combinations of applied composite stresses which are frequently encountered in practical applications.

TABLE OF CONTENTS

Contents PAGE

Contents

ACKNOWLEDGMENT

The authors wish to acknowledge the financial support of this work by the U. S. Army Materials and Mechanics Research Center, and the scientific supervision of Dr. John M. Slepetz. Dr. E. Lenoe made many useful suggestions in the course of this investigation. Professor Senol Utku provided advice on the use of the ELAS computer program, and on several aspects of the numerical solutions.

The theoretical foundation of the present work was developed under financial sponsorship by the U. S. Army Research Office. It is summarized for completeness in Chapters III and IV.

LIST OF FIGURES

LIST OF TABLES

PART I

PLASTICITY THEORY UNIDIRECTIONAL FIBER-REINFORCED METAL MATRIX COMPOSITES

CHAPTER I

INTRODUCTION

Composites with their high strength to density, and stiffness to density ratios have become very useful in many technological applications. From the engineering point of view a composite may be defined as "a man-made material, consisting of at least two mechanically distinct materials with distinct interface separating the constituents, the properties of which could not be achieved by any one of the constituents acting alone". An important class of composites consists of a softer, low modulus matrix, and stiffer high modulus inclusions. The inclusions may be of arbitrary shape or of specified geometry. They may be distributed in the matrix randomly or form a regular array.

Depending upon the shape of the inclusions, composites can be classified into two major types: particle-reinforced composites, and fiber-reinforced composites. As the names imply, in particle-reinforced composites, the inclusions are in the form of fine particles, and in fiber-reinforced composites the inclusions are in the form of thin fibers. The size of the particles and the diameter of the fiber may range from a fraction of a micron to several mils. Only the fiber-reinforced composites are considered in the present study.

The main advantage in using composites is derived from their superior mechanical properties such as stiffness, toughness, yield and ultimate strengths, etc. By varying the volume fraction of the inclusions, their geometry and shape, and the material selection for the matrix and inclusions, one could achieve many desired combinations of the mechanical properties.

1.1 Composite Models

To utilize a composite in structural applications, one must be able to specify its mechanical properties. For this purpose, the heterogeneous composite is idealized as a homogeneous anisotropic material, such that the mechanical properties of the idealized homogeneous anisotropic material are equal to some "average" properties of the composite. The homogeneous anisotropic material is termed as an "effective material" (Rosen [1]) for the composite. The idealization of the composite, by the effective material, is justified from the consideration that the lateral dimensions of the inclusions (particles or fibers) are extremely small when compared to the dimensions of the structure, such as the thickness of a plate made of the composite. Thus, by definition, the response of a structure made of the effective material to imposed boundary tractions or displacements is equal to the average response of the same structure made of the actual composite.

Strictly speaking, the constituents in a composite are randomly distributed in any given domain. Thus, the physical constants of the material are, in general, random space functions. Thus, the analysis of the composite, even under the simple boundary conditions required for the determination of the mechanical constants of the effective material presents formidable difficulties. Consequently, the composite is often idealized by a model consisting of a matrix in which the inclusions of a specified geometry form regular arrays. The solution of the composite required for the determination of the properties of the effective material is then obtained by analyzing a "Representative Volume Element", which is defined by a repeating domain of the idealized composite model. Some commonly used idealizations of fiber-reinforced composites [2-10] have been: circular fibers forming hexagonal arrays in the matrix; circular fibers forming square arrays; circular fibers forming rectangular arrays in the matrix; and randomly arranged composite cylinders. The idealization of the composite by one of these models is essential for the description of both the elastic as well as the inelastic behavior of the effective material.

1.2 Analysis of Composite Models

To determine both the elastic and inelastic behavior of the effective material by an analysis of an idealized composite

model, one needs to introduce several ssumptions in order to obtain a reasonably simple solution. For fibrous composites these assumptions include the following: (1) The composite is macroscopically homogeneous and orthotropic, (2) The fibers are homogeneous and linearly elastic, (3) The matrix is homogeneous, linearly elastic, or elastic-perfectly plastic, (4) Fibers and matrix are free of voids and cracks, (5) There is perfect bonding at the interface of the constituents and there is no transitional region between them, (6) The composite is free of initial stresses, (7) The composites can be idealized by simple models such as hexagonal, rectangular, or composite cylinders, and the material behavior could be determined completely by an analysis of a representative volume element of the idealized composite model. This assumption implicitly indicates that there are no end effects. End effects should be considered for points in the material near a structural boundary. However, in the absence of the end effects the boundary conditions for a representative volume element are completely determined from the requirements of periodicity of the idealized composite, and from the generalized plane strain condition in the transverse plane (plane perpendicular to the direction of the fibers).

A complete description of mechanical behavior (both elastic and inelastic), requires the solution of the representative volume element of the idealized corposite model under six "Composite Stresses". The Composite Stresses may be defined as those stresses acting at a point in a structure, if it were made

of the effective material. By the definition of the effective material, composite stresses are the "average" stresses in a representative volume element of a composite model. If we consider a hexagonal composite model shown in Figure 1-1, the representative volume element may be defined by OABC. If we consider a coordinate system x_1, x_2, x_3, such that, the axes x_1 and x_2 are in the transverse plane, and x_3 is in the direction of the fibers, the six composite stresses may be represented as T_{11}, T_{22}, T_{33}, T_{12}, T_{13}, and T_{23}. The composite stresses T_{11}, T_{22}, and T_{33} are the normal stresses in the directions x_1, x_2, and x_3, respectively; T_{12} is the transverse shear stress in x_1x_2-plane; T_{13} and T_{23} are the longtitudinal shear stresses in x_1x_3- and x_2x_3-planes, respectively. In analogy with the composite strains ε_{11}, ε_{22}, ε_{33}, ε_{12}, ε_{13}, and ε_{23} are the strains at a point in a structure made of the effective material. Again, by the definition of the effective material, the composite strains are appropriate volume integrals of the strains in the representative volume element of the idealized composite model. The local stresses and strains in the representative volume element are called the microstresses and microstrains, respectively.

1.3 Elastic Behavior

The elastic behavior of a fiber-reinforced composite as an orthotropic and macroscopically homogeneous material, requires the definition of nine elastic constants (Green and Zerna [11])

relating the composite stresses T_{ij} to the composite strains ε_{ij}. These elastic constants may be selected as: three Young's moduli E_1, E_2, E_3 in directions x_1, x_2, x_3; three shear moduli G_{12}, G_{13}, G_{23} in planes x_1x_2, x_1x_3, x_2x_3; and three Poisson's ratios ν_{12}, ν_{13}, ν_{23}. Other selection of the elastic constants may be the tensorial coefficients C_{rs}^{ij} in the stress-strain relation $T_{ij} = C_{rs}^{ij} \varepsilon_{rs}$. For an orthotropic material only nine coefficients of C_{rs}^{ij} are independent [11].

The elastic constants of the composites have been studied very extensively in the past decade. Most of these studies have been aimed at the prediction of some or all of the elastic constants, on the basis of different composite idealizations. Several solution methods were used. For instance, Shaffer [2] using a hexagonal model, Abolin'sh [3] and Springer [4] by using a square model obtained the estimates of the elastic constants by approximate methods; Hashin et al [5] using a cylinder model, obtained the bounds for the elastic constants by variational principles; Hill [6] and Whitney et al. [7] estimated the elastic constants by self-consistent cylindrical models; Bloom et al. [8] using a hexagonal model, and Adams et al. [9, 10] using a rectangular model, obtained the elastic constants by exact methods. A review of these and other methods of determination of the elastic constants has been made by Chamis et al. [12]. Also, Hashin [13] made a historical review of general heterogeneous materials, which also includes some references to the fiber-reinforced composites.

1.4 Plastic Behavior

The theories on prediction of inelastic properties of composites are of recent origin. When fiber-reinforced composites are loaded to failure, McDaniels et al. [14] stated that there exists in general, four stages of deformation:

Stage I - Elastic deformation of fiber; elastic deformation of matrix

Stage II - Elastic deformation of fiber; plastic deformation of matrix

Stage III - Plastic deformation of fiber; plastic deformation of matrix

Stage IV - Failure of the composite.

It can be noted that the deformation of the composite in Stage I is completely elastic, and can be determined from the knowledge of the elastic constants of the composite discussed in the previous section. The boundary between Stages I and II corresponds to initial yielding in the composite. Studies on the initial yield of the composites have been made by Lin, et al. [15], and Dvorak et al. [16, 17]. The former study considered the yielding of a composite lamina under the combined influence of the two normal stresses in the transverse and fiber directions, and the latter generalized the procedure for all the stress combinations.

Dvorak et al. [17] also described a procedure for determining the generalized initial yield surfaces of unidirectional fiber-reinforced composites under both external loads and uniform temperature changes.

The deformation of the composite in Stage II is characterized by microplastic flow in the matrix material and the generation of the residual stresses in the composite. In order to predict realistically the macroscopic behavior of the composite, one should be able to determine the nature of the microscopic residual stresses. The macroscopic behavior includes the definition of a hardening rule, which determines the loading conditions, and of a flow rule which determines the stress-strain response of the composite.

The deformation of the composite in Stage III is similar to that in Stage II, except that, in this stage even the fiber undergoes plastic deformation. However, as the fibers often are made of high strength and/or brittle materials such as boron, beryllium, tungsten, glass, etc., this stage of deformation may not be significant in most composites. The failure (Stage IV) follows the Stage III (if it was present) or the Stage II.

The present work is primarily concerned with the deformation of fiber-reinforced metal matrix composites in Stage II in the "axisymmetric" mode. The axisymmetric mode of deformation is a special case of general deformation pattern that can occur during the plastic flow, and is caused by a hydrostatic transverse composite stress ($T_{11} = T_{22}$), and the axial composite stress (T_{33}).

The composite shear stresses vanish ($T_{12} = T_{13} = T_{23} = 0$). In this mode of deformation the composite is idealized as a composite cylinder under generalized plane strain, loaded by a radial stress equal to the uniform transverse stresses ($T_{11} = T_{22}$) on the outer radial boundary and by an axial stress (T_{33}). Comparison of initial yield surfaces for the composite cylinders obtained during the course of the present work, with those obtained earlier by Dvorak et al. [16] for hexagonal models (Figure 1-1), showed that the composite cylinder idealization is very satisfactory for the axisymmetric mode of deformation.

On the basis of exploratory studies of plastic flow in boron-aluminum and beryllium-aluminum composite cylinders by the finite element method [20], the hardening and flow rules were formulated for fiber-reinforced metal matrix composites with elastic-perfectly plastic matrices, under axisymmetric deformation ($T_{11} = T_{22}$, T_{33}) in Chapters II and III. The proposed formulation was verified by the finite element method under several loading conditions.

The residual stresses developed in a composite due to plastic flow in the matrix do have an influence on the fatigue and fracture behavior. Therefore, an approximate solution was formulated for the microstresses during plastic deformation in axisymmetric mode in Chapter IV.

The generation of microstresses during the heat treatment of the composites in which the coefficients of thermal expansion of the constituents are different is of interest in

fabrication of these materials. The thermomechanical analogy developed earlier [17] for uniform temperature changes is extended to the quenching and aging problems in Chapter V. The linear volume changes that may occur due to the metallurgical transformations of the matrix material during aging are also incorporated into the thermomechanical analogy. By using the thermomechanical analogy and the plasticity theories described in Chapters III and IV, microstresses generated during heat-treatment are found for tungsten-aluminum and boron-aluminum composites in Chapter V. Heat treatment sequences that may possibly improve the initial yield, fatigue and fracture properties of boron-aluminum composites are also suggested in the same chapter.

The theoretical foundations of the present study have been already reported elsewhere [18, 19] and are summarized here for completeness.

CHAPTER II

THE PLASTICITY THEORY OF COMPOSITES

2.1 Introduction

This chapter is concerned with the deformation of unidirectional composites consisting of an elastic-perfectly plastic matrix, and continuous elastic fibers. The existing plasticity theories for such composites have evolved from the early work which identified the possible failure mechanisms (e.g., Stowell and Liu [21], Kelly and Davies [22], and Cratchley [23]) - Yielding in the matrix on planes parallel to the fibers, both in the longitudinal and transverse directions, and brittle or ductile failure of the fibers. In particular, Drucker [24], Hashin [25], Shu and Rosen [26], Mulhern, et al. [27], Prager [28], and Butler and Sullivan [29], considered Shear deformation of the matrix in the presence of rigid fibers; Mulhern, et al. [30], later relaxed the rigidity assumption and permitted elastic strains in the fiber direction; while Lance and Robinson [31], and McLaughlin and Batterman [32] allowed for plastic yielding of the fibers, and constructed limit surfaces of the composites.

The early work also suggested that matrix can deform plastically when the composite is loaded in the direction of the elastically strained fibers, and the existence of a hysteresis loop in cyclic loading was demonstrated both experimentally and by simple theoretical considerations [21-22, 33]. The axial and other axisymmetric deformation modes in unidirectional composites were discussed by Hill [34]; Mulhern, et al. [35] constructed an exact plasticity solution for a composite cylinder containing an elastic fiber, under cyclic axial loading; and Dvorak, et al. [16, 17] showed that plastic yielding in the matrix can be caused by any axisymmetric stress state, e.g., by a hydrostatic stress, or by a small uniform thermal change. However, a continuum theory allowing for such deformation modes of fibrous composites remained to be developed.

The axisymmetric stress states, such as tension in the fiber direction, and a uniform thermal change are very frequently applied in practice. Although in the presence of strong elastic fibers the composite can not fail in an axisymmetric manner, the deformation of the matrix is bound to affect the shear strength of the composite. For example, if a nonhardening matrix becomes completely plastic under a composite tension stress in the fiber direction, the composite shear strength may decrease. The axisymmetric plastic strains can also generate microstresses in both constituents which may influence the magnitudes of composite proportional limits.

The purpose of the present work is to construct a plasticity theory which accounts for these and other aspects of the axisymmetric plastic deformation of unidirectional composites.

2.2 The Loading Surface

The unidirectional fibrous composite is regarded as a transversely isotropic, mascroscopically homogeneous solid consisting of an elastic-perfectly plastic matrix of the Mises type, and elastic fibers. A perfect bond is assumed to exist between the constituents. On the microscale, the fibers are circular cylinders arranged in such a way that their axes are parallel, however, they can have different diameters and they can be randomly distributed, except for the requirement that the fiber volume fraction V_f must be nearly uniform in the transverse plane.

In the formulation of the yield function, we shall adopt the assumption about the existence of the yield function and plastic potential. No restrictions will be made on the form of the yield function except for those implied by the transverse isotropy of the material, and by the compatibility of both elastic and inelastic deformations of the constituents.

Let x_i denote a Cartesian system of coordinates such that the axes x_1, x_2 are in transverse plane and x_3 is parallel to the fiber direction. The stresses applied to the composite in the x_i coordinate system are denoted at T_{ij}, $(i = 1, 2, 3)$. If the composite is initially free of internal stresses, the yield function must be invariant under rotation about the x_3 axis, and under

the transformations $x_3' = - x_3$. The appropriate invariants of the stress tensor T_{ij} can be obtained by analogy with the well-known strain invariants (e.g., Green and Zerna [36]). In notation similar to that used by Mulhern, et al. [30],

$$I_1 = \frac{1}{2}[T_{11} + T_{22}],\ I_2 = T_{33},\ I_3 = T_{13}^2 + T_{23}^2,$$

$$I_4 = \frac{1}{2}[T_{11} - T_{22}]^2 + 2\,T_{12}^2$$

$$I_5 = \frac{1}{2}[T_{11} - T_{22}][T_{13}^2 - T_{23}^2] + 2\,T_{12}\,T_{23}\,T_{31} \qquad (2.1)$$

Then, the yield function for a stress-free composite can be written as [30]:

$$f = f[I_1, I_2, I_3, I_4, I_5] \qquad (2.2)$$

If the composite is regarded as a homogeneous solid, the yield function f defines a hypersurface in the stress space which bounds the region of completely reversible elastic deformation, i.e., it represents an initial yield surface of the composite. Recent studies of the properties of these surfaces by Dvorak, et al. [16, 17], have revealed that the microscopic nonhomogeneity of the composite has a profound influence on the actual form of the yield function f. In particular, it was found that the distinction between the yield surfaces for composites made of different constituents, or with different fiber volume fractions, is

reflected primarily in the dependence of f on the invariants I_1 and I_2. It follows that the composite must be plastically extensible in the fiber direction, and compressible. If ε_{ij}^{p} are the composite plastic strains, one must assume that

$$d\varepsilon_{33}^{p} \neq 0, \quad d\varepsilon_{kk}^{p} \neq 0 \tag{2.3}$$

These assumptions recognize the fact that a part of the permanent composite strains is caused by elastic, but not completely reversible strains of the fiber. Inasmuch as the plastic strain increments $d\varepsilon_{33}^{p}$ and $d\varepsilon_{kk}^{p}$ were neglected in all earlier continuum models of fibrous composites, the assumptions 2.3 represents a departure towards a more realistic plasticity theory for composite materials. The plastic dilatation has been analyzed so far only for particular composites under isotropic stress; Chu and Hashin [38].

Let us now determine the functional dependence of f on the invariants I_1 and I_2. Since all composite stress states which depend on these invariants must be symmetric about the axis of each fiber, it is possible to assume that the local microstress states will be also approximately symmetric about the fiber axis, both in the fiber, and in the immediate vicinity of the fiber-matrix interface. Under such circumstances, the composite microstructure can be modeled as a system of right circular cylinders which consist of fibers surrounded by uniform layers of the matrix material [37]. If the fiber volume fraction V_f is nearly uniform in the transverse plane, it is sufficient to consider a single

composite cylinder of external diameter a, containing a cylindrical fiber of radius R; $V_f = (R/a)^2$.

The previous studies of initial yield surfaces of regular hexagonal composite arrays [16, 17] have shown that yielding starts most frequently in the matrix at the fiber-matrix interface. During the course of the present work, extensive calculations have been made, with the use of the finite element method [20], to explore the plastic deformation and unloading of composite cylinders subjected to axisymmetric composite stresses along different loading paths in the I_1I_2-plane. (The details of these calculations are given in Chapter III. The results of these calculations have suggested the following assumption:

> "If the composite cylinder is loaded along any path in the I_1I_2-plane, the plastic zone in the matrix is an annular ring adjoining the fiber-matrix interface".

This assumption, if not always true, represents a fairly accurate approximation. Specifically, if the plastic zone starts to form away from the interface, it spreads rapidly towards the fiber and reaches the interface within a very short segment of the loading path. This assumption suggests that both the onset and the termination of plastic flow in the matrix are restricted to the interface. Therefore, the loading surface of the composite refers only to the matrix points at the interface, which are within a homogeneous stress field for any instantaneous combination of the composite stress invariants I_1 and I_2.

The properties of the composite loading surfaces will now be explored. Let us introduce cylindrical coordinates r, ϕ, x_3, such that r and ϕ are in the transverse plane of the cylinder, the origin is at the axis of the fiber, and x_3 coincides with the fiber direction. The cylinder is in the state of generalized plane strain under any combination of the composite stresses I_1 and I_2. The local microstresses σ_{ij} in the elastic range can be determined as in [16, 17]. Using an analogous notation microstresses in the elastic range for the present case can be represented as:

$$\{\sigma_{rr}\ \sigma_{\phi\phi}\ \sigma_{33}\} = [A]\ \{I_1\ I_2\}$$

$$\{\sigma_{r\phi}\ \sigma_{\phi 3}\ \sigma_{3r}\} = 0 \qquad (2.4)$$

where { } represents a column matrix (the elements may be listed horizontally or vertically), and

$$[A] = \begin{bmatrix} A_{11} & A_{12} \\ A_{21} & A_{22} \\ A_{31} & A_{32} \end{bmatrix} \qquad (2.5)$$

The coefficients A_{ij} are evaluated in the matrix at the interface r = R, and depend on the four elastic constants of the constituents, and on the fiber volume fraction. These can be derived from the closed form solution for the microstresses in the composite

cylinder which is given in Chapter IV.

The equation of initial yield surface of a stress-free composite cylinder follows from the Mises yield condition and Equation (2-4):

$$\{I_1\ I_2\}^T\ [A]^T\ [c]\ [A]\ \{I_1\ I_2\} - Y^2 = 0 \qquad (2.6)$$

where superscript T represents transpose, Y the matrix yield stress in simple tension, and

$$[c] = \frac{1}{2} \begin{bmatrix} 2 & -1 & -1 \\ & 2 & -1 \\ \text{SYM.} & & 2 \end{bmatrix}. \qquad (2.7)$$

It follows that the axisymmetric section of the initial yield surface represented by the quadratic form in Equation (2.6), is an ellipse in I_1I_2-plane, with the center at the origin, $I_1 = I_2 = 0$.

The deviatoric components of the microstresses in Equation 2.4 are:

$$\{S\} = \{S_{rr}\ S_{\phi\phi}\ S_{33}\} = \frac{2}{3}\ [c]\ [A]\ \{I_1\ I_2\}$$

$$\{S_{r\phi}\ S_{\phi 3}\ S_{3r}\} = 0, \qquad (2.8)$$

So that Equation 2.6 can be written as

$$\frac{3}{2} \{S\}^T \{S\} - Y^2 = 0 \qquad (2.9)$$

Since $S_{kk} \equiv 0$, the first of Equation 2.8 can also be written as

$$\{S_{\phi\phi} \; S_{33}\} = [P] \{I_1 \; I_2\} \qquad (2.10)$$

or in two other analogous forms for the remaining pairs of the principal deviatoric stresses. When Equation 2.10 is selected,

$$[P] = \frac{1}{3} \begin{bmatrix} -1 & 2 & -1 \\ & & \\ -1 & -1 & 2 \end{bmatrix} [A] \qquad (2.11)$$

Assume that the composite cylinder has been loaded to a certain axisymmetric plastic state, L, such that $I_1 = I_1^L$ and $I_2 = I_2^L$, the deviatoric microstresses at the interface are $\{S^L\}$, and satisfy Equation 2.9. If the composite is now unloaded to a point $I_1 = I_1^U$, $I_2 = I_2^U$ from $I_1 = I_1^L$, $I_2 = I_2^L$, and if complete elastic unloaded were to take place, the change in the microstresses at the interface will be elastic. The deviatoric components of this microstress change can be obtained from Equation 2.10, by relacing $\{I_1 I_2\}$ by $\{(I_1^L - I_1^U) \; (I_2^L - I_2^U)\}$. The deviatoric stresses $S_{\phi\phi}^U$ and S_{33}^U at the unloading point $\{I_1^U \; I_2^U\}$ can then be written as

$$\{S_{\phi\phi}^U \; S_{33}^U\} = \{S_{\phi\phi}^L \; S_{33}^L\} - [P] \{(I_1^L - I_1^U) \; (I_2^L - I_2^U)\} \qquad (2.12)$$

Equation 2.12 suggests that we can find an unloading point $I_1^U = \alpha_1$, $I_2^U = \alpha_2$ such that $S_{\phi\phi}^U = S_{33}^U = 0$. In such a situation the values of α_1 and α_2 should satisfy the following relation.

$$\{I_1^L \; I_2^L\} - \{\alpha_1 \; \alpha_2\} = [P]^{-1} \; \{S_{\phi\phi}^L \; S_{33}^L\} \qquad (2.13)$$

It can be verified that [P] in Equation 2.10 is of rank 2,

and is positive definite if and only if the vectors [P] {0 I_2} and [P] {I_1 0} are not coaxial. That is generally the case when the elastic constants of the constituents are independent. Specifically, from Equations 2.5 and 2.11:

$$\frac{1}{6}|P| = A_{12}(A_{31} - A_{21}) + A_{22}(A_{11} - A_{31}) + A_{32}(A_{21} - A_{11}) \neq 0 \qquad (2.14)$$

In actual metal matrix composites consisting of a stiffer fiber and a low modulus matrix, one finds that A_{12} and A_{22} are one order of magnitude smaller than $(A_{21} - A_{11})$, and the other coefficients of [A] matrix are given in Equation 2.5 (explicit values of the coefficients of [A] matrix are given in Appendix I for some metal matrix composites). Therefore, the last term in Equation 2.14 is dominant; [P] is a nonsingular matrix, and Equation 2.13 has a unique solution for α_1 and α_2. A notable exception is found in case of a homogeneous cylinder where $A_{11} = A_{21} = A_{32} = 1$, $A_{31} = A_{12} = A_{22} = 0$, so that $|P| = 0$, Equation 2.14, and the solution of Equation 2.13 do not exist.

It follows from Equation 2.13

$$\{S_{\phi\phi}{}^L \; S_{33}{}^L\} = [P]\{\{I_1{}^L \; I_2{}^L\} - \{\alpha_1 \quad \alpha_2\}\} \qquad (2.15)$$

So that the equation of the section of the loading surface in the I_1I_2-plane is, from Equations 2.6 to 2.9, 2.13, 2.15:

$$f \equiv \{I_1-\alpha_1 \quad I_2-\alpha_2\}^T [A]^T[c][A] \{I_1-\alpha_1 \quad I_1-\alpha_2\} - Y^2 = 0 \tag{2.16}$$

A comparison of Equations 2.6 and 2.16 leads to the conlusion that:

"At each point of the leading path in I_1I_2 composite stress plane, the loading surface of the composite cylinder is identical with a translated initial yield surface, such that the center of the loading surface is at $I_1 = \alpha_1$, $I_2 = \alpha_2$."

This indicates the existence of kinematic hardening of the composite cylinder under axisymmetric loading. Accordingly the required form of the loading function of an elastic-plastic fibrous composite with a nonhardening matrix is

$$f = f[I_1-\alpha_1 \ , \ I_2-\alpha_2 \quad I_3, \ I_4, \ I_5] \tag{2.17}$$

2.3 The Plasticity Equations

Let us now write the equations governing the plastic flow in the fiber-reinforced composites with a nonhardening matrix. The treatment will be formal in the sense that it is tentatively assumed that a yield function exists, and the normality condition holds. It will also be assumed that the loading surface is always identical to a translated yield surface at any stage of loading.

Yield Condition:

The initial yield condition is

$$f = f(I_1, I_2, I_3, I_4, I_5) = 0 \qquad (2.18)$$

The subsequent yield condition is

$$f = f(I_1 - \alpha_1, I_2 - \alpha_2, I_3, I_4, I_5) = 0 \qquad (2.19)$$

The explicit forms of Equations 2.18 and 2.19 for $I_3 = I_4 = I_5 = 0$ are respectively given by Equations 2.6 and 2.16. The general form of these equations can be derived from analysis for the generalized yield surfaces [17].

Plastic flow occurs in the composite if

$$df = \frac{\partial f}{\partial I_1} dI_1 + \frac{\partial f}{\partial I_2} dI_2 + \frac{\partial f}{\partial I_3} dI_3 + \frac{\partial f}{\partial I_4} dI_4 + \frac{\partial f}{\partial I_5} dI_5 > 0 \qquad (2.20)$$

The translation of the yield surface due to plastic flow is reflected as a change in the parameters α_1, α_2 as $d\alpha_1$, $d\alpha_2$. The determination of these parameters requires the specification of a hardening rule which will be discussed in Chapter III.

Plastic Strain-rate:

It is assumed that the plastic strain increments $d\varepsilon_{ij}^{p}$ obey the normality condition, so that

$$d\varepsilon_{ij}^{p} = d\lambda \frac{\partial f}{\partial T_{ij}} \quad \text{for } f = 0 \text{ and } df > 0,$$

and (2.21)

$$d\varepsilon_{ij}^{p} = 0 \quad \text{for } f \leq 0 \text{ and } df < 0$$

where $d\lambda$ in a scalar constant.

The value of the scalar constant can be estimated from the knowledge of plastic strain rate when loaded in radial directions. However, formulae will be derived to determine the value of $d\lambda$ in conjunction with the hardening rules in axisymmetric deformation in Chapter III.

CHAPTER III.

THE AXISYMMETRIC PLASTICITY THEORY

3.1 Introduction

In Chapter II we outlined a general plasticity theory for the fiber reinforced composites. We noted that there exists a kinematic motion of the loading surface in the axisymmetric $I_1 I_2$ composite stress plane, during plastic flow. We observed further, that if the microscopic yielding is localized at the fiber-matrix interface, during plastic flow, then the loading surface is identical to the initial yield surface in a translated position in the $I_1 I_2$-plane. The translation of the loading surface is associated with the plastic straining of the matrix and the consequent generation of residual stresses. In Appendix II it is proved that there exists an infinite combination of residual stress fields and the associated initial strain fields, such that the microstresses generated by external composite stresses combined with the existing residual stresses satisfy the yield condition at both the micro- and macro-levels, and also the equilibrium requirements. By establishing the correspondence between microstress increments generated by the applied composite stress increments, we shall formulate the hardening and the associated

flow rules governing the kinematic motion of the loading surface, and the macrostrains, respectively, in the I_1I_2-plane. By doing so, we determine the particular combination of the residual stress field and the associated strain field out of the infinite possible combinations, such that they are consistent with the microplastic flow.

3.2 Micro- and Macro-Stress Correspondence

In Chapter II we observed that the microstresses satisfy the yield condition given by Equation 2.9, and the macrostresses satisfy the yield condition given by Equation 2.16. It should be noted, that these two yield conditions are identical, except they are written for different stress systems. Whereas Equation 2.9 refers to the local deviatoric stresses at the fiber-matrix interface, Equation 2.16 is an analogous form in which the local stresses are expressed in terms of the composite stress state. Figure 3-1. shows schematically the Equation 2.9 and 2.16. The center of the Mises Circle (Equation 2.9) in the deviatoric stress plane always corresponds to the center of the ellipse (Equation 2.16), in the composite stress plane, since according to Equation 2.12, 2.13, and 2.15, the composite stresses α_1, α_2 can cause only isotropic stress changes at the interface. Similarly, any loading state L can be represented by a vector given by Equation 2.12 from the center of each loading surface (the subsequent yield surfaces, Equations 2.9 and 2.16, are referred to as the loading

surfaces). When loading continues from L to L', the loading path in the deviatoric plane must follow the Mises Circle, because of the nonhardening matrix.

The above considerations suggest that any composite stress increment can cause the following stress changes in the matrix at the fiber-matrix interface during plastic flow:

(a) A hydrostatic stress increment which always contributes to the translation of the loading surface in the composite stress plane.

(b) A neutral stress increment which causes only elastic strains and has no effect on the motion of the composite loading surface.

(c) A deviatoric stress increment which causes plastic strains in the matrix, and thus affects the motion of the composite loading surface.

Each of these stress changes can be associated with a component of the composite stress increment as follows:

Stress Increment (a) - the hydrostatic stress change (a) is caused by

$$\{dI_1 \; dI_2\} = \{d\alpha_1 \; d\alpha_2\} \tag{3.1}$$

where $\{d\alpha_1 \; d\alpha_2\}$ is the translation of the loading surface in composite stress plane. The corresponding microstress change at the interface is of the form

$$\{d\sigma_{rr}^{m} \; d\sigma_{\phi\phi}^{m} \; d\sigma_{33}^{m}\} = dp \; \{1 \quad 1 \quad 1\}$$

$$\{d\sigma_{r\phi}^{m} \; d\sigma_{\phi 3}^{m} \; d\sigma_{3r}^{m}\} = 0 \qquad (3.2)$$

Indeed, the composite stress change of Equation 3.1 does not violate the Equation 2.16, and the microstress change of Equation 3.2 does not change the Equation 2.9.

Stress Increment (b) - the neutral stress change (b) is caused by a neutral loading (L L'' in Figure 3-1) in the I_1I_2-plane, given by

$$\{dI_1 \; dI_2\} = d\mu' \left\{ - \frac{\partial f}{\partial I_2} \; \frac{\partial f}{\partial I_1} \right\} \qquad (3.3)$$

where $d\mu'$ is a scalar multiplier.

Proof: Let us prove that the composite stress increment given by Equation 3.3 causes neutral stress change locally.

From Equations 2.16 and 2.8

$$\begin{Bmatrix} \partial f/\partial I_1 \\ \partial f/\partial I_2 \end{Bmatrix} = 2 \; [A]^T \; [c] \; [A] \begin{Bmatrix} I_1 - \alpha_1 \\ I_2 - \alpha_2 \end{Bmatrix} = 3 \; [A]^T \; \{S\} \qquad (3.4)$$

The deviatoric stress increments at the interface caused by $\{dI_1 \; dI_2\}$ in Equation 3.3 are given by Equation 2.8 as:

$$\{dS\} = \frac{2}{3}\, d\mu' \, [c] \, [A] \begin{Bmatrix} -\partial f/\partial I_2 \\ \partial f/\partial I_1 \end{Bmatrix} \tag{3.5}$$

A substitution for the derivatives from Equation 3.4 leads to

$$\{dS\} = 2\mu' \, [c] \, [d] \, \{S\} \tag{3.6}$$

where

$$[d] = \begin{bmatrix} 0 & d_1 & -d_2 \\ -d_1 & 0 & d_3 \\ d_2 & -d_3 & 0 \end{bmatrix} \tag{3.7}$$

and from Equations 2.5 and 3.6

$$\begin{aligned} d_1 &= A_{12}A_{21} - A_{11}A_{22} \\ d_2 &= A_{11}A_{32} - A_{12}A_{31} \\ d_3 &= A_{22}A_{31} - A_{21}A_{32} \end{aligned} \tag{3.8}$$

From Equations 3.6 to 3.8

$$\{S\}^T\{dS\} = 0 \tag{3.9}$$

which proves, in connection with Equation 2.9, that the neutral loading given by Equation 3.3 causes only neutral loading in the deviatoric stress plane. Conversely, a neutral loading in the

deviatoric stress plane is a consequence of the neutral loading in the composite stress plane. As a corollary, it follows that plastic deformation is caused by a composite stress other than given by Equation 3.3.

Stress Increment (c) - the stress increment (c) is a neutral stress change along with plastic deformation in the matrix, and thus affects the translation of the loading surface in the composite stress plane. The composite stress increment corresponding to this stress change is similar to (b) and is given by

$$\{dI_1 \; dI_2\} = d\mu'' \left\{ -\frac{\partial f}{\partial I_2} \; \frac{\partial f}{\partial I_1} \right\} \qquad (3.10)$$

where $d\mu''$ is a scalar constant. The micro-stresses corresponding to this stress increment are neutral in nature, and purely deviatoric. This is in contrast to the stress increment (b) caused by composite stresses in Equation 3.3, where the microstresses could have a hydrostatic component. The deviator component of micro-stress change (c) at the interface can be expressed in analogy with Equation 3.6 as

$$\{dS\} \equiv \{d\sigma\} = 2\,\mu''\,[c]\,[d]\,\{S\} \qquad (3.11)$$

3.3 The Hardening Rules

The superposition of the composite stress increments given by Equations 3.1, 3.3, and 3.10, corresponding to the three types of stress changes at the interface leads to the following equation.

$$\begin{Bmatrix} dI_1 \\ dI_2 \end{Bmatrix} = \begin{Bmatrix} d\alpha_1 \\ d\alpha_2 \end{Bmatrix} + d\mu \begin{Bmatrix} -\partial f/\partial I_2 \\ \partial f/\partial I_1 \end{Bmatrix} \qquad (3.12)$$

where $d\mu = d\mu' + d\mu''$. The elementary translation of the loading surface during this composite stress increment is due to the microstress increments (a) and (c). The deviatoric rotation (c) causes the loading surface to travel along the instantaneous tangent to the loading surface. This stress increment can be considered as a consequence of two composite stress increments both in the direction of the instantaneous tangent, the first one causing an elastic stress change rotating the stress vector in the deviatoric plane, and the second one which is equal and opposite to the first one but causing an isotropic stress change. The first of the above does not change the position of the loading surface, and the second causes the loading surface to move along the tangent. The net effects of this process are, that a deviatoric neutral microstress increment is "locked" in the composite at the fiber matrix interface as residual stress, and the loading surface has moved along the tangent with the loading point fixed

in the I_1I_2-plane. Such translation of the loading surface is reflected in the Equation 3.12 by suitable selection of the multiplier $d\mu$. This will be done in the formulation of the two hardening rules that will follow.

3.3.1 Hardening Rule I

In order to determine the value of $d\mu$ in Equation 3.12, it will be assumed that the vector $\{d\alpha_1\ d\alpha_2\}$ is directed always in the "radial direction", where a "radial direction" is defined as the direction in the I_1I_2-plane passing through the center of the instantaneous loading surface and the current loading point. This suggests that the tangential component of the composite stress increment is always elastic, and the microstress change (c) is absent along radial paths.

The nature of the stress change (c) has been investigated in the course of the finite element analysis of elasto-plastic composite cylinders by the ELAS65 program [20]. Figure 3-2 shows the results for a boron-aluminum composite cylinder which has been loaded along several radial paths defined by $I_2 = \beta I_1$, well into plastic range. The matrix becomes completely plastic in each case. The details of the loading will be described later in this chapter. The shaded fans in Figure 3-2 represent the range of directions of the resultant deviator stress vectors at the fiber-matrix interface during plastic straining of the composite cylinders. It is observed that radial loading in the composite stress space causes essentially isotropic stress increments at the interface during plastic flow of the matrix. Therefore,

the effect of stress state (c) is quite limited along radial paths. Similar results are obtained for other composites, such as beryllium-aluminum, and also for different fiber volume fractions, but are not presented here.

On the basis of the above observations, a simple hardening rule, which will be referred to as Hardening Rule I henceforth, can be stated as follows:

"A load increment along an arbitrary path in axisymmetric composite plane $I_1 I_2$ can be resolved into radial and tangential components. The radial component which is responsible for the translation of the composite loading surface, causes an isotropic stress increment (a), and a plastic strain increment at the interface; the tangential component which does not affect the position of the loading surface leads to neutral loading (b) and elastic interface strains."

Thus the Hardening Rule I can be obtained from the Equation 3.12 with $d\mu''$ as zero and $d\mu'$ determined from the assumption of radial translation made above. The Hardening Rule I can thus be written as

$$\begin{Bmatrix} d\alpha_1 \\ d\alpha_2 \end{Bmatrix} = \begin{Bmatrix} dI_1 \\ dI_2 \end{Bmatrix} - d\mu_I \begin{Bmatrix} -\partial f/\partial I_2 \\ \partial f/\partial I_1 \end{Bmatrix} \qquad (3.13)$$

where $d\mu_I \equiv d\mu'$, and $\{d\alpha_1 \; d\alpha_2\}$ is the elementary translation of the loading surface.

The scalar constant $d\mu_I$ can be found from the requirement that the vector $\{d\alpha_1 \; d\alpha_2\}$ is in the radial direction (See

Figure 3-1.). Specifically the vectors

$$\{(I_1 - \alpha_1 + dI_1)\ (I_2 - \alpha_2 + dI_2)\} \qquad \text{and}$$

$$\{(I_1 - \alpha_1 - d\mu_I\ \partial f/\partial I_2)\ (I_2 - \alpha_2 + d\mu_I\ \partial f/\partial I_1)\}$$

must be coaxial, i.e., their cross-product must be equal to zero. Neglecting the second order terms in the cross-product and simplifying we obtain

$$d\mu_I = \frac{(I_1 - \alpha_1)\ dI_2 - (I_2 - \alpha_2)\ dI_1}{(I_1 - \alpha_1)\ \partial f/\partial I_1 + (I_2 - \alpha_2)\ \partial f/\partial I_2} \qquad (3.14)$$

Therefore, the translation $\{d\alpha_1\ d\alpha_2\}$ of the loading surface can be found for each given load increment from Equations 3.13 and 3.14. Note that $d\mu_I = 0$ for any radial path $(I_1 - \alpha_1)/(I_2 - \alpha_2) = dI_1/dI_2$.

3.3.2 Hardening Rule II

We formulated earlier the Hardening Rule I, which neglected the deviatoric increment (c), and the translation of the loading surface being assumed always taking place in the radial direction. The considerations led us to a simple minded hardening rule, which may be very useful in the formulation of a not-too-complicated plasticity theory of composites under general loading conditions. In the present section we shall abolish the radiality assumption of the translation of the loading surface, and consider the deviatoric stress increment (c) to be present, to formulate a more accurate hardening rule.

The Hardening Rule II will be formally stated in analogy to Hardening Rule I as follows:

"A load increment along any arbitrary path in axisymmetric composite plane I_1I_2 can be resolved into translation and tangential components. The translation component which is responsible for the translation of the composite loading surface, causes an isotropic stress increment of type (a), and a plastic strain increment at the interface; the tangential component which does not affect the position of the loading surface leads to neutral loading of type (b) and elastic interface strains."

It should be noted that the translation component is a consequence of the two microstress increments (a) and (c), and the tangential component is a consequence of (b) and (c). Thus the Hardening Rule can be written as

$$\begin{Bmatrix} d\alpha_1 \\ d\alpha_2 \end{Bmatrix} = \begin{Bmatrix} dI_1 \\ dI_2 \end{Bmatrix} - d\mu_{II} \begin{Bmatrix} -\partial f/\partial I_2 \\ \partial f/\partial I_1 \end{Bmatrix} \qquad (3.15)$$

where $d\mu_{II}$ is a scalar constant and $\{d\alpha_1 \; d\alpha_2\}$ is the elementary translation of the loading surface. Equation 3.15 is formally similar to Equation 3.13 which defines Hardening Rule I. However, the vector $\{d\alpha_1 \; d\alpha_2\}$ calculated from Equation 3.15 may no longer in the radial direction, and $d\mu_I \neq d\mu_{II}$. Instead, we must require that each elementary composite increment $\{dI_1 \; dI_2\} = \{d\alpha_1 \; d\alpha_2\}$, where $\{d\alpha_1 \; d\alpha_2\}$ is defined by Equation 3.15, causes only isotropic stress changes at the interface. This requirement follows from Equation 2.16, which suggests that the center of the current loading surface is at $I_1 = \alpha_1$, $I_2 = \alpha_2$, the composite stresses α_1 and α_2 causes only isotropic changes at the interface, for any loading path in the I_1I_2-plane.

In order to determine the scalar multiplier $d\mu_{II}$ it will be assumed that under the action of the composite stress increment $\{d\alpha_1 \; d\alpha_2\}$, not only the interface, but also the entire matrix will experience an isotropic change only. On the basis of this assumption and stress equilibrium requirements between the local and composite stresses we can write the local stress increments in the matrix and the fiber as follows:

In the matrix,

$$\{d\sigma_{rr}^{\,m} \; d\sigma_{\phi\phi}^{\,m} \; d\sigma_{33}^{\,m}\} = d\alpha_1 \{1 \;\; 1 \;\; 1\} \qquad (3.16)$$

In the fiber,

$$\{d\sigma_{rr}^{f}\ d\sigma_{\phi\phi}^{f}\ d\sigma_{33}^{f}\} = \{d\alpha_1\ d\alpha_1\ d\sigma_{33}^{f}\} \qquad (3.17)$$

and $d\sigma_{33}^{f}$ is determined from the equilibrium requirement in the axial direction

$$d\sigma_{33}^{f} V_f + d\sigma_{33}^{m} (1 - V_f) = d\alpha_2 \qquad (3.18)$$

From Equations 3.16 and 3.18,

$$d\sigma_{33}^{f} = [- (1 - V_f)\ d\alpha_1 + d\alpha_2]/V_f \qquad (3.19)$$

The existence of perfect bond between the constituents requires that the local displacement increments in the radial direction be equal, so that,

$$du_r^{f} = du_r^{m} \text{ at } r = R \qquad (3.20)$$

In view of the radial symmetry, $du_r = r d\varepsilon_{\phi\phi}$, and the local strains at the interface are:

$$d\varepsilon_{\phi\phi}^{f} = d\varepsilon_{\phi\phi}^{m} \text{ at } r = R$$

$$d\varepsilon_{33}^{f} = d\varepsilon_{33}^{m} \text{ at } 0 \leq r \leq a \qquad (3.21)$$

The second relation is a consequence of the generalized plane strain in the axial direction of the composite cylinder.

Since the fiber remains elastic, one can find from Equations 3.17 and 3.19:

$$d\varepsilon_{\phi\phi}^{f} = \frac{1}{E_f} \left([(1 - \nu_f) - \nu_f(1 - \frac{1}{V_f})] \, d\alpha_1 - \frac{\nu_f}{V_f} \, d\alpha_2 \right)$$

$$d\varepsilon_{33}^{f} = \frac{1}{E_f} \left([-2 \, \nu_f + (1 - \frac{1}{V_f})] \, d\alpha_1 + \frac{1}{V_f} \, d\alpha_2 \right) \qquad (3.22)$$

The matrix strains will have an elastic part by the microstresses given by Equation 3.16, and a plastic part, due to the local deviatoric stresses S_{ij} at the loading point $\{I_1 \; I_2\}$. For a nonhardening matrix of Mises type:

$$d\varepsilon_{\phi\phi}^{m} = \frac{d\alpha_1}{3K_m} + d\,\lambda^m S_{\phi\phi}$$

$$d\varepsilon_{33}^{m} = \frac{d\alpha_1}{3K_m} + d\lambda^m S_{33} \qquad (3.23)$$

where K_m is the bulk modulus of the matrix, and $d\lambda^m$ is a scalar multiplier. From Equations 3.21 to 3.23

$$\{d\alpha_1 \; d\alpha_2\} = d\lambda^m \, [F]^{-1} \, \{S_{\phi\phi} \; S_{33}\} \qquad (3.24)$$

where

$$[F] = \begin{bmatrix} F_{11} & F_{12} \\ F_{21} & F_{22} \end{bmatrix}$$

$$F_{11} = \frac{1}{E_f}\left((1 - \nu_f) - \nu_f\left(1 - \frac{1}{V_f}\right)\right) - \frac{1}{3K_m},$$

$$F_{21} = \frac{1}{E_f}\left(-2\,\nu_f + 1 - \frac{1}{V_f}\right) - \frac{1}{3K_m},$$

$$F_{12} = -\frac{\nu_f}{E_f\,V_f}, \quad F_{22} = \frac{1}{E_f\,V_f},$$

and E_f, ν_f are the elastic constants of the fiber.

The deviatoric stresses in the matrix at the loading point $\{I_1\ I_2\}$ can be found from the Equation 2.15,

$$\{S_{\phi\phi}\ \ S_{33}\} = [P]\,\{(I_1 - \alpha_1)\,(I_2 - \alpha_2)\} \qquad (3.25)$$

when [P] is defined by Eqution 2.11, and α_1, α_2 are the coordinates of the center of the current loading surface (Equation 2.16) in the I_1I_2-plane. The unknown parameters $d\mu_{II}$ and $d\lambda^m$ can now be found from Equations 2.16, 3.15, 3.24, and 3.25,

$$\{(d\lambda^m\,E_m)\,d\mu_{II}\} = [R]^{-1}\,\{dI_1\ dI_2\} \qquad (3.26)$$

where E_m the Young's Modulus of the matrix, has been introduced for dimensional reasons.

The coefficients of the matrix [R] are:

$$\begin{Bmatrix} R_{11} \\ R_{21} \end{Bmatrix} = \frac{1}{E_n} [F]^{-1} [P] \begin{Bmatrix} I_1 - \alpha_1 \\ I_2 - \alpha_2 \end{Bmatrix} \tag{3.27}$$

$$\begin{Bmatrix} R_{12} \\ R_{22} \end{Bmatrix} = \begin{Bmatrix} -\partial f/\partial I_2 \\ \partial f/\partial I_1 \end{Bmatrix}$$

Selected numerical values for the determination of these coefficients are listed in Appendix III.

The components $d\alpha_1$, $d\alpha_2$ of the elementary translation of the loading surface can now be determined by using the Hardening Rule II given by Equation 3.15, where the scalar multiplier $d\mu_{II}$ is found from Equation 3.26.

3.4 The Strains

The micromechanical considerations employed in the previous sections are useful insofar as they permit a fairly accurate examination of the essential effects of the micrononhomogeneity of the composite on its macroscopic deformation behavior. On the other hand, the formulation of macroscopic constitutive relations for the composite must be made on the basis of macrohomogeneous, anisotropic continuum model of an elastic-plastic solid. As before, the

emphasis will be on the axisymmetric stress states, and the resulting deformation modes. The composite will be regarded as a homogeneous solid, loaded in the I_1I_2-plane, with the loading surface given by Equation 2.16, which may be controlled by either Hardening Rule I (Equations 3.13 and 3.14), or the Hardening Rule II (Equations 3.15 and 3.26). The load surface (Equation 2.16) is an ellipse in I_1I_2-plane with its center at $I_1 = \alpha_1$, $I_2 = \alpha_2$. The plastic component of a strain increment, if it exists, must coincide with the outward normal to the loading surface [39, 40].

Let ε_{rr} and $\varepsilon_{33} = \varepsilon_2$ denote the total composite strains in the radial, and axial directions, respectively. The area strain in the transverse plane which is the ratio between the change in transverse area to the original area is $\varepsilon_1 = 2\,\varepsilon_{rr}$.

The elastic components of the total strains ε_1 and ε_2 can be found from the knowledge of the composite compliances (See Appendix I) as

$$\begin{Bmatrix} \varepsilon_1^{\,e} \\ \varepsilon_2^{\,e} \end{Bmatrix} = \begin{bmatrix} \kappa_{11} & \kappa_{12} \\ \kappa_{21} & \kappa_{22} \end{bmatrix} \begin{Bmatrix} I_1 \\ I_2 \end{Bmatrix} \tag{3.28}$$

where $\varepsilon_1^{\,e}$ and $\varepsilon_2^{\,e}$ are elastic components of the total strains ε_1 and ε_2, respectively, and κ_{ij} are the composite compliances.

The plastic components of the total strains ε_1 and ε_2 can be obtained by integrating the plastic strain increments, which can be written by using the normality condition [39] as

$$d\varepsilon_1^p = d\lambda \frac{\partial f}{\partial I_1}$$

$$d\varepsilon_2^p = d\lambda \frac{\partial f}{\partial I_2} \qquad (3.29)$$

where $d\lambda$ is a scalar multiplier, and f is the loading function given by Equation 2.16.

The scalar multiplier $d\lambda$ may be found from a suitable estimate of the plastic strain increments under loading in the radial direction, such as was, for instance, by Hill [34]. Instead we shall derive another formula for $d\lambda$ which will be consistent with the formulation of the hardening rules.

In the formulation of the hardening rules in the earlier sections, we observed that there exists a component $\{d\alpha_1 \; d\alpha_2\}$ of the applied composite stress increment $\{dI_1 \; dI_2\}$, which is responsible for the translation of the loading surface in I_1I_2-plane, during plastic deformation. This component was in the radial direction for Hardening Rule I, and was in a special direction depending upon the current microstresses at the fiber-matrix interface for Hardening Rule II. Closer observation of these rules would reveal that, the only component of the composite stress increment $\{dI_1 \; dI_2\}$ that causes plastic deformation is $\{d\alpha_1 \; d\alpha_2\}$, when $\{d\alpha_1 \; d\alpha_2\}$ is determined from Equation 3.13 for Hardening Rule I and from Equation 3.15 for Hardening Rule II. The other component which is tangential to the loading surface at the loading point, causes only elastic strains. In both hardening rules it has been postulated that $\{d\alpha_1 \; d\alpha_2\}$ causes only

isotropic stress change in the matrix at the fiber matrix interface. It was assumed further in the formulation of Hardening Rule II that, not only the interface, but also the entire matrix experiences only isotropic change during the loading $\{d\alpha_1\ d\alpha_2\}$. Noting that Equation 3.22 is equally valid with $\{d\alpha_1\ d\alpha_2\}$ found from Hardening Rule I (Equation 3.13), subject to the same assumptions, and considering the generalized plane strain in the fiber direction, the total composite strain increment $d\varepsilon_2$ in the axial direction is equal to the strain increment $d\varepsilon_{33}^{f}$. The value of $d\varepsilon_{33}^{f}$ can be found from Equation 3.22. Thus

$$d\varepsilon_2 = \frac{1}{E_f}\left([-2\ \nu_f + (1 - \frac{1}{V_f})]\ d\alpha_1 + \frac{1}{V_f}\ d\alpha_2\right) \qquad (3.30)$$

The plastic component of the total strain $d\varepsilon_2$ can be obtained by subtracting its elastic component. Thus

$$d\varepsilon_2^{p} = d\varepsilon_2 - (\kappa_{21}\ d\alpha_1 + \kappa_{22}\ d\alpha_2) \qquad (3.31)$$

where κ_{21} and κ_{22} are elastic compliances as defined in Equation 3.28.

The scalar constant $d\lambda$ can now be found from Equations 3.29, 3.30, and 3.31 as

$$d\lambda = \frac{1}{\partial f/\partial I_2}\ \left[\left(-\frac{2\nu_f + (1 - V_f)/V_f}{E_f} - \kappa_{21}\right) d\alpha_1 + \right.$$

$$\left. + \left(\frac{1}{E_f\ V_f} - \kappa_{22}\right) d\alpha_2\right] \qquad (3.32)$$

The plastic strain increments can now be obtained from Equations 3.29 with $d\lambda$ determined from Equation 3.32. The plastic strains at any loading step can be obtained by integration of Equation 3.29 along the loading path where there is plastic flow (See Equation 2.21). The total strains can then be obtained by adding these to the elastic strains obtained from Equation 3.28.

3.5 Comparison of Approximate and Exact Solutions

The validity of the hardening and flow rules proposed in previous chapters will now be verified by extensive comparisons of the results obtained from these rules, with the exact plasticity solutions. Three loading programs are selected for the purpose. The first in proportional loading and the other two are zig-zag paths consisting of linear segments in I_1I_2-plane. Two composites, a boron-aluminum composite with a volume fraction of 0.3, and a beryllium-aluminum composite with a volume fraction of 0.5, have been used in the analysis. The elastic constants of these composites and their constituents are given in Appendix I.

3.5.1 Exact solution

The exact solution for each loading program are obtained by using ELAS65 computer program [20], which is based on the finite element method. The finite element mesh for the composite cylinder (Figure 5-3) under axisymmetric deformation consists of a layer of

the cylinder with unit thickness in the axial direction, which has a shape of a 10-degree sector of the transverse circular section. The axisymmetric condition is specified by prescribing zero normal displacements on the radial faces of the sector, and the generalized plane strain is specified by prescribing uniform displacements in the thickness direction. A total of 19 hexahedral finite elements are used to cover the entire domain, 15 of them in the matrix. The fiber is considered as an isotropic linear elastic material, and the matrix as an isotropic elastic-plastic nonhardening material of Mises type. The composite stresses are simulated by prescribing appropriate nodal forces. Whenever required the ELAS65 program is restarted at the end of each linear segment of the loading programs to change the loading direction in the I_1I_2-plane by changing the nodal forces suitably. The error in the finite element solution [20] is expected to be less than 7%. The loading surfaces are constructed at the end of each linear segment of the zig-zag loading programs. These surfaces are constructed by considering the microstresses present at any loading point $\{I_1\ I_2\}$ in the I_1I_2-plane as residual stresses; constructing the yield surface corresponding to these residual stresses; translating the origin of the coordinate system of the above to $\{-I_1, -I_2\}$. The procedure of determining the yield surfaces with residual stresses is outlined in Appendix IV.

3.5.2 Approximate solutions

The approximate solutions for each loading program are constructed by integrating the hardening and flow rules numerically

by piecewise linearization. The center of the loading surface and the total strains are found at each step of the loading. The loading surface at the step is obtained by translating the stress free initial yield surface such that its center coincides with the center determined by the hardening rules.

3.5.3 Results and comparison

The three loading programs selected for the purpose of checking the validity of the proposed plasticity theory with exact finite element plasticity solutions are as follows:

i) proportional loading

This loading program consists of loading a stress free composite along a proportional path defined by $I_2 = \beta I_1$ in the $I_1 I_2$-plane. The values of β selected are 0, 1, 1.34, 2, ∞ and -1. In order to facilitate comparison of the representation of the results obtained along various paths, a parameter t is introduced, such that $I_1 = p_1 t$ and $I_2 = p_2 t$ where $p_2 = \beta p_1$ and $t = Y$ at initial yield; Y is the tensile yield stress of the matrix, and is selected as 40,000 psi in all calculations.

ii) zig-zag loading I

This loading program consists of loading a stress free composite along a zig-zag path. The path consists of 8 linear continuous segments in $I_1 I_2$-plane (Figure 3-4) and contains a total of 38 loading steps. The corners of the zig-zag segments of the loading are at loading steps 2, 7, 6, 19, 22, and 31. In the approximate solution each of the above steps is further subdivided into 10 substeps to increase the accuracy.

iii) zig-zag loading II

Like zig-zag loading I, this loading program also consists of loading a stress free composite along a zig-zag path, but another combination of the 8 linear segments (Figure 3-6). This loading program contains 46 loading steps. The corners of the zig-zag linear segments are at loading steps 3, 9, 19, 24, 32, 38, and 39. As before each step is further subdivided into 10 substeps in the approximate solution.

The results of loading along a proportional path $I_2 = \beta I_1$ for a B-Aℓ ($V_f = 0.3$) are shown in Figure 3-3. The micro-stresses obtained from ELAS65 program were also used for Figure 3-2. The composite is loaded well into plastic range. Figure 3-3 shows the composite strains for all values of β except 1.34, and 2 in comparison with the theoretical predictions. It is observed that the stress-strain curves obtained from Hardening Rule I and the associated flow rule are almost identical with those found by the finite element method. Equally good agreement was found for the other two values of β. These comparisons provide a direct verification of Equation 3.30 for the total axial composite strain ε_2, and the flow-rule derived earlier. The stress-strain curves obtained from Hardening Rule II and the associated flow rule are almost identical to those obtained from Hardening Rule I, and so are not shown.

The results obtained here will also be used in the determination of plastic dilatations, later in this chapter.

A stress free B-Aℓ ($V_f = 0.3$) composite is loaded along the zig-zag loading path I. The location of the loading surface

and the total composite strains are obtained by using both the finite element method and the proposed theory. The results are shown in Figures 3-4 and 3-5. Figure 3-4 shows the loading path, and the loading surfaces at Steps 1, 7, 15, 19, 22, 31 and 38, calculated from the microstresses obtained from the finite element method as well as the theoretical predictions from Hardening Rule I. The initial yield surface at Step I is, of course, common to both the finite element and theoretical methods. During the loading process, the yield surface is translated without deformation, according to the Hardening Rule I. The agreement with the finite element solution is examined by finding the centers of the yield surfaces, both from Hardening Rule I, and from the finite element solution. In the later case, it has been necessary to find the centers of hypothetical loading surfaces based on the microstresses in the interface element, rather than for the actual overall loading surfaces, which include some times parts of loading surfaces of matrix points away from the interface and are not entirely regular.

The differences between actual and interface loading surfaces are found to be negligible. It is readily seen that the calculated overall loading surfaces are almost exact replicas of the initial yield surface, in agreement with Equation 2.16. The centers of the loading surfaces obtained by using Hardening Rule I (Equation 3.13) are very close to those obtained from the finite element method, but there is small discrepancy for certain segments of the loading path. On the contrary, the centers of the loading surfaces obtained by using Hardening Rule

II (Equation 3.15), have coincided (not shown on the figure) exactly with their counterparts obtained by the finite element method, which seem to indicate that the Hardening Rule II is more accurate.

Figure 3-5 shows a comparison of the total strains calculated from the hardening and flow rules, and from the finite element method. The elastic strains, Equation (I-1) are also plotted for each point of the loading path. Again, the strains calculated from the rules are in good agreement with the exact results.

A stress free Be-Aℓ (V_f = 0.5) is loaded along the zig-zag loading path II. The location of the loading surface and the total composite strains are obtained by using the finite element method as well as the proposed theory. The results are shown in Figures 3-6 and 3-7.

Figure 3-6 shows the zig-zag loading path II, and centers of the loading surfaces at Steps 1, 3, 9, 19, 24, 32, 38, and 46, calculated both from the finite element method and the Hardening Rules I and II. The initial yield surface for the Be-Aℓ (V_f = 0.5) composite is very large, and is shown in a separate Figure 4-1. Figure 3-6 contains only a part of the initial yield surface, to illustrate the extent of loading along the described path. The kinematic motion of the loading proceeded again by rigid body translation, with no deformation (negligible in the finite element solution), since the onset of yielding at the fiber-matrix interface has been predominant. It can be seen that Hardening Rule II gives very accurate prediction of the exact

method based on the finite element method. On the contrary, the centers of the loading surfaces predicted by Hardening Rule I deviate significantly from the exact results, at some segments of the path.

The accuracy of the flow rules associated with the hardening rules is verified by a comparison of the predicted total strains with those obtained by the finite element method, and the results are shown in Figure 3-7. It can be observed from this figure the total strains obtained from the two hardening rules on essentially same, and are very close to the finite element solution.

3.6 Plastic Dilatation

The magnitude of macroscopic plastic dilatation of the B-Aℓ composite has been evaluated for the proportional loading $I_2 = \beta I_1$, for the values of β described earlier, and also for additional values of the same.

The hydrostatic composite stress increment is

$$dT_{kk} = 2\, dI_1 + dI_2 = (2 + \beta)\, dI_1. \qquad (3.33)$$

The elastic isotropic strain increment is

$$d\varepsilon_{kk} = d\varepsilon_1^{\,e} + d\varepsilon_2^{\,e}. \qquad (3.34)$$

Then, from Equations 3.33, 3.34 and (I-1)

$$\frac{d\varepsilon_{kk}^{e}}{d\,T_{kk}} = [(\kappa_{11} + \kappa_{21}) + \beta(\kappa_{12} + \kappa_{22})]/(2 + \beta) \tag{3.35}$$

The elementary plastic dilatation $d\varepsilon_{kk}^{p} = d\,\varepsilon_{kk} - d\,\varepsilon_{kk}^{e}$ has been found both by using the flow rule associated with Hardening Rule I and the finite element method. Figure 3-8 shows the ratios $d\,\varepsilon_{kk}^{p}/d\,\varepsilon_{kk}^{e}$, and $d\,\varepsilon_{kk}^{e}/d\,T_{kk}^{e}$, as functions of the angle $\phi = \tan^{-1}\beta$ (Note that ϕ is not the angular coordinate here). These ratios are approximately constant for a given value of β, since the composite stress-strain curves for the proportional loading are nearly bilinear, Figure 3-3. Note that $d\,\varepsilon_{kk}^{e} = 0$ at $\phi = 0.597\,\pi$, and $d\,T_{kk} = 0$ at $\phi = 0.647\,\pi$.

It is observed that the plastic dilatation is of the same order of magnitude as the elastic dilatation for most values of ϕ.

3.7 Discussion

The results of the previous sections indicate that the Hardening and the associated Flow Rules proposed, provide a respectable approximation of the exact hardening and flow behavior of the fibrous composites. The rules are simple enough, that they can be used with simple, computer programs to perform the integration or even without computer assistance for simple loading paths, providing that the necessary material constants

are known. Appendix I shows a summary of these constants for B-Aℓ and Be-Aℓ composites.

The Hardening Rule I is somewhat similar to the Ziegler's modification of the Prager's kinematic hardening rule [43, 44]. The basic difference is, of course, that the present rule is not an assumed one; instead, it has been derived from the constraints on plastic deformation imposed by the nonhomogeneity of the microstructure of fibrous composites with a nonhardening matrix. It is not beyond the realm of possibility that the kinematic hardening in macrohomogeneous metals has a similar physical basis.

The Hardening Rule II represents a higher order approximation than the Hardening Rule I. As a consequence the results obtained by this rule are very close (in some cases exact) to the exact finite element solution. This rule gives a very accurate description of microplastic flow at the fiber matrix interface and its effect on the macrobehavior.

The flow rule proposed is based to some extent on the "rule of mixtures" for the stresses in the axial direction. However, it should be noted that the equilibrium of stresses by rule of mixtures has been required only for that part of the component $\{d\alpha_1, d\alpha_2\}$ of the composite stress increment $\{dI_1, dI_2\}$, which has been responsible for the plastic deformation. In spite of this assumption, the total strains predicted by the proposed theory agree with the exact finite element solution. Conversely, the agreement seems to prove the accuracy of the assumption made in the evaluation of $d\mu_{II}$ (Equation 3.26) and $d\lambda$ (Equation 3.32),

that the entire matrix experiences isotropic stress change when loaded along a path defined by $\{d\alpha_1\ d\alpha_2\}$.

CHAPTER IV.

DETERMINATION OF MICROSTRESSES

In the preceding chapter we developed a continuum theory for elasto-plastic deformation in fibrous composites under axisymmetric conditions. We observed that the theory developed provides a satisfactory approximation of the macro-elasto-plastic response. In the present chapter we shall formulate approximate evaluation of the internal microstress fields in the composite during the elasto-plastic deformation of the matrix, under axisymmetric conditions.

4.1 The Model

Consider again that the composite is represented by a right circular cylinder, x_3 is both the fiber and cylinder axis. The cross section of the cylinder is in the transverse $r\phi$ plane, consists of a fiber region $0 \leq r \leq R$, and a matrix region $R \leq r \leq a$. The cylinder is loaded by composite stresses in I_1I_2-plane. Like in the formulation of the hardening rules in the earlier chapters, it will be assumed that the plastic zone, if it exists,

must adjoin the fiber matrix interface. Therefore, the matrix can be divided into plastic region $R \leq r \leq c$, and an elastic region $c \leq r \leq a$, Figure 5-3.

4.2 The Loading

Consider that the cylinder has been loaded along a general path to the plastic state $\{I_1, I_2\}$, and that another load increment $\{dI_1, dI_2\}$ is applied. According to Hardening Rules I and II (Chapter III) the composite stress increment $\{dI_1, dI_2\}$ has two components $\{d\alpha_1 \; d\alpha_2\}$ and $d\mu \; \{-\partial f/\partial I_2 \;\; \partial f/\partial I_1\}$, where $d\mu$ is a scalar constant depending upon the hardening rule ($d\mu_I$ or $d\mu_{II}$) and f is the loading function (Equation 2.16). We observed in Chapter III that the first component is responsible for the elasto-plastic deformation and causes isotropic stress changes in the matrix at the fiber-matrix interface, while the second component causes pure elastic changes. In this chapter we shall consider the components $\{d\alpha_1 \; d\alpha_2\}$ and $d\mu \;\; \{-\partial f/\partial I_2 \;\; \partial f/\partial I_1\}$ of $\{dI_1 \; dI_2\}$ separately and formulate the microstress solutions.

At this point, it should be noted that, in the determination of $d\mu_{II}$ (Equation 3.26) and $d\lambda$ (Equation 3.32) in Chapter III, we assumed that $\{d\alpha_1, d\alpha_2\}$ causes isotropic stress changes not only at the fiber-matrix interface but also in the entire matrix. Based on this assumption we can construct a simple microstress solution (See Appendix V). However, in this solution only interface yields throughout the loading and the rest

of the matrix remain elastic. In order to account for partial or full plasticity in the matrix, it will be assumed in the following solution, that only the plstic region in the matrix adjoining the interface experience the isotropic stress change.

4.3 Microstress Evaluation

Let $\{d\alpha_1\ d\alpha_2\}$, determined from the Hardening Rule I or II, be the component of the applied composite stress increment $\{dI_1\ dI_2\}$ causing the plastic deformation, and $d\alpha_2 = \beta\ d\alpha_1$, where β is a constant. The stress and displacement fields caused by $d\alpha_1$ and $d\alpha_2 = \beta\ d\alpha_1$ are:

In the fiber ($0 \leq r \leq R$),

$$d\sigma_{rr}^{f} = d\sigma_{\phi\phi}^{f} = dp$$

$$d\sigma_{33}^{f} = E_f\ d\ \varepsilon_{33} + 2\ \nu_f\ dp. \tag{4.1}$$

$$d\ u_r^{f} = \frac{1}{E_f}\ (1 + \nu_f)\ (1 - 2\ \nu_f)\ r\ dp - \nu_f\ r d\varepsilon_2 \tag{4.2}$$

In the matrix,

$$d\sigma_{rr}^{mp} = d\sigma_{\phi\phi}^{mp} = d\sigma_{33}^{mp} = dp \text{ for } R \leq r \leq c \tag{4.3}$$

and

$$d\sigma_{rr}^{me} = \{[\frac{1}{r^2} - \frac{1}{c^2}]\, d\alpha_1 - [\frac{1}{r^2} - \frac{1}{a^2}]\, dp\}/[\frac{1}{a^2} - \frac{1}{c^2}]$$

$$d\sigma_{\phi\phi}^{me} = \{-[\frac{1}{r^2} + \frac{1}{c^2}]\, d\alpha_1 + [\frac{1}{r^2} + \frac{1}{a^2}]\, dp\}/[\frac{1}{a^2} - \frac{1}{c^2}]$$

$$d\sigma_{33}^{me} = E_m\, d\varepsilon_2 + 2\,\nu_m\,[-\frac{d\alpha_1}{c^2} + \frac{dp}{a^2}]/[\frac{1}{a^2} - \frac{1}{c^2}] \qquad (4.4)$$

$$d\,u_r^{me} = \frac{1}{E_m}(1 + \nu_m)(1 - 2\,\nu_m)\, r\, d\alpha_1 - \nu_m\, r\, d\varepsilon_2 + \\ + \frac{(d\alpha_1 - dp)(1 + \nu_m)}{E_m\,(a^2/c^2 - 1)}\,[(1 - 2\,\nu_m)r + \frac{a^2}{r} \qquad (4.5)$$

for $c \leq r \leq a$.

In these equations, $d\varepsilon_2 = d\varepsilon_{33}$ is the axial composite strain increment, dp is a constant which is not necessarily equal to $d\alpha_1$, and E_f, ν_f, E_m, ν_m are the elastic constants of the fiber and matrix, respectively.

Equilibrium in x_3 direction requires that

$$d\alpha_2 = \beta d\alpha_1 = V_f\, d\sigma_{33}^{f} + \frac{c^2 - R^2}{a^2}\, d\sigma_{33}^{mp} + \frac{a^2 - c^2}{a^2}\, d\sigma_{33}^{me} \qquad (4.6)$$

From Equations 4.1, 4.3, 4.4, and 4.6:

$$[-(1 - 2\,\nu_f)R^2/a^2 + (1 - 2\,\nu_m)c^2/a^2]\, dp + [E_f\, R^2/a^2 + \\ + E_m\,(1 - c^2/a^2)]\, d\varepsilon_2 = (\beta - 2\,\nu_m)d\alpha_1 \qquad (4.7)$$

The dilatation caused by the stress increment given by Equation 4.3 in the plastic part of the matrix must be uniform and elastic. If $V_p = \pi x_3^o (c^2 - R^2)$ is the original volume of an elementary layer of thickness x_3^o, the dilatation is:

$$\frac{dV_p}{V_p} = 2 \left(\frac{dc}{c} - \left(\frac{R}{c}\right)^2 \frac{dR}{R}\right)/\left(1 - \left(\frac{R}{c}\right)^2 + d\varepsilon_2 \right. \qquad (4.8)$$

and

$$\frac{dV_p}{V_p} = \frac{dp}{K_m} \qquad (4.9)$$

where K_m is the bulk modulus of the matrix. During the elastic dilatation:

$$dc = d\, u_r^{me}\Big|_{r=c} , \quad dR = d\, u_r^{f}\Big|_{r=R} \qquad (4.10)$$

These equations, in combination with Equations 4.2 and 4.5, lead to another equation relating dp and d ε_2 to d α_1. The later and Equation 4.7 can be written in matrix form

$$\begin{Bmatrix} dp/E_m \\ d\varepsilon_2 \end{Bmatrix} = \begin{bmatrix} a_{11} & a_{12} \\ a_{21} & a_{22} \end{bmatrix}^{-1} \begin{Bmatrix} c_1 \\ c_2 \end{Bmatrix} \frac{d\alpha_1}{E_m} \qquad (4.11)$$

where

$$a_{11} = -(1 - 2\nu_f)(R/a)^2 + (1 - 2\nu_m)(c/a)^2$$

$$a_{12} = (E_f/E_m)(R/a)^2 + (1 - (c/a)^2)$$

$$a_{21} = -2(1 + \nu_m)(1 + (1 - 2\nu_m)(c/a)^2) - 3(1 - 2\nu_m)$$

$$(1 - (R/c)^2)(1 - (c/a)^2) - 2(1 + \nu_f)(1 - 2\nu_f)$$

$$(E_m/E_f)(R/c)^2(1 - (R/a)^2) \qquad (4.11a)$$

$$a_{22} = ((1 - 2\nu_m) - (1 - 2\nu_f)(R/c)^2)(1 - (c/a)^2)$$

$$c_1 = \beta - 2\nu_m,\ c_2 = -4(1 + \nu_m)(1 - \nu_m). \qquad (4.11b)$$

Finally, the stresses in the plastic part of the matrix must satisfy the yield condition. If ${\sigma_{ij}}^m$ are the stresses in the matrix before the application of the load increment, the yield condition at the end of the loading step is

$$\left(g({\sigma_{ij}}^m) + \frac{\partial g}{\partial \alpha_1} d\alpha_1\right)_{r=c} = 0 \qquad (4.12)$$

where g is the Mises yield, and r = c is the position of the elastic-plastic boundary. Equations 4.11 and 4.12 can be used, together with Equation 4.4, to find unknowns dp, $d\varepsilon_2$, and c. The procedure which readily yields itself to a numerical solution

consists in the selection of the position of c of the elastic plastic boundary, and in the determination of the corresponding load increment $d\alpha_1$. Write

$$g(\sigma_{ij}^{m}) = g(r) = g(r-dr) + \frac{\partial g}{\partial r} dr \qquad (4.13)$$

Since $g(r-dr) = 0$ for $r = c$, a substitution of Equation 4.13 into Equation 4.12 gives after rearrangement

$$\frac{d\alpha_1}{dc} = - \left(\frac{\partial g/\partial r}{\partial g/\partial \alpha_1}\right)_{r=c} \qquad (4.14)$$

Note that dc in Equation 4.14 is different from that in Equations 4.8 and 4.10.

If the elasto-plastic boundary is located at $r = c - dc \geq R$ before this application $d\alpha_1$, Equations 4.11 and 4.16 can be used to find the increments dp, $d\varepsilon_2$, and $d\alpha_1$, corresponding to dc. The substitution of these results in Equations 4.1 to 4.5 yields the local stresses and displacements corresponding to the component $d\alpha_1$ and $d\alpha_2 = \beta d\alpha$ of the composite stress increments dI_1 and dI_2.

In the formulation so far we assumed that the constant $\beta = d\alpha_2/d\alpha_1$ exists. In cases where $d\alpha_1 \equiv 0$, β becomes infinity. However, the formulation can still be used if we rewrite the quantity $c_1 d\alpha_1/E_m$ in Equation 4.11 by using Equation 4.11b as follows

$$c_1 d\alpha_1/E_m = (\beta - 2\,\nu_m)d\alpha_1/E_m = (d\alpha_2 - 2\,\nu_m d\alpha_1)/E_m \qquad (4.15)$$

The effect of component $d\mu\{-\partial f/\partial I_2 \;\; \partial f/\partial I_1\}$ of $\{dI_1 \;\; dI_2\}$, where $d\mu = d\mu_I$ or $d\mu_{II}$, can be obtained from the elastic solution as

$$\{d\sigma_{rr} \;\; d\sigma_{\phi\phi} \;\; d\sigma_{33}\} = d\mu\,[A]\,\{-\partial f/\partial I_2 \;\; \partial f/\partial I_1\} \qquad (4.16)$$

where [A] must be evaluated at the appropriate radius r [e.g., Equation 2.4]. The multipliers $d\mu_I$, or $d\mu_{II}$, which were found for the fiber matrix interface in Chapter III are now assumed to apply to the entire matrix $R \leq r \leq a$. Further refinements, perhaps, could be obtained if one can define different values for $d\mu_I$, or $d\mu_{II}$ in the elastic and plastic zones of the matrix.

The complete solution for the stress increments in the composite can now be found by superposition of solutions given by the Equations 4.1, 4.3, 4.4 and the Equation 4.16, provided [A] is found at any value of the radius r.

A computer program has been written integrate numerically the hardening rules (I and II) and the microstress solution, and also the associated flow rules by piece-wise linearization. This program can evaluate the centers of the loading surface, the composite strains, and the microstresses during plastic deformation of the composite in the axisymmetric $I_1 I_2$ composite stress plane. The program can also solve the thermal and aging problems which fall in the same axisymmetric deformation mode, the details of

which will be discussed in Chapter V.

4.4 Numerical Results

The stress evaluation procedure has been verified by comparison of the results with the exact finite element solution from the ELAS65 program. The composites B-Aℓ (V_f = 0.3) and Be-Aℓ (V_f = 0.5) have been used along with the three loading programs discussed in Chapter III.

Table 4-1 shows the comparison for the case of the B-Aℓ composite loaded along the zig-zag path I in Chapter III (Figure 3-4). The microstresses have been determined from ELAS65, computer-aided numerical integration of Hardening Rules I and II coupled with the microstress evaluation procedure, and also by using the approximate formula, Equation (V-1) with the Hardening Rule I.

Table 4-2 shows the comparison for the case of the Be-Aℓ composite loaded along the zig-zag path II in Chapter III (Figure 3-6). The microstresses have been determined from ELAS65, and the numerical integration of Hardening Rule II coupled with the microstress evaluation procedure.

It can be observed from Table 4-1 and 4-2 that all three approximate methods give a satisfactory estimation of the exact finite element solution, both at r = R, and r = a. However, the Hardening Rule II gives the best precision, with only few errors greater than 3 percent of the exact value. As one would expect,

Table 4-1. Microstresses in the matrix of the B-Aℓ composite cylinder (V_f = 0.3) at selected points of the loading path of Figure 3-4. (Stresses in 10^3 psi).

a. At the fiber-matrix interface, r = R.

Loading Step	2	7	15	19	22	31	35
			σ_{rr}				
ELAS65	-3.262	105.5	208.1	206.4	-19.15	-312.1	-91.04
H.R.I	-2.001	107.5	206.5	206.6	-17.95	-318.1	-99.18
H.R.II	-2.810	107.5	207.3	205.2	-20.50	-315.5	-97.80
Eqn. (V-1)	-3.160	105.0	206.6	205.3	-15.56	-309.5	-90.86
			$\sigma_{\phi\phi}$				
ELAS65	5.674	90.88	188.3	191.1	26.82	-285.4	-117.1
H.R.I	3.789	86.41	192.9	196.6	27.36	-291.4	-125.2
H.R.II	5.700	93.50	188.5	190.1	25.70	-287.1	-121.0
Eqn.(V-1)	6.023	90.55	187.2	189.7	29.90	-281.8	-117.6
			σ_{33}				
ELAS65	40.45	136.1	162.0	161.5	0	-265.9	-137.5
H.R.I	40.61	132.5	162.0	161.6	-2.982	-269.9	-145.1
H.R.II	40.60	138.7	160.8	159.3	-2.800	-267.5	-144.1
Eqn. (V-1)	40.58	136.0	160.6	159.8	1.090	-262.8	-136.6

b. At the cylinder surface, r = a.

Loading Step	2	7	15	19	22	31	35
			σ_{rr}				
ELAS65	0	100	200	200	0	-300	-100
H.R.I	0	100	200	200	0	-300	-100
H.R.II	0	100	200	200	0	-300	-100
Eqn.(V-1)	0	100	200	200	0	-300	-100

Table 4-1. Continued

$\sigma_{\phi\phi}$

ELAS65	2.988	95.64	194.0	195.7	18.56	-290.5	-110.0
H.R.I	1.874	92.71	190.5	192.3	16.13	-277.4	- 96.2
H.R.II	2.890	86.40	192.2	195.9	20.10	-281.9	-100.0
Eqn.(V-1)	2.943	95.38	193.7	195.0	14.65	-291.1	-108.6

σ_{33}

ELAS65	41.39	137.9	158.0	158.6	- 1.513	-257.4	-144.4
H.R.I	40.88	135.9	148.7	148.1	-11.73	-247.1	-138.0
H.R.II	41.32	131.6	156.7	158.1	- 1.719	-251.1	-140.1
Eqn.(V-1)	40.58	136.0	160.6	159.8	1.089	-262.8	-136.6

Table 4-2. Microstresses in the matrix of the Be-Aℓ composite cylinder (V_f = 0.5) at selected points of the loading path of Figure 3-6. (Stresses in 10^3 psi).

Loading Step	3	9	19	24	32	38	40
			$\sigma_{rr}(r = R)$				
ELAS65	-85.80	-288.4	-155.0	-74.14	208.0	411.6	-7.18
H.R.II	-85.80	-286.3	-154.5	-74.10	206.5	409.0	-6.15
			$\sigma_{\phi\phi}(r = R)$				
ELAS65	-63.40	-262.9	-178.1	-98.65	181.3	376.5	18.03
H.R.II	-62.80	-261.0	-178.0	-98.70	180.0	373.7	19.61
			$\sigma_{33}(r = R)$				
ELAS65	-39.70	-242.3	-201.2	-120.4	161.9	368.1	39.14
H.R.II	-39.50	-240.0	-200.6	-120.0	160.5	365.0	40.00
			$\sigma_{rr}(r = a)$				
ELAS65	-80	-280	-160	-80	200	400	0
H.R.II	-80	-280	-160	-80	200	400	0
			$\sigma_{\phi\phi}(r = a)$				
ELAS65	-67.30	-267.0	-173.6	-94.40	185.3	379.7	13.10
H.R.II	-67.60	-266.1	-171.4	-92.29	186.3	397.9	12.00
			$\sigma_{33}(r = a)$				
ELAS65	-37.20	-236.4	-205.4	-125.3	155.8	356.2	44.20
H.R.II	-35.39	-235.1	-204.4	-124.6	155.0	354.1	44.39

the larger errors are usually at the low stress magnitudes.

4.5 The Completely Plastic State

When the composite is loaded beyond initial yield surface, or a current loading surface, the plastic zone expands gradually from the fiber matrix interface towards the external surface of the cylinder (cases contrary to this do exist, but will not be considered here). The stress evaluation methods discussed earlier can be used to determine the position of the elasto-plastic boundary at any stage of loading in I_1I_2-plane. In order to illustrate the extent of the plastic zone in the composites, surfaces corresponding to the completely plastic state have been constructed for the case of proportional loading. Both ELAS65 finite element solution, and the approximate stress determination method with the Hardening Rule II have been used in the analysis. The results are shown in conjunction with the initial yield surfaces in Figures 4-1 and 4-2, for the Be-Aℓ (V_f = 0.5) and B-Aℓ (V_f = 0.3) composites, respectively. As one would expect, the plastic zone spreads most rapidly when the loading path is not directed in the hydrostatic stress direction $I_1 = I_2$. The matrix becomes completely plastic immediately after the onset of yielding if the loading path is in the second and fourth quadrants, $I_2/I_1 < 0$, or in a direction adjacent to the stress axes. The results of Figure 4-1 seem to suggest that the

vertex of the complete plasticity surface is obtained on a path which intersects the initial yield surface at a point where $\partial f/\partial I_2 = 0$. However, further confirmation is required regarding this phenomenon.

Note that neither the initial yield surface nor the complete plasticity surface can be regarded as failure surfaces of a composite, since the axisymmetric failure modes are limited by the strength of the fiber. However, the axisymmetric deformation can effect the shear strength of a composite. Further studies are required in this direction.

4.6 Discussion

The plasticity solution developed in this chapter for a composite cylinder is primarily based on two assumptions. First, yielding always starts in the matrix at the fiber-matrix interface and proceeds outwards away from the center of the cylinder, and the second, the deviator stress rotations in the deviatoric stress plane during plastic flow are elastic and given by Equation 3.5 for the interface and similar equations for other points in the matrix with different [A] matrix, the rotational constant $d\mu'$ being same for all the points in the matrix, although it has been determined only with respect to interface, in the hardening rules. The first assumption is fairly accurate one, at least, along radials paths for a stress free composite cylinder. The second assumption leads to the conclusion that the stress increments other

than the elastic deviatoric rotations are purely hydrostatic and uniform in the entire plastic region. The deviatoric rotations were observed to be a consequence of only the constraint of the elastic fiber in the derivation of the Hardening Rule II in Chapter III, the elastic regions in the matrix were implicitly assumed to offer no constraint to cause any deviatoric rotations. Although, no direct verification of these assumptions could be made, a hollow cylinder under internal pressure has been solved making similar assumptions in Appendix VI by using Tresca's yield condition. This problem was originally solved by Hill [41, 45]. It can be seen that the equations for the inplane stresses in both solutions are identical, and the σ_{33} stress is slightly different in the plastic region.

CHAPTER V.
THERMOPLASTIC DEFORMATION AND RESIDUAL MICROSTRESSES IN HEAT-TREATED COMPOSITES

5.1 Introduction

The manufacturing process of fiber-reinforced metal matrix composites often involves heat treatment which provides desirable mechanical properties of the matrix material and of the interfacial bond with the fiber. Similarly, a composite can be exposed to temperature cycles in structural applications. As a result of differential thermal expansion of the constituents, only temperature change leads to the development of microscopic strain and stress fields in the composite. It was found in earlier studies [16, 17], that only moderate temperature changes are needed to cause yielding in most metal matrix composite systems. Accordingly, thermoplastic strains and the attendant residual stresses exist in many composites which have been subjected to large thermal changes.

The residual stresses in superposition with the microstresses caused by external loads, form a part of the total

internal stress field in the composite. Their determination is of interest for two principal reasons. First, the residual microstresses can affect the onset of yielding in the matrix and, therefore, influence the macroscopic mechanical properties of the composite. Second, they can have an affect on the nucleation and growth of imperfections in the composite microstructure both during heat treatment and subsequent loading. Specifically, the presence of residual microstresses in the matrix can significantly reduce the fatigue strength of the composite by promoting fatigue failure of the matrix. Related studies on this problem had been done by Hoffman [52, 53] and Fedon et al. [54], who estimated the residual stress states in copper-tungsten composites due to temperature changes by approximate techniques.

In this chapter a thermo-mechanical analogy will be formulated, which will permit the plasticity theories developed in the earlier chapters, be utilized in the solution of thermoplastic problems. The proposed hardening rules will be extended for cases where the matrix yield stress is a function of temperature.

The theories developed will be used in the prediction of the internal microstresses in fibrous metal matrix composites caused by heat treatment during the fabrication process. The theory will be verified by a comparison of the predicted and the available experimental data.

5.2 The Thermo-Mechanical Analogy

When composites are subjected to the differential volume changes in the constituents, internal residual microstresses are developed. The volume changes may be due to uniform temperature change of the entire composite, and due to the linear dimensional changes occurring during the aging of certain alloys, because of the metallurgical transformations. In this section we will develop a procedure which relates the residual microstresses due to the volume changes, to the microstresses developed in the composite due to axisymmetric composite loading.

Consider a composite the temperature of which has been changed from θ_o to θ. Let $(\Delta L/L)_m$ and $(\Delta L/L)_f$ be the linear dimensional changes due to metallurgical transformations in the matrix and the fiber, respectively. Then the total linear dimensional changes during this time are

$$\xi_f = \alpha_f(\theta - \theta_o) + (\Delta L/L)_f$$

$$\xi_m = \alpha_m(\theta - \theta_o) + (\Delta L/L)_m \qquad (5.1)$$

where ξ_f and ξ_m are total linear dimensional changes, and α_f and α_m are coefficients of the thermal expansion of the fiber and matrix, respectively.

Now consider the composite the constituents of which are subjected to the total linear dimensional changes ξ_f and ξ_m and also a composite stress system $I_1 = I_2 = S$ in the axisymmetric I_1I_2 composite plane. We notice that a microstress response given by

$$\begin{aligned} \{\sigma_{rr}^{\ f} \ \sigma_{\phi\phi}^{\ f} \ \sigma_{33}^{\ f}\} &= S \ \{1 \quad 1 \quad 1\} \\ \{\sigma_{rr}^{\ m} \ \sigma_{\phi\phi}^{\ m} \ \sigma_{33}^{\ m}\} &= S \ \{1 \quad 1 \quad 1\} \end{aligned} \tag{5.2}$$

in the fiber and the matrix, respectively (the shear stresses being zero), form an exact solution of the problem under consideration, if we select S such that there is uniform total microstrain field in the entire composite. That is,

$$\varepsilon_{rr}^{\ f} = \varepsilon_{\phi\phi}^{\ f} = \varepsilon_{33}^{\ f} = \varepsilon_{rr}^{\ m} = \varepsilon_{\phi\phi}^{\ m} = \varepsilon_{33}^{\ m} \tag{5.3}$$

where ε_{ij} are the total strains and the superscripts f and m refers to fiber and matrix respectively.

The total strains in the fiber and matrix due to the linear dimensional changes ξ_f and ξ_m in Equation 5.1, and the microstresses in Equation 5.2 are as follows:

$$\begin{aligned} \varepsilon_{rr}^{\ f} = \varepsilon_{\phi\phi}^{\ f} = \varepsilon_{33}^{\ f} &= \xi_f + \frac{S}{3K_f} \\ \varepsilon_{rr}^{\ m} = \varepsilon_{\phi\phi}^{\ m} = \varepsilon_{33}^{\ m} &= \xi_m + \frac{S}{3K_m} \end{aligned} \tag{5.4}$$

where K_f and K_m are bulk moduli of the fiber and the matrix, respectively.

From Equations 5.3 and 5.4

$$S = 3 \frac{\xi_f - \xi_m}{(1/K_m) - (1/K_f)} \qquad (5.5)$$

Thus, if we subject the composite to the total linear dimensional changes in Equation 5.1 and the composite stresses $I_1 = I_2 = S$, where S is given by Equation 5.5, then we obtain the microstresses and microstrains given by Equation 5.2 and 5.3. We observe that, no yielding occurs in the composite because of the isotropic nature of the microstresses in Equation 5.2. It should be noted that this is an exact solution as we satisfied both the equilibrium and compatibility requirements.

In order to obtain the solution for the microstresses in a composite subjected only to the linear dimensional changes ξ_f and ξ_m in Equation 5.1, we can solve the composite under the action of $I_1 = I_2 = -S$, when S is given by Equation 5.5, by the plasticity theory developed in Chapters III and IV and superimpose the microstresses obtained on the stress field in Equation 5.2. This procedure is illustrated in Figure 5-1. The composite strains can be obtained from the flow rule for the composite stress state $I_1 = I_2 = -S$ and adding them to the uniform strains in Equation 5.4. Care should be taken to add twice the uniform strain in Equation 5.4 to ε_1 the area strain in the transverse plane.

It can be noted that the analogy developed here is similar to that developed in [17] and also to the formulation for residual stresses in Appendix II, except the second part of the solution is elasto-plastic in the present case.

The analogy developed here can be easily incorporated in the numerical integration procedure for the microstresses formulated in Chapter IV.

5.3 Solution Procedures

The results obtained in this chapter are obtained by any one of the two methods. The first is the finite element method [20], which has been realized by means of the ELAS65 computer program for the solution of equilibrium thermoplasticity problems in solids and structures. Two types of models have been used to represent a composite, in conjunction with the finite element method. The first model consists of a composite in which the fibers form hexagonal arrays as shown in Figure 1-1. A representative volume element in Figure 5-2 has been considered in the analysis. The representative volume element is divided into 33 finite elements. Under uniform temperature changes in the composite, the hexagonally symmetric deformation is prescribed by specifying zero normal displacements on faces OB and OC (Figure 5-2), uniform normal displacement over the face BC, and generalized plane strain in the thickness direction. The second model consists of a composite cylinder as shown in Figure 5-3.

The finite element description of this model is identical to that used in the verification of the proposed plasticity theory (See 3.5.1).

The second method, which has been used most extensively in this chapter in the microstress solution developed in Chapter IV, along with the hardening and flow rules developed in Chapter III. In order to account for the variation of matrix yield stress with temperature the hardening rules were to be modified as shown in Appendix VII. The procedure for the application of this method is illustrated in Appendix VIII for a 7075-T6M Aℓ-B composite, the required details being shown in Figure 5.4. The governing equations have been integrated numerically by using a computer program.

Both the finite element method and the method based on the proposed plasticity theory permit to evaluate the local stresses at each point of the composite cylinder, also the composite strains, and the loading surfaces, at each loading step. In addition, the finite element method gives the local displacements and strains also, which are not emphasized in this chapter.

5.4 Verification of Theoretical Predictions

In order to illustrate the accuracy of the method based on the proposed plasticity theory, the problem of determination of the microstresses developed during the heat treatment and the stress-strain curve of a 2024-T6 Aℓ-W composite has been considered. Calculations have been made to simulate the experimental

work by Cheskis and Heckel [46]. These experiments appear to be the sole source of experimental data on in-situ stress distribution in a metal matrix fibrous composite.

The heat treatment process of 2024-T6 Aℓ-W involves [46], quenching from the solutions using temperature of 920 deg. F. to room temperature of 70 deg. F., followed by aging at 365 deg. F., and subsequent cooling to 70 deg. F. The matrix yield stress before and after aging as shown in Figure 5-5 has been estimated on the basis of the data obtained from References [47] and [48]. Note that the matrix yield stress in the as-quenched state (W) is much lower than in the T6 state. During the heat treatment simulation the matrix is considered as elastic-perfectlyplastic. By using the computer-aided numerical integration of the proposed plasticity theory and also the ELAS65 program with both the cylindrical and hexagonal models, the microstresses σ_{rr}, $\sigma_{\phi\phi}$, σ_{33}, and the equivalent stress $\bar{\sigma}$ at each point in the composite are found during the heat treatment process. The elastic-plastic boundary c defined in Figure 5-3 has also been monitored in the former procedure. Figure 5-5 shows the values of the microstresses in the matrix at the fiber-matrix interface, and the position of the elastic-plastic boundary c as a function of temperature. It can be observed that the matrix is completely plastic during most of the quenching period, and only partially plastic during the period of reheating to the aging temperature. In view of the speed of the quenching process, which lasts only for several seconds one can consider the deformation as invicid, and the use of classical plasticity theory as appropriate. Some creep effects could occur

during the aging period which is rather long. However, the matrix yield stress increases very rapidly during the initial interval of the aging period. Therefore, the duration of plastic straining will be short (or even be absent), and the time dependent deformation components can be neglected. Further, the microstresses generated due to the volume changes due to metallurgical transformations of 2024 Aℓ alloy during aging [48] have been found to be insignificant, and so, are not considered in the present case.

Figure 5-6 distribution of the residual stresses at the end of heat treatment as a function of the radius. The invariant quantities, $\bar{\sigma}$ the equivalent stress and the hydrostatic stress component $\sigma_{kk} = \sigma_{rr} + \sigma_{\phi\phi} + \sigma_{33}$ are represented by the dotted lines. The matrix average stresses which are the volumetric averages of the microstresses are also presented on the same figure.

The tensile test of Cheskis and Heckel [46] is now simulated numerically taking into account the residual microstresses obtained during the heat treatment process. In order to account for the strain hardening in 2024-T6 Aℓ, this part of the numerical simulation is obtained by using the ELAS65 program [20]. The stress-strain curves for the tungsten fiber and the aluminum matrix are shown in Figure 5-7. Although the ELAS65 program does not handle problems involving residual stresses it has been modified in the present case to load the composite with residual stresses to 125 ksi in the axial direction and to unload. The composite stress-strain curve, the fiber stress and the matrix

average stress in the axial direction are plotted in Figure 5-8. The experimental values of Cheskis and Heckel are also presented. It is seen that the agreement between the experimental and predicted results is extremely good. In spite of the nonhardening matrix assumption for the results at $\varepsilon_{33} = 0$, the experimental and the predicted values of the average stresses are very close. This provides direct verification of the proposed plasticity theory by the experimental results.

In order to illustrate the motion of the loading surface during a tensile test, the composite is loaded to 100 ksi and unloaded. By using the Hardening Rule II, the center of loading surface is obtained during the entire loading sequence. Figure 5-9 shows the loading surfaces and the motion of their centers.

Figure 5-10 shows the coefficients of thermal expansion of the composite during the heat treatment process predicted by both the finite element method and the Hardening Rule II. The procedure for the determination of the coefficients of thermal expansion in the latter case is outlined in Appendix IX.

5.5 Thermal Stresses in 6061 Aℓ-B Composites

A 6061 Aℓ-B of volume fraction 0.3 has been considered. The variation of the matrix yield stress with temperature before and after aging has been estimated from the data in References [47] and [48]. The following heat treatments of this composite

have been investigated by using the proposed plasticity theory:

(a) Quenching from 862 deg. F. to 70 deg. F., followed by aging at 320 deg. F., and cooling to 70 deg. F. The unit dimensional changes [48] due to the metallurgical transformations during aging are small and are neglected. The matrix stresses at the interface and the positions of the plastic zone are shown in Figure 5-11; the stress distribution at the end of the heat treatment in Figure 5-12. It is seen that relatively large stresses are present, especially at the fiber-matrix interface. Specifically, both the equivalent and hydrostatic stresses have maxima at the interface. The residual stress distribution would seem to favor the initiation and growth of imperfections in the interface region.

(b) Quenching from 862 deg. F. to -320 deg. F., followed by aging and cooling, as in (a). This is T6M temper which was used by Hancock [49] to improve the properties of the fiber-matrix interface bonds. Figures 5-13 and 5-14 show the stress distributions. It is seen that the final stresses are comparable to those obtained in the previous case.

(c) The T6M treatment described in (b), followed by subsequent quenching to -320 deg. F. and reheating to 70 deg. F.

(d) The T6M treatment followed by quenching to -450 deg. F. and reheating to 70 deg. F.

The last two heat treatments have been designed to cause a change in the magnitude and the distribution of the room temperature residual stresses after heat treatment. No metallurgical effects are caused by the cooling cycles. Figure 5-15 shows the

equivalent stress $\bar{\sigma}$, at the interface, and the position of the plastic zone during the thermal load sequence. Figures 5-16 and 5-17 show the final distribution of the residual stresses in the composite. It is observed that considerable redistribution of the residual stresses takes place, especially at the fiber-matrix interface. The average matrix stresses are also reduced. The stress redistribution is obviously very favorable since all stresses in the matrix at the fiber-matrix interface are now compressive, and the magnitude of these compressive stresses increases with the decrease in the cooling temperature. The positions of the plastic zone shown in Figure 5-15 indicate the development of the additional plastic strains in the matrix during the cooling cycles. The final residual stresses at the room temperature are caused by elastic unloading from the low temperature plastic state, and their magnitude is related both to the extent of plastic straining during cooling, and to the extent of the unloading path. These two factors, of course, will be more pronounced when the cooling temperature is lower.

Figure 5-18 shows the loading surfaces of the composite during various stages of the heat treatment. The intercept of the yield surface with the $I_2 = T_{33}$ axis indicates the proportional limit of the composite in tension in the fiber direction. It is observed that the cooling sequences (c) and (d) cause an increase in the proportional limit of the 6061-T6M Aℓ-B composite in tension from approximately 40 ksi to 100 ksi. This figure also illustrates the kinematic motion of the loading surface in the I_1I_2-plane during thermal changes.

5.6 Thermal Stresses in 7075 Aℓ-B Composites

The investigation of thermal stresses in the 7075 Aluminum must include the effect of the dimensional changes due to metallurgical transformations during aging. The dimensional changes have been described in Reference [48], and appear to be rather significant in the 7075 aluminum. This was not the case with 6061 Aluminum considered earlier, where such effects were negligible. Figure 5-19 shows the unit dimensional change $\Delta L/L$, and also the yield stress as a function of aging time at 250 deg. F. The aging time for the 7075 Aℓ-B composites considered here is 25 hours. The matrix yield stress variation before and after aging with respect to temperature has been estimated from the data in References [47] and [48]. The following heat treatment sequences have been investigated using the proposed plasticity theory:

(a) Quenching from 862 deg. F. to 70 deg. F., followed by aging at 250 deg. F. for 25 hours. This corresponds to T6 treatment. The microstresses in the matrix at the fiber-matrix interface during the T6 temper are shown in Figure 5-20. The reheating to aging temperature did not cause any plastic straining but there is a discontinuous change in the microstresses at the aging temperature. This is an effect of the dimensional changes at the aging temperature, and is more clearly visible in Figure 5-21, where the matrix and fiber microstresses are given for both the actual dimensional change, and for a zero dimensional change.

(b) Quenching from 862 deg. F. to -320 deg. F. and aging and cooling as in (a). This corresponds to the T6M temper. This case has been selected as an illustrative example in Appendix VIII. The microstresses in the matrix at the fiber-matrix interface during the T6M treatment, are shown in Figure 5-22. Here, there exists plastic straining during the period of reheating to the aging temperature. Figure 5-23 shows the stresses in the composite at the end of T6M temper. It is seen that the T6M temper produces considerably smaller microstresses than the T6 temper, and the distribution is entirely different. These effects are attributed to the plastic deformation sequence in the matrix during the heat treatment.

The loading surfaces of the 7075 Aℓ-B composite at various stages of the heat treatment are shown in Figure 5-24. The T6M treatment gives a somewhat higher proportional limit than T6 treatment in simple tension.

It has been observed that the cooling of 7075-T6M Aℓ-B to -320 deg. F. or -450 deg. F., did not affect the microstresses as in the case of 6061-T6M Aℓ-B. This can be easily observed from Figure 5-22, where the equivalent stress $\bar{\sigma}$ does not attain the magnitude of the yield stresses during cooling after aging. The same is true for T6 temper (See Figure 5-20). Therefore, it does not appear that a change in the microstress in the two 7075 Aℓ-B composites can be achieved by a heat treatment that would not affect the metallurgical characteristics. Nor does it seem that such treatment is necessary, since both the microstresses, and the proportional limit of the 7075-T6M Aℓ-B composite are quite favorable.

5.7 Thermal Expansion Coefficients for B-Aℓ Composites

Since the composite laminae experiences plastic straining during the heat treatment, the thermal expansion coefficients vary between the elastic and plastic states. These effects should be considered in problems involving heat treatment of composite laminates and other structures. The thermal expansion coefficients of B-Aℓ composites have to be determined by the proposed plasticity theory, the procedure being outlined in Appendix IX.

Figure 5-25 shows the variation of the thermal expansion coefficient for 6061 Aℓ-B composites during the T6 and T6M tempers. The coefficient of thermal expansion in the fiber direction, α_{ca}, is about equal to that of the fiber, α_f, when the matrix is fully plastic and increases in the elastic case. Similarly, the coefficient of thermal expansion in the transverse direction, α_{ct}, is nearly equal to that of the matrix, α_m, for a completely plastic matrix, and decreases in elastic case.

Figure 5-26 shows similar results for the 7075 Aℓ-B composites.

5.8 The Effect of Residual Microstresses on the Fatigue Limits of the B-Aℓ Composites*

The microstresses which were found for the B-Aℓ composites in Figures 5-12, 5-14, 5-16, 5-17, 5-21, and 5-23 can be used to evaluate, at least tentatively, the fatigue limits (at 10^6 cycles) of the composites for loading in the fiber direction, and the effect of the various heat treatments on these limits. The evaluation procedure is described by Dvorak et al. [50]. In principle, the fatigue limit of the composite can be derived from that which has been experimentally established for the matrix material, on the premise that the matrix or fiber stresses during the cyclic loading do not exceed the fatigue limits of the respective materials. This assumption was successfully tested on a number of as-fabricated 6061 Aℓ-B composites, and other composites by Dvorak et al. [50]. Also, available data from tests on heat treated composites were examined by the same authors and showed a good agreement. However, the number of test results available were too small to establish a definite relationship for the latter group. Therefore, the following results should be regarded as a very tentative basis of a possible working hypothesis, but at least reflect the relative effect of the internal microstresses

---

*The author wishes to thank Dr. G. J. Dvorak for the results of this section.

on fatigue strength of heat-treated composites.

Figure 5-27 shows the Goodman diagram for the 6061-T6 aluminum alloy, which was derived experimentally in Reference [51]. These stress magnitudes were considered admissible for the σ_{33} stresses in the matrix if the fatigue failure of the matrix was to be avoided. Then, the average matrix stress σ_{33} was calculated by superposition of the average residual stresses in the matrix which were evaluated in this work, and of the matrix stresses caused by the composite load applied in the fiber direction. The latter stresses were derived from the rule of mixture equation. The resulting curves for the 6061-T6M Aℓ-B, with and without subsequent cooling to -450 deg. F., are shown in Figure 5-27. The dashed line refers to the as-fabricated 6061-0 Aℓ-B composite, assuming that both the fatigue and yield strength of the matrix are equal to 12 ksi. The horizontal portion of this line was verified experimentally for several 6061 Aℓ-B composites in Reference [51]. The sloping part of the dashed line indicates a limitation caused by the boron fiber fatigue limit which was selected as 300 ksi. Such limitation does not affect the tempered composites, matrix fatigue failure always precedes that of the fibers.

Figure 5-28 shows similar results for the 7075 Aℓ-B composites.

It is observed that the reduction of the residual stresses in the matrix by heat treatment does indeed hold a promise for improvement of the composite fatigue limits. However, more experimental work is needed to verify the calculated curves of Figures 5-27 and 5-28.

5.9 Conclusions

1. The plasticity theory proposed in Chapters III and IV, coupled with the thermomechanical analogy developed in this chapter, makes it possible to evaluate the residual microstresses in metal matrix fibrous composites during heat treatment. The comparison with the available in-situ experimental measurements of these microstresses indicates that the theoretical predictions are very accurate.

2. The microstresses in 6061 Aℓ-B composites evaluated for T6 and T6M temper were found to be very high, and unfavorably distributed in the matrix. Also, the proportional limit for loading in the fiber direction was found to be rather low. The new heat treatment consisting of cooling the tempered composites to -320 or -450 deg. F., changes the residual stresses in the composite without changing the metallurgical characteristics of the matrix. The thermal loads imposed by these cooling cycles cause plastic flow in the matrix. Elastic unloading follows during reheating to the room temperature. As a result of these treatments, the microstress distribution in the matrix improved drastically, and the proportional limit of the composite increased by a factor of 2.5.

3. The microstresses obtained for the 7075-Aℓ-B composites for T6 and T6M tempers were more favorable than those obtained in case of 6061 Aℓ-B composites. It was found that the stress distribution in the T6M case are most favorable, and the proportional limits were high for both tempers. No improvements of the microstress distributions, or of proportional limits could be achieved by the new heat treatment as in the case of the 6061 Aℓ-B composites.

4. The thermal expansion coefficients of the 6061-T6 Aℓ-B, 6061-T6M Aℓ-B, 7075-T6 Aℓ-B, and 7075-T6M Aℓ-B were evaluated as functions of temperatures during heat treatment. It was found that significant changes of both axial and transverse thermal expansion coefficients are caused by plastic straining of the matrix during the heat treatment.

5. Tentative calculations were made of the expected fatigue limits of the heat treated composites. It was found that the process designed to reduce the residual stresses in the matrix may also significantly improve the fatigue strengths of the composites.

CHAPTER VI.

SUMMARY, GENERAL DISCUSSION, AND RECOMMENDED RESEARCH

The plasticity theory for fiber-reinforced metal matrix composites formulated here is based on micromechanical considerations. The microplastic flow caused in the axisymmetric deformation mode is related to the macroscopic behavior of the composite through the hardening and flow rules. The salient features of the formulation of the plasticity theory will now be summarized.

6.1 Summary

The plastic deformation of a fiber reinforced composite can be represented by a set of five invariants which are functions of the applied composite stresses. The first two invariants I_1 and I_2 are responsible for the axisymmetric deformation in the composite. The axisymmetric deformation mode is characterized by uniform normal composite stresses on planes parallel to the fiber,

and an axial composite stress on a plane perpendicular to the fiber. When the composite is loaded into plastic range in the axisymmetric deformation mode, the resulting microplastic flow produces nonrecoverable strains and residual stresses in the composite. Under the assumption that yielding always starts in the matrix at the fiber-matrix interface, it has been established that the subsequent yield surface is identical to the initial yield surface translated to a new position in the I_1I_2-plane, and thus establishing the kinematic hardening in this plane.

During microplastic flow, for loading in the axisymmetric mode, it has been found that three types of microstress increments take place due to a composite stress increment in the matrix at the fiber-matrix interface. These three microstress increments correspond in turn to two components of the applied stress increment. The first of the two components of the composite stress increments corresponds to an isotropic microstress increment, and the second to a neutral elastic microstress increment. It has been established that the former type of the composite stress increment is responsible to the translation of the loading surface in the I_1I_2-plane. On the assumption that the first component of the composite stress increment is always in the radial direction, the Hardening Rule I has been formulated. Later it has been found that there exists a special direction in the I_1I_2-plane for each loading point, such that, if loading takes place along this direction only isotropic microstress change results during plastic flow. This finding resulted in the formulation of a more accurate Hardening Rule II. The plastic components of the

composite stress increments have been determined by using the flow rule based on normality. The proportionality constant in the normality condition has been determined by an estimate of the total strain in the fiber direction. The proposed hardening and flow rules have been verified by using the finite element method. The agreement between the results predicted by the proposed theory and the finite element method has been very satisfactory.

In order to determine the microstresses in the entire composite under axisymmetric deformation, an approximate solution has been developed. The solution has been based on composite cylinder idealization of the composite. Again, comparisons between the results obtained from the approximate microstress solution and the finite element method, showed a very satisfactory agreement.

Finally, to determine the responses of composites under thermal loading, a thermomechanical analogy has been developed, such that the microstresses and composite strains during thermal loading can be evaluated by solving an associated problem of loading in the axisymmetric mode. The thermomechanical analogy is equally valid for determining the effects of volume changes in the constituent phases of a composite due to metallurgical transformations during heat treatment. By modifying the proposed plasticity theory to account for the change in matrix yield stress due to temperature changes, serval heat treatment problems have been solved. The results obtained agree with the existing experimental results. On the basis of the proposed plasticity theory, new heat treatment sequences that may improve the initial yielding, fatigue

and fracture behavior of boron-aluminum composites have been proposed.

6.2 General Discussion

Effects of microplastic flows occurring during plastic deformation are related to the macroplastic deformation of the composite in the axisymmetric deformation mode. The constraint offered by the elastic fibers is essentially reflected as the kinematic motion of the loading surface during plastic deformation. The hardening rules predicting the motion of the loading surfaces are based on the study of the microstresses in the matrix at the fiber-matrix interfaces. The Hardening Rule I is a simple one, and could be easily incorporated in a general plasticity theory. The Hardening Rule II which offers more accurate prediction of the composite behavior is not as simple, but nevertheless could be incorporated in a general plasticity theory, if more accuracy is required. Either hardening rule gives sufficiently accurate prediction of the kinematic hardening behavior in the axisymmetric deformation mode, both under mechanical as well as thermal loads. The flow rule proposed is closely related to the hardening rules in its formulation, and gives accurate prediction of the composite plastic strains.

The microstress solution formulated for a composite cylinder under plastic flow is an approximate one, the approximation introduced being that, the regions remote from the fiber-matrix interfaces are controlled mainly by the interface response.

This is due to the coupling of the hardening rules which essentially monitor the interface responses, and the microstress solution for radial loading of a stress free composite cylinder. A consequence of the above is that, the solution procedure and the associated assumptions may break down under severe reversed plastic flow in the matrix, in which instance, the plastic flow may no longer start at the interface but in a region remote from the interface. However, it should be noted that the kinematic motion of the loading surface is still expected because of the assurance of the existence of a residual stress field that could translate the loading surfaces, the contained nature of the microplastic flow, and the well known shake down theorems [55]. Under moderate plastic flow the procedure of determination of the microstresses is expected to give reasonably accurate results on the assumption that, even if the yielding were to start in a region remote from the interface, it would spread rapidly towards the interface within a short segment of a loading path.

The above suggests that a multipoint input into the hardening rules instead of the single interface point may be required under severe reversed plastic flow. The loading surface in that situation would be the interior envelope of all the yield surfaces corresponding to the different points selected. The residual stresses which are responsible for the translation of the yield surfaces, being different at different points selected move the respective subsequent yield surfaces to different positions. Thus, the centers of the subsequent yield surfaces would move according to different rules depending upon the nature of

the residual stresses generated at the selected points. The new loading surface would then be given by an interior envelope of all the subsequent yield surfaces. However, it should be noted that the loading surface obtained by the interface controlled hardening rule of the present work is an upper bound of the true loading surface, or any multipoint controlled loading surface suggested (See Reference [56] for proof).

The plasticity theory developed is useful for the axi-symmetric part of the overall deformation, and gives the effect of the invariants I_1 and I_2. The influence of the invariants I_3, I_4, and I_5 on the plastic deformation is yet to be studied. However, it is the opinion of this investigator, that, because of the relative closeness of the initial yield and limit loads for composite stress systems corresponding to these invariants, no significant residual stresses could be stored in a composite made of a non-hardening matrix. In such cases it would seem that an elastic-perfectly plastic idealization of the deformation behavior is appropriate for stress systems corresponding to these invariants. The hardening in I_1I_2-plane would however influence the yielding in these stress systems. Further investigations on these aspects is suggested.

The thermomechanical analogy formulated is an effective tool in the determination of the residual stresses and the mechanical behavior of heat-treated composites. The major obstruction in the way however is the lack of experimental data on the behaviour of the matrixalloys of the metal matrix composites during heat treatment. The variation of the yield stress during the heat treatment and the volume changes due to metallurgical

transformations during aging for the aluminum alloys used in the present work have been estimated from the available experimental data. As evident from the results obtained for the two boron-aluminum composites made of 6061 and 7075 aluminum alloys, the variation of the yield stress plays a very important role and affects both the magnitude and distribution of the residual microstresses in the heat-treated composites.

6.3 Recommended Research

Based on the earlier discussion, as well as the ideas that crossed the mind of the author during the course of the present work, the following areas of research seem to be of interest in the extension, refinement, and application of the present work.

1. Multipoint controlled hardening and flow rules.
2. Interaction between axisymmetric and shear deformation modes.
3. Effects of cyclic loads where there is reversed plastic flow.
4. Effect of strain hardening of the matrix material on the hardening and flow rules of the composite.
5. Experimental verification of the hardening and flow rules, and also the residual stresses in heat-treated composites.
6. Experiments for the determination of the variation of yield stress during heat treatment and the volume changes during aging of the matrix materials.

7. Investigation of new heat-treatment sequences that may improve the initial yield, fatigue and fracture behavior of heat-treated composites.

8. Kinematic hardening in multilayered composites where each layer is made of a uniaxial fibrous composite. In these materials kinematic hardening is expected in the entire normal stress space as well as for the transverse shear stress.

PART II

PLASTICITY THEORY OF MULTILAYERED COMPOSITES - INITIAL YIELDING

CHAPTER VII.

INTRODUCTION

The initial yielding in composites under externally applied composite fractions, is primarily governed by the micromechanical interaction between the constituents. In a unidirectional fiber-reinforced composite, one should consider the interaction between the parallel fibers and the matrix. On the other hand, in a multi-layered composite made of a series of unidirectional fiber-reinforced composite layers, one should consider in addition, the interaction between the non-parallel fibers in two successive layers.

The initial yielding of unidirectional fiber-reinforced composites has been studied earlier by Lin et al. [15] and Dvorak et al. [16]. The interaction between the parallel fibers and the matrix has been successfully included in the analysis by the analysis of representative volume element of the composite idealizations with appropriate boundary conditions. However, to the author's knowledge no such solutions are available for the multilayered composites.

The purpose of the Part II is to evaluate the microstresses and construct the initial yield surfaces for multilayered composites under external composite tractions. The multilayered composites considered are made of unidirectional hexagonal composite layers, and the fibers in two successive layers are perpendicular to each other (0-90 composite).

The analysis consists of two parts, namely: the "Regular Solution" which neglects the interaction between the fibers in two successive layers (cross-over effects); and the "cross-over solution" which includes the cross-over effects.

On the assumption, that the Saint-Venants principle [57] is applicable for the cross-over effects, the microstresses farther away from the interface of two successive layers (layer-layer interface) may be evaluated by the regular solution. In the vicinity of the layer-layer interface the microstresses are given by the cross-over solution. One could consider the two solutions separately, and construct the initial yield surfaces corresponding to the microstresses obtained from the two solutions. The initial yield surface for the multilayered composite is then given by the interior envelope of the yield surfaces obtained by the two solutions.

CHAPTER VIII.

REGULAR SOLUTION

In order to construct the regular solution, the multilayered composite is considered as a material consisting of a series of "balanced" anisotropic layers with different elastic moduli. A balanced multilayered composite is defined as a composite which when acted upon by uniform composite strains on the principal planes of the composite do not produce any bending effects. This assumption implicitly uncouples the composite normal and shear stresses. An example of a balanced multilayered composite is, a three-layer composite; the top and bottom layers of equal thickness made of one anisotropic material, and the middle layer of twice the thickness of the other two made of another anisotropic material; the principal planes of anisotropy of the two materials being parallel.

In the present chapter one half of the three-layered composite discussed above is considered (Figure 8-1). The total thickness of the model is 2 t. The x and y axes lie in plane parallel to the interface of the two layers, and the z axis in a direction perpendicular to the interface. The principal axes of anisotropy are assumed to be coincident with the xyz-directions.

The model is subjected to composite normal stresses, S_{11}, S_{22}, and S_{33} in the directions x, y, and z, respectively; and composite shears S_{12}, S_{13}, and S_{23} in the planes xy, xz, and yz, respectively. Now the problem is to find the individual components of the applied composite stresses, acting on the two individual layers. The microstresses in the individual layers could then be determined by considering the nonhomogeneities in the layers.

8.1 Solution for Normal Stresses

Let $\{E_{11}\ E_{22}\ E_{33}\}$ be the normal composite strains produced under the action of the normal composite stresses $\{S_{11}\ S_{22}\ S_{33}\}$ in x, y, and z directions, respectively. (The braces { } always represent a column matrix; the elements may be listed horizontally or vertically). The strains produced in the individual layers (Figure 2-1) may then be written as

$$\{E_{xx}^{L}\ E_{yy}^{L}\ E_{zz}^{L}\} = \{E_{11}\ E_{22}\ (E_{33} + d_{33})\} \qquad (8.1)$$

$$\{E_{xx}^{U}\ E_{yy}^{U}\ E_{zz}^{U}\} = \{E_{11}\ E_{22}\ (E_{33} - d_{33})\} \qquad (8.2)$$

$\{E_{xx}^{L}\ E_{yy}^{L}\ E_{zz}^{L}\}$ are strain in the lower layer (Figure 8-1), $\{E_{xx}^{U}\ E_{yy}^{U}\ E_{zz}^{U}\}$ are strains in the upper layer, and d_{33} is the antisymmetric component of the z-strain in the two layers.

Let $[C^L]$ and $[C^U]$ be the elastic moduli of the lower and upper layers, respectively, when considered independently for normal strains, and $\left\{S_{xx}^{\ L}\ S_{yy}^{\ L}\ S_{zz}^{\ L}\right\}$ and $\left\{S_{xx}^{\ U}\ S_{yy}^{\ U}\ S_{zz}^{\ U}\right\}$ be the stresses in the two layers due to $\left\{S_{11}\ S_{22}\ S_{33}\right\}$. The stress-strain relations for the individual layers are as follows:

Lower layer

$$[C^L]\left\{E_{xx}^{\ L}\ E_{yy}^{\ L}\ E_{zz}^{\ L}\right\} = \left\{S_{xx}^{\ L}\ S_{yy}^{\ L}\ S_{zz}^{\ L}\right\} \qquad (8.3)$$

Upper layer

$$[C^U]\left\{E_{xx}^{\ U}\ E_{yy}^{\ U}\ E_{zz}^{\ U}\right\} = \left\{S_{xx}^{\ U}\ S_{yy}^{\ U}\ S_{zz}^{\ U}\right\} \qquad (8.4)$$

From Equations 8.1 to 8.4

$$[C^L]\left\{E_{11}\ E_{22}\ E_{33}\right\} + [C^L]\left\{0\quad 0\quad d_{33}\right\} = \left\{S_{xx}^{\ L}\ S_{yy}^{\ L}\ S_{zz}^{\ L}\right\} \qquad (8.5)$$

$$[C^U]\left\{E_{11}\ E_{22}\ E_{33}\right\} - [C^U]\left\{0\quad 0\quad d_{33}\right\} = \left\{S_{xx}^{\ U}\ S_{yy}^{\ U}\ S_{zz}^{\ U}\right\} \qquad (8.6)$$

For the overall equilibrium of the model (Figure 8-1), we require

$$S_{xx}^{L} + S_{yy}^{U} = 2\,S_{11}$$

$$S_{yy}^{L} + S_{yy}^{U} = 2\,S_{22} \qquad (8.7)$$

$$S_{zz}^{L} = S_{33}$$

$$S_{zz}^{U} = S_{33}$$

Equations 8.5 to 8.7 constitute 10 equations for the 10 unknown d_{33}, E_{11}, E_{22}, E_{33}, S_{xx}^{L}, S_{yy}^{L}, S_{zz}^{L}, S_{xx}^{U}, S_{yy}^{U}, and S_{zz}^{U} in terms of the applied composite stresses S_{11}, S_{22}, and S_{33}. Solution of these equations yields the following relations for unknown.

$$d_{33} = \frac{1}{(C_{33}^{L} + C_{33}^{U})} \left\{ (C_{31}^{U} - C_{31}^{L})\ (C_{32}^{U} - C_{32}^{L})\ (C_{33}^{U} - C_{33}^{L}) \right\}^{T} [C]^{-1} \begin{Bmatrix} S_{11} \\ S_{22} \\ S_{33} \end{Bmatrix} \qquad (8.8)$$

$$\left\{ E_{11}\ E_{22}\ E_{33} \right\} = [C]^{-1} \left\{ S_{11}\ S_{22}\ S_{33} \right\} \qquad (8.9)$$

$$\left\{ S_{xx}^{L}\ S_{yy}^{L}\ S_{zz}^{L} \right\} = [H^{L}] \left\{ S_{11}\ S_{22}\ S_{33} \right\} \qquad (8.10)$$

$$\left\{ S_{xx}^{U}\ S_{yy}^{U}\ S_{zz}^{U} \right\} = [H^{U}] \left\{ S_{11}\ S_{22}\ S_{33} \right\} \qquad (8.11)$$

where

$$[C] = \frac{1}{2}\,[[C^L] + [C^U]] + \frac{1}{2(C_{33}^{\,L} + C_{33}^{\,U})} \cdot \begin{Bmatrix} C_{13}^L - C_{13}^U \\ C_{23}^L - C_{23}^U \\ C_{33}^L - C_{33}^U \end{Bmatrix} \begin{Bmatrix} C_{31}^U - C_{31}^L \\ C_{32}^U - C_{32}^L \\ C_{33}^U - C_{33}^L \end{Bmatrix}^T \tag{8.12}$$

$$[H^L] = [C^L][C]^{-1} + \frac{1}{(C_{33}^{\,L} + C_{33}^{\,U})} \begin{Bmatrix} C_{13}^L \\ C_{23}^L \\ C_{33}^L \end{Bmatrix} \cdot \begin{Bmatrix} C_{31}^U - C_{31}^L \\ C_{32}^U - C_{32}^L \\ C_{33}^U - C_{33}^L \end{Bmatrix}^T [C]^{-1} \tag{8.13}$$

$$[H^U] = [C^U][C]^{-1} - \frac{1}{(C_{33}^{\,L} + C_{33}^{\,U})} \begin{Bmatrix} C_{13}^U \\ C_{13}^U \\ C_{33}^U \end{Bmatrix} \cdot \begin{Bmatrix} C_{31}^U - C_{31}^L \\ C_{32}^U - C_{32}^L \\ C_{33}^U - C_{33}^L \end{Bmatrix} [C]^{-1} \tag{8.14}$$

In the above equations the matrix [C] represents the elastic moduli of the multilayered composite. The superscript T over matrices indicates the transpose.

8.2 Solution for Shear Stresses

Let S_{12}, S_{13}, and S_{23} be the composite shear stresses acting on the planes xy, xz, and yz, respectively. We assume that each shear stress is uncoupled with the other stresses. That is, application of a composite shear strain produces only the corresponding shear stress and none other. Thus, the stress-strain relations in the shear for the two individual layers in Figure 8-1 are

$$\begin{aligned} C_{44}^{L} E_{xy}^{L} &= S_{xy}^{L} \\ C_{55}^{L} E_{xz}^{L} &= S_{xz}^{L} \\ C_{66} E_{yz}^{L} &= S_{yz}^{L} \end{aligned} \tag{8.15}$$

$$\begin{aligned} C_{44}^{U} E_{xy}^{U} &= S_{xy}^{U} \\ C_{55}^{U} E_{xz}^{U} &= S_{xz}^{U} \\ C_{66}^{U} E_{yz}^{U} &= S_{yz}^{U} \end{aligned} \tag{8.16}$$

where C_{44}^{L}, C_{55}^{L}, C_{66}^{L}, and C_{44}^{U}, C_{55}^{U}, C_{66}^{U} are the elastic moduli; S_{xy}^{L}, S_{xz}^{L}, S_{yz}^{L}, and S_{xy}^{U}, S_{xz}^{U}, S_{yz}^{U} are the shear stresses; E_{xy}^{L}, E_{xz}^{L}, E_{yz}^{L}, and E_{xy}^{U}, E_{xz}^{U}, E_{yz}^{U} are the shear strains; subscript L being lower domain, and U being the upper domain (Figure 8-1).

Under the action of shear stresses S_{13} and S_{23}, the two layers of the model (Figure 8-1) respond in "series". One has to satisfy the equilibrium on the interface between the two layers. This would require that, the shear stresses in the two individual layers be equal. Thus,

$$S_{xz}^{L} = S_{xz}^{U} = S_{13}$$
$$S_{yz}^{L} = S_{yz}^{U} = S_{23} \qquad (8.17)$$

The total strains are given by

$$E_{13} = E_{xz}^{L} + E_{xz}^{U}$$
$$E_{23} = E_{yz}^{L} + E_{yz}^{U} \qquad (8.18)$$

From Equations 8.15 to 8.18, we can obtain the overall stress strain relations as

$$S_{13} = C_{55} E_{13}$$
$$S_{23} = C_{66} E_{23} \qquad (8.19)$$

where

$$C_{55} = C_{55}^{L} C_{55}^{U}/(C_{55}^{L} + C_{55}^{U})$$

$$C_{66} = C_{66}^{L} C_{66}^{U}/(C_{66}^{L} + C_{66}^{U}) \qquad (8.20)$$

The constants C_{55} and C_{66} represent the overall shear moduli.

Under the action of shear stress S_{12}, the two layers of the model respond in "parallel".In this case, one has to satisfy the compatibility on the interface. This would require that the shear strains in the two layers be equal. Thus the governing equations are as follows:

$$E_{xy}^{L} = E_{xy}^{U} = E_{12} \qquad (8.21)$$

$$S_{xy}^{L} = C_{44}^{L} E_{xy}^{L}$$

$$S_{xy}^{U} = C_{44}^{U} E_{xy}^{U} \qquad (8.22)$$

$$S_{12} = C_{44} E_{12} \qquad (8.23)$$

Solution of Equation 8.21 to 8.23 leads to,

$$S_{xy}^{L} = \frac{C_{44}^{L}}{C_{44}} S_{12}$$

$$S_{xy}^{U} = \frac{C_{44}^{U}}{C_{44}} S_{12} \qquad (8.24)$$

$$C_{44} = \frac{1}{2} \left(C_{44}^{L} + C_{44}^{U}\right) \tag{8.25}$$

Now, the stresses in the individual layers corresponding to applied composite stresses can be determined from Equations 8.10, 8.11, 8.17, and 8.24. In analogy with the normal stresses (Equations 8.10 and 8.11) the shear stresses in the individual layers can be written as

$$\left\{S_{12}^{L} \; S_{13}^{L} \; S_{23}^{L}\right\} = [G^{L}] \left\{S_{12} \; S_{13} \; S_{23}\right\} \tag{8.26}$$

$$\left\{S_{12}^{U} \; S_{13}^{U} \; S_{23}^{U}\right\} = [G^{U}] \left\{S_{12} \; S_{13} \; S_{23}\right\} \tag{8.27}$$

where

$$G_{11}^{L} = C_{44}^{L}/C_{44}; \; G_{11}^{U} = C_{44}^{U}/C_{44};$$

$$G_{22}^{L} = G_{22}^{U} = G_{33}^{L} = G_{33}^{U} = 1;$$

$$G_{ij}^{k} = 0 \quad \text{for} \quad i \neq j \,, \; k = L \text{ and } U.$$

8.3 Microstresses for Regular Solution

Having determined the stresses in the individual layers corresponding to an applied combination of the composite stresses, we can determine the microstresses in the individual layers by considering the nonhomogeneities. We shall assume that each individual layer is made of a unidirectional composites with fibers forming hexagonal arrays. The fibers in two successive layers are considered to be perpendicular to each other. Figure 8-2 shows an isometric projection of the composite under consideration. The unidirectional composites with hexagonal arrays of fibers have been solved in earlier studies [16, 17] for the microstresses. These results will now be utilized in the formulation of the regular solution for microstresses in a multilayered composite.

Figure 8-2 shows the "local coordinate system" for the representative volume elements, which are in correspondence with the coordinate system of unidirectional composites considered in earlier studies [16, 17]. The transformation equations for the stresses in the local and overall coordinate systems are as follows:

$$\{\sigma^{L,\ell}\} = [T^L]\ \{\sigma^{L,0}\}$$

$$\{\sigma^{U,\ell}\} = [T^U]\ \{\sigma^{U,0}\} \qquad (8.28)$$

$$\{S^{L,\ell}\} = [T^L]\ \{S^{L,0}\}$$

$$\{S^{U,\ell}\} = [T^U]\ \{S^{U,0}\} \qquad (8.29)$$

In these equations $\{\sigma\} = \{\sigma_{xx}\ \sigma_{yy}\ \sigma_{zz}\ \sigma_{xy}\ \sigma_{xz}\ \sigma_{yz}\}$ are the microstresses; $\{S\} = \{S_{xx}\ S_{yy}\ S_{zz}\ S_{xy}\ S_{xz}\ S_{yz}\}$ are the composite stresses; the first superscript represent the domain identification, L for lower, and U for upper domain; the second superscript for the coordinate identification, ℓ for local coordinates, and 0 for overall coordinates. Note that $\{S^{L,0}\}$ and $\{S^{U,0}\}$ are identical to $\{S^L\}$ and $\{S^U\}$ determined in earlier sections. The transformation matrices $[T^L]$ and $[T^U]$ are given by

$$[T^L] = \begin{bmatrix} 0 & 0 & 1 & 0 & 0 & 0 \\ 1 & 0 & 0 & 0 & 0 & 0 \\ 0 & 1 & 0 & 0 & 0 & 0 \\ 0 & 0 & 0 & 0 & 1 & 0 \\ 0 & 0 & 0 & 0 & 0 & 1 \\ 0 & 0 & 0 & 1 & 0 & 0 \end{bmatrix} \qquad (8.30)$$

$$[T^U] = \begin{bmatrix} 0 & 0 & 1 & 0 & 0 & 0 \\ 0 & 1 & 0 & 0 & 0 & 0 \\ 1 & 0 & 0 & 0 & 0 & 0 \\ 0 & 0 & 0 & 0 & 0 & -1 \\ 0 & 0 & 0 & 0 & -1 & 0 \\ 0 & 0 & 0 & 1 & 0 & 0 \end{bmatrix} \tag{8.31}$$

In analogy with the microstress determination in unidirectional composites [16, 17] we can write the microstresses in the form

$$\begin{aligned} \{\sigma^{L,\ell}\} &= [A]\{S^{L,\ell}\} \\ \{\sigma^{U,\ell}\} &= [A]\{S^{U,\ell}\} \end{aligned} \tag{8.32}$$

where [A] is a 6 x 6 matrix which was referred to as [Σ] in Reference [17].

The stresses $\{S^{L,0}\}$ and $\{S^{U,0}\}$ can be obtained in terms of the applied composite stresses $\{S\} = \{S_{11}\ S_{22}\ S_{12}\ S_{13}\ S_{23}\}$ by combining Equation 8.10 with 8.26, and Equation 8.11 with 8.27, as

$$\begin{aligned} \{S^{L,0}\} &= [J^L]\{S\} \\ \{S^{U,0}\} &= [J^U]\{S\} \end{aligned} \tag{8.33}$$

where $[J^L]$ is obtained by appropriate combination of $[H^L]$ and $[G^L]$ in Equations 8.10 and 8.26, and $[J^U]$ by combination of $[H^U]$ and $[G^U]$ in Equations 8.11 and 8.27.

Noting that the inverses of $[T^L]$ and $[T^U]$ are their transposes, and solving Equations 8.28, 8.29, 8.32, and 8.33 we obtain

$$\{\sigma^{L,0}\} = [A^L]\{S\}$$
$$\{\sigma^{U,0}\} = [A^U]\{S\} \qquad (8.34)$$

where

$$[A^L] = [T^L]^T [A] [T^L] [J^L], \text{ and}$$

$$[A^U] = [T^U]^T [A] [T^U] [J^U]$$

Equation 8.34 represents the regular microstress solution for a multilayered composite. The matrices $[A^L]$ and $[A^U]$ are derived essentially, from the analysis of unidirectional fibrous composite for different points in the composite domain.

8.4 Construction of Initial Yield Surfaces

We can now determine the initial yield surfaces based on the regular solution (Equation 8.34). The procedure is identical to that used for the unidirectional composites [16, 17], except the matrices $[A^L]$ and $[A^U]$ are used for the determination of the microstresses. The procedure for the determination of initial yield surfaces in briefly outlined below:

1. Select a path defined by

$$\left\{ S \right\} = p \left\{ t_{11} \; t_{22} \; t_{33} \; t_{12} \; t_{13} \; t_{23} \right\}, \tag{8.35}$$

in the {S} space, when t_{ij} are known constants and p in an unknown defining the magnitude of the loading along the path.

2. Form the Mises' yield condition for the microstresses developed at a point due to composite stresses in Equation 8.35. This is given by

$$p^2 \{t\}^T [A^i]^T [c] [A^i] \{t\} = Y^2 \tag{8.36}$$

where $[A^i]$ is the matrix defining the microstresses at the point which is equal to $[A^L]$ or $[A^U]$ in Equation 8.34, Y is the yield stress, and

$$[c] = \frac{1}{2}\begin{bmatrix} 2 & -1 & -1 & 0 & 0 & 0 \\ & 2 & -1 & 0 & 0 & 0 \\ & & 2 & 0 & 0 & 0 \\ & & & 6 & 0 & 0 \\ & \text{SYM.} & & & 6 & 0 \\ & & & & & 6 \end{bmatrix}$$

Note that the left hand side of Equation 8.35 represents the square of the equivalent stress.

3. Equation 8.36 yields two equal and opposite roots for p. Step 2 is repeated for all the matrix points. The minimum value of the positive roots and the maximum value of the negative roots for p, when substituted into Equation 8.35 give two points on the yield surface along the path defined.

4. Steps 1 to 3 are repeated along several paths until enough number of points are obtained on the required yield surface.

CHAPTER IX.

CROSS-OVER SOLUTION

In Chapter VIII we considered the regular solution of a multilayered composite assuming that, there is no interaction between the fibers in two successive layers. Such a solution gives sufficiently accurate representation of the microstresses for points farther away from the layer-layer interfaces. But in the vicinity of the layer-layer interfaces the microstresses are bound to be affected by the presence of the discontinuity in the material description. In 0-90 multilayered composites, the fibers being aligned in perpendicular directions in two successive layers, the discontinuity in the material description is caused by an abrupt change in the alignment of the fibers across the layer-layer interface. In order to determine the microstresses in a cross-over problem, one should include the layer-layer interface in any representative model describing the composite. In this chapter, two methods are discussed to include the effects of layer-layer interface in the analysis. The first method is the two layer method which involves selecting a representative domain near the layer-layer interface consisting of a part of each layer, adjoining the interface of a multilayer composite in Figure 8.2.

The second is the one layer method, and involves solving a representative domain near the layer-layer interface consisting of only one layer, the layer-layer interface being simulated by appropriate specification of the boundary conditions, which will be discussed later.

9.1 Solution Method

The solution method for the cross-over problems essentially consists of: subjecting the representative volume elements to unit composite strains; solving the stresses in the composite by analytical or finite element method [20] for each composite strain; evaluating the microstresses due to unit composite stresses from the unit strain responses. The procedure is identical to that used for the unidirectional composites [16, 17]. If the finite element method were to be used then, the microstresses in each element can be written as

$$\{\sigma\} = [B]\{E\} \tag{9.1}$$

where $\{\sigma\} = \{\sigma_{xx}\ \sigma_{yy}\ \sigma_{zz}\ \sigma_{xy}\ \sigma_{xz}\ \sigma_{yz}\}$

$\{E\} = \{E_{11}\ E_{22}\ E_{33}\ E_{12}\ E_{13}\ E_{23}\}$

[B] is a 6 x 6 matrix for each finite element in the composite, such that each column of [B] represents the microstresses $\{\sigma\}$ in the finite element due to a unit composite strain.

The microstress responses due to the composite stresses {S} can be obtained by using the composite stress-strain relation, given by

$$\{S\} = [C]\{E\} \tag{9.2}$$

where $\{S\} = \{S_{11}\ S_{22}\ S_{33}\ S_{12}\ S_{13}\ S_{23}\}$

[C] is the composite moduli matrix.

By using Green's identities and the uncoupling between composite normal and shear deformations as well as between the shear deformations, it can be proved

$$[C] = \frac{1}{V} \int_V [B]\ dv \tag{9.3}$$

where V is the volume of the representative volume domain in which [B] are computed, and the integral is taken over the volume of the representative volume element. The microstress responses due to composite strains can now be obtained from Equations 9.1 and 9.2 as

$$\{\sigma\} = [A]\{S\} \tag{9.4}$$

where $[A] = [B][C]^{-1}$

9.2 Material Planes of Symmetry

The basis of the formulation of the boundary conditions for the representative models of the cross-over problem which will be discussed later, is the identification of the "Material Planes of Symmetry". The material planes of symmetry are defined as the planes about which the material properties are symmetric. In a composite, these planes can be identified as the periodic planes of the composite about which the composite repeats itself.

Consider a point 0 on the material plane symmetry as shown in Figure 9-1. Let ξ, η, ζ represent an orthogonal coordinate system at the point 0, with ξ in the direction perpendicular to the material plane of symmetry, and η, ζ lying in the plane. Let the displacements of the point 0 be u_ξ, u_η, u_ζ, and the stresses on the plane at point 0 be, σ_ξ, τ_η, τ_ζ, where σ_ξ is the normal stress and τ_η, τ_ζ are the shear stresses on the plane in the directions η and ζ, respectively.

It is observed that the displacements and stresses at points like 0 on the material plane of symmetry under the action of the external loads, symmetric or antisymmetric with respect to the plane, with symmetric boundary conditions have the properties shown in Table 9-1.

Table 9-1. Boundary Conditions on a Material Plane of Symmetry.

Loads	u_ξ	u_η	u_ζ	σ_ξ	τ_η	τ_ζ
Sym.	Const.	-	-	-	0	0
Anti-Sym.	-	Const.	Const.	0	-	-

In Table 9-1. the displacements marked "Const." are constant on the entire material plane of symmetry, the stresses marked 0 are zero on the entire plane; and the quantities marked - are unknowns to be determined. Thus, one can prescribe on a material plane of symmetry three quantities, one displacement and two stresses, or, two displacements and one stress.

It is interesting to note that if a composite can be represented by a representative volume element, which is bounded by the material planes of symmetry, then, there is no coupling between the normal and shear deformations, nor, between the shear deformations. That is, if the composite is subjected to normal composite strains, then, no composite shear stresses are generated, and the vice versa. Also, if the composite is subjected to a composite shear strain, only the corresponding shear stress is generated and none of the other.

Based on the concept of the material plane of symmetry we shall now formulate the boundary conditions for the cross-over models based on the two- and one-layer methods.

9.3 The Two-Layer Method

The two-layer method for evaluating the fiber cross-over effects involves the solution of a representative volume model of the multilayer composite near the layer-layer interface consisting of part of two successive layers. In Figure 9-2, this model can be represented by a domain bounded by the planes $x = 0$, $x = a$,

$y = 0$, $y = a$, $z = z_1$, and $z = z_2$. Where z_1 and z_2 are selected such that the effects of layer-layer interface are attenuated near these planes. In the present case z_1 and z_2 are assumed to be 0 and 2t, respectively. The dimensions a and t are selected from the consideration that the individual layers are made of unidirectional hexagonal composites, so that, $a = R(\pi/(3.464\ v_f))^{1/2}$, $t = 0.866\ a$, where R is the radius of the fibers, and v_f is the fiber volume fraction. It is observed that the planes $x = 0$, $x = a$, $y = 0$, $y = a$ bounding the representative model are material planes of symmetry. Due to the assumption that the plane $z = 0$ and $z = 2t$ are sufficiently farther away from the layer-layer interface, and the effects of layer-layer interface are attenuated at this distance, even these planes can be considered as material planes of symmetry, the symmetry being with respect to the unidirectional composites of which the layers are made.

Based on the above considerations, the boundary conditions for the model of the two-layer method are formulated as shown in Table 9-2, under the action of the composite strains E_{11}, E_{22}, E_{33}, E_{12}, E_{13}, and E_{23}. Note that the shear strains E_{12}, E_{13}, and E_{23} are tensorial, and u, v, and w are displacements at a point in x, y, and z directions, respectively.

Table 9-2. Boundary Conditions for a Two-Layer Model.

Strain State	x = 0	x = a	y = 0	y = a	z = 0	z = 2t
E_{11}, E_{22}, E_{33}	$u=-E_{11}a/2$ $\sigma_{xy} = 0$ $\sigma_{xz} = 0$	$u=E_{11}a/2$ $\sigma_{xy} = 0$ $\sigma_{xz} = 0$	$v=-E_{22}a/2$ $\sigma_{xy} = 0$ $\sigma_{yz} = 0$	$v=E_{22}a/2$ $\sigma_{xy} = 0$ $\sigma_{yz} = 0$	$w=-E_{33}t$ $\sigma_{xz} = 0$ $\sigma_{yz} = 0$	$w=E_{33}t$ $\sigma_{xz} = 0$ $\sigma_{yz} = 0$
E_{12}	$v=-E_{12}a/2$ $w = 0$ $\sigma_{xx}=0$	$v=E_{12}a/2$ $w = 0$ $\sigma_{xx}=0$	$u=-E_{12}a/2$ $w = 0$ $\sigma_{yy}=0$	$u=E_{12}a/2$ $w = 0$ $\sigma_{yy}=0$	$w = 0$ $\sigma_{xz}=0$ $\sigma_{yz}=0$	$w = 0$ $\sigma_{xz}=0$ $\sigma_{yz}=0$
E_{13}	$w=-E_{13}a/2$ $v = 0$ $\sigma_{xx}=0$	$w=E_{13}a/2$ $v = 0$ $\sigma_{xx}=0$	$v = 0$ $\sigma_{xy} = 0$ $\sigma_{xz}=0$	$v = 0$ $\sigma_{xy} = 0$ $\sigma_{yz}=0$	$u=-E_{13}t$ $v = 0$ $\sigma_{zz}=0$	$u=E_{13}t$ $v = 0$ $\sigma_{zz}=0$
E_{23}	$u = 0$ $\sigma_{xy}=0$ $\sigma_{xz}=0$	$u = 0$ $\sigma_{xy}=0$ $\sigma_{xz}=0$	$w=-E_{23}a/2$ $u = 0$ $\sigma_{yy}=0$	$w=E_{23}a/2$ $u = 0$ $\sigma_{yy}=0$	$v=-E_{13}t$ $u = 0$ $\sigma_{zz}=0$	$v=E_{13}t$ $u = 0$ $\sigma_{zz}=0$

9.4 The One-Layer Method

The two-layer method discussed earlier, requires excessive amounts of computer time and core if finite element method were to be used in the solution. In order to avoid this and obtain the solution more efficiently, a one-layer method will be discussed here. In the one-layer method, the representative model of the multi-layer composite in Figure 8-2 consists of a part of only one layer near the layer-layer interface. In Figure 9-2 this model is represented by the domain bounded by the planes $x = 0$, $x = a$, $y = 0$, $y = a$, $z = z_1$, and $z = t$. The parameters a and t are identical to those given for the two-layer model discussed earlier. The distance z_1 is again selected such that the effects of layer-layer interface are attenuated at this distance. In the present model the value of z_1 is taken as $-t$. The plane $z = t$ represents layer-layer interface.

In order to solve this model, the composite strains E_{11}, E_{22}, E_{33}, E_{12}, E_{13}, and E_{23} are resolved into six associated strain fields defined below:

$$
\begin{aligned}
&1.\quad E_{11} = E_{22} = F_{11} \\
&2.\quad E_{11} = -E_{22} = F_{22} \\
&3.\quad E_{33} = F_{33} \\
&4.\quad E_{12} = F_{12} \\
&5.\quad E_{13} = -E_{23} = F_{13} \\
&6.\quad E_{13} = E_{23} = F_{23}
\end{aligned}
\tag{9.5}
$$

The strain fields associated with F_{11}, F_{33}, F_{12}, and F_{13} are considered as "symmetric", as under the action of these strain fields the displacements at a point ($x = c_1$, $y = c_2$, $z = c_3$) in the lower layer (Figure 9-2) are related to an identical point ($x = c_1$, $y = c_2$, $z = 2t - c_3$) in the upper layer, the center of the interface being fixed, are related by

$$
\begin{aligned}
u^L &= v^U \\
v^L &= u^U \\
w^L &= -w^U
\end{aligned}
\tag{9.6}
$$

where u^L, v^L, w^L are the dispalcement at a point in the lower layer in x, y, z directions, respectively, and u^U, v^U, w^U are the displacements at an identical point in the upper layer. The stresses at the corresponding points under the symmetric strain fields are related by

$$
\{\sigma_{xx}^L \sigma_{yy}^L \sigma_{zz}^L \sigma_{xy}^L \sigma_{xz}^L \sigma_{yz}^L\} = \{\sigma_{yy}^U \sigma_{xx}^U \sigma_{zz}^U \sigma_{yx}^U -\sigma_{yz}^U -\sigma_{xz}^U\} \tag{9.7}
$$

If we consider the layer-layer interface (Figure 9-3) under the action of symmetric strain fields, the dispalcements at points A($x = c_1$, $y = c_2$, $z = t$) and B ($x = c_1$, $y = c_2$, $z = t$) which are symmetrically placed with respect to the line $x = y$ are realted by equations similar to those in Equation 9.6, because one can consider A to be a part of the lower layer and B as a part of the upper layer, or vice versa. Thus, the boundary conditions on the layer-layer interface for symmetric strain states are as follows:

$$\begin{aligned} u_A &= v_B \\ v_A &= u_B \\ w_A &= -w_B \end{aligned} \qquad (9.8)$$

$$u = v = w = 0 \qquad \text{at} \qquad x = y \; a/2, \; z = t$$

where u_A, v_A, w_A are displacements at point A and u_B, v_B, w_B are are displacements at point B.

The strain fields associated with F_{22} and F_{23} in Equations 9.5, are considered as "antisymmetric", as under the action of these strain fields the displacements at a point ($x = c_1$, $y = x_2$, $z = c_3$) in the lower layer (Figure 9-2) are related to an identical point in the upper layer ($x = c_2$, $y = c_1$, $z = 2t - c_3$), the center of the layer-layer interface being fixed, are related by

$$
\begin{aligned}
u^L &= - v^U \\
v^L &= - u^U \\
w^L &= w^U
\end{aligned}
\tag{9.9}
$$

The stresses at the corresponding points are related by

$$
\{\sigma_{xx}^L \ \sigma_{yy}^L \ \sigma_{zz}^L \ \sigma_{xy}^L \ \sigma_{xz}^L \ \sigma_{yz}^L\} = \{-\sigma_{yy}^U \ -\sigma_{xx}^U \ -\sigma_{zz}^U \ -\sigma_{xy}^U \ \sigma_{yz}^U \ \sigma_{xz}^U\}
\tag{9.10}
$$

If we consider the layer-layer interface (Figure 9-3) under the action of antisymmetric strain fields, the displacements at points A ($x = c_1$, $y = c_2$, $z = t$) and B ($x = c_2$, $y = c_1$, $z = t$) are related by equations similar to those in Equation 9.9. Thus boundary conditions on the layer-layer interface for antisymmetric strain fields are as follows:

$$
\begin{aligned}
u_A &= - v_B \\
v_A &= - u_B \\
w_A &= w_B
\end{aligned}
\tag{9.11}
$$

$$
u = v = w = 0 \qquad \text{at} \qquad x = y = a/2, \ z = t
$$

The boundary conditions on the lateral faces are prescribed on the consideration that these are material planes of symmetry. However, one would encounter a difficulty in prescribing the boundary conditions on the lateral faces for the strain states

represented by F_{13} and F_{23} in Equations 9.5, because these faces would no longer remain as the material planes of symmetry, and would not fall in any case of Table 9-1. To overcome this difficulty one could solve four associated problems: E_{13} with boundary conditions in Equation 9.8 on the layer-layer interface and boundary conditions in Table 9-2 on the other faces; E_{13} with boundary conditions in Equation 9.9 on the layer-layer interface and boundary conditions in Table 9-2 on the other faces; and two other similar problems with E_{23}. Appropriate combination of these four associated problems would give the solution for strain states F_{13} and F_{23} in Equations 9.5. Uncoupling of F_{13} and F_{23} would give the solution for composite strains E_{13} and E_{23}. Alternately, one could consider a model similar to the two-layer model and prescribe the boundary conditions in Table 9-2 to obtain a direct solution for E_{13} and E_{23}.

The boundary conditions on the face $z = - t$ for the one-layer model could be prescribed on the assumption that the influence of the layer-layer interface has attenuated at this distance. As a result, the boundary conditions on this face correspond to those existing in unidirectional composite. It should be pointed out that the choice of the distance $z = - t$ of this face from the layer-layer interface is arbitrary. One could as well consider any distance equal to an integral multiple of t for this purpose. If this face were to be located at $z = 0, - 2t, - 4t$, etc., then the boundary conditions for this face would be identical to those described for the two-layer model at $z = 0$ in Table 9-2.

On the other hand if the face were to be located at $z = -3t$, $z = -5t$, etc., then the boundary conditions on this face would be identical to those for a face at $z = -t$.

Based on the above considerations the boundary conditions for the one-layer model are stated in Table 9-3.

9.5 Microstresses for Cross-Over Solution

The microstresses for the cross-over models corresponding to an applied system of composite stresses can be found from the microstress solution for the composite strains by either method. The solution procedure could be either analytical if one could be found or a finite element solution. In the latter case the [B] matrices in Equation 9.1 are first found. The [A] matrices in Equation 9.4 can then be obtained by determining [C] by Equation 9.3. Care should be taken to omit the coupling terms corresponding to the normal stresses and shear strains, shear stresses and normal strains, shear stresses and those shear strains that do not correspond. This is necessary because, the models in both methods represent only one half of a periodic domain, and stresses in the other half of the domain are complementary to those in the domain considered by the models.

For the two-layer method the above procedure is directly applicable as the [B] matrices (Equation 9.1) are determined directly. On the other hand, for the one-layer method one has to

Table 9-3. Boundary Conditions for a One-Layer Model.

Strain State	x = 0	x = a	y = 0	y = a	z = -t	z = t
$E_{11}=E_{22}=F_{11}$	$u=-F_{11}a/2$ $\sigma_{xy} = 0$ $\sigma_{xz} = 0$	$u =F_{11}a/2$ $\sigma_{xy} = 0$ $\sigma_{xz} = 0$	$v=-F_{11}a/2$ $\sigma_{xy} = 0$ $\sigma_{yz} = 0$	$v=F_{11}a/2$ $\sigma_{xy} = 0$ $\sigma_{yz} = 0$	$u(x)+u(a-x)=0$	Equation 9.8
$E_{11}=-E_{22}=F_{22}$	$u=-F_{22}a/2$ $\sigma_{xy} = 0$ $\sigma_{xz} = 0$	$u=F_{22}a/2$ $\sigma_{xy} = 0$ $\sigma_{xz} = 0$	$v=F_{22}a/2$ $\sigma_{xy} = 0$ $\sigma_{yz} = 0$	$v=-F_{22}a/2$ $\sigma_{xy} = 0$ $\sigma_{yz} = 0$	$v(x)-v(a-x)=0$ $w(x)+w(a-x)=0$	Equation 9.11
$E_{33} = F_{33}$	$u = 0$ $\sigma_{xy} = 0$ $\sigma_{xz} = 0$	$u = 0$ $\sigma_{xy} = 0$ $\sigma_{xz} = 0$	$v = 0$ $\sigma_{xy} = 0$ $\sigma_{yz} = 0$	$v = 0$ $\sigma_{xy} = 0$ $\sigma_{yz} = 0$	$u(x)+u(a-x)=0$ $v(x)-v(z-x)=0$ $w(x)+w(a-x)=-2F_{33}t$	Equation 9.8
$E_{12} = F_{12}$	$v=-F_{12}a/2$ $w = 0$ $\sigma_{xx} = 0$	$v=F_{12}a/2$ $w = 0$ $\sigma_{xx} = 0$	$u=-F_{12}a/2$ $w = 0$ $\sigma_{yy} = 0$	$u=F_{12}a/2$ $w = 0$ $\sigma_{yy} = 0$	$u(x)-u(a-x)=0$ $v(x)+v(a-x)=0$ $w(x)-w(a-x)=0$	Equation 9.8

determine the stresses in the adjoining layer from the stress identities in Equations 9.7 and 9.10; the solution should then be uncoupled to obtain the [B] matrices.

Using the [A] matrices obtained for the cross-over models, the initial yield surfaces can be constructed. The procedure for the determination of the initial yield surfaces is identical to that outlined in the preceding chapter. The procedure remains the same except the $[A^i]$ matrices in Equation 8.35 should be replaced by the new cross-over [A] matrices.

CHAPTER X.

RESULTS, DISCUSSION, AND CONCLUSIONS

On the basis of the formulations made in Chapters 8 and 9, a multilayered composite the layers of which are made of unidirectional fiber-reinforced boron-aluminum composites with fiber volume fraction of 0.3, has been analyzed. The [A]-matrices corresponding to the regular solution have been determined from Equation 8.34 by using the results obtained earlier in References [16] and [17] for unidirectional fiber-reinforced composites. The [A]-matrices corresponding to the cross-over problem (Equation 9.4) have been obtained by using the two-layer method discussed in Chapter IX. The solution is found by using the finite element method [20], with finite element mesh shown in Figure 10-1.

10.1 Results

A computer print-out of the microstresses σ_{xx}, σ_{yy}, σ_{xy}, σ_{xz}, σ_{yz}, their hydrostatic component $\sigma_{kk} = \sigma_{xx} + \sigma_{yy} + \sigma_{zz}$, and the equivalent stress $\bar{\sigma}$ corresponding to the composite stresses S_{11}, S_{22}, S_{33}, S_{12}, S_{13}, and S_{23} equal to 100 units are shown in

Tables 10-1 to 10-6. In these tables the microstresses are printed as SXX, SYY, etc. instead of σ_{xx}, σ_{yy}, etc.; the hydrostatic component as SKK instead of σ_{kk}; the equivalent stress as EQS instead of $\bar{\sigma}$; the composite stresses as S11, S22, etc. instead of S_{11}, S_{22}, etc. Each line in these tables shows the microstresses in four successive finite elements printed at the beginning of the line under the column ELTS (for example, for the line containing 53-56 under ELTS, the first 8 entries correspond to the element 53, second 8 entries to element 54, third 8 entries to element 55, fourth eight entries to element 56). The element positions in these table are as shown in Figure 10-1. It should be noted that, the elements not visible in Figure 10-1 are directly located below the immediate lowest element visible, and may be in one of the other three rows, the elements being numbered sequentially in the positive direction of y-axis in the lower layer, and in the negative direction of the x-axis in the upper layer.

The non-zero components of the microstresses in the matrix at the fiber-matrix interface in the lower layer are plotted in Figures 10-2 to 10-7 at two sections, y = a/8 and a = 7a/8, for the cross-over problem. The stresses σ_{rr}, $\sigma_{\phi\phi}$, σ_{yy}, $\sigma_{r\phi}$, σ_{ry}, $\sigma_{\phi y}$ are in radial coordinates, the rϕ-plane being lying in the xz-plane, r measured from x = z = 0, measured in the anti-clockwise direction from the x-axis (Figure 10-1). The corresponding regular solution is also shown for the purpose of comparison (except in Figure 10-3).

The initial yield surfaces based on both the regular and cross-over solutions have been constructed in the sub-composite-stress-spaces S_{11} - S_{22}, S_{11} - S_{33}, S_{11} - S_{12}, and S_{11} - S_{13}

TABLE 10-1

CROSS-OVER PROBLEM, B-AL (VF=0.30)

MICROSTRESS DISTRIBUTION FOR COMPOSITE STRESS S11=100

ELTS	SXX	SYY	SZZ	SXY	SXZ	SYZ	SKK	EQS	SXX	SYY	SZZ	SXY	SXZ	SYZ	SKK	EQS	SXX	SYY	SZZ	SXY	SXZ	SYZ	SKK	EQS	SXX	SYY	SZZ	SXY	SXZ	SYZ	SKK	EQS
1- 4	102	-45	-11	0	0	0	46	133	102	-45	-11	0	0	0	46	133	101	-45	-10	0	0	0	46	133	101	-46	-10	0	0	0	45	133
5- 8	101	-45	-11	0	0	0	45	133	101	-45	-11	0	0	0	45	133	101	-46	-10	0	0	0	45	133	101	-46	-10	0	0	0	45	133
9- 12	102	-45	-12	0	0	0	45	134	102	-45	-11	0	0	0	46	134	102	-45	-11	0	0	0	46	134	102	-46	-10	0	0	0	46	134
13- 16	102	-45	-11	0	-1	0	46	133	102	-45	-11	0	-1	0	46	133	102	-45	-10	0	-1	0	47	134	102	-46	-9	0	-1	0	47	134
17- 20	101	-45	-11	0	-1	0	45	132	101	-45	-10	0	-1	0	46	132	100	-46	-9	0	-1	0	45	132	100	-46	-9	0	-1	0	45	132
21- 24	99	-45	-11	0	0	0	43	131	99	-45	-10	0	0	0	44	131	99	-46	-9	0	0	0	44	131	99	-46	-9	0	0	0	44	131
25- 28	104	-44	-12	0	0	0	48	135	104	-45	-11	0	0	0	48	135	104	-45	-11	0	0	0	48	135	104	-45	-10	0	0	0	49	135
29- 32	103	-44	-11	0	-2	0	48	134	103	-45	-11	0	-2	0	47	134	103	-45	-10	0	-2	0	48	135	103	-45	-10	0	-2	0	48	135
33- 36	101	-45	-12	0	-1	0	44	133	101	-45	-11	0	-1	0	45	133	101	-46	-10	0	-2	0	45	133	101	-46	-10	0	-2	0	45	133
37- 40	99	-45	-11	0	-2	0	43	131	99	-45	-10	0	-2	0	44	131	99	-46	-9	0	-2	0	44	131	99	-46	-9	0	-2	0	44	131
41- 44	98	-45	-10	0	-1	0	43	129	98	-45	-9	0	-1	0	44	129	98	-46	-8	0	-1	0	44	129	98	-46	-7	0	-1	0	45	129
45- 48	97	-45	-10	0	0	0	42	129	97	-45	-9	0	0	1	43	129	97	-46	-8	0	0	0	43	129	97	-46	-7	0	0	0	44	129
49- 52	108	33	27	0	-2	0	168	77	108	32	27	0	-2	0	167	77	108	32	27	0	-2	0	167	77	108	32	27	0	-2	0	167	77
53- 56	102	28	19	0	-3	0	149	79	102	28	19	0	-3	0	149	79	102	28	19	0	-3	0	149	79	102	28	19	0	-3	0	149	79
57- 60	94	22	10	0	-2	0	126	78	94	22	10	0	-2	0	126	78	94	22	11	0	-2	0	127	77	94	22	11	0	-2	0	127	77
61- 64	85	18	5	0	0	0	108	74	85	18	6	0	0	0	109	74	85	18	6	0	0	0	109	74	85	18	6	0	0	0	109	73
65- 68	69	8	-7	0	6	0	70	71	69	8	-7	0	6	0	70	70	69	8	-6	0	6	0	71	70	69	8	-6	0	6	0	71	70
69- 72	59	3	-13	0	10	0	49	68	59	3	-12	0	10	0	50	67	59	3	-11	0	10	0	51	67	59	3	-10	0	10	0	52	66
73- 76	42	-3	-17	0	12	0	22	58	42	-3	-16	0	12	0	23	57	42	-3	-15	0	12	0	24	57	43	-2	-14	0	12	0	27	56
77- 80	24	-8	-17	0	6	0	-1	40	25	-8	-16	0	6	1	1	40	25	-8	-14	0	6	1	3	39	26	-8	-13	0	6	0	5	39
81- 84	106	28	13	0	0	0	147	86	106	27	13	0	0	0	146	86	106	27	14	0	0	0	147	86	106	27	14	0	0	0	147	86
85- 88	97	24	12	0	2	0	133	79	97	24	12	0	2	0	133	79	97	24	12	0	2	0	133	78	97	24	13	0	2	0	134	78
89- 92	83	19	11	0	2	0	113	68	83	19	11	0	2	0	113	68	83	19	11	0	2	0	113	68	83	19	12	0	2	0	114	68
93- 96	70	15	10	0	1	0	95	58	70	15	10	0	1	0	95	58	71	14	11	0	1	0	96	58	71	14	11	0	1	0	96	58
97-100	62	11	6	0	1	0	79	53	62	10	6	0	1	0	78	53	62	10	7	0	1	0	79	53	62	10	7	0	1	0	79	53
101-104	56	6	-2	0	1	0	60	54	56	6	-1	0	1	0	61	54	56	6	0	0	1	0	62	54	56	6	0	0	1	0	62	53
105-108	47	0	-11	0	2	0	36	54	47	0	-10	0	2	0	37	53	47	0	-9	0	2	0	38	53	47	0	-8	0	2	0	39	52
109-112	37	-4	-18	0	1	0	15	51	37	-4	-17	0	1	1	16	50	38	-4	-15	0	1	0	19	49	38	-4	-13	0	1	0	21	48
113-116	103	25	8	0	1	0	136	88	103	25	8	0	1	0	136	87	103	25	8	0	1	0	136	87	103	24	8	0	1	0	135	87
117-120	92	22	9	0	2	0	123	77	92	21	9	0	2	0	122	77	92	21	9	0	2	0	122	77	92	21	9	0	2	0	122	77
121-124	77	17	11	0	2	0	105	63	78	17	11	0	2	0	106	63	78	17	11	0	2	0	106	63	78	17	11	0	1	0	106	63
125-128	65	13	11	0	0	0	89	52	65	13	11	0	0	0	89	52	65	13	12	0	0	0	90	53	65	13	12	0	0	0	90	53
129-132	56	11	9	0	0	0	78	48	58	10	9	0	0	0	77	48	59	10	10	0	0	0	79	48	59	10	10	0	0	0	79	48
133-136	55	8	2	0	-1	0	65	49	55	7	3	0	-1	0	65	49	55	7	4	0	-1	0	66	49	55	7	5	0	-1	0	67	49
137-140	50	3	-7	0	-1	0	46	53	50	2	-6	0	-1	0	46	53	50	2	-5	0	-1	0	47	52	51	2	-4	0	-1	0	49	52
141-144	44	-1	-17	0	0	0	26	56	45	-1	-16	0	0	1	28	55	45	-2	-14	0	0	1	29	54	45	-2	-12	0	0	0	31	54
145-148	101	23	6	0	0	0	130	87	101	23	6	0	0	0	130	87	101	23	6	0	0	0	130	87	101	23	6	0	0	0	130	87
149-152	89	20	8	0	1	0	117	75	89	20	8	0	1	0	117	75	89	20	8	0	1	0	117	75	89	20	9	0	1	0	118	75
153-156	74	16	10	0	0	0	100	60	74	16	11	0	0	0	101	60	74	16	11	0	0	0	101	60	74	16	11	0	0	0	101	60
157-160	61	12	10	0	0	0	83	50	61	12	10	0	0	0	83	50	62	11	11	0	0	0	84	50	62	11	11	0	0	0	84	50
161-164	56	10	10	0	-1	0	76	46	56	10	10	0	-1	0	76	46	56	10	10	0	-1	0	76	46	56	9	11	0	-1	0	76	46
165-168	54	8	5	0	-2	0	67	48	55	8	6	0	-2	0	69	48	55	8	6	0	-2	0	69	48	55	7	7	0	-2	0	69	47
169-172	52	4	-5	0	-3	0	51	53	52	4	-4	0	-3	1	52	53	52	3	-2	0	-3	0	53	52	53	3	-1	0	-3	0	55	52
173-176	48	0	-16	0	-1	0	32	58	49	0	-14	0	-1	1	35	57	49	0	-12	0	-1	1	37	57	50	0	-10	0	-1	0	40	56
177-180	55	10	11	0	-1	0	76	44	53	8	3	0	-2	0	64	48	51	4	-6	0	-3	0	49	54	50	2	-14	0	-1	0	38	59
181-184	55	10	11	0	-1	0	76	44	53	7	4	0	-2	0	64	48	52	4	-4	0	-3	1	52	53	51	1	-11	0	-1	1	41	58
185-188	55	9	11	0	-1	0	75	44	53	7	5	0	-3	0	65	48	52	3	-2	0	-3	1	53	53	52	1	-9	0	-1	1	44	57
189-192	55	9	11	0	-2	0	75	44	53	6	5	0	-3	0	64	48	53	3	-1	0	-4	0	55	53	52	1	-7	0	-1	0	46	56
193-196	53	8	10	0	-1	0	71	44	53	6	5	0	-3	0	64	48	53	3	-1	0	-3	0	55	53	54	2	-6	0	-1	0	50	56
197-200	52	7	8	0	-1	0	67	45	53	6	5	0	-2	0	64	48	54	4	0	0	-3	0	58	52	55	3	-3	0	-1	0	55	55

TABLE 10-1 (Contd.)

CROSS-OVER PROBLEM, B-AL (VF=0.30)

MICROSTRESS DISTRIBUTION FOR COMPOSITE STRESS S11=100

ELTS	SXX	SYY	SZZ	SXY	SXZ	SYZ	SKK	EQS	SXX	SYY	SZZ	SXY	SXZ	SYZ	SKK	EQS	SXX	SYY	SZZ	SXY	SXZ	SYZ	SKK	EQS	SXX	SYY	SZZ	SXY	SXZ	SYZ	SKK	EQS
201-204	52	6	7	0	0	0	65	45	53	5	4	0	-1	0	62	48	55	5	1	0	-1	0	61	51	56	4	0	0	0	0	60	54
205-208	53	6	6	0	0	0	65	46	53	5	5	0	0	0	63	48	55	5	2	0	0	0	62	51	56	5	0	0	0	0	61	53
209-212	54	10	10	0	-1	0	74	44	53	7	2	0	-3	0	62	48	52	4	-7	0	-3	0	49	54	51	2	-14	0	-1	0	59	59
213-216	54	9	10	0	-1	0	73	44	53	7	3	0	-3	1	63	48	52	4	-4	0	-3	1	52	54	52	2	-11	0	-1	2	43	58
217-220	53	8	10	0	-1	0	71	44	53	6	4	0	-3	1	63	48	53	4	-2	0	-3	1	55	53	53	2	-8	0	-1	2	47	57
221-224	53	8	10	0	-1	0	71	44	53	6	5	0	-3	0	64	48	53	3	-1	0	-3	1	55	53	54	2	-6	0	-1	1	50	57
225-228	53	7	9	0	-1	0	69	44	53	6	5	0	-3	0	64	48	54	4	0	0	-3	0	58	52	54	2	-4	0	-1	1	52	56
229-232	52	6	8	0	-1	0	66	45	53	5	5	0	-2	0	63	48	54	4	0	0	-2	0	58	52	55	3	-2	0	-1	0	56	55
233-236	53	6	7	0	0	0	66	46	53	5	5	0	-1	0	63	48	55	5	1	0	-1	0	61	51	55	4	0	0	0	0	59	53
237-240	53	6	7	0	0	0	66	46	54	5	5	0	0	0	64	48	55	5	2	0	0	0	62	51	56	5	0	0	0	0	61	53
241-244	54	10	9	0	-1	0	73	45	53	7	2	0	-3	0	62	49	51	4	-7	0	-3	0	48	54	50	2	-15	0	-1	0	57	59
245-248	54	9	9	0	-1	0	72	45	53	7	2	0	-3	1	62	48	52	4	-5	0	-3	1	51	54	52	2	-11	0	-1	2	43	58
249-252	53	8	8	0	-1	0	69	45	53	6	3	0	-3	1	62	48	53	4	-3	0	-3	2	54	53	53	2	-8	0	-1	2	47	57
253-256	53	7	8	0	-1	0	68	45	53	6	4	0	-3	1	63	48	53	4	-1	0	-3	1	56	53	54	2	-5	0	-1	2	51	56
257-260	53	7	8	0	-1	0	68	45	53	6	4	0	-2	1	63	48	54	4	0	0	-2	1	58	52	54	3	-3	0	-1	1	54	55
261-264	53	6	7	0	0	0	66	46	53	5	5	0	-2	1	63	48	54	4	1	0	-2	1	59	51	55	3	-1	0	0	1	57	54
265-268	53	6	7	0	0	0	66	46	54	5	5	0	-1	0	64	48	55	4	2	0	-1	1	61	51	55	4	0	0	0	1	59	53
269-272	53	5	7	0	0	0	65	47	54	5	5	0	0	0	64	48	55	5	3	0	0	0	63	50	55	4	1	0	0	0	60	52
273-276	55	10	8	0	-1	0	73	46	53	7	1	0	-4	0	61	50	50	4	-8	0	-4	0	46	54	48	1	-15	0	-1	0	34	57
277-280	55	9	8	0	-1	1	72	46	53	7	1	0	-3	1	61	49	51	5	-6	0	-3	1	50	53	50	3	-12	0	-1	1	41	57
281-284	54	8	7	0	-1	1	69	46	53	7	2	0	-2	1	62	49	52	5	-3	0	-3	2	54	53	51	4	-9	0	-1	2	46	55
285-288	54	7	7	0	-1	1	68	47	53	6	3	0	-2	1	62	49	53	5	-2	0	-2	2	56	52	53	4	-5	0	-1	3	52	55
289-292	54	7	7	0	0	1	68	47	54	6	4	0	-2	2	64	49	54	5	0	0	-2	2	59	51	54	4	-2	0	0	3	56	53
293-296	54	6	7	0	0	1	67	47	54	5	5	0	-1	2	64	49	54	4	2	0	-1	2	60	51	54	4	0	0	0	3	58	53
297-300	54	5	8	0	0	1	67	47	54	5	6	0	0	1	65	49	54	4	3	0	0	2	61	50	55	3	2	0	0	2	60	52
301-304	54	5	8	0	0	0	67	47	54	4	7	0	0	0	65	48	55	4	5	0	0	0	64	50	55	3	4	0	0	1	62	51
305-308	281	4	5	0	-2	0	290	274	283	4	0	0	-4	0	287	279	285	3	-7	0	-4	0	281	285	287	2	-13	0	-2	0	276	290
309-312	281	4	5	0	-2	0	290	274	283	3	0	0	-4	0	286	279	285	3	-7	0	-4	0	281	285	287	2	-13	0	-2	0	276	291
313-316	280	4	4	0	-1	0	288	274	282	3	0	0	-3	0	285	279	286	3	-6	0	-3	0	283	285	288	2	-11	0	-1	0	279	290
317-320	280	4	3	0	-1	0	287	274	282	3	0	0	-2	0	285	279	286	3	-6	0	-2	0	283	285	288	2	-10	0	-1	0	280	290
321-324	280	4	3	0	-1	0	287	274	282	3	0	0	-2	0	285	278	286	3	-6	0	-2	0	283	285	289	2	-10	0	-1	0	281	290
325-328	280	4	3	0	0	0	287	274	282	3	0	0	0	0	285	279	286	3	-6	0	0	0	283	285	288	2	-9	0	0	0	281	290
329-332	280	4	3	0	-1	0	287	275	283	3	0	0	-2	0	286	279	285	3	-6	0	-2	0	282	285	288	3	-10	0	-1	0	281	289
333-336	280	4	3	0	-1	0	287	275	283	3	0	0	-2	0	286	279	286	3	-6	0	-2	0	283	285	288	3	-10	0	-1	0	281	289
337-340	280	4	2	0	0	0	286	275	283	3	-1	0	-1	0	285	279	286	3	-6	0	-1	0	283	285	288	3	-10	0	0	0	281	289
341-344	280	4	2	0	0	0	286	275	283	3	-1	0	0	0	285	279	286	3	-6	0	0	0	283	285	288	3	-9	0	0	0	282	289
345-348	280	3	2	0	0	0	285	275	283	3	-1	0	-1	0	285	279	286	3	-6	0	-1	0	283	285	288	3	-10	0	0	0	281	289
349-352	281	4	2	0	0	0	287	275	283	3	-1	0	0	0	285	279	285	3	-6	0	0	0	282	285	288	3	-10	0	0	0	281	289

TABLE 10-2

CROSS-OVER PROBLEM, B-AL (VF=0.30)

MICROSTRESS DISTRIBUTION FOR COMPOSITE STRESS S22=100

ELTS	SXX	SYY	SZZ	SXY	SXZ	SYZ	SKK	EQS	SXX	SYY	SZZ	SXY	SXZ	SYZ	SKK	EQS	SXX	SYY	SZZ	SXY	SXZ	SYZ	SKK	EQS	SXX	SYY	SZZ	SXY	SXZ	SYZ	SKK	EQS
1- 4	3	288	-10	0	0	0	281	289	3	285	-6	0	0	0	282	285	3	283	-1	0	0	0	285	279	4	281	2	0	0	0	287	275
5- 8	3	288	-10	0	0	0	281	289	3	285	-6	0	0	1	282	285	3	283	-1	0	0	1	285	279	3	280	2	0	0	0	285	275
9- 12	3	288	-9	0	0	0	282	289	3	286	-6	0	0	0	283	285	3	283	-1	0	0	0	285	279	4	280	2	0	0	0	286	275
13- 16	3	288	-10	0	0	0	281	289	3	286	-6	0	0	1	283	285	3	283	-1	0	0	1	285	279	4	280	2	0	0	0	286	275
17- 20	3	288	-10	0	0	1	281	289	3	285	-6	0	0	2	282	285	3	283	0	0	0	2	286	279	4	280	3	0	0	1	287	275
21- 24	3	288	-10	0	0	1	281	289	3	285	-6	0	0	2	282	285	3	283	0	0	0	2	286	279	4	280	3	0	0	1	287	275
25- 28	2	289	-9	0	0	0	281	290	3	286	-6	0	0	0	283	285	3	282	0	0	0	0	285	279	4	280	3	0	0	0	287	274
29- 32	2	288	-10	0	0	1	280	290	3	286	-6	0	0	2	283	285	3	282	0	0	0	2	285	278	4	280	3	0	0	1	287	274
33- 36	2	288	-10	0	0	1	280	290	3	286	-6	0	0	2	283	285	3	282	0	0	0	2	285	279	4	280	3	0	0	1	287	274
37- 40	2	288	-11	0	0	1	279	290	3	286	-6	0	0	3	283	285	3	282	0	0	0	3	285	279	4	280	4	0	0	1	288	274
41- 44	2	287	-13	0	0	2	276	291	3	285	-7	0	0	4	281	285	3	283	0	0	0	4	286	279	4	281	5	0	0	2	290	274
45- 48	2	287	-13	0	0	2	276	290	3	285	-7	0	0	5	281	285	4	283	0	0	0	4	287	279	4	281	5	0	0	2	290	274
49- 52	3	55	4	0	-1	0	62	51	4	55	5	0	0	0	64	50	4	54	7	0	0	0	65	48	5	54	8	0	0	0	67	47
53- 56	3	55	2	0	-2	0	60	52	4	54	3	0	-2	0	61	50	5	54	6	0	-1	0	65	49	5	54	8	0	-1	0	67	47
57- 60	4	54	0	0	-3	0	58	53	4	54	2	0	-2	1	60	51	5	54	5	0	-2	1	64	49	6	54	7	0	-1	0	67	47
61- 64	4	54	-2	0	-3	0	56	53	5	54	0	0	-2	2	59	51	6	54	4	0	-2	2	64	49	7	54	7	0	-1	0	68	47
65- 68	4	53	-5	0	-3	1	52	55	5	53	-1	0	-2	2	57	52	6	53	3	0	-1	2	62	49	7	54	7	0	-1	1	68	47
69- 72	4	51	-9	0	-2	1	46	55	5	52	-4	0	-2	3	53	53	7	53	2	0	-1	3	62	49	8	54	7	0	-1	1	69	46
73- 76	3	50	-12	0	-1	1	41	57	5	51	-6	0	-1	3	50	53	7	53	1	0	-1	3	61	49	9	55	8	0	-1	1	72	46
77- 80	1	48	-15	0	0	1	34	57	4	50	-8	0	0	4	46	54	7	53	1	0	0	4	61	50	10	55	8	0	0	1	73	46
81- 84	4	55	1	0	0	0	60	52	5	55	3	0	0	0	63	50	5	54	5	0	0	0	64	48	5	53	7	0	0	0	65	47
85- 88	4	55	0	0	-1	0	59	53	4	55	2	0	-1	1	61	51	5	54	5	0	0	1	64	48	6	53	7	0	0	0	66	46
89- 92	3	55	-1	0	-1	0	57	54	4	54	1	0	-1	2	59	51	5	53	5	0	-1	2	63	48	6	53	7	0	0	0	66	46
93- 96	3	54	-3	0	-1	1	54	55	4	54	0	0	-1	2	58	52	6	53	4	0	-1	2	63	48	7	53	8	0	0	1	68	45
97-100	2	54	-5	0	-2	1	51	56	4	53	-1	0	-1	3	56	53	6	53	4	0	-1	3	63	48	7	53	8	0	0	1	68	45
101-104	2	53	-8	0	-2	1	47	57	4	53	-3	0	-1	3	54	53	6	53	3	0	-1	3	62	48	8	53	8	0	0	1	69	45
105-108	2	52	-11	0	-2	1	43	58	4	52	-5	0	-1	3	51	54	7	53	2	0	-1	3	62	48	9	54	9	0	0	1	72	45
109-112	2	50	-15	0	0	1	37	59	4	51	-7	0	0	3	48	54	7	53	2	0	0	3	62	49	10	54	9	0	0	1	73	45
113-116	5	56	0	0	0	0	61	53	5	55	2	0	0	0	62	51	5	54	5	0	0	0	64	48	6	53	7	0	0	0	66	46
117-120	4	55	0	0	0	0	59	53	5	55	2	0	0	1	62	51	5	53	5	0	0	1	63	48	6	53	7	0	0	0	66	46
121-124	3	55	-2	0	0	1	56	55	4	54	0	0	0	2	58	52	5	53	5	0	0	2	63	48	6	52	8	0	0	1	66	45
125-128	2	54	-4	0	0	1	52	56	4	54	0	0	0	3	58	52	6	53	5	0	0	3	64	48	7	53	9	0	0	1	69	44
129-132	2	54	-6	0	-1	1	50	57	3	53	-1	0	-1	3	55	53	6	53	5	0	0	3	64	48	8	53	10	0	0	1	71	44
133-136	2	53	-8	0	-1	1	47	57	4	53	-2	0	-1	3	55	53	6	53	4	0	-1	3	63	48	8	53	10	0	0	1	71	44
137-140	2	52	-11	0	-2	1	43	58	4	52	-4	0	-1	3	52	54	7	53	3	0	-1	3	63	48	9	54	10	0	0	1	73	44
141-144	2	51	-14	0	0	1	39	59	4	52	-7	0	0	3	49	54	7	53	2	0	0	3	62	48	10	54	10	0	0	1	74	44
145-148	5	56	0	0	0	0	61	53	5	55	2	0	0	0	62	51	5	53	5	0	0	0	63	48	6	53	6	0	0	0	65	46
149-152	4	56	0	0	0	0	60	54	5	55	1	0	0	1	61	51	5	53	4	0	0	1	62	48	6	52	7	0	0	0	65	45
153-156	3	55	-3	0	0	1	55	55	4	54	0	0	0	3	58	52	6	53	5	0	0	2	64	48	7	52	8	0	0	1	67	45
157-160	2	54	-6	0	0	1	50	56	3	53	-1	0	0	4	55	53	6	53	5	0	0	3	64	48	8	53	10	0	0	1	71	44
161-164	1	52	-7	0	0	1	46	56	3	53	-1	0	0	4	55	53	6	53	5	0	0	3	64	48	9	55	11	0	0	2	75	44
165-168	1	52	-9	0	-1	1	44	57	3	52	-2	0	-1	3	53	53	7	53	5	0	0	3	65	48	9	55	11	0	0	1	75	44
169-172	1	51	-11	0	-1	1	41	58	4	52	-4	0	-1	3	52	53	7	53	4	0	0	2	64	48	10	55	11	0	0	1	76	44
173-176	2	50	-14	0	0	1	38	59	4	51	-6	0	0	3	49	54	8	53	3	0	0	2	64	48	10	55	11	0	0	1	76	44
177-180	0	50	-10	0	0	1	40	56	0	49	-12	0	-1	1	37	57	0	49	-14	0	-1	1	35	57	0	48	-16	0	0	1	32	58
181-184	3	53	-1	0	0	3	55	52	3	52	-2	0	0	3	53	52	4	52	-4	0	-1	3	52	52	4	52	-5	0	0	3	51	53
185-188	7	55	7	0	0	2	69	47	8	55	6	0	0	2	69	48	8	55	6	0	0	2	69	48	8	54	5	0	0	2	67	48
189-192	9	56	11	0	0	1	76	46	10	56	10	0	0	1	76	46	10	56	10	0	0	1	76	46	10	56	10	0	0	1	76	46
193-196	11	62	11	0	0	0	84	50	11	61	11	0	0	0	83	50	12	61	10	0	0	0	83	50	12	61	10	0	0	0	83	50
197-200	16	74	11	0	0	0	101	60	16	74	11	0	0	0	101	60	16	74	11	0	0	0	101	60	16	74	10	0	0	0	100	60

TABLE 10-2 (Contd.)

CROSS-OVER PROBLEM, B-AL (VF=0.30)

MICROSTRESS DISTRIBUTION FOR COMPOSITE STRESS S22=100

ELTS	SXX	SYY	SZZ	SXY	SXZ	SYZ	SKK	EQS	SXX	SYY	SZZ	SXY	SXZ	SYZ	SKK	EQS	SXX	SYY	SZZ	SXY	SXZ	SYZ	SKK	EQS	SXX	SYY	SZZ	SXY	SXZ	SYZ	SKK	EQS
201-204	20	89	9	0	0	-1	118	75	20	89	8	0	0	-1	117	75	20	89	8	0	0	-1	117	75	20	89	8	0	0	-1	117	75
205-208	23	101	6	0	0	0	130	87	23	101	6	0	0	0	130	87	23	101	6	0	0	0	130	87	23	101	6	0	0	0	130	87
209-212	-2	45	-12	0	0	0	31	54	-2	45	-14	0	-1	0	29	54	-1	45	-16	0	-1	0	28	55	-1	44	-17	0	0	0	26	56
213-216	2	51	-4	0	0	1	49	52	2	50	-5	0	0	1	47	52	2	50	-6	0	0	1	46	53	3	50	-7	0	0	1	46	53
217-220	7	55	5	0	0	1	67	49	7	55	4	0	0	1	66	49	7	55	3	0	0	1	65	49	8	55	2	0	0	1	65	49
221-224	10	59	10	0	0	0	79	48	10	59	10	0	0	0	79	48	10	58	9	0	0	0	77	48	11	58	9	0	0	0	78	48
225-228	13	65	12	0	0	0	90	53	13	65	12	0	0	0	90	53	13	65	11	0	0	0	89	52	13	65	11	0	0	0	89	52
229-232	17	78	11	0	0	-1	106	63	17	78	11	0	0	-1	106	63	17	78	11	0	0	-2	106	63	17	77	10	0	0	-2	104	63
233-236	21	92	9	0	0	-2	122	77	21	92	9	0	0	-2	122	77	21	92	9	0	0	-2	122	77	22	92	9	0	0	-2	123	77
237-240	24	103	8	0	0	-1	135	87	25	103	8	0	0	-1	136	87	25	103	8	0	0	-1	136	87	25	103	8	0	0	-1	136	88
241-244	-4	38	-13	0	0	-1	21	48	-4	38	-15	0	0	-1	19	49	-4	37	-17	0	-1	-1	16	50	-4	37	-18	0	0	-1	15	51
245-248	0	47	-8	0	0	-2	39	52	0	47	-9	0	0	-2	38	53	0	47	-10	0	0	-2	37	53	0	47	-11	0	0	-2	36	54
249-252	6	56	0	0	0	-1	62	53	6	56	0	0	0	-1	62	54	6	56	-1	0	0	-1	61	54	6	56	-2	0	0	-1	60	54
253-256	10	62	7	0	0	-1	79	53	10	62	7	0	0	-1	79	53	10	62	6	0	0	-1	78	53	11	62	6	0	0	-1	79	53
257-260	14	71	11	0	0	-1	96	58	14	71	11	0	0	-1	96	58	15	70	10	0	0	-1	95	58	15	70	10	0	0	-1	95	58
261-264	19	83	12	0	0	-2	114	68	19	83	11	0	0	-2	113	68	19	83	11	0	0	-2	113	68	19	83	11	0	0	-2	113	68
265-268	24	97	12	0	0	-2	133	78	24	97	12	0	0	-2	133	78	24	97	12	0	0	-2	133	78	24	97	12	0	0	-2	133	79
269-272	27	106	14	0	0	0	147	86	27	106	14	0	0	0	147	86	27	106	13	0	0	0	146	86	28	106	13	0	0	0	147	86
273-276	-8	26	-13	0	0	-6	5	39	-8	25	-14	0	0	-6	3	39	-8	25	-16	0	-1	-6	1	40	-8	24	-17	0	0	-6	-1	40
277-280	-2	42	-14	0	0	-12	26	56	-3	42	-15	0	0	-12	24	57	-3	42	-16	0	0	-12	23	57	-3	42	-17	0	0	-12	22	58
281-284	3	59	-10	0	0	-10	52	67	3	59	-11	0	0	-10	51	67	3	59	-12	0	0	-10	50	67	3	59	-12	0	0	-10	50	68
285-288	8	69	-6	0	0	-6	71	70	8	69	-6	0	0	-6	71	70	8	69	-7	0	0	-6	70	70	8	69	-7	0	0	-6	70	71
289-292	18	85	6	0	0	0	109	73	18	85	6	0	0	0	109	74	18	85	6	0	0	0	109	74	18	85	5	0	0	0	108	74
293-296	22	94	11	0	0	2	127	77	22	94	10	0	0	2	126	77	22	94	10	0	0	2	126	78	22	94	10	0	0	2	126	78
297-300	28	102	19	0	0	3	149	79	28	102	19	0	0	3	149	79	28	102	19	0	0	4	149	79	28	102	19	0	0	4	149	79
301-304	32	108	27	0	0	2	167	77	32	108	27	0	0	2	167	77	32	108	27	0	0	2	167	77	32	108	27	0	0	2	167	77
305-308	-46	97	-7	0	0	0	44	129	-46	97	-8	0	0	0	43	129	-45	97	-9	0	-1	0	43	129	-45	97	-10	0	0	0	42	129
309-312	-46	98	-7	0	0	1	45	129	-46	98	-8	0	0	1	44	129	-45	98	-9	0	0	1	44	129	-45	98	-10	0	0	1	43	129
313-316	-46	99	-9	0	0	2	44	131	-46	99	-9	0	0	2	44	131	-45	99	-10	0	0	2	44	131	-45	99	-11	0	0	2	43	131
317-320	-46	101	-10	0	0	2	45	133	-46	101	-10	0	0	2	45	133	-45	101	-11	0	0	1	45	133	-45	101	-12	0	0	1	44	133
321-324	-45	103	-10	0	0	2	48	135	-45	103	-10	0	0	2	48	135	-45	103	-11	0	0	2	47	134	-44	103	-11	0	0	2	48	134
325-328	-45	104	-10	0	0	0	49	135	-45	104	-11	0	0	0	48	135	-45	104	-11	0	0	0	48	135	-44	104	-12	0	0	0	48	135
329-332	-46	99	-9	0	0	0	44	131	-46	99	-9	0	0	0	44	131	-45	99	-10	0	0	0	44	131	-45	99	-11	0	0	0	43	131
333-336	-46	100	-9	0	0	1	45	132	-46	100	-9	0	0	1	45	132	-45	100	-10	0	0	1	45	132	-45	100	-11	0	0	1	44	132
337-340	-46	102	-9	0	0	1	47	134	-45	102	-10	0	0	1	47	134	-45	102	-11	0	0	1	46	133	-45	102	-11	0	0	1	46	133
341-344	-46	102	-10	0	0	0	46	134	-45	102	-11	0	0	0	46	134	-45	102	-11	0	0	0	46	134	-45	102	-12	0	0	0	45	134
345-348	-46	101	-10	0	0	0	45	133	-46	101	-10	0	0	0	45	133	-45	101	-11	0	0	0	45	133	-45	101	-11	0	0	0	45	133
349-352	-46	101	-10	0	0	0	45	133	-45	101	-10	0	0	0	46	133	-45	101	-11	0	0	0	45	133	-45	102	-11	0	0	0	46	133

TABLE 10-3

CROSS-OVER PROBLEM, B-AL (VF=0.30)

MICROSTRESS DISTRIBUTION FOR COMPOSITE STRESS S33=100

ELTS	SXX	SYY	SZZ	SXY	SXZ	SYZ	SKK	EQS	SXX	SYY	SZZ	SXY	SXZ	SYZ	SKK	EQS	SXX	SYY	SZZ	SXY	SXZ	SYZ	SKK	EQS	SXX	SYY	SZZ	SXY	SXZ	SYZ	SKK	EQS
1- 4	-1	-68	141	0	0	0	72	186	-2	-65	136	0	0	-1	69	178	-2	-61	129	0	0	-1	65	168	-2	-58	123	0	0	0	63	160
5- 8	-1	-69	141	0	0	0	71	186	-1	-65	136	0	0	-1	70	178	-1	-61	128	0	0	-1	66	167	-1	-57	123	0	0	0	65	160
9- 12	-2	-69	140	0	0	0	69	185	-2	-65	135	0	0	-1	68	178	-2	-61	128	0	0	-1	65	167	-3	-57	123	0	0	0	63	160
13- 16	-1	-69	141	0	0	-1	71	186	-2	-65	135	0	0	-3	68	178	-2	-61	128	0	0	-2	65	167	-3	-57	122	0	0	-1	62	160
17- 20	0	-69	142	0	0	-1	73	186	-1	-65	136	0	0	-4	70	178	-1	-60	127	0	0	-4	66	167	-1	-57	121	0	0	-1	63	158
21- 24	0	-69	142	0	0	-2	73	186	0	-65	136	0	0	-4	71	178	0	-60	127	0	0	-4	67	166	0	-57	121	0	0	-2	64	157
25- 28	-2	-70	140	0	0	0	68	186	-3	-66	134	0	0	-1	65	178	-3	-61	127	0	0	-1	63	167	-4	-57	121	0	0	0	60	159
29- 32	-1	-70	140	0	1	-1	69	186	-2	-66	134	0	1	-3	66	177	-3	-61	126	0	1	-3	62	166	-3	-57	120	0	1	-1	60	158
33- 36	0	-69	142	0	0	-1	73	187	-1	-65	136	0	0	-4	70	178	-1	-60	127	0	0	-4	66	166	-2	-56	121	0	1	-1	63	158
37- 40	0	-69	144	0	1	-2	75	188	0	-65	136	0	1	-6	71	179	0	-60	127	0	1	-5	67	166	-1	-56	120	0	1	-2	63	156
41- 44	1	-69	145	0	0	-3	77	189	1	-65	136	0	0	-8	72	178	0	-60	125	0	0	-7	65	164	0	-56	117	0	0	-3	61	153
45- 48	2	-69	145	0	0	-3	78	189	1	-65	136	0	0	-8	72	178	0	-60	125	0	0	-8	65	164	0	-56	117	0	0	-3	61	153
49- 52	-11	-7	45	0	6	0	27	55	-11	-7	43	-1	6	0	25	54	-12	-6	40	-1	6	0	22	51	-12	-5	39	0	5	0	22	50
53- 56	-8	-2	58	0	15	0	48	70	-9	-2	56	-1	15	-1	45	68	-10	-1	53	-1	14	-1	42	65	-11	-1	51	0	14	0	39	62
57- 60	-4	3	76	0	18	-1	75	82	-5	4	72	-1	17	-2	71	79	-6	4	68	-1	16	-2	66	75	-7	5	65	0	15	-1	63	72
61- 64	0	8	88	0	16	-1	96	88	-1	9	84	-1	15	-3	92	85	-2	9	79	-1	14	-3	86	79	-3	10	75	0	13	-1	82	76
65- 68	13	21	112	0	9	-1	146	96	12	21	106	-1	9	-4	139	91	11	21	99	-1	8	-4	131	84	10	21	93	0	7	-1	124	79
69- 72	19	27	127	0	5	-2	173	104	17	27	119	-1	4	-5	163	98	15	26	109	-1	4	-5	150	89	14	25	102	0	3	-2	141	83
73- 76	33	37	144	0	0	-2	214	108	31	36	134	-1	0	-6	201	100	27	34	121	-1	-1	-6	182	91	25	32	112	0	-1	-2	109	83
77- 80	50	46	154	0	-2	-3	250	105	46	44	142	0	-2	-8	232	97	41	40	127	0	-2	-7	208	86	38	37	116	0	-2	-3	191	78
81- 84	-14	-3	65	0	1	0	48	75	-15	-2	63	0	1	0	46	73	-15	0	60	0	1	0	45	69	-16	0	58	0	1	0	42	67
85- 88	-6	0	71	0	4	0	65	75	-7	1	68	0	4	-1	62	72	-8	3	64	0	3	-1	59	68	-9	4	61	0	3	0	56	65
89- 92	4	6	79	0	5	-1	89	74	3	7	75	0	5	-3	85	70	1	8	70	0	5	-3	79	65	0	10	66	0	4	-1	76	62
93- 96	16	11	86	0	6	-2	113	73	14	12	81	0	6	-4	107	69	12	14	74	0	6	-4	100	62	10	15	69	0	5	-2	94	57
97-100	22	15	95	0	7	-2	133	78	20	17	90	0	7	-5	127	72	18	19	81	0	6	-5	118	65	16	20	75	0	6	-2	111	58
101-104	25	21	113	0	9	-2	159	90	23	23	105	0	9	-6	151	83	20	24	94	0	8	-5	138	74	18	24	87	0	7	-2	129	67
105-108	30	30	134	0	7	-3	194	104	28	30	123	0	7	-6	181	95	24	30	110	0	6	-6	164	84	21	30	101	0	5	-2	152	75
109-112	37	38	151	0	2	-3	226	113	34	38	139	0	2	-7	211	103	30	37	123	0	1	-7	190	90	27	36	111	0	1	-3	174	80
113-116	-14	0	74	0	0	0	60	82	-14	0	72	0	0	0	58	80	-15	2	68	0	0	0	55	76	-15	3	66	0	0	0	54	74
117-120	-4	2	77	0	0	-1	75	78	-5	4	74	0	0	-2	73	75	-5	6	70	0	0	-2	71	70	-6	7	67	0	0	-1	63	67
121-124	9	7	82	0	2	-1	98	73	8	9	77	0	2	-4	94	69	6	11	72	0	2	-3	89	63	5	13	67	0	1	-1	85	59
125-128	21	12	89	0	3	-2	121	72	19	13	82	0	3	-5	114	66	16	16	74	0	3	-5	106	58	14	17	68	0	3	-2	99	52
129-132	26	14	94	0	6	-3	134	75	24	17	87	0	5	-6	128	68	21	19	77	0	5	-6	117	59	18	20	70	0	5	-3	108	52
133-136	27	18	107	0	9	-3	152	85	25	21	98	0	9	-7	144	77	21	22	87	0	8	-6	130	67	19	23	79	0	8	-3	121	59
137-140	29	25	128	0	10	-3	182	102	26	27	117	0	9	-8	170	92	22	28	103	0	8	-6	153	79	19	29	93	0	8	-3	141	70
141-144	31	32	148	0	4	-3	211	116	28	34	135	0	4	-8	197	104	24	34	118	0	3	-7	176	90	21	34	106	0	3	-3	161	79
145-148	-12	0	78	0	0	0	66	85	-13	2	75	0	0	0	64	82	-13	4	72	0	0	0	63	78	-14	5	69	0	0	0	60	75
149-152	-2	3	80	0	0	-1	81	79	-2	5	76	0	0	-2	79	75	-3	7	72	0	0	-2	76	70	-4	9	69	0	0	-1	74	67
153-156	12	8	84	0	0	-2	104	74	11	10	79	0	0	-4	100	69	9	13	73	0	0	-4	95	62	7	14	68	0	0	-2	89	57
157-160	25	13	92	0	2	-3	130	73	22	16	85	0	2	-6	123	67	19	18	76	0	2	-6	113	58	17	19	69	0	2	-3	105	51
161-164	29	15	96	0	4	-3	140	75	26	18	87	0	4	-7	131	67	23	20	77	0	4	-6	120	57	19	20	68	0	4	-3	107	49
165-168	29	18	106	0	8	-3	153	84	26	20	95	0	8	-8	141	75	22	22	83	0	7	-6	127	63	18	22	74	0	7	-3	114	55
169-172	28	23	125	0	10	-4	176	100	25	25	113	0	9	-8	163	89	21	27	98	0	9	-7	146	76	17	27	87	0	8	-3	131	67
173-176	29	29	145	0	5	-4	203	116	25	31	131	0	4	-8	187	103	21	32	113	0	4	-7	166	88	17	31	101	0	4	-3	149	77
177-180	31	17	101	0	3	-4	149	77	32	21	113	0	7	-4	166	88	31	25	131	0	9	-4	187	103	29	29	145	0	4	-4	203	116
181-184	26	17	87	0	3	-8	130	67	27	21	98	0	7	-9	146	76	25	25	112	0	8	-9	162	89	23	28	125	0	4	-10	176	100
185-188	22	18	74	0	3	-7	114	55	22	22	83	0	7	-7	127	63	20	26	95	0	8	-8	141	75	18	29	106	0	4	-8	153	84
189-192	20	19	68	0	3	-4	107	49	20	23	77	0	6	-4	120	57	18	26	87	0	8	-4	131	67	15	29	96	0	3	-4	140	75
193-196	19	17	69	0	3	-1	105	51	18	19	76	0	6	-2	113	58	16	22	85	0	7	-2	123	67	13	25	92	0	3	-2	130	73
197-200	14	7	68	0	2	0	89	57	13	9	73	0	4	0	95	62	10	11	79	0	4	0	100	69	8	12	84	0	2	0	104	74

TABLE 10-3 (Contd.)

CROSS-OVER PROBLEM, B-AL (VF=0.30)

MICROSTRESS DISTRIBUTION FOR COMPOSITE STRESS S33=100

ELTS	SXX	SYY	SZZ	SXY	SXZ	SYZ	SKK	EQS	SXX	SYY	SZZ	SXY	SXZ	SYZ	SKK	EQS	SXX	SYY	SZZ	SXY	SXZ	SYZ	SKK	EQS	SXX	SYY	SZZ	SXY	SXZ	SYZ	SKK	EQS
201-204	9	-4	69	0	1	0	74	67	7	-3	72	0	2	0	76	71	5	-2	76	0	2	0	79	75	4	-2	80	0	1	0	82	79
205-208	5	-14	69	0	0	0	60	75	4	-13	72	0	0	0	63	78	2	-13	75	0	0	0	64	82	0	-12	78	0	0	0	66	85
209-212	34	21	106	0	3	-3	161	79	34	24	118	0	7	-3	176	90	34	28	135	0	8	-4	197	104	32	31	148	0	3	-4	211	116
213-216	29	19	93	0	3	-8	141	70	28	22	103	0	6	-8	153	79	27	26	117	0	7	-9	170	92	25	29	128	0	3	-9	182	102
217-220	23	19	78	0	3	-8	120	59	22	21	87	0	6	-8	130	67	21	25	98	0	7	-9	144	77	18	27	107	0	3	-9	152	85
221-224	20	18	71	0	3	-5	109	52	19	21	78	0	6	-5	118	59	17	24	87	0	6	-5	128	68	14	26	94	0	3	-6	134	75
225-228	17	14	68	0	2	-3	99	52	16	16	74	0	5	-3	106	58	13	19	82	0	5	-3	114	66	12	21	88	0	2	-3	121	72
229-232	13	5	67	0	1	-1	85	59	11	6	72	0	4	-2	89	63	9	8	77	0	4	-2	94	69	7	9	82	0	1	-2	98	73
233-236	7	-6	67	0	1	0	68	67	6	-5	70	0	2	0	71	70	4	-4	74	0	2	0	74	75	2	-4	77	0	1	0	75	78
237-240	3	-15	66	0	0	0	54	74	2	-15	68	0	0	0	55	76	0	-14	72	0	0	0	58	80	0	-14	74	0	0	0	60	83
241-244	36	27	111	0	3	-1	174	80	37	30	123	0	7	-1	190	90	38	34	139	0	7	-2	211	103	38	37	151	0	3	-2	226	113
245-248	30	21	101	0	2	-5	152	75	30	24	110	0	6	-6	164	84	30	28	123	0	7	-6	181	95	30	30	134	0	3	-7	194	104
249-252	24	18	87	0	2	-7	129	67	24	20	94	0	5	-8	138	74	23	23	105	0	6	-8	151	83	21	25	113	0	2	-9	159	90
253-256	20	16	75	0	2	-6	111	58	19	18	81	0	5	-6	118	64	17	20	90	0	5	-7	127	72	15	22	96	0	2	-7	133	78
257-260	15	10	69	0	2	-5	94	57	14	12	74	0	4	-5	100	62	12	14	81	0	4	-6	107	69	11	16	86	0	2	-6	113	73
261-264	10	0	66	0	1	-4	76	62	8	1	70	0	3	-5	79	65	7	3	75	0	3	-5	85	70	6	4	79	0	1	-5	89	74
265-268	4	-9	61	0	0	-3	56	65	3	-8	64	0	1	-3	59	68	1	-7	68	0	2	-3	62	72	0	-6	71	0	0	-4	65	75
269-272	0	-16	58	0	0	-1	42	67	0	-15	60	0	0	-1	45	69	-2	-15	63	0	0	-1	46	73	-3	-14	65	0	0	-1	48	75
273-276	37	37	116	0	3	2	190	78	40	41	127	0	7	2	208	86	44	46	142	0	8	2	232	97	46	50	154	0	3	2	250	105
277-280	32	25	112	0	2	1	169	83	34	27	121	-1	6	1	182	91	36	31	134	-1	6	0	201	101	38	33	144	0	2	0	215	108
281-284	25	13	102	0	2	-3	140	83	26	15	109	-1	5	-4	150	89	27	17	119	-1	5	-4	163	98	27	19	127	0	2	-5	173	104
285-288	21	10	93	0	1	-7	124	79	21	11	99	-1	4	-7	131	84	21	12	106	-1	4	-8	139	91	21	13	112	0	1	-9	146	96
289-292	10	-3	75	0	1	-13	82	76	9	-2	79	-1	3	-14	86	79	9	-1	84	-1	3	-15	92	85	8	0	88	0	1	-15	96	88
293-296	5	-7	65	0	1	-15	63	72	4	-6	68	-1	2	-16	66	75	4	-5	72	-1	2	-16	71	79	3	-4	76	0	1	-17	75	82
297-300	-1	-11	51	0	0	-13	39	62	-1	-10	53	-1	1	-14	42	65	-2	-9	56	-1	1	-14	45	68	-2	-8	59	0	0	-15	43	70
301-304	-5	-12	39	0	0	-5	22	50	-6	-12	40	-1	0	-6	22	51	-7	-11	43	-1	0	-6	25	54	-7	-10	45	0	0	-6	28	55
305-308	-56	0	117	0	3	0	61	153	-60	0	125	0	8	0	65	164	-65	1	136	0	8	0	72	178	-69	2	145	0	3	0	78	189
309-312	-56	0	117	0	3	0	61	153	-60	0	125	0	7	0	65	164	-65	1	136	0	8	0	72	178	-69	1	145	0	3	0	77	189
313-316	-56	-1	120	0	2	-1	63	156	-60	0	127	0	5	-1	67	166	-65	0	136	0	6	-1	71	179	-69	0	144	0	2	-1	75	188
317-320	-56	-2	121	0	1	-1	63	158	-60	-1	127	0	4	0	66	166	-65	-1	136	0	4	0	70	178	-69	0	142	0	1	0	73	187
321-324	-57	-3	120	0	1	-1	60	158	-61	-3	126	0	3	-1	62	166	-66	-2	134	0	3	-1	66	177	-70	-1	140	0	1	-1	69	186
325-328	-57	-4	122	0	0	0	61	159	-61	-3	127	0	1	0	63	167	-66	-2	135	0	1	0	67	178	-70	-2	140	0	0	0	68	186
329-332	-57	0	121	0	2	0	64	157	-60	0	127	0	4	0	67	166	-65	0	136	0	4	0	71	178	-69	0	142	0	2	0	73	186
333-336	-57	-1	122	0	1	0	64	158	-60	-1	127	0	4	0	66	167	-65	-1	136	0	4	0	70	178	-69	0	142	0	1	0	73	186
337-340	-57	-3	122	0	1	0	62	160	-61	-2	128	0	3	0	65	167	-65	-2	136	0	3	0	69	178	-69	-1	141	0	1	0	71	186
341-344	-57	-3	123	0	0	0	63	160	-61	-2	128	0	1	0	65	168	-65	-2	135	0	1	0	68	178	-69	-1	141	0	0	0	71	185
345-348	-57	-1	123	0	0	0	65	160	-60	-1	128	0	1	0	67	168	-65	-1	136	0	1	0	70	178	-69	-1	142	0	0	0	72	186
349-352	-58	-2	123	0	0	0	63	160	-61	-2	128	0	1	0	65	168	-65	-2	136	0	1	0	69	178	-68	-1	142	0	0	0	73	186

TABLE 10-4

CROSS-OVER PROBLEM, B-AL (VF=0.30)

MICROSTRESS DISTRIBUTION FOR COMPOSITE STRESS S12=100

ELTS	SXX	SYY	SZZ	SXY	SXZ	SYZ	SKK	EQS	SXX	SYY	SZZ	SXY	SXZ	SYZ	SKK	EQS	SXX	SYY	SZZ	SXY	SXZ	SYZ	SKK	EQS	SXX	SYY	SZZ	SXY	SXZ	SYZ	SKK	EQS
1- 4	0	0	0	137	0	0	0	236	0	0	0	140	0	0	0	241	0	0	0	143	0	0	0	247	0	0	0	146	0	0	0	251
5- 8	0	0	0	137	0	0	0	235	0	0	0	139	-1	0	0	240	0	0	0	143	-1	0	0	247	0	0	0	146	0	0	0	251
9- 12	0	0	0	138	0	0	0	238	0	-1	0	141	0	0	-1	242	0	-1	0	144	0	0	-1	248	0	0	0	146	0	0	0	252
13- 16	0	0	0	138	0	0	0	237	0	-1	0	140	-1	-1	-1	241	0	-1	0	144	-1	-1	-1	248	0	0	0	146	0	-1	0	252
17- 20	0	0	0	136	0	0	0	234	0	0	0	139	-2	0	0	239	0	0	0	143	-2	0	0	247	0	0	0	146	0	-1	0	252
21- 24	0	0	0	134	-1	0	0	231	0	0	0	138	-2	0	0	238	0	0	0	143	-2	0	0	246	0	0	0	146	-1	0	0	252
25- 28	0	-1	0	141	0	0	-1	242	0	-3	1	143	0	0	-2	246	0	-3	1	145	0	0	-2	250	0	-1	0	147	0	-1	-1	254
29- 32	0	-1	0	140	0	-2	-1	240	0	-4	0	142	-1	-2	-4	245	0	-4	0	145	-1	-3	-4	250	0	-1	0	147	0	-3	-1	254
33- 36	0	-1	0	137	-1	-1	-1	235	0	-2	1	140	-2	-1	-1	241	0	-2	1	144	-2	-2	-1	248	0	-1	0	147	-1	-3	-1	252
37- 40	0	0	0	134	-1	-1	0	231	0	-2	1	138	-4	-1	-1	238	0	-2	1	143	-3	-2	-1	247	0	-1	0	147	-1	-3	-1	253
41- 44	0	0	0	131	-2	0	0	226	0	-2	0	137	-5	0	-2	235	0	-2	0	143	-5	-2	-2	247	0	0	0	148	-2	-3	0	254
45- 48	0	0	0	131	-2	0	0	225	0	0	0	136	-5	0	0	234	0	0	0	143	-5	0	0	246	0	0	0	147	-2	-1	0	254
49- 52	0	0	0	132	0	9	0	227	0	-1	0	133	0	9	-1	229	0	-1	0	134	0	9	-1	231	0	0	0	135	0	9	0	232
53- 56	0	0	0	121	0	25	0	213	-1	-1	0	122	0	25	-2	215	-1	-1	0	123	0	25	-2	217	0	0	0	124	0	26	0	219
57- 60	0	0	0	106	0	34	0	192	-1	-1	0	107	-1	34	-2	194	-1	-1	0	108	-1	35	-2	196	0	0	0	109	0	35	0	198
61- 64	0	0	0	92	-1	37	0	170	-1	0	0	93	-2	37	-1	173	-1	0	0	94	-2	38	-1	175	0	0	0	96	0	38	0	177
65- 68	0	0	0	77	-1	43	0	152	-2	-1	0	78	-3	43	-3	154	-2	-1	0	81	-2	43	-3	158	0	0	0	82	-1	43	0	160
69- 72	-1	0	0	61	-1	43	-1	129	-3	-1	0	63	-3	43	-4	132	-3	-1	0	65	-3	43	-4	135	-1	0	0	67	-1	44	-1	138
73- 76	-1	0	0	42	-2	34	-1	95	-3	-1	0	44	-5	35	-4	98	-3	-1	0	47	-5	35	-4	102	-1	0	0	48	-2	35	-1	104
77- 80	0	0	0	28	-3	14	0	55	-2	0	0	30	-7	14	-2	59	-1	0	0	32	-7	14	-1	63	0	0	0	34	-2	14	0	64
81- 84	0	0	0	120	0	6	0	207	0	0	0	121	0	6	0	208	0	0	0	122	0	6	0	210	0	0	0	122	0	6	0	211
85- 88	0	0	0	111	0	15	0	193	-1	0	0	112	-1	15	-1	194	-1	0	0	113	0	16	-1	196	0	0	0	114	0	16	0	198
89- 92	0	0	0	98	0	20	0	172	-1	0	0	99	-2	20	-1	174	-1	0	0	100	-2	20	-1	177	0	0	0	101	0	20	0	178
93- 96	0	0	0	85	-1	20	0	151	-1	0	0	87	-3	20	-1	155	-1	0	0	89	-3	20	-1	158	0	0	0	91	-1	20	0	161
97-100	0	0	0	75	-2	24	0	136	-1	0	0	77	-4	24	-1	140	-1	0	0	81	-4	24	-1	145	0	0	0	83	-1	24	0	148
101-104	0	0	0	63	-2	28	0	120	-1	0	0	66	-5	28	-1	125	-1	0	0	70	-5	28	-1	130	0	0	0	72	-2	28	0	134
105-108	0	0	0	48	-2	25	0	94	-1	0	-1	51	-6	25	-2	100	-1	0	-1	55	-6	25	-2	106	0	0	0	57	-2	26	0	109
109-112	0	0	0	35	-3	10	0	64	0	0	0	38	-7	11	0	71	0	0	0	43	-7	11	0	77	0	0	0	45	-2	11	0	81
113-116	0	0	0	113	0	3	0	195	0	0	0	114	0	3	0	197	0	0	0	115	0	3	0	198	0	0	0	116	0	3	0	199
117-120	0	0	0	105	0	8	0	181	-1	0	0	106	-1	8	-1	183	-1	0	0	107	-1	8	-1	185	0	0	0	108	0	8	0	186
121-124	0	0	0	92	-1	10	0	160	-1	0	0	94	-2	10	-1	163	-1	0	0	96	-2	10	-1	167	0	0	0	97	-1	10	0	169
125-128	0	0	0	81	-2	9	0	140	0	0	0	83	-5	9	0	145	0	0	0	87	-4	10	0	151	0	0	0	89	-1	10	0	154
129-132	0	0	0	71	-2	13	0	125	0	0	0	75	-6	13	0	133	0	0	0	80	-6	13	0	141	0	0	0	83	-2	13	0	145
133-136	0	0	0	63	-3	19	0	113	0	0	0	67	-7	19	0	121	0	0	0	72	-6	19	0	130	0	0	0	76	-2	19	0	135
137-140	0	0	0	50	-3	19	0	93	0	0	-1	55	-8	19	-1	102	0	0	-1	61	-7	19	-1	111	0	0	0	64	-3	19	0	116
141-144	0	0	0	39	-3	8	0	70	0	0	0	44	-8	8	0	80	0	0	0	50	-8	8	0	89	0	0	0	54	-3	8	0	95
145-148	0	0	0	110	0	1	0	189	0	0	0	111	0	1	0	191	0	0	0	112	0	1	0	192	0	0	0	112	0	1	0	193
149-152	0	0	0	101	0	2	0	174	0	0	0	102	-1	2	0	176	0	0	0	104	-1	2	0	178	0	0	0	104	0	2	0	180
153-156	0	0	0	88	-1	2	0	152	-1	0	0	90	-3	2	-1	156	-1	0	0	93	-3	3	-1	161	0	0	0	95	-1	3	0	163
157-160	0	0	0	76	-2	2	0	130	-1	0	0	80	-6	2	-1	138	0	0	0	85	-6	2	0	147	0	0	0	86	-2	2	0	151
161-164	0	0	0	66	-3	6	0	116	0	0	0	73	-8	6	0	127	0	0	0	80	-7	6	0	139	0	0	0	84	-3	6	0	145
165-168	0	0	0	60	-4	12	0	107	0	0	-1	67	-9	12	-1	119	0	0	-1	74	-8	12	-1	131	0	1	0	79	-3	12	1	138
169-172	0	0	0	50	-4	14	0	91	0	0	-1	57	-10	14	-1	104	0	0	-1	65	-9	14	-1	116	0	1	0	70	-3	15	1	123
173-176	0	0	0	41	-4	7	0	73	0	0	0	48	-10	7	0	87	0	0	0	56	-9	7	0	100	0	0	0	61	-3	7	0	106
177-180	0	0	0	61	-7	3	0	107	0	0	0	56	-6	9	0	100	0	0	0	48	-6	11	0	87	0	0	0	41	-6	4	0	73
181-184	1	0	0	70	-14	3	1	123	0	0	-1	65	-14	9	-1	116	0	0	-1	57	-14	10	-1	104	0	0	0	50	-14	4	0	91
185-188	1	0	0	79	-12	3	1	138	0	0	-1	74	-12	9	-1	131	0	0	-1	67	-12	9	-1	119	0	0	0	60	-12	4	0	107
189-192	0	0	0	84	-5	3	0	145	0	0	0	80	-5	8	0	139	0	0	0	73	-6	8	0	127	0	0	0	66	-6	3	0	116
193-196	0	0	0	88	-2	2	0	151	0	0	0	85	-2	6	0	147	0	-1	0	80	-2	6	-1	138	0	0	0	75	-2	2	0	130
197-200	0	0	0	95	-3	1	0	163	0	-1	0	93	-2	3	-1	161	0	-1	0	90	-2	3	-1	156	0	0	0	88	-2	1	0	152

TABLE 10-4 (Contd.)

CROSS-OVER PROBLEM, B-AL (VF=0.30)

MICROSTRESS DISTRIBUTION FOR COMPOSITE STRESS S12=100

ELTS	SXX	SYY	SZZ	SXY	SXZ	SYZ	SKK	EQS	SXX	SYY	SZZ	SXY	SXZ	SYZ	SKK	EQS	SXX	SYY	SZZ	SXY	SXZ	SYZ	SKK	EQS	SXX	SYY	SZZ	SXY	SXZ	SYZ	SKK	EQS
201-204	0	0	0	104	-2	0	0	180	0	0	0	104	-2	1	0	178	0	0	0	102	-2	1	0	176	0	0	0	101	-2	0	0	174
205-208	0	0	0	112	-1	0	0	193	0	0	0	111	-1	0	0	192	0	0	0	111	-1	0	0	191	0	0	0	110	-1	0	0	189
209-212	0	0	0	54	-8	3	0	95	0	0	0	50	-8	8	0	89	0	0	0	44	-8	9	0	80	0	0	0	39	-8	3	0	70
213-216	0	0	0	64	-19	3	0	116	0	0	-1	61	-19	7	-1	111	0	0	-1	55	-19	8	-1	102	0	0	0	50	-19	3	0	93
217-220	0	0	0	76	-18	2	0	135	0	0	0	72	-18	6	0	130	0	0	0	67	-18	7	0	121	0	0	0	63	-19	3	0	113
221-224	0	0	0	83	-13	2	0	146	0	0	0	80	-13	6	0	141	0	0	0	75	-13	6	0	133	0	0	0	71	-13	2	0	125
225-228	0	0	0	89	-9	1	0	154	0	0	0	87	-9	4	0	151	0	0	0	83	-9	5	0	145	0	0	0	81	-9	2	0	140
229-232	0	0	0	97	-10	1	0	169	0	-1	0	96	-10	2	-1	167	0	-1	0	94	-10	3	-1	163	0	0	0	92	-10	1	0	160
233-236	0	0	0	108	-8	0	0	186	0	-1	0	107	-8	1	-1	185	0	-1	0	106	-8	1	-1	183	0	0	0	105	-8	0	0	181
237-240	0	0	0	116	-3	0	0	199	0	0	0	115	-3	0	0	198	0	0	0	114	-3	0	0	196	0	0	0	113	-3	0	0	195
241-244	0	0	0	45	-10	2	0	81	0	0	0	43	-10	7	0	77	0	-1	0	38	-10	7	-1	71	0	0	0	35	-10	3	0	64
245-248	0	0	0	57	-25	2	0	109	0	-1	-1	55	-25	6	-2	106	0	-1	-1	51	-25	6	-2	100	0	0	0	48	-25	2	0	94
249-252	0	0	0	72	-28	2	0	134	0	-1	0	70	-28	5	-1	130	0	-1	0	66	-28	5	-1	125	0	0	0	63	-28	2	0	120
253-256	0	0	0	83	-23	1	0	148	0	-1	0	80	-23	4	-1	145	0	-1	0	77	-23	4	-1	140	0	0	0	75	-24	2	0	136
257-260	0	0	0	91	-20	1	0	161	0	-1	0	89	-20	3	-1	158	0	-1	0	87	-20	3	-1	155	0	0	0	85	-19	1	0	151
261-264	0	0	0	101	-20	0	0	178	0	-1	0	100	-20	2	-1	177	0	-1	0	99	-20	2	-1	174	0	0	0	98	-19	0	0	172
265-268	0	0	0	114	-15	0	0	198	0	-1	0	113	-15	1	-1	196	0	-1	0	112	-15	1	-1	194	0	0	0	111	-15	0	0	193
269-272	0	0	0	122	-6	0	0	211	0	0	0	122	-6	0	0	210	0	0	0	121	-6	0	0	208	0	0	0	120	-6	0	0	207
273-276	0	0	0	34	-14	2	0	64	0	-1	0	32	-14	7	-1	63	0	-2	0	30	-13	7	-2	59	0	0	0	28	-13	3	0	55
277-280	0	-1	0	48	-35	2	-1	104	-1	-3	0	47	-34	5	-4	102	-1	-3	0	44	-34	5	-4	98	0	-1	0	42	-34	2	-1	95
281-284	0	-1	0	67	-43	1	-1	138	-1	-3	0	65	-42	3	-4	136	-1	-3	0	63	-42	3	-4	132	0	-1	0	61	-42	1	-1	129
285-288	0	0	0	82	-42	1	0	160	-1	-2	0	80	-42	2	-3	158	-1	-2	0	78	-42	3	-3	154	0	0	0	77	-42	1	0	152
289-292	0	0	0	96	-37	0	0	177	0	-1	0	94	-37	2	-1	175	0	-1	0	93	-36	2	-1	173	0	0	0	92	-36	1	0	170
293-296	0	0	0	109	-34	0	0	198	-1	-1	0	108	-34	1	-2	196	-1	-1	0	107	-34	1	-2	194	0	0	0	106	-33	0	0	192
297-300	0	0	0	124	-25	0	0	219	-1	-1	0	123	-25	0	-2	217	-1	-1	0	122	-25	0	-2	215	0	0	0	121	-25	0	0	213
301-304	0	0	0	135	-9	0	0	232	-1	0	0	134	-9	0	-1	231	-1	0	0	133	-9	0	-1	229	0	0	0	132	-9	0	0	227
305-308	0	0	0	148	1	2	0	254	0	0	0	143	0	5	0	246	0	0	0	136	0	5	0	234	0	0	0	131	0	2	0	225
309-312	0	0	0	148	3	2	0	254	-2	0	0	143	2	5	-2	247	-2	0	0	137	0	5	-2	235	0	0	0	131	0	2	0	226
313-316	0	0	0	147	3	1	0	253	-2	0	1	143	2	4	-1	247	-2	0	1	138	2	4	-1	238	0	0	0	134	1	1	0	231
317-320	-1	0	0	147	3	1	-1	253	-2	0	1	144	2	2	-1	248	-2	0	1	140	1	2	-1	241	-1	0	0	137	1	1	-1	235
321-324	-1	0	0	147	3	0	-1	254	-4	0	0	145	3	1	-4	250	-4	0	0	142	2	1	-4	245	-1	0	0	140	2	0	-1	241
325-328	-1	0	0	147	1	0	-1	254	-3	0	1	146	0	0	-2	250	-3	0	1	143	0	0	-2	246	-1	0	0	141	0	0	-1	242
329-332	0	0	0	146	0	1	0	252	0	0	0	143	0	2	0	246	0	0	0	138	0	2	0	237	0	0	0	134	0	1	0	231
333-336	0	0	0	146	1	0	0	252	0	0	0	143	0	2	0	247	0	0	0	139	0	2	0	239	0	0	0	136	0	0	0	234
337-340	0	0	0	146	1	0	0	252	-1	0	0	144	1	1	-1	248	-1	0	0	140	1	1	-1	241	0	0	0	138	0	0	0	237
341-344	0	0	0	146	0	0	0	252	-1	0	0	144	0	0	-1	248	-1	0	0	141	0	0	-1	242	0	0	0	138	0	0	0	238
345-348	0	0	0	146	0	0	0	251	0	0	0	143	0	1	0	247	0	0	0	139	0	1	0	240	0	0	0	137	0	0	0	235
349-352	0	0	0	146	0	0	0	251	0	0	0	143	0	0	0	247	0	0	0	140	0	0	0	241	0	0	0	137	0	0	0	236

TABLE 10-5

CROSS-OVER PROBLEM, 9-AL (VF=0.30)

MICROSTRESS DISTRIBUTION FOR COMPOSITE STRESS S13=100

ELTS	SXX	SYY	SZZ	SXY	SXZ	SYZ	SKK	EQS	SXX	SYY	SZZ	SXY	SXZ	SYZ	SKK	EQS	SXX	SYY	SZZ	SXY	SXZ	SYZ	SKK	EQS	SXX	SYY	SZZ	SXY	SXZ	SYZ	SKK	EQS
1- 4	0	0	0	0	124	0	0	213	0	0	0	0	122	0	0	209	0	0	0	0	119	0	0	205	0	0	0	0	117	0	0	201
5- 8	-2	0	0	0	124	0	-2	214	-1	0	0	-1	122	0	-1	211	-1	0	0	-1	119	0	-1	206	-1	0	0	0	117	0	-1	202
9- 12	-1	0	0	0	123	0	-1	212	-1	0	0	0	121	0	-1	209	-1	0	0	0	118	0	-1	204	-1	0	0	0	117	0	-1	201
13- 16	-5	-1	0	0	127	0	-6	218	-5	-1	0	-1	124	0	-6	214	-5	-1	0	-1	121	0	-6	209	-4	-1	0	0	119	0	-5	206
17- 20	-8	-1	-1	-1	129	0	-10	222	-7	-1	-1	-3	127	0	-9	218	-6	-1	-1	-3	123	0	-8	213	-6	-1	-1	-1	121	0	-8	209
21- 24	-4	0	0	-1	129	0	-4	222	-3	0	0	-4	127	0	-3	218	-3	0	0	-4	123	0	-3	212	-2	0	0	-1	121	0	-2	208
25- 28	-5	0	0	0	123	0	-5	212	-5	0	0	0	121	1	-5	209	-5	-1	0	0	119	1	-6	205	-4	-1	0	0	117	0	-5	202
29- 32	-8	-1	0	0	127	0	-9	219	-8	-1	0	-2	125	1	-9	215	-8	-2	0	-2	122	1	-10	210	-8	-2	0	0	120	0	-10	207
33- 36	-12	-2	0	-1	129	0	-14	223	-12	-2	0	-3	127	1	-14	219	-12	-2	0	-3	123	1	-14	213	-12	-3	0	-1	121	0	-15	209
37- 40	-9	-1	0	-2	134	0	-10	230	-9	-1	0	-3	130	0	-10	225	-9	-2	0	-4	126	0	-11	218	-9	-2	0	-2	123	0	-11	213
41- 44	-11	-2	-2	-3	139	0	-15	240	-10	-2	-2	-7	135	1	-14	233	-10	-2	-2	-7	130	1	-14	224	-10	-3	-2	-2	126	0	-15	218
45- 48	-3	0	0	-3	139	0	-3	239	-3	0	0	-7	134	0	-3	232	-3	0	0	-7	129	0	-3	222	-3	-1	0	-3	125	0	-4	215
49- 52	2	7	18	0	94	0	27	162	2	6	18	0	93	0	26	161	2	6	17	0	92	0	25	159	2	6	17	0	91	0	25	158
53- 56	12	19	46	0	86	0	77	152	11	19	46	0	85	0	76	151	11	18	45	0	84	0	74	149	10	18	44	0	83	0	72	147
57- 60	27	28	58	0	80	0	113	142	26	27	58	-1	79	0	111	140	24	27	57	-1	77	0	108	137	24	26	56	0	76	0	106	135
61- 64	37	31	59	0	80	0	127	141	36	31	59	-1	79	0	126	138	35	31	58	-1	76	0	124	134	33	30	58	0	75	0	121	131
65- 68	51	37	63	-1	79	0	151	138	49	37	62	-2	76	0	148	134	47	36	61	-2	74	0	144	129	46	35	60	0	72	0	141	126
69- 72	63	40	60	-1	80	0	183	140	61	39	58	-2	77	0	158	135	58	38	57	-2	74	0	153	129	56	37	55	-1	71	0	148	124
73- 76	66	35	41	-1	93	0	142	163	64	34	40	-3	89	0	138	156	60	32	38	-2	84	0	130	147	58	31	37	-1	81	0	126	142
77- 80	32	14	13	-1	116	0	59	200	30	14	12	-3	110	0	56	191	28	13	11	-2	103	0	52	179	27	13	11	-1	99	0	51	171
81- 84	6	5	8	0	76	0	19	132	6	5	8	0	76	0	19	131	6	4	8	0	75	0	18	129	6	4	8	0	74	0	18	128
85- 88	19	13	22	0	81	0	54	139	19	13	21	0	80	0	53	138	18	13	21	0	78	0	52	135	17	13	21	0	77	0	51	134
89- 92	28	18	28	0	89	0	74	154	26	18	28	-1	87	0	72	151	25	17	27	-1	85	0	69	147	24	17	27	0	84	0	68	145
93- 96	27	18	31	-1	99	0	76	171	26	18	31	-2	96	0	75	166	25	18	30	-2	93	0	73	160	24	18	30	0	91	0	72	156
97-100	27	21	40	-1	103	0	88	177	26	21	39	-3	99	0	86	172	25	21	38	-3	95	0	84	165	24	21	37	-1	92	0	82	160
101-104	32	26	51	-2	101	0	109	176	31	26	50	-4	97	0	107	169	29	26	48	-4	92	0	103	160	28	26	47	-1	89	0	101	155
105-108	33	26	49	-2	100	0	108	174	32	25	47	-3	95	0	104	165	30	25	45	-4	89	0	100	155	29	24	43	-1	85	0	96	148
109-112	16	11	20	-2	103	0	47	177	15	11	20	-5	97	0	46	168	14	11	19	-5	90	0	44	156	14	11	18	-2	86	0	43	148
113-116	6	3	4	0	69	0	13	120	6	3	4	0	69	0	13	119	5	3	4	0	68	0	12	118	5	3	3	0	68	0	11	117
117-120	16	8	10	0	79	0	34	137	15	8	10	0	78	0	33	135	14	8	10	0	77	0	32	133	14	8	10	0	76	0	32	131
121-124	19	10	14	0	94	0	43	162	18	10	13	-2	92	0	41	159	16	10	13	-1	90	0	39	155	15	10	13	0	88	0	38	152
125-128	13	8	15	-1	107	0	36	185	12	8	15	-4	104	0	35	179	11	9	14	-3	99	0	34	171	11	9	14	-1	96	0	34	166
129-132	12	11	26	-2	111	0	49	192	11	11	25	-6	107	0	47	185	10	12	24	-5	101	0	46	175	10	12	23	-2	98	0	45	169
133-136	15	17	42	-3	110	0	74	191	15	18	41	-6	105	0	74	182	14	18	39	-5	98	0	71	171	13	18	37	-2	94	0	68	164
137-140	16	19	47	-3	104	0	82	181	15	19	45	-7	98	0	79	171	14	19	43	-6	90	0	76	159	13	19	41	-2	86	0	73	150
141-144	8	9	22	-3	93	0	39	170	7	9	21	-8	92	0	37	159	7	9	20	-7	84	0	36	145	7	9	19	-2	79	0	35	137
145-148	4	2	2	0	67	0	8	115	3	1	1	0	66	0	5	114	3	1	1	0	66	0	5	113	3	1	1	0	65	0	5	113
149-152	9	4	5	0	81	0	18	139	8	4	4	-1	80	0	16	137	8	4	4	-1	78	0	16	135	7	3	4	0	77	0	14	133
153-156	8	4	5	-1	99	0	17	171	7	4	4	-2	97	0	15	167	6	3	4	-2	94	0	13	162	5	3	4	-1	92	0	12	158
157-160	2	1	3	-2	113	0	6	194	1	1	3	-6	108	0	5	187	0	1	2	-5	103	0	3	178	0	1	2	-2	99	0	3	171
161-164	0	4	15	-4	117	0	19	202	0	4	14	-9	111	0	18	192	1	5	13	-7	104	0	19	180	1	5	13	-3	99	0	19	172
165-168	6	11	34	-4	116	0	51	201	5	12	32	-9	109	-1	49	190	5	12	30	-8	101	0	47	175	4	12	28	-3	96	0	44	166
169-172	7	14	43	-5	108	0	64	189	6	15	40	-10	100	-1	61	176	6	15	38	-8	91	0	59	161	5	15	36	-3	86	0	56	151
173-176	4	7	21	-5	98	0	32	170	3	7	20	-11	90	0	30	157	3	7	19	-9	81	0	29	141	3	7	18	-3	75	0	28	131
177-180	-3	1	10	-6	128	0	8	220	2	9	31	-6	121	0	42	211	1	9	35	-6	112	0	45	195	0	4	15	-6	102	0	19	176
181-184	-2	2	9	-12	116	0	9	201	1	9	27	-13	110	-1	37	192	0	9	31	-13	100	-1	40	177	0	4	14	-14	90	0	18	158
185-188	-1	2	8	-11	105	0	9	182	0	9	24	-11	99	-1	33	174	0	9	27	-12	89	-1	36	157	0	4	12	-12	79	0	16	138
189-192	-1	2	7	-5	99	0	8	172	0	9	22	-6	94	0	31	163	-1	9	25	-6	83	0	33	145	-1	4	11	-6	72	0	14	126
193-196	-1	2	7	-3	95	0	8	163	-2	7	18	-3	89	0	23	155	-2	7	20	-3	79	0	25	138	-1	3	9	-3	69	0	11	120
197-200	-1	1	4	-4	82	0	4	142	-3	4	12	-4	77	0	13	134	-3	4	12	-3	69	0	13	120	-1	1	5	-3	62	0	5	107

TABLE 10-5 (Contd.)

CROSS-OVER PROBLEM, B-AL (VF=0.30)

MICROSTRESS DISTRIBUTION FOR COMPOSITE STRESS S12=100

ELTS	SXX	SYY	SZZ	SXY	SXZ	SYZ	SKK	EQS	SXX	SYY	SZZ	SXY	SXZ	SYZ	SKK	EQS	SXX	SYY	SZZ	SXY	SXZ	SYZ	SKK	EQS	SXX	SYY	SZZ	SXY	SXZ	SYZ	SKK	EQS
201-204	0	0	2	-3	68	0	2	118	-2	2	6	-3	64	0	6	111	-2	2	6	-3	58	0	6	100	-1	0	2	-3	53	0	1	91
205-208	0	0	0	-1	58	0	0	101	0	0	2	-1	55	0	2	95	0	0	2	-1	49	0	2	86	0	0	0	-1	45	0	0	79
209-212	0	2	11	-8	132	0	13	229	1	7	29	-8	127	0	37	220	1	8	33	-8	117	0	42	203	0	3	14	-8	107	0	17	186
213-216	0	2	9	-17	119	0	11	207	0	7	25	-18	113	-1	32	199	0	8	28	-18	103	-1	36	183	0	3	12	-18	94	0	15	166
217-220	0	2	8	-17	105	0	10	184	-1	7	21	-17	100	-1	27	176	-2	7	23	-18	90	-1	28	160	-1	3	10	-18	81	0	12	144
221-224	-1	2	7	-11	97	0	8	168	-2	6	18	-12	91	-1	22	160	-3	7	20	-12	81	-1	24	144	-1	3	9	-13	72	0	11	128
225-228	-1	2	6	-10	93	0	7	156	-2	5	15	-10	84	0	18	148	-3	6	17	-10	75	0	20	133	-1	2	7	-10	67	0	8	118
229-232	0	1	4	-11	77	0	5	135	-2	3	10	-11	73	0	11	128	-2	3	11	-11	65	0	12	115	-1	1	4	-11	59	0	4	104
233-236	0	0	2	-9	64	0	2	112	-1	1	5	-9	61	0	5	106	-1	1	6	-9	55	0	6	96	0	0	2	-8	50	0	2	88
237-240	0	0	0	-3	55	0	0	96	0	0	1	-3	52	0	1	90	0	0	1	-3	47	0	1	81	0	0	0	-3	43	0	0	75
241-244	1	2	10	-11	140	0	13	242	4	8	28	-10	134	0	40	232	4	8	31	-10	123	0	43	215	1	3	13	-10	115	0	17	199
245-248	0	2	9	-25	124	0	11	218	2	6	24	-25	118	-1	32	209	1	7	26	-24	109	-1	34	193	0	3	11	-24	100	0	14	178
249-252	0	2	7	-27	105	0	9	189	0	6	19	-27	101	-1	25	181	0	6	21	-27	92	-1	27	167	0	2	9	-27	84	0	11	153
253-256	0	2	6	-22	94	0	8	167	-1	5	15	-22	89	-1	19	159	-2	5	16	-22	80	-1	19	145	-1	2	7	-22	73	0	8	133
257-260	0	1	5	-21	84	0	6	151	-1	5	12	-21	80	-1	16	143	-1	5	13	-21	72	-1	17	130	0	2	6	-21	65	0	8	119
261-264	0	1	3	-21	71	0	4	129	-1	3	8	-21	67	-1	10	123	-1	3	9	-20	61	-1	11	112	0	1	4	-20	56	0	5	103
265-268	0	0	1	-16	58	0	1	104	0	1	4	-16	54	0	5	99	0	1	5	-15	49	-1	6	90	0	0	2	-15	45	0	2	83
269-272	0	0	0	-6	49	0	0	85	0	0	1	-5	46	0	1	80	0	0	1	-5	41	0	1	72	0	0	0	-5	38	0	0	66
273-276	3	3	10	-15	152	0	16	263	9	9	27	-14	145	0	45	251	9	10	30	-13	133	0	49	231	4	4	13	-13	124	0	21	215
277-280	2	2	9	-36	133	0	13	237	6	6	23	-35	126	0	35	227	6	7	25	-33	116	0	38	210	2	3	11	-32	108	0	16	195
281-284	1	1	7	-43	109	0	9	203	3	4	18	-42	104	-1	25	195	4	4	19	-40	96	-1	27	180	1	2	8	-39	89	0	11	168
285-288	0	1	5	-41	92	0	6	175	1	2	13	-40	88	-2	16	167	1	2	14	-38	81	-2	17	155	0	1	6	-37	75	-1	7	145
289-292	0	0	3	-42	77	0	3	152	0	2	9	-40	73	-2	11	146	0	2	10	-39	67	-2	12	135	0	1	4	-37	62	-1	5	126
293-296	0	0	2	-37	62	0	2	125	0	2	6	-36	58	-2	8	120	0	2	7	-34	53	-2	9	110	0	1	3	-33	49	0	4	103
297-300	0	0	1	-26	46	0	1	93	0	1	4	-25	44	-1	5	89	0	1	4	-24	40	-1	5	81	0	0	1	-23	37	0	1	76
301-304	0	0	0	-9	37	0	0	66	0	0	1	-9	34	-1	1	62	0	0	1	-8	31	-1	1	56	0	0	0	-8	28	0	0	52
305-308	0	0	7	1	167	0	7	287	1	2	19	1	157	0	22	271	1	2	20	0	142	0	23	245	0	1	9	0	129	0	10	222
309-312	0	0	7	4	167	0	7	287	1	2	18	4	157	0	21	271	1	2	20	2	142	0	23	244	0	0	8	1	129	0	8	222
313-316	0	0	5	3	164	0	5	282	0	0	14	3	155	0	14	266	0	1	15	2	140	0	16	241	0	0	6	1	128	0	6	220
317-320	0	0	3	4	162	0	3	279	0	0	10	3	153	-1	10	263	0	0	10	2	138	-1	10	238	0	0	4	2	127	0	4	218
321-324	0	0	3	3	161	0	3	277	0	1	8	2	151	-1	9	261	0	1	8	1	136	-1	9	235	0	0	3	0	125	0	3	215
325-328	0	0	1	1	159	0	1	274	0	0	2	1	150	-1	2	258	0	0	3	0	136	-1	3	234	0	0	1	0	125	0	1	215
329-332	0	0	4	1	164	0	4	282	-1	0	10	0	155	0	9	266	-1	0	11	0	140	0	10	242	0	0	4	0	129	0	4	223
333-336	0	0	3	2	164	0	3	281	0	0	9	2	154	0	9	266	-1	0	9	1	140	0	8	241	0	0	4	0	129	0	4	222
337-340	0	0	2	1	162	0	2	279	0	1	6	1	153	0	7	263	0	1	6	0	139	0	7	240	0	0	2	0	128	0	2	221
341-344	0	0	0	0	160	0	0	276	0	0	2	0	151	0	2	261	0	0	2	0	138	0	2	237	0	0	0	0	127	0	0	219
345-348	0	0	1	0	162	0	1	279	-1	0	4	0	153	0	3	264	-1	0	4	0	140	0	3	241	0	0	1	0	130	0	1	223
349-352	0	0	0	0	162	0	0	278	0	0	1	0	153	0	1	263	0	0	1	0	139	0	1	240	0	0	0	0	129	0	0	222

TABLE 10-6

CROSS-OVER PROBLEM, B-AL (VF=0.30)

MICROSTRESS DISTRIBUTION FOR COMPOSITE STRESS S23=100

ELTS	SXX	SYY	SZZ	SXY	SXZ	SYZ	SKK	EQS	SXX	SYY	SZZ	SXY	SXZ	SYZ	SKK	EQS	SXX	SYY	SZZ	SXY	SXZ	SYZ	SKK	EQS	SXX	SYY	SZZ	SXY	SXZ	SYZ	SKK	EQS
1- 4	0	0	0	0	0	129	0	222	0	0	-1	0	0	139	-1	240	0	0	-1	0	0	153	-1	263	0	0	0	0	0	162	0	278
5- 8	0	0	-1	0	0	130	-1	223	0	1	-4	0	0	140	-3	241	0	1	-4	0	0	153	-3	264	0	0	-1	0	0	162	-1	279
9- 12	0	0	0	0	0	127	0	219	0	0	-2	0	0	138	-2	237	0	0	-1	0	0	151	-1	261	0	0	0	0	0	160	0	276
13- 16	0	0	-2	0	0	128	-2	221	-1	0	-6	0	0	139	-7	240	-1	0	-6	-1	0	153	-7	263	0	0	-2	-1	0	162	-2	279
17- 20	0	0	-4	0	0	129	-4	222	0	1	-9	-1	0	140	-8	241	0	0	-9	-1	0	154	-9	266	0	0	-3	-2	0	164	-3	281
21- 24	0	0	-4	0	0	129	-4	223	0	1	-11	0	0	140	-10	242	0	1	-10	0	0	155	-9	266	0	0	-4	-1	0	164	-4	282
25- 28	0	0	-1	0	0	125	-1	215	0	0	-3	0	-1	136	-3	234	0	0	-2	-1	-1	150	-2	258	0	0	-1	-1	0	159	-1	274
29- 32	0	0	-3	0	0	125	-3	215	-1	0	-8	-1	-1	136	-9	235	-1	0	-8	-2	-1	151	-9	261	0	0	-3	-3	0	161	-3	277
33- 36	0	0	-4	-2	0	127	-4	218	0	0	-10	-2	-1	138	-10	238	0	0	-9	-3	-1	153	-9	263	0	0	-3	-4	0	162	-3	279
37- 40	0	0	-6	-1	0	128	-6	220	-1	0	-14	-2	0	140	-15	241	0	0	-13	-3	0	155	-13	266	0	0	-5	-3	0	164	-5	282
41- 44	0	0	-8	-1	0	129	-8	222	-2	-1	-19	-2	0	142	-22	244	-2	-1	-18	-3	0	157	-21	271	0	0	-7	-4	0	167	-7	287
45- 48	-1	0	-8	0	0	129	-9	222	-2	-1	-20	0	0	142	-23	245	-2	-1	-18	-1	0	157	-21	271	0	0	-7	-1	0	167	-7	287
49- 52	0	0	0	8	0	28	0	52	0	0	-1	9	-1	31	-1	56	0	0	-1	9	-1	34	-1	62	0	0	0	10	0	37	0	66
53- 56	0	0	-1	23	0	37	-1	76	-1	0	-4	25	-1	40	-5	81	-1	0	-4	26	-1	44	-5	89	0	0	-1	27	0	46	-1	93
57- 60	-1	0	-3	33	0	49	-4	103	-2	0	-7	35	-2	53	-9	110	-2	0	-6	37	-2	58	-8	120	0	0	-2	38	0	62	-2	125
61- 64	-1	0	-4	38	-1	62	-5	126	-2	0	-9	39	-2	67	-11	135	-2	0	-9	41	-2	73	-11	146	0	0	-3	42	0	77	-3	152
65- 68	-1	0	-6	38	-1	75	-7	145	-2	-1	-14	39	-2	81	-17	155	-2	-1	-13	40	-2	88	-16	167	-1	0	-5	42	0	92	-6	175
69- 72	-2	-1	-8	39	0	89	-11	168	-4	-3	-19	41	-1	96	-26	180	-4	-3	-18	43	-1	104	-25	195	-1	-1	-7	44	0	109	-9	203
73- 76	-3	-2	-10	33	0	108	-15	195	-7	-6	-24	34	0	116	-37	210	-6	-6	-22	36	0	126	-34	227	-2	-2	-8	37	0	133	-12	237
77- 80	-4	-4	-13	13	0	124	-21	215	-10	-9	-29	14	0	133	-48	231	-9	-8	-26	15	0	145	-42	251	-3	-3	-10	15	0	152	-16	263
81- 84	0	0	0	5	0	38	0	66	0	0	-1	6	0	41	-1	72	0	0	-1	6	0	46	-1	80	0	0	0	6	0	49	0	85
85- 88	0	0	-2	15	0	45	-2	83	-1	0	-5	15	-1	49	-6	90	-1	0	-4	16	0	54	-5	99	0	0	-1	17	0	58	-1	104
89- 92	-1	0	-3	20	0	56	-4	103	-3	1	-9	21	-1	61	-11	112	-3	1	-8	21	-1	67	-10	123	-1	0	-3	22	0	71	-4	129
93- 96	-2	0	-5	21	0	65	-7	119	-5	1	-13	21	-1	72	-17	130	-4	1	-12	21	-1	80	-15	143	-1	0	-4	22	0	84	-5	151
97-100	-2	1	-7	23	0	73	-8	133	-5	2	-16	22	-1	80	-19	145	-5	1	-15	22	-1	89	-19	159	-2	0	-5	22	0	94	-7	167
101-104	-2	0	-9	27	0	84	-11	153	-6	0	-20	27	-1	92	-26	167	-5	0	-18	27	-1	101	-23	181	-2	0	-7	27	0	106	-9	189
105-108	-3	0	-11	25	0	100	-14	178	-7	-1	-25	25	-1	109	-33	193	-6	-1	-23	25	-1	118	-30	209	-2	0	-9	25	0	124	-11	218
109-112	-3	-1	-13	10	0	115	-17	199	-8	-3	-30	11	0	123	-41	215	-7	-4	-28	11	0	134	-39	232	-2	-1	-10	11	0	140	-13	242
113-116	0	0	0	3	0	43	0	75	0	0	-1	3	0	47	-1	81	0	0	-1	3	0	52	-1	90	0	0	0	3	0	55	0	96
117-120	0	0	-2	9	0	50	-2	88	-1	1	-5	9	0	55	-5	96	-1	1	-5	9	0	61	-5	106	0	0	-2	9	0	64	-2	112
121-124	-1	1	-4	11	0	59	-4	104	-3	3	-10	11	0	65	-10	115	-3	2	-10	11	0	73	-11	128	-1	0	-3	11	0	77	-4	135
125-128	-2	1	-7	11	0	67	-8	118	-6	3	-16	10	0	75	-19	133	-5	2	-15	10	0	84	-18	148	-2	1	-5	10	0	90	-6	156
129-132	-2	1	-8	13	0	72	-9	128	-6	3	-20	12	-1	81	-23	144	-6	2	-18	12	-1	91	-22	160	-2	1	-6	12	0	97	-7	168
133-136	-3	1	-10	19	0	81	-12	144	-7	2	-23	14	-1	90	-28	160	-7	1	-21	18	-1	100	-27	176	-2	0	-7	17	0	105	-9	184
137-140	-3	0	-12	19	0	94	-15	166	-8	0	-27	18	-1	103	-35	183	-7	0	-25	18	-1	113	-32	199	-2	0	-9	18	0	119	-11	207
141-144	-3	0	-14	8	0	107	-17	186	-8	-1	-32	8	0	117	-41	203	-7	-1	-29	8	0	127	-37	220	-2	0	-10	8	0	132	-12	229
145-148	0	0	0	1	0	45	0	79	0	0	-2	1	0	49	-2	86	0	0	-1	1	0	55	-1	95	0	0	0	1	0	58	0	101
149-152	0	1	-2	3	0	53	-1	91	-2	2	-6	3	0	58	-6	100	-2	2	-6	3	0	64	-6	111	0	0	-2	3	0	68	-2	118
153-156	-1	1	-5	3	0	62	-5	107	-4	3	-12	4	0	69	-13	120	-4	3	-11	4	0	77	-12	134	-1	1	-4	4	0	82	-4	142
157-160	-3	1	-9	3	0	69	-11	120	-7	2	-20	3	0	79	-25	138	-6	2	-18	3	0	89	-22	155	-2	1	-6	3	0	95	-7	163
161-164	-3	1	-11	6	0	72	-13	126	-9	1	-24	6	0	83	-32	145	-8	0	-22	6	0	94	-30	163	-2	1	-7	5	0	99	-8	172
165-168	-4	0	-12	13	0	79	-16	138	-9	0	-26	12	-1	89	-35	157	-8	0	-24	11	-1	99	-32	174	-2	1	-8	11	0	105	-9	182
169-172	-4	0	-13	14	0	90	-17	158	-9	0	-30	14	-1	100	-39	177	-8	-1	-27	13	-1	110	-36	192	-2	2	-9	12	0	116	-9	201
173-176	-4	0	-15	6	0	102	-19	176	-9	-1	-34	6	0	112	-44	195	-8	-2	-31	6	0	121	-41	211	-1	3	-10	6	0	128	-8	220
177-180	-7	-3	-18	3	0	75	-28	131	-7	-3	-19	9	0	81	-29	141	-7	-3	-20	11	0	90	-30	157	-7	-3	-21	5	0	98	-31	170
181-184	-15	-5	-35	3	0	86	-55	151	-15	-6	-37	9	0	91	-58	161	-14	-6	-40	10	-1	100	-60	176	-14	-7	-42	5	0	108	-63	189
185-188	-12	-4	-28	3	0	96	-44	166	-12	-4	-29	8	0	101	-45	175	-11	-5	-32	10	-1	109	-48	190	-11	-6	-34	4	0	116	-51	201
189-192	-5	-1	-12	3	0	99	-18	172	-5	-1	-13	7	0	104	-19	180	-4	0	-14	9	0	111	-18	192	-4	0	-15	4	0	117	-19	202
193-196	-1	0	-2	2	0	99	-3	171	-1	0	-2	5	0	103	-3	178	-1	-1	-3	6	0	108	-5	187	-1	-2	-3	2	0	113	-6	194
197-200	-3	-5	-3	1	0	92	-11	158	-3	-6	-4	2	0	94	-13	162	-3	-7	-4	2	0	97	-14	167	-4	-8	-5	1	0	99	-17	171

TABLE 10-6 (Contd.)

CROSS-OVER PROBLEM, B-AL (VF=0.30)

MICROSTRESS DISTRIBUTION FOR COMPOSITE STRESS S22=100

ELTS	SXX	SYY	SZZ	SXY	SXZ	SYZ	SKK	EQS	SXX	SYY	SZZ	SXY	SXZ	SYZ	SKK	EQS	SXX	SYY	SZZ	SXY	SXZ	SYZ	SKK	EQS	SXX	SYY	SZZ	SXY	SXZ	SYZ	SKK	EQS
201-204	-3	-7	-4	0	0	77	-14	133	-4	-8	-4	1	0	78	-16	135	-4	-8	-4	1	0	80	-16	137	-4	-9	-4	0	0	81	-17	139
205-208	-1	-3	-1	0	0	65	-5	113	-1	-3	-1	0	0	66	-5	113	-1	-3	-1	0	0	66	-5	114	-1	-4	-2	0	0	67	-7	115
209-212	-9	-6	-19	2	0	79	-34	137	-9	-7	-20	7	0	84	-36	145	-9	-7	-21	8	0	92	-37	159	-9	-7	-22	3	0	98	-38	170
213-216	-19	-13	-40	2	0	86	-72	150	-19	-14	-42	6	0	90	-75	159	-19	-15	-44	7	0	98	-78	171	-19	-15	-46	3	0	104	-80	181
217-220	-18	-13	-37	2	0	94	-68	164	-17	-13	-38	6	0	98	-68	171	-17	-14	-40	6	0	105	-71	182	-17	-15	-41	3	0	110	-73	191
221-224	-12	-10	-23	2	0	98	-45	169	-12	-10	-23	5	0	101	-45	175	-11	-11	-25	6	0	107	-47	185	-11	-11	-26	2	0	111	-48	192
225-228	-9	-11	-14	1	0	96	-34	166	-9	-11	-14	3	0	99	-34	171	-8	-12	-14	4	0	104	-34	179	-8	-13	-15	1	0	107	-36	185
229-232	-9	-15	-12	0	0	88	-36	152	-9	-16	-13	1	0	90	-38	155	-10	-17	-13	2	0	92	-40	159	-10	-18	-14	0	0	94	-42	162
233-236	-8	-13	-9	0	0	76	-30	131	-8	-14	-10	0	0	77	-32	133	-8	-15	-10	0	0	78	-33	135	-8	-16	-10	0	0	79	-34	137
237-240	-3	-5	-3	0	0	68	-11	117	-3	-5	-3	0	0	68	-11	118	-3	-6	-4	0	0	69	-13	119	-3	-6	-4	0	0	69	-13	120
241-244	-10	-14	-17	2	0	86	-41	148	-11	-14	-18	5	0	90	-43	156	-11	-15	-19	5	0	97	-45	168	-11	-16	-20	2	0	103	-47	177
245-248	-24	-28	-42	1	0	85	-94	148	-24	-29	-44	4	0	89	-97	155	-25	-31	-46	5	0	95	-102	165	-25	-32	-48	2	0	100	-105	174
249-252	-25	-28	-46	1	0	89	-99	155	-25	-29	-47	4	0	92	-101	160	-26	-30	-49	4	0	97	-105	169	-26	-32	-50	2	0	101	-108	176
253-256	-21	-24	-36	1	0	92	-81	160	-21	-24	-37	3	0	95	-82	165	-21	-26	-38	3	0	99	-85	172	-20	-27	-39	1	0	103	-86	177
257-260	-18	-24	-29	0	0	91	-71	156	-18	-25	-29	2	0	93	-72	160	-18	-26	-30	2	0	96	-74	166	-18	-27	-30	1	0	99	-75	171
261-264	-17	-23	-26	0	0	84	-66	145	-17	-24	-27	1	0	85	-68	147	-17	-26	-27	1	0	87	-70	151	-17	-27	-28	0	0	89	-72	154
265-268	-12	-17	-20	0	0	77	-49	134	-12	-17	-21	0	0	78	-50	135	-13	-18	-21	0	0	80	-52	138	-13	-19	-21	0	0	81	-53	139
269-272	-4	-6	-8	0	0	74	-18	128	-4	-6	-8	0	0	75	-18	129	-4	-6	-8	0	0	76	-18	131	-5	-6	-8	0	0	76	-19	132
273-276	-12	-27	-11	1	0	99	-50	171	-13	-28	-11	3	0	103	-52	179	-14	-30	-12	3	0	110	-56	191	-14	-31	-12	1	0	116	-57	200
277-280	-31	-56	-36	1	0	81	-123	142	-32	-59	-37	2	0	84	-128	147	-33	-62	-39	3	0	89	-134	156	-34	-65	-40	1	0	93	-139	163
281-284	-36	-55	-54	1	0	71	-145	124	-37	-57	-56	2	0	74	-150	129	-38	-60	-57	2	0	77	-155	135	-39	-62	-58	1	0	80	-159	140
285-288	-35	-45	-59	0	0	72	-139	126	-35	-46	-60	2	0	74	-141	129	-36	-48	-61	2	0	76	-145	134	-36	-50	-62	1	0	79	-148	138
289-292	-30	-33	-56	0	0	75	-119	131	-30	-34	-57	1	0	76	-121	134	-30	-35	-58	1	0	79	-123	138	-31	-37	-58	0	0	80	-126	141
293-296	-26	-23	-55	0	0	76	-104	135	-26	-24	-56	1	0	77	-106	137	-27	-25	-56	1	0	79	-108	140	-27	-27	-57	0	0	80	-111	142
297-300	-18	-10	-43	0	0	83	-71	147	-18	-10	-44	0	0	84	-72	149	-18	-11	-45	0	0	85	-74	151	-19	-12	-45	0	0	86	-76	152
301-304	-6	-2	-17	0	0	91	-25	158	-6	-2	-17	0	0	92	-25	159	-6	-2	-17	0	0	93	-25	161	-6	-2	-17	0	0	94	-25	162
305-308	1	3	0	3	0	125	4	215	0	3	0	7	0	129	3	222	0	3	0	8	0	134	3	232	0	3	0	3	0	139	3	239
309-312	3	10	2	2	0	126	15	218	2	10	2	7	1	130	14	224	2	11	2	7	1	135	15	233	2	11	2	3	0	139	15	240
313-316	2	9	0	2	0	123	11	213	2	9	0	5	0	126	11	218	1	9	0	5	0	130	10	225	1	9	0	2	0	134	10	230
317-320	3	12	0	1	0	121	15	209	2	12	0	3	1	123	14	213	2	12	0	3	1	127	14	219	2	13	0	1	0	129	15	223
321-324	2	8	0	0	0	120	10	207	2	8	0	2	1	122	10	210	1	8	0	2	1	125	9	215	1	8	0	0	0	127	9	219
325-328	1	5	0	0	0	117	6	202	1	5	0	0	1	119	6	205	0	5	0	0	1	121	5	209	0	5	0	0	0	123	5	212
329-332	0	2	0	1	0	121	2	208	0	3	0	4	0	123	3	212	0	3	0	4	0	127	3	218	0	4	0	1	0	129	4	222
333-336	1	6	1	1	0	121	8	209	1	6	1	3	0	123	8	213	1	7	1	3	0	127	9	218	1	8	1	1	0	129	10	222
337-340	1	4	0	0	0	119	5	206	1	5	0	1	0	121	6	209	1	5	0	1	0	124	6	214	1	5	0	0	0	127	6	218
341-344	0	1	0	0	0	117	1	201	0	1	0	0	0	118	1	204	0	1	0	0	0	121	1	209	0	1	0	0	0	123	1	212
345-348	0	1	0	0	0	117	1	202	0	1	0	1	0	119	1	206	0	1	0	1	0	122	1	211	0	2	0	0	0	124	2	214
349-352	0	0	0	0	0	117	0	201	0	0	0	0	0	119	0	205	0	0	0	0	0	122	0	209	0	0	0	0	0	124	0	213

spaces. The composite stresses are normalized with respect to the matrix yield stress (Y).

10.2 Discussion

The 0-90 multilayer composite has been analyzed for the microstresses both for regions farther away from the interface of two successive layers and also in the vicinity of the interface under composite fractions. For regions in the former case, the microstresses are given by the regular solution which is an uncoupled solution derived from the analysis of unidirectional composites, and for regions in the latter case the microstresses are evaluated from the cross-over solution. Two methods, two layer method and one layer method, have been discussed for the cross-over solution. The two layer method is a simple one and gives straightforward solution. On the other hand, the one layer method involves linear transformation of composite strains fields into associated strain fields; solving the cross-over problem in terms of the associated strain field; finding the stresses in the adjoining layer by appropriate stress equalities; and finding the desired solution from the solution of the associated strain fields. The primary advantage of the one-layer method over the two-layer method is: in a finite element solution the computer time and the core requirements are reduced almost by one-half in the former method compared to the latter, if the same finite element mesh configuration were to be used.

The microstress distribution in the matrix at the fiber-matrix interface for a multilayer B-Aℓ (v_f = 0.3) composite as shown in Figures 10-2 to 10-7 is almost identical for both the cross-over and regular solutions, for all the composite stresses. Even the initial yield surfaces shown in Figures 10-8 to 10-11 are almost identical for both solutions. It is seen from the yield surfaces that the composite stresses acting on planes parallel to the layer-layer interface of two layers generally increase the stress concentrations, while the other composite stresses generally reduce the stress concentrations. However, these effects are not very significant. The reason for this is attributed to the low fiber volume fraction of the composite.

The rate of attenuation of the effects of layer-layer interface reflected by the change in stress concentration discussed above is very rapid, and the microstresses reaches the regular solution within a distance of t. This is evident from the microstress distributions in Figures 10-2 to 10-7 where for $\emptyset$ = 0 the microstresses for the cross-over and regular solutions almost coincide.

10.3 Conclusions

Based on the above discussion the following inferences can be drawn for multilayered composites with low volume fractions.

1. Fiber cross-over effects are minor for low volume fractions.

2. The only composite stresses that may possibly increase the stress concentration are those acting on planes parallel to the layer-layer interface. The stress concentration due to the other stresses are reduced.

3. Yield surfaces obtained by regular solution are fairly accurate, and there is no necessity to consider the cross-over effects for low volume fractions.

10.4 General Remarks and Suggestions for Future Researchers

An accepted philosophy in research has been to report the successes, but not the failures. However, in the present case even the contrary seems to be justified if one considers the enormous time of both the researcher as well as the computer, and also the expenditure involved in the solution of the multi-layered composites for the cross-over effects. We shall devote this section to the failures and also the pitfalls which an unsuspecting researcher might encounter in the solution of the cross-over problems. The author believes that these should serve as the warning signs for the future researchers.

Solution of the multilayered composites for the cross-over effects by the finite element method is simple, at least in theory. However, this apparent simplicity becomes an illusion when one considers the astronomical memory requirements of these problems. In spite of the "large" memory area available for the user on the

IBM370/165 computer at Duke University, which is 1,000K (a quarter million words) many finite element models for the cross-over problems that have been attempted could not be accommodated in the core, even with the relabelling available on the ELAS programs. The memory requirement depends not only on the number of the finite elements but also on the boundary conditions. For example, the two layer model in Figure 10-1 requires about 700K memory for most strain states. If one attempts to solve the same model as a stress problem instead of a strain problem, by prescribing composite stresses instead of composite strains with appropriate boundary conditions, the limit of 1,000K memory would be exceeded.

Another hurdle in the solution of cross-over problems by finite element method is the accuracy. Under the computational constraints discussed in the previous paragraph, there seems to be no way to increase the number of finite elements without exceeding the available memory. This only seems to suggest the desirability of the one-layer method which requires a much smaller memory than the two layer method. However, a case of failure is worth reporting in this connection: The solution of a boron-aluminum multilayer composite for a volume fraction of 0.65 has been attempted by using the one-layer method, the boundary conditions in Table 9-3, and a finite element configuration identical to that used in Figure10-1. The results are not reported here because there has been no satisfactory equilibrium check between the stresses in several regions. The reason has been attributed to the lack of uniformity in the size of the finite elements. The dimensions R and t (See Figure10-1) are almost equal for a volume

fraction of 0.65, which made the finite elements in the matrix extremely small compared to those in the fiber. Incidentally, the memory requirement for this problem has been about 700K for most of the strain states.

REFERENCES

REFERENCES

1. Roson, W., "Strength and Stiffness of Fibrous Composites", Modern Composite Materials, Edited by Broutman, L. J., and Krock, R. H., pp. 106-119, Addison-Wesley Publishing Co., 1967.

2. Shaffer, B. W., "Stress-Strain Relations of Reinforced Plastics Parallel and Normal to the Internal Filaments", AIAA Journal, Vol. 2, No. 2, pp. 348-352, 1964.

3. Abolin'sh, D. S., "Compliance Tensor for an Elastic Material Reinforced in One Direction", Polymer Mechanics, Vol. 1, No. 1, p. 28, 1965.

4. Springer, S. G., and Tsai, S. W., "Thermal Conductivities of Unidirectional Materials", Journal of Composite Materials, Vol. 1, No. 2, pp. 166-173, 1967.

5. Hashin, Z., and Rosen, B. W., "The Elastic Moduli of Fiber-Reinforced Materials", Journal of Applied Mechanics, Vol. 31, No. 2, p-. 223-230, 1964 [Errata-Journal of Applied Mechanics, Vol. 32, p. 219, 1965].

6. Hill, R., "Theory of Mechanical Properties of Fiber-Strengthened Materials: III. Self-Consistent Model", Journal of the Mechanics and Physics of Solids, Vol. 13, No. 6, pp. 189-198, 1965.

7. Whitney, J. M., Riley, M. B., "Elastic Properties of Fiber-Reinforced Materials", AIAA Journal, Vol. 4, No. 9, pp. 1537-1542, 1966.

8. Bloom, J. M., and Wilson, H. B., "Axial Loading of a Unidirectional Composite", Journal of Composite Materials, Vol. 1, No. 1, pp. 268-277, 1967.

9. Adams, D. F., and Doner, D. R., "Longitudinal Shear Loading of a Unidirectional Composite", Journal of Composite Materials, Vol. 1, No. 1, pp. 4-17, 1967.

10. Adams, D. F., and Doner, D. R., "Transverse Normal Loading of a Unidirectional Composite", Journal of Composite Materials, Vol. 1, No. 2, pp. 152-184, 1967.

11. Green, A. E., and Zerna, W., Theoretical Elasticity, pp. 154-155, Oxford, 1968.

12. Chamis, C. C., and Sendeckyj, G. P., "Critique on Theories Predicting Thermoelastic Properties of Fibrous Composites", Journal of Composite Materials, Vol. 2, No. 3, pp. 332-358, 1968.

13. Hashin, Z., "Theory of Mechanical Behavior of Heterogeneous Media", Applied Mechanics Reviews, Vol. 17, No. 1, pp. 1-9, 1964.

14. McDaniels, D. L., Jech, R. W., and Weeton, J. W., "Stress-Strain Behavior of Tungsten-Fiber Reinforced Copper Composites", NASA TN D-1881, 1963.

15. Lin, T. H., Salinas, D., and Ito, M., "Initial Yield Surface of a Unidirectionally Reinforced Composite", Journal of Applied Mechanics, Vol. 39, No. 2, pp. 321-326.

16. Dvorak, G. J., Rao, M. S. M., Tarn, J. Q., "Yielding in Unidirectional Composites under External Loads and Temperature Changes", Journal of Composite Materials, Vol. 7, No. 2, pp. 194-216, 1973.

17. Dvorak, G. J., Rao, M. S. M., Tarn, J. Q., "Generalized Initial Yield Surfaces for Unidirectional Composites", Journal of Applied Mechanics, Vol. 41, No. 1, pp. 249-253, 1974.

18. Dvorak, G. J., Rao, M. S. M., "Plasticity Theory of Fibrous Composites: Part I", Duke University, School of Engineering, Solid Mechanics Series No. 8, 1973 (To appear in International Journal of Engineering Science).

19. Rao, M. S. M., Dvorak, G. J., "Plasticity Theory of Fibrous Composites: Part II", Duke University, School of Engineering, Solid Mechanics Series No. 9, 1973 (To appear in International Journal of Engineering Science).

20. Utku, S., Rao, M. S. M., and Dvorak, G. J., "ELAS65 Computer Program for Equilibrium Problems of Elastic-Thermoplastic Solids and Structures", Duke University, School of Engineering, Structured Mechanics Series No. 15, 1973 (to appear in International Journal of Computers and Structures).

21. Stowell, E. Z., and Liu, T. S., "On the Mechanical Behavior of Fiber-Reinforced Crystalline Materials", Journal of the Mechanics and Physics of Solids, Vol. 9, No. 4, pp. 242-260, 1961.

22. Kelly, A., and Davies, G. J., "The Principles of Fiber Reinforcement of Metals", Metallurgical Reviews, Vol. 10, No. 37, pp. 1-77, 1965.

23. Cratchley, D., "Experimental Aspects of Fiber-Reinforced Metals", Metallurgical Reviews, Vol. 10, No. 37, pp. 79-144, 1965.

24. Drucker, D. C., "High Strength Materials", V. F. Zackay, ed., Wiley, New York, pp. 795-833, 1965.

25. Hashin, Z., "Theory of Fiber-Reinforced Materials", NASA CR 207, 1965.

26. Shu, L. S., and Rosen, B. W., "Strength of Fiber-Reinforced Composites by Limit Analysis Methods", Journal of Composite Materials, Vol. 1, No. 4, pp. 366-381, 1967.

27. Mulhern, J. F., Rogers, T. G., and Spencer, A. J. M., "A Continuum Model for Fiber-Reinforced Plastic Materials", Proceeding of Royal Society, Vol. 301, No. A1467, pp. 473-492, 1967.

28. Prager, W., "Plastic Failure of Fiber-Reinforced Composites", Journal of Applied Mechanics, Vol. 36, No. 3, pp. 542-544, 1969.

29. Butler, T. W., and Sullivan, E. J., "On the Transverse Strength of Fiber-Reinforced Materials", Journal of Applied Mechanics, Vol. 40, No. 2, pp. 523-526, 1973.

30. Mulhern, J. F., Rogers, T. G., and Spencer, A. J. M., "A Continuum Theory of a Plastic-Elastic Fiber-Reinforced Material", International Journal of Engineering Science, Vol. 7, No. 2, pp. 129-152, 1969.

31. Lance, R. H., and Robinson, D. N., "Maximum Shear Stress Theory of Plastic Failure of Fiber-Reinforced Materials", Journal of the Mechanics and Physics of Solids, Vol. 19, No. 2, pp. 49-60, 1971.

32. McLaughlin, Jr., P. V., and Batterman, S. C., "Limit Analysis of Fibrous Materials", International Journal of Solids and Structures, Vol. 6, No. 10, pp. 1357-1376, 1970.

33. Baker, A. A., and Cratchley, D., "Stress-Strain Behavior and Toughness of a Fiber-Reinforced Metal", Applied Materials Research, Vol. 5, pp. 92-103, 1966.

34. Hill, R., "Theory of Mechanical Properties of Fiber-Reinforced Materials: II. Inelastic Behavior", Journal of the Mechanics and Physics of Solids, Vol. 12, No. 4, pp. 213-218, 1964.

35. Mulhern, J. F., Rogers, T. G., and Spencer, A. J. M., "Cyclic Extension of an Elastic Fiber with an Elastic-Plastic Coating", Journal of the Mathematics and its Applications, Vol. 3, No. 1, pp. 24-40, 1967.

36. Green, A. E., and Zerna, W., Theoretical Elasticity, p. 160, Oxford, 1953.

37. Hashin, Z., "The Elastic Moduli of Heterogeneous Materials", Journal of Applied Mechanics, Vol. 29, No. 1, pp. 143-150, 1962.

38. Chu, T. Y., and Hashin, Z., "Plastic Behavior of Composites and Porous Media under Isotropic Stress", International Journal of Engineering Science, Vol. 9, No. 10, pp. 971-994, 1971.

39. Hill, R., "The Essential Structure of Constitutive Laws for Metal Composites and Polycrystals", Journal of the Mechanics and Physics of Solids", Vol. 15, No. 2, pp. 79-95, 1967.

40. Rice, J. R., "Inelastic Constitutive Relations for Solids: An Internal-Variable Theory and its Applications to Metal Plasticity", Journal of the Mechanics and Physics of Solids, Vol. 19, No. 6, pp. 433-455, 1971.

41. Hill, R., Lee, E. H., and Tupper, S. J., "The Theory of Combined Plastic and Elastic Deformation with Particular Reference to a Thick Tub under Internal Pressure", Proceedings of the Royal Society of London, Vol. 191, No. A1024, pp. 278-303, 1947.

42. Hill, R., "Theory of Mechanical Properties of Fiber-Strengthened Materials: I. Elastic Behavior", Journal of the Mechanics and Physics of Solids, Vol. 12, No. 4, pp. 199-212, 1964.

43. Ziegler, H., "A Modification of Prager's Hardening Rule", Quarterly of Applied Mathematics, Vol. 17, No. 1, pp. 55-65, 1959.

44. Prager, W., "The Theory of Plasticity: A Survey of Achievements", Proceedings of Institute of Mechanical Engineers, Vol. 169, p. 41, 1955.

45. Hill, R., The Mathematical Theory of Plasticity, Oxford, 1956.

46. Cheskis, H. P., and Heckel, R. W., "Deformation Behavior of Continuous-Fiber Metal-Matrix Composite Materials", Metallurgical Transactions, Vol. 1, No. 7, pp. 1931-1942, 1970.

47. Metals Handbook, Vol. 1, American Society for Metals, 1961.

48. Van Horn, K. R., editor, "Aluminum", Vol. I, American Society for Metals, Metals Park, Ohio, 1967.

49. Hancock, J. R., "The Initiation and Growth of Fatigue Cracks in Filament-Reinforced Aluminum Alloys", Composite Materials: Testing and Design (Second Conference), ASTM STP 497, American Society for Testing and Materials, pp. 483-502, 1972.

50. Dvorak, G. J., and Tarn, J. Q., "Fatigue and Shake-Down in Metal Matrix Composites", Duke University, School of Engineering, Solid Mechanics Series No. 7, November, 1973.

51. Shimizu, H., and Dolowy, J. F., "Fatigue Testing and Thermal Mechanical Treatment Effects on Aluminum Boron Composites", Composite Materials: Testing and Design, ASTM STP 460, American Society for Testing and Materials, pp. 192-202, 1969.

52. Hoffman, C. A., "Effects of Thermal Loading on Composites with Constituents of Differing Thermal Expansion", NASA TN D-5926, 1970.

53. Hoffman, C. A., "Effects of Thermal Loading on Fiber Reinforced Composites with Constituents of Differing Thermal Expansitivities", Journal of Basic Engineering, Vol. 95, No. 1, pp. 1-8, 1973.

54. Feder, R. J., and Ebert, E. J., "A Study of the Tensile Properties of Filamentary Composites", Journal of Engineering Materials and Technology, Vol. 95, No. 2, pp. 69-75, 1973.

55. Symonds, P. S., "Shakedown in Continuous Media", Journal of Applied Mechanics, Vol. 73, No. 1, pp. 85-89, 1951.

56. Tarn, J. Q., Dvorak, G. J., and Rao, M. S. M., "Shakedown of Unidirectional Composites", Duke University, School of Engineering, Solid Mechanics Series No. 10, pp. 18-20, 1974.

57. Fung, Y. C., Foundations of Solid Mechanics, Prentice-Hall, pp. 304-309, 1965.

APPENDICES

APPENDIX I

ELASTIC CONSTANTS

This appendix lists the elastic constants, the quantities which are needed for evaluation of the microstresses at the interface in Equation 2.4, the yield surface in Equation 2.16, and the elastic composite strains ε_1^e, ε_2^e. Specifically, the coefficients of the [A] matrix in Equation 2.5, and the [κ] matrix in Equation 3.28 are given. The dimensions of κ_{ij} are in pound-inch units, and $\kappa_{21} = \kappa_{12}$.

The elastic constants of aluminum, boron, and beryllium used extensively in the present work are as follows:

	$E(10^6$ psi)	$G(10^6$ psi)	ν
Al	10.5	3.95	0.3291
B	58.0	23.97	0.2098
Be	40.0	19.60	0.0204

Coefficients of [A] and [κ] Matrices

	B-Aℓ			Be-Aℓ		
	V_f=0.30	V_f=0.50	V_f=0.68	V_f=0.30	V_f=0.50	V_f=0.68
A_{11}	1.1604	1.1069	1.0651	1.1161	1.0710	1.0411
A_{12}	-0.0227	-0.0113	-0.0056	-0.0703	-0.0377	-0.0196
A_{21}	0.7020	0.6792	0.6584	0.7843	0.7869	0.7844
A_{22}	0.0422	0.0338	0.0293	0.1306	0.1130	0.1027
A_{31}	0.3689	0.4265	0.4481	0.3805	0.4752	0.5248
A_{32}	0.4300	0.3136	0.2529	0.5554	0.4358	0.3681
$\kappa_{11} \times 10^8$	7.8465	6.0316	4.7020	8.4976	7.0931	6.1642
$\kappa_{12} \times 10^8$	-2.3240	-1.5364	-1.1343	-2.3333	-1.2974	-0.7236
$\kappa_{22} \times 10^8$	4.0338	2.9158	2.3343	5.1006	3.9144	3.2456

APPENDIX II

RESIDUAL STRESS FIELDS

In this appendix we shall prove existence of micro-residual stress fields that could translate the matrix controlled initial yield surface to any position without change of shape in the $I_1 I_2$-plane, for an arbitrary fibrous composite. Consider the composite being subjected simultaneously to the initial strains $\{e_{rr}^m \; e_{\phi\phi}^m \; e_{33}^m\}$ in the matrix, $\{e_{rr}^f \; e_{\phi\phi}^f \; e_{33}^f\}$ in the fiber, and the microstresses $\alpha_1 \{1 \quad 1 \quad 1\}$ in the matrix and $\{\alpha_1 \; \alpha_1 \; \alpha_{33}^f\}$ in the fiber, and the composite stresses $I_1 = \alpha_1$, $I_2 = \alpha_2$. We note that the above combination of stresses and initial strains satisfy the compatibility at the fiber matrix interface if we prescribe uniform total strain fields in the transverse as well as axial directions. The equilibrium at the interface is satisfied because of the microstresses in the transverse plane are uniform. The equilibrium of the transverse stresses is already satisfied, and the axial composite stress α_2 can be equilibrated by equating the rule of mixture resultant of the axial microstresses to α_2. The uniform strain fields in the transverse plane requires the initial strains e_{rr} and $e_{\phi\phi}$ be equal in both matrix and fiber.

Thus, the above forms an exact solution for a fibrous composite of an arbitrary geometry subjected to the composite stresses $I_1 = \alpha_1$, $I_2 = \alpha_2$ and the initial strains e_{rr}^m, $e_{\phi\phi}^m = e_{rr}^m$, e_{33}^m, e_{33}^m in the matrix, and e_{rr}^f, $e_{\phi\phi}^f = e_{rr}^f$, e_{33}^f in the fiber, subject to the following equations.

Uniform total strain field in transverse direction requires

$$e_{rr}^m + \frac{\alpha_1}{3K_m} = e_{rr}^f + \frac{1}{E_f}\left[(1 - \nu_f)\ \alpha_1 - \nu_f\ \sigma_{33}^f\right] \qquad \text{(II-1)}$$

Uniform total strain field in the axial direction requires

$$e_{33}^m + \frac{\alpha_1}{3K_m} = e_{33}^f + \frac{1}{E_f}\left[-2\ \nu_f\ \alpha_1 + \sigma_{33}^f\right] \qquad \text{(II-2)}$$

Equilibrium in the fiber direction requires

$$V_f\ \sigma_{33}^f + (1 - V_f)\ \alpha_1 = \alpha_2 \qquad \text{(II-3)}$$

The above form three equations for the three unknowns α_1, α_2, and σ_{33}^f in terms of $(e_{rr}^m - e_{rr}^f)$ and $(e_{33}^m - e_{33}^f)$. The microstress fields for the above problem are as follows:

In the matrix

$$\{\sigma_{rr}^m\ \sigma_{\phi\phi}^m\ \sigma_{33}^m\} = \alpha_1\ \{1\ \ 1\ \ 1\} \qquad \text{(II-4)}$$

In the fiber

$$\{\sigma_{rr}^f\ \sigma_{\phi\phi}^f\ \sigma_{33}^f\} = \{\alpha_1\ \ \alpha_1\ \ \sigma_{33}^f\} \qquad \text{(II-5)}$$

If we unload the composite from the above stress state elastically we introduce additional stresses. The net residual stress field is then given by

In the matrix

$$\begin{Bmatrix} \rho_{rr}^{m} \\ \rho_{\phi\phi}^{m} \\ \rho_{33}^{m} \end{Bmatrix} = \alpha_1 \begin{Bmatrix} 1 \\ 1 \\ 1 \end{Bmatrix} - [A] \begin{Bmatrix} \alpha_1 \\ \alpha_2 \end{Bmatrix} \qquad \text{(II-6)}$$

In the fiber

$$\begin{Bmatrix} \rho_{rr}^{f} \\ \rho_{\phi\phi}^{f} \\ \rho_{33}^{f} \end{Bmatrix} = \begin{Bmatrix} \alpha_1 \\ \alpha_1 \\ \alpha_{33}^{f} \end{Bmatrix} - [A] \begin{Bmatrix} \alpha_1 \\ \alpha_1 \end{Bmatrix} \qquad \text{(II-7)}$$

where ρ_{ij}^{m} and ρ_{ij}^{f} are the residual stresses in the matrix and fiber, respectively, the shear stresses being zero, [A] is a matrix which varies from point to point in the composite (See for example Equation 2.4).

The matrix controlled yield surface, with the residual stress state in Equation (II-6) is given by

$$\left| \{(I_1 - \alpha_1)\ (I_2 - \alpha_2)\}^T\ [A]^T\ [c][A]\ \{(I_1 - \alpha_1)\ (I_2 - \alpha_2)\} \right|_{MAX} - Y^2 = 0 \qquad \text{(II-8)}$$

where the first term is the square of the equivalent stress with [c] defined by Equation 2.7, and Y is the matrix yield stress. The maximum value of the first term is taken for the entire matrix.

Noting that Equation (II-8) represents the yield surface of a stress free composite for $\alpha_1 = \alpha_2 = 0$, this equation is a translated version of the stress free initial yield surface, the new center being located at $I_1 = \alpha_1$, $I_2 = \alpha_2$ in the I_1I_2-plane. This indicates that for a given loading point in the I_1I_2-plane one can find an infinite combination of the parameters α_1 and α_2 in Equation (II-8). All combinations α_1 and α_2 are permissible, because one can find a state of initial strain in Equations (II-1) to (II-3), corresponding to the selected combination.

APPENDIX III.

CONSTANTS OF HARDENING RULES

This appendix presents the constants of the initial yield surface (Equation 2.16 for $\alpha_1 = \alpha_2 = 0$) which is in the form

$$f \equiv k_1 I_1^2 + k_2 I_1 I_2 + k_3 I_2^2 - Y^2 = 0, \qquad \text{(III-1)}$$

and the matrix [R] in Equation 3.27. The matrix [R] depends upon the current load level. The coefficients can be determined by using Equations 2.16 and 3.27. A simplification of these equations gives:

$$\begin{Bmatrix} R_{11} \\ R_{21} \end{Bmatrix} = \begin{bmatrix} H_{11}' & H_{12}' \\ H_{21}' & H_{22}' \end{bmatrix} \begin{Bmatrix} I_1 - \alpha_1 \\ I_2 - \alpha_2 \end{Bmatrix} \qquad \text{(III-2)}$$

$$\begin{Bmatrix} R_{12} \\ R_{22} \end{Bmatrix} = \begin{bmatrix} H_{11}'' & H_{12}'' \\ H_{21}'' & H_{22}'' \end{bmatrix} \begin{Bmatrix} I_1 - \alpha_1 \\ I_1 - \alpha_2 \end{Bmatrix}$$

The components of [H'] and [H''] are also presented.

Coefficients k, H', and H''

Constant	B-Aℓ			Be-Aℓ		
	V_f=0.30	V_f=0.50	V_f=0.68	V_f=0.30	V_f=0.50	V_f=0.68
k_1	0.4738	0.3548	0.2951	0.4072	0.2664	0.2000
k_2	-0.5173	-0.3110	-0.2207	-0.6986	-0.4255	-0.3000
k_3	0.1798	0.0929	0.0590	0.3062	0.1755	0.1178
H_{11}'	0.4205	0.4316	0.4307	-0.1770	-0.0324	-0.0470
H_{21}'	-0.0357	-0.1453	-0.2222	-0.6294	-0.6141	-0.6120
H_{12}'	0.1704	0.1255	0.1020	0.7346	0.5661	0.4711
H_{22}'	0.7014	0.7641	0.7964	1.2103	1.1687	1.1448
H_{11}''	0.5173	0.3110	0.2207	0.6986	0.4255	0.3000
H_{21}''	0.9495	0.7097	0.5902	0.8144	0.5329	0.4000
H_{12}''	-0.3595	-0.1858	-0.1180	-0.6124	-0.3511	-0.2357
H_{22}''	-0.5173	-0.3110	-0.2207	-0.6986	-0.4255	-0.3000

APPENDIX IV

YIELDING WITH RESIDUAL STRESSES

Consider a composite with residual stresses in x, y, z coordinates

$$\{\rho\} = \{\rho_{xx}\ \rho_{yy}\ \rho_{zz}\ \rho_{xy}\ \rho_{xz}\ \rho_{yz}\}, \qquad \text{(IV-1)}$$

which may be different at different points in the composite.

The microstresses produced in the composite due to application of external loads T_{ij} could be obtained from the earlier results [16, 17] as

$$\{\sigma\} = [\Sigma]\ \{T\} \qquad \text{(IV-2)}$$

where

$$\{\sigma\} = \{\sigma_{xx}\ \sigma_{yy}\ \sigma_{zz}\ \sigma_{xy}\ \sigma_{xz}\ \sigma_{yz}\},$$

$$\{T\} = \{T_{11}\ T_{22}\ T_{33}\ T_{12}\ T_{13}\ T_{23}\},$$

and [Σ] is defined in [17], and varies from point to point in the composite.

The equivalent stress of the stresses obtained by superposition of stress states (IV-1) and (IV-2) for a point in the composite is given by,

$$\bar{\sigma}^2 = \{\rho + \sigma\}^T [C] \{\rho + \sigma\} \qquad \text{(IV-3)}$$

where

$$[C] = \begin{bmatrix} 1 & -\frac{1}{2} & -\frac{1}{2} & 0 & 0 & 0 \\ & 1 & -\frac{1}{2} & 0 & 0 & 0 \\ & & 1 & 0 & 0 & 0 \\ \text{SYM} & & & 3 & 0 & 0 \\ & & & & 3 & 0 \\ & & & & & 3 \end{bmatrix}$$

From Equations (IV-2) and (IV-3)

$$\bar{\sigma}^2 = \{T\}^T [\Sigma]^T [C] [\Sigma] \{T\} + 2 \{\rho\}^T [C] [\Sigma] \{T\} + \{\rho\}^T [C] \{\rho\} \qquad \text{(IV-4)}$$

The Mises Yield condition for the microstress is given by

$$\bar{\sigma}^2 = Y^2 \qquad \text{(IV-5)}$$

where Y yield stress of the material at which the stresses are being considered.

Define a radial path in {T} space by

$$\{T\} = p \{t_{11}\ t_{22}\ t_{33}\ t_{12}\ t_{13}\ t_{23}\} \qquad \text{(IV-6)}$$

where t_{ij} are known constants and p is a constant defining the stress level along the path {t}

Substituting Equations (IV-5) and (IV-6) into (IV-4) We obtain

$$a_1 p^2 + a_2 p + a_3 = 0 \qquad \text{(IV-7)}$$

where $a_1 = \{t\}^T [C] [\Sigma] \{t\}$

$a_2 = 2\ \{\rho\}^T [C] [\Sigma] \{t\}$

$a_3 = \{\rho\}^T [C]\ \{\rho\} - Y^2$

Equation (IV-7) gives two rooks p_1 and p_2 for p, p_1 being the smaller and p_2 being the larger. Equation (IV-7) should be formed for all points in the composite (elements if the finite element method is used to determine [Σ]). Then the algebraically largest value of p_1 and smallest of p_2 when substituted into Equation (IV -6) for p, gives two points on the yield surface with the residual stresses.

The procedures could be repeated with different paths with varying t_{ij} until sufficient number of points are obtained on the yield surface. It should be noted that if the roots of Equation (IV-7) are complex then the chosen path in Equation (IV -6) does not intersect the yield surface.

In some cases, it has been found, that a nonradical path defined by $\{T\} = \{t^o\} + p\{ t\}$ where $\{t^o\}$ and $\{t\}$ are known vectors, gives quicker results. The procedure however remains same, except the vector $\{\rho\}$ in the determination of the constants a_2 and a_3 of Equation (IV-7) is replaced by $\{\rho\} + [\Sigma]\ \{t^o\}$.

The stresses in the above analysis are in the Cartesian coordinate system. However, the same analysis could be used even in a cylindrical coordinate system.

APPENDIX V.

SIMPLE MICROSTRESS SOLUTION

A simple formula for the microstresses in the matrix could be derived from the considerations in Chapter III. We assumed that component $\{d\alpha_1 \; d\alpha_2\}$ of the composite increment $\{dI_1 \; dI_2\}$ causes always an isotropic stress change in the entire matrix (Equation 3.16), and the other component $\{(dI_1 - d\alpha_1) \; (dI_2 - d\alpha_2)\}$ causes always an elastic stress change. Thus, from Equations 2.4 and 3.16, we can write the microstresses in the matrix as

$$\{\sigma_{rr}^{m} \; \sigma_{\phi\phi}^{m} \; \sigma_{33}^{m}\} = \alpha_1 \{1 \;\; 1 \;\; 1\} + [A] \{I_1 - \alpha_1) \; (I_2 - \alpha_2)\} \qquad (V\text{-}1)$$

where [A] is found as a function of r, and α_1, α_2 are found from either hardening rule.

APPENDIX VI.

CYLINDER UNDER INTERNAL PRESSURE

(PLANE STRAIN)

In this appendix we shall solve the problem of a hollow cylinder under internal pressure under plane strain. This problem was originally solved by Hill et al. [41] and Hill [45]. A solution to this problem is attempted here by a procedure similar to that used for the composite cylinder in Chapter IV.

Consider a hollow cylinder of external radius a, internal radius b, made of an elastic-perfectly plastic material. Let the cylinder be loaded under internal pressure p beyond initial yielding, so that, the region $b \leq r \leq \rho$ is plastic, and the region $\rho \leq r \leq a$ is elastic, where r is the distance measured from the center of the cylinder, and $r = \rho$ defines the elastic-plastic interface.

Now, if the internal pressure is increased by dp, the plastic zone spreads from $r = \rho$ to $r = \rho + d\rho$. In analogy with the composite cylinder solution in Chapter IV, the following stress changes are assumed to have taken place during this time.

Plastic region ($b \leq r \leq \rho$)

$$d\,\sigma_{rr}^{p} = -dp$$

$$d\,\sigma_{\phi\phi}^{p} = -dp \qquad \text{(VI-1)}$$

$$d\,\sigma_{33}^{p} = -dp$$

Elastic region ($\rho \leq r \leq a$)

$$d\sigma_{rr}^{e} = -dp\ (\frac{a^2}{r^2} - 1)/(\frac{a^2}{\rho^2} - 1)$$

$$d\sigma_{\phi\phi}^{e} = dp\ (\frac{a^2}{r^2} + 1)/(\frac{a^2}{\rho^2} - 1) \qquad \text{(VI-2)}$$

$$d\sigma_{33}^{e} = 2\ \nu\ dp/(\frac{a^2}{\rho^2} - 1)$$

In these equations r, ϕ, 3 define the radial coordinate system, and ν is the Poisson's ratio. The stress increments in the elastic region correspond to the elastic solution of hollow cylinder of internal radius ρ and external radius a, with plane strain condition, under internal pressure dp.

The stresses in the elastic region ($\rho \leq r \leq a$) can be written by considering the radial stress at $r = \rho$ as $-p'$, where $dp'/dp = 1$ as a consequence of the stress state (VI-1) in the plastic region. Thus

$$\sigma_{rr}^{e} = -p' \left(\frac{a^2}{2} - 1\right)/\left(\frac{a^2}{\rho^2} - 1\right)$$

$$\sigma_{\phi\phi}^{e} = p' \left(\frac{a^2}{r^2} + 1\right)/\left(\frac{a^2}{\rho^2} - 1\right) \qquad \text{(VI-3)}$$

$$\sigma_{33}^{e} = 2\nu p'/\left(\frac{a^2}{\rho^2} - 1\right)$$

The Tresca's yield condition for $\sigma_{\phi\phi} > \sigma_{33} > \sigma_{rr}$ is

$$f = \sigma_{\phi\phi}^{e} - \sigma_{rr}^{e} - Y = 0$$

where Y is the yield stress.

Substituting for $\sigma_{\phi\phi}^{e}$ and σ_{rr}^{e} from (VI-3) we get

$$f = 2p' \frac{a^2}{r^2}/\left(\frac{a^2}{\rho^2} - 1\right) - Y \qquad \text{(VI-4)}$$

In order to satisfy the yield condition at $r = \rho$ we require $f = 0$ at $r = \rho$. Thus, from Equation (VI-4) we get

$$p' = \frac{Y}{2}\left(1 - \frac{\rho^2}{a^2}\right) \qquad \text{(VI-5)}$$

Now if we wish to propagate the plastic zone from $r = \rho$ to $r = \rho + d\rho$ by increasing the radial pressure at $r = \rho$ from p' to $p' + dp'$, we require to satisfy the yield condition at $r = \rho + d\rho$ at the end of the pressure increase. Thus

$$\frac{\partial f}{\partial p'} dp' + \frac{\partial f}{\partial r} dr \Big|_{r=\rho} = 0 \qquad \text{(VI-6)}$$

From (VI-4) and (VI-6)

$$\frac{dp'}{d\rho} = \frac{2\ p'}{\rho} \qquad \text{(VI-7)}$$

From (VI-5) and (VI-7), and noting dp' = dp

$$\frac{dp'}{d\rho} = \frac{dp}{d\rho} = \frac{Y}{\rho}\left(1 - \frac{\rho^2}{a^2}\right) \qquad \text{(VI-8)}$$

Now consider that the plastic zone has been propagated to r = c by increasing the internal pressure. The stresses in the plastic region ($b \leq r \leq c$) can be considered in two parts:

i) Stresses developed during the time when the point was elastic.

ii) Stresses developed during the time when the point was plastic. Thus

$$\sigma_{ij}{}^{p} = \sigma_{ij}{}^{o} + \int_{\rho=b}^{\rho=r} \frac{d\sigma_{ij}{}^{e}}{d\rho}\, d\rho + \int_{\rho=r}^{\rho=c} \frac{d\sigma_{ij}{}^{p}}{d\rho}\, d\rho \qquad \text{(VI-9)}$$

where i, j = r, ϕ, 3; $\sigma_{ij}{}^{o}$ are stresses at the point at the initial yield; the second term corresponds to the part (i), and the third term to part (ii) above. The derivatives $d\sigma_{ij}{}^{e}/d\rho$ and $d\sigma_{ij}{}^{p}/d\rho$ are obtained from (VI-2) and (VI-1), respectively, by replacing

the incremental variables with the derivatives with respect to ρ.

The stresses at initial yield σ_{ij}^{o} could be obtained from (VI-3) and (VI-5) by substituting $\rho = b$ and $p' = p$.

Performing the integrations in (VI-9) by using (VI-1), (VI-2), and (VI-8) and simplifying we obtain the stresses in the plastic region as,

$$\frac{\sigma_{rr}^{p}}{Y} = -\frac{1}{2} - \ell n\left(\frac{c}{r}\right) + \frac{c^2}{2a^2}$$

$$\frac{\sigma_{\phi\phi}^{p}}{Y} = \frac{1}{2} - \ell n\left(\frac{c}{r}\right) + \frac{c^2}{2a^2} \qquad c \leq r \leq a \qquad \text{(VI-10)}$$

$$\frac{\sigma_{33}^{p}}{Y} = -\ell n\left(\frac{c}{r}\right) + \frac{c^2 - (1 - 2\nu)r^2}{2\,a^2}$$

The stresses in the elastic region can be obtained from (VI-3) and (VI-5) by putting $\rho = c$, as

$$\frac{\sigma_{rr}^{e}}{Y} = -\frac{1}{2}\left(\frac{c^2}{r^2} - \frac{c^2}{a^2}\right)$$

$$\frac{\sigma_{\phi\phi}^{e}}{Y} = \frac{1}{2}\left(\frac{c^2}{r^2} + \frac{c^2}{a^2}\right) \qquad \text{(VI-11)}$$

$$\frac{\sigma_{33}^{e}}{Y} = \nu\,\frac{c^2}{a^2}$$

The internal pressure corresponding to elastic-plastic interface at c can be obtained by integrating (VI-8) between $\rho = b$ and $\rho = c$, and adding the internal pressure p^o at initial yielding, which is equal to p' for $\rho = b$ in (VI-5). Thus

$$\frac{p}{Y} = \ell n \left(\frac{c}{b}\right) + \frac{1}{2}\left(1 - \frac{c^2}{a^2}\right) \qquad \text{(VI-12)}$$

It can be observed that Equations (VI-11), (VI-12), and the first two equations of (VI-10) are identical to those obtained by Hill [45], except the notation is different here. The σ_{33} stress in the plastic region given by the third equation of (VI-10) is found to be slightly different from Hill. It is speculated, that the discrepancy is due to the stress state (VI-1) assumed in the plastic region. The Tresca yield condition used is not influenced by the σ_{33} stress, and consequently any selection of $d\sigma_{33}^{p}$ in (VI-1) would not have affected the yield condition. It is expected that the procedure would yield better results if Mises yield condition were to be used, in which case all three stress components should be considered, and stress state (VI-1) forms a major part of the stress increments in the plastic region.

APPENDIX VII.

MODIFICATION OF HARDENING RULES

In this appendix, the Hardening Rules (I and II) formulated in Chapter III will be modified to account for the change in the matrix yield stress with temperature.

We noted in Chapter III that, "for a given point $\{I_1 \; I_2\}$ on the loading surface with its center at $\{\alpha_1 \quad \alpha_2\}$, if plastic deformation were to occur, then there exists a special direction in the I_1I_2-plane along which any incremental $\{d\alpha_1 \; d\alpha_2\}$ would be directed".

Thus the hardening rules (Equations 3.13 and 3.15) may be rewritten as

$$\{d\alpha_1 \; d\alpha_2\} = d\eta \quad \{\ell_1 \; \ell_2\} \tag{VII-1}$$

where $d\eta$ is some constant and $\{\ell\}$ is a known vector depending upon the hardening rule, and is given by

$$\text{for Rule I:} \quad \{\ell_1 \; \ell_2\} \quad = \{(I_1 - \alpha_1) \; (I_2 - \alpha_2)\} \text{and} \tag{VII-2}$$

$$\text{for Rule II:} \quad \{\ell_1 \; \ell_2\} \quad = \{R_{11} \; R_{21}\}$$

where R_{11} and R_{21} are obtained from Equation 3.27.

Thus, if at any loading point $\{I_1\ I_2\}$ on a loading surface, the yield stress is changed from Y to Y + dY, by keeping the loads constant, then for $dY < 0$. The loading surface has to travel in order to maintain the yield condition, the direction of motion being governed by Equation (VII-1).

In order to determine $d\eta$ corresponding to the change of yield stress, dY, one can use the yield condition at the end of the yield stress change (consistency equation), which is given by

$$df = \frac{\partial f}{\partial \alpha_1}\ d\alpha_1 + \frac{\partial f}{\partial \alpha_1}\ d\alpha_2 + \frac{\partial f}{\partial Y}\ dY \qquad \text{(VII-3)}$$

where f is the loading fun-tion defined by Equation 2.16, and $dI_1 = dI_2 = 0$.

By noting $\frac{\partial f}{\partial \alpha_1} = -\frac{\partial f}{\partial I_1}$ and $\frac{\partial f}{\partial \alpha_2} = -\frac{\partial f}{\partial I_2}$, Equations (VII-1) and (VII-3) yield,

$$d\eta = \frac{\frac{\partial f}{\partial Y}\ dY}{\ell_1 \frac{\partial f}{\partial I_1} + \ell_2 \frac{\partial f}{\partial I_2}} \qquad \text{(VII-4)}$$

Thus, if the yield stress were to change during a load increment $\{dI_1\ dI_2\}$, the Hardening Rules may be rewritten as

$$\begin{Bmatrix} d\alpha_1 \\ \\ d\alpha_2 \end{Bmatrix} = \begin{Bmatrix} dI_1 \\ \\ dI_2 \end{Bmatrix} - d\mu \begin{Bmatrix} -\partial f/\partial I_2 \\ \\ \partial f/\partial I_1 \end{Bmatrix} + d\eta \begin{Bmatrix} \ell_1 \\ \\ \ell_2 \end{Bmatrix} \qquad \text{(VII-5)}$$

$d\mu$ is identical to $d\mu_I$ or $d\mu_{II}$ in Chapter III, but should be determined from Equation 3.14 or 3.26, by replacing $\{dI_1\ dI_2\}$ with $\{(dI_1 + d\eta\ell_1)\ (dI_2 + d\eta\ell_2)\}$, respectively, with corresponding $\{\ell_1\ \ell_2\}$ from (VII-2). We note that, the change dY of the matrix yield stress in (VII-4) may be because of any cause including a change in temperature, in which case $dY \equiv \frac{dY}{d\theta}\, d\theta$, where θ is the temperature.

APPENDIX VIII.

ILLUSTRATION OF USE OF THERMOMECHANICAL ANALOGY

In this appendix we shall illustrate the use of thermo-mechanical analogy in the solution of heat treatment problems. First, the general numerical procedure will be outlined, then the numerical procedure will be illustrated by an example.

A. Numerical Procedure:

1. Select the temperature variation $\theta(t)$ as a function of t (numerical step) depending upon the temperature history of heat-treatment.

2. Find the unit dimensional changes due to volume changes of the matrix material during aging from experiments and incorporate them in the procedure by specifying it as a function of t.

3. Find the matrix yield stress variation as a function of temperature and aging time from experiments and incorporate this in the procedure by specifying it as a function of t.

4. Determine the value of $S(t)$ as a function of t by using temperature variation $\theta(t)$ in Step 1 and unit dimensional

changes in step 2 by using the thermo-mechanical analogy (Equation 5.5).

5. Determine the first part of the solution by Equation 5.2.

6. Determine the second part of the microstress solution by using $I_1(t) = I_2(t) = -S(t)$ and $Y(t)$ found in Step 3 in the Hardening Rule (I or II) in Appendix VII, and the approximate microstress solution for the cylinder in Chapter IV, as follows:

(a) Determine the initial yield along the path $I_1 = I_2$ for yield stress $Y(0)$. The shift of the yield surface is zero for this part of the problem at this step. i.e., $\alpha_1 = \alpha_2 = 0$.

(b) Find the change of I_1 and I_2 during t and $t + \Delta t$ as $I_1 = I_2 = -\frac{dS}{dt}\Delta t$, and the change in yield stress as $\Delta Y = \frac{dY}{dt}\Delta t$, where S is as found in Step 4 and Y in Step 3.

(c) If $\frac{\partial f}{\partial I_1}\Delta I_1 + \frac{\partial f}{\partial I_2}\Delta Y > 0$, find $\Delta\alpha_1$ and $\Delta\alpha_2$ by using the Hardening Rule (I or II), and determine the changes in the microstresses as an elastic part due to $\Delta I_1 - \Delta\alpha_1$ and $\Delta I_2 - \Delta\alpha_2$, and as an elasto-plastic part due to $\Delta\alpha_1$ and $\Delta\alpha_2$ using approximate cylinder solution. Otherwise, determine the elastic stress increment due to dI_1 and dI_2.

(d) Update the microstresses and the shifts of the yield surfaces by the incremental values obtained in (c).

(e) Repeat (b) to (d) for the entire heat-treatment history.

7. Determine the complete solution of the heat-treatment problem as a superposition of the two parts of the solution obtained in Steps 5 and 6. The center of the yield surface at any

step is located at $I_1 = S(t) + \alpha_1(t)$, $I_2 = S(t) + \alpha_2(t)$ in the I_1I_2-plane.

B. Example: Heat Treatment of 7075-T6M Aℓ-B

For the heat treatment of the 7075-T6M Aℓ-B the steps in numerical procedure are as follows:

1. Temperature variation selected is shown in Figure 5-4.

Steps 1-112: Quenching from 862 deg. F. to -320 deg. F.

Steps 113-140: Reheating from -320 deg. F. to 250 deg. F.

Steps 141-207: Aging at 250 deg. F. for 25 hours.

Steps 208-223: Cooling from 250 deg. F. to 70 deg. F.

2. The experimental values of unit dimensional changes during aging are shown in Figure 5-19, and are incorporated in the numerical procedure between steps 141-207 as shown in Figure 5-4.

3. The matrix yield stress variation 7075 Aℓ in w state is assumed to be varying linearly from 1 ksi at 862 deg. F. to 28 ksi at -320 deg. F. The variation of yield stress during aging is shown in Figure 5-19. These variations are incorporated in the numerical procedure as shown in Figure 5-4.

4. The value of S(t) is determined by using the thermo-mechanical analogy (Equation 5.5).

5. The first part of the microstress solution is obtained for the entire process by using Equation 5.2.

6. The second part of solution is obtained as in Step 6 in the numerical procedure.

7. The complete solution is obtained by the superposition of the solutions obtained in 5 and 6.

APPENDIX IX.

THERMAL EXPANSION COEFFICIENTS

In this appendix we shall outline a procedure to determine the composite coefficients of thermal expansion from the composite strains obtained from the plasticity theory in Chapter III, and the thermomechanical analogy formulated in Chapter V, when a composite is subjected to uniform thermal changes. The thermomechanical analogy (Chapter V) states that a problem of a composite subjected to uniform thermal change can be considered as a superposition of two problems, the first involving uniform strain fields in the composite and subjected to a uniform composite stress in all directions, and the second involving an elastoplastic composite subjected to uniform composite in all directions (Figure 5-1). The composite stresses in the two problems are equal and opposite and is given by S in Equation 5.5.

Now consider a composite subjected to uniform temperature change $\Delta\theta$. Ignoring $\Delta L/L$ in Equation 5.1 and substituting it in Equation 5.5 we obtain ΔS corresponding to $\Delta\theta$ as

$$\Delta S = 3 \cdot \frac{\alpha_f - \alpha_m}{(1/K_m) - (1/K_f)} \cdot \Delta\theta \qquad \text{(IX-1)}$$

The composite strains $\Delta\varepsilon_1'$ $2\,\Delta\varepsilon_{rr}'$ and $\Delta\varepsilon_2'$ in the I_1I_2-plane for the first problem can be obtained from Equations 5-1, 5-4 and (IX-1) by observing that this is a problem of uniform strain fields. Thus

$$\frac{1}{2}\quad \Delta\varepsilon_1' = \Delta\varepsilon_2' = \frac{K_m\,\alpha_f - K_f\,\alpha_m}{K_m - K_f}\cdot\Delta\theta \qquad \text{(IX-2)}$$

The composite strains $\Delta\varepsilon_1''$ and $\Delta\varepsilon_2''$ in the I_1I_2-plane corresponding to the second problem ($dI_1 = dI_2 = -dS$) can be obtained from the plasticity theory in Chapter III (Equations 3.28 and 3.29) can be written as

$$\begin{aligned}\Delta\varepsilon_1'' &= -(\kappa_{11} + \kappa_{12})\,\Delta S - \frac{d\varepsilon_1^{\,p}}{dS}\,\Delta S \\ \Delta\varepsilon_2'' &= -(\kappa_{21} + \kappa_{22})\,\Delta S - \frac{d\varepsilon_2^{\,p}}{dS}\,\Delta S\end{aligned} \qquad \text{(IX-3)}$$

where κ_{ij} are the composite compliances and the derivatives of the plastic strains $d\varepsilon_1^{\,p}/dS$ and $d\varepsilon_2^{\,p}/dS$ can be obtained by considering all the incremental parameters in Chapter III as derivatives with respect to S, where $I_1 = I_2 = S$.

The total strain increments are a superposition of the strain increments of the above two problems. Thus

$$\begin{aligned}\Delta\varepsilon_1 &= \Delta\varepsilon_1' + \Delta\varepsilon_1'' \\ \Delta\varepsilon_2 &= \Delta\varepsilon_2' + \Delta\varepsilon_2''\end{aligned} \qquad \text{(IX-4)}$$

From Equations (IX-1) to (IX-4)

$$\frac{\Delta\varepsilon_1}{\Delta\theta} = 2\frac{K_m\alpha_1 - K_f\alpha_m}{K_m - K_f} - 3\frac{(\alpha_f - \alpha_m)}{(1/K_f) - (1/K_m)}\left\{\kappa_{11} + \kappa_{12} + \frac{d\varepsilon_1^p}{dS}\right\}$$

$$\frac{\Delta\varepsilon_2}{\Delta\theta} = \frac{K_m\alpha_f - K_f\alpha_m}{K_m - K_f} - 3\frac{(\alpha_f - \alpha_m)}{(1/K_f) - (1/K_m)}\left\{\kappa_{21} + \kappa_{22} + \frac{d\varepsilon_2^p}{dS}\right\} \qquad \text{(IX-5)}$$

Now the composite coefficients of thermal expansion α_{ct} in the transverse direction, and α_{ca} in the axial direction can be obtained from Equation (IX-5) by using the definitions

$$\alpha_{ct} = \frac{1}{2}\frac{\Delta\varepsilon_1}{\Delta\theta}$$

$$\alpha_{ca} = \frac{\Delta\varepsilon_2}{\Delta\theta} \qquad \text{(IX-6)}$$

The elastic coefficients of thermal expansion can be obtained from Equations (IX-5) and (IX-6) by setting $d\varepsilon_1^p/dS$ and $d\varepsilon_2^p/dS$ to zero and using the appropriate composite compliances.

APPENDIX X.

FIGURES

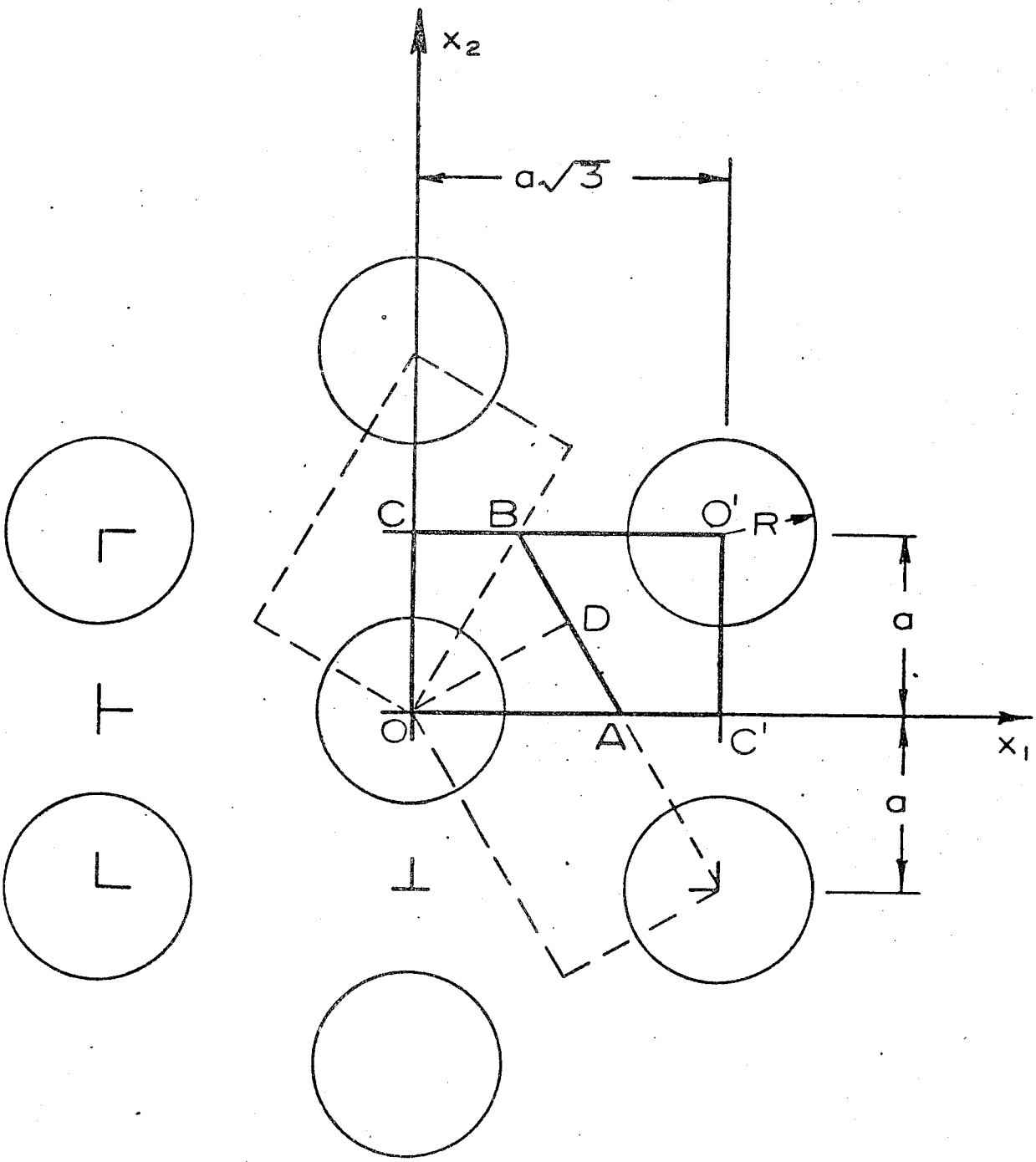

Figure 1-1. A regular hexagonal model of a fiber-reinforced composite, and repeating elementary domains.

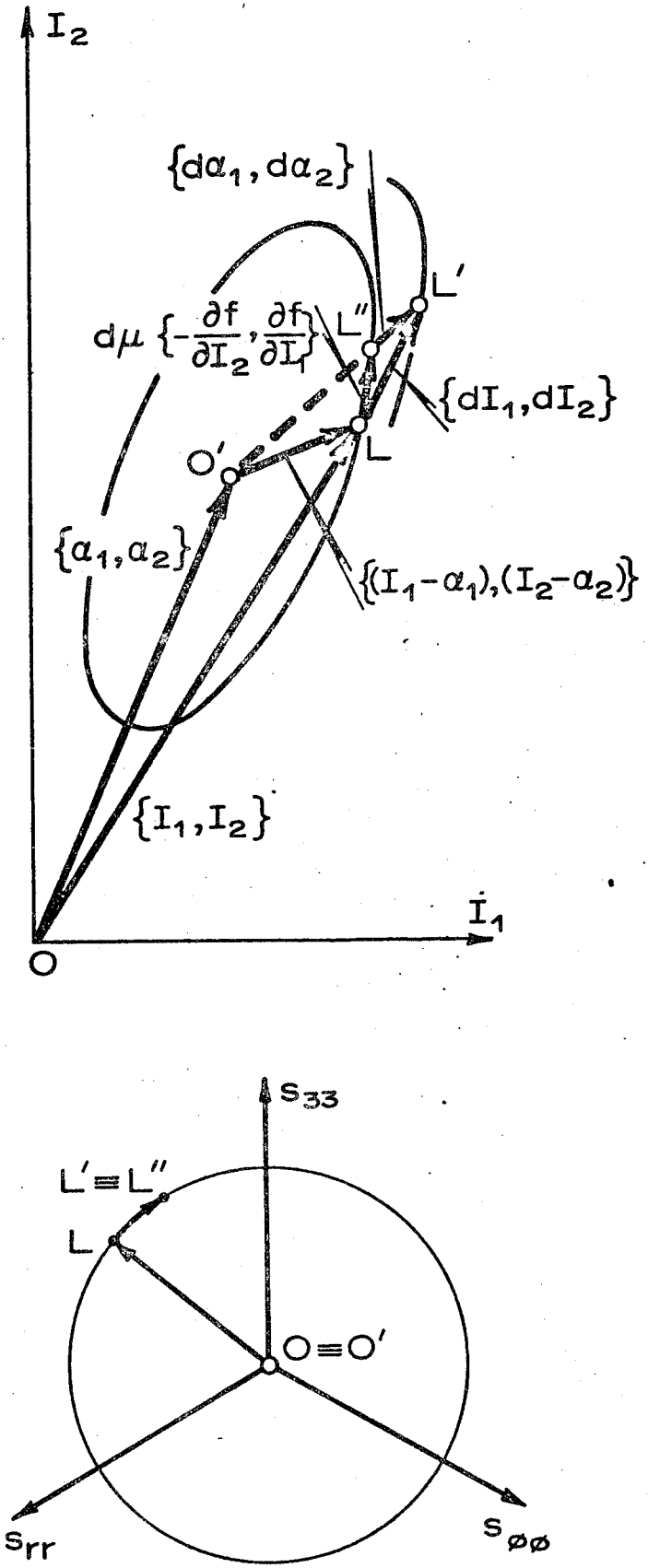

Figure 3-1. Schematic Representation of Stress Increments in the Composite, and the Deviatoric Stress Planes.

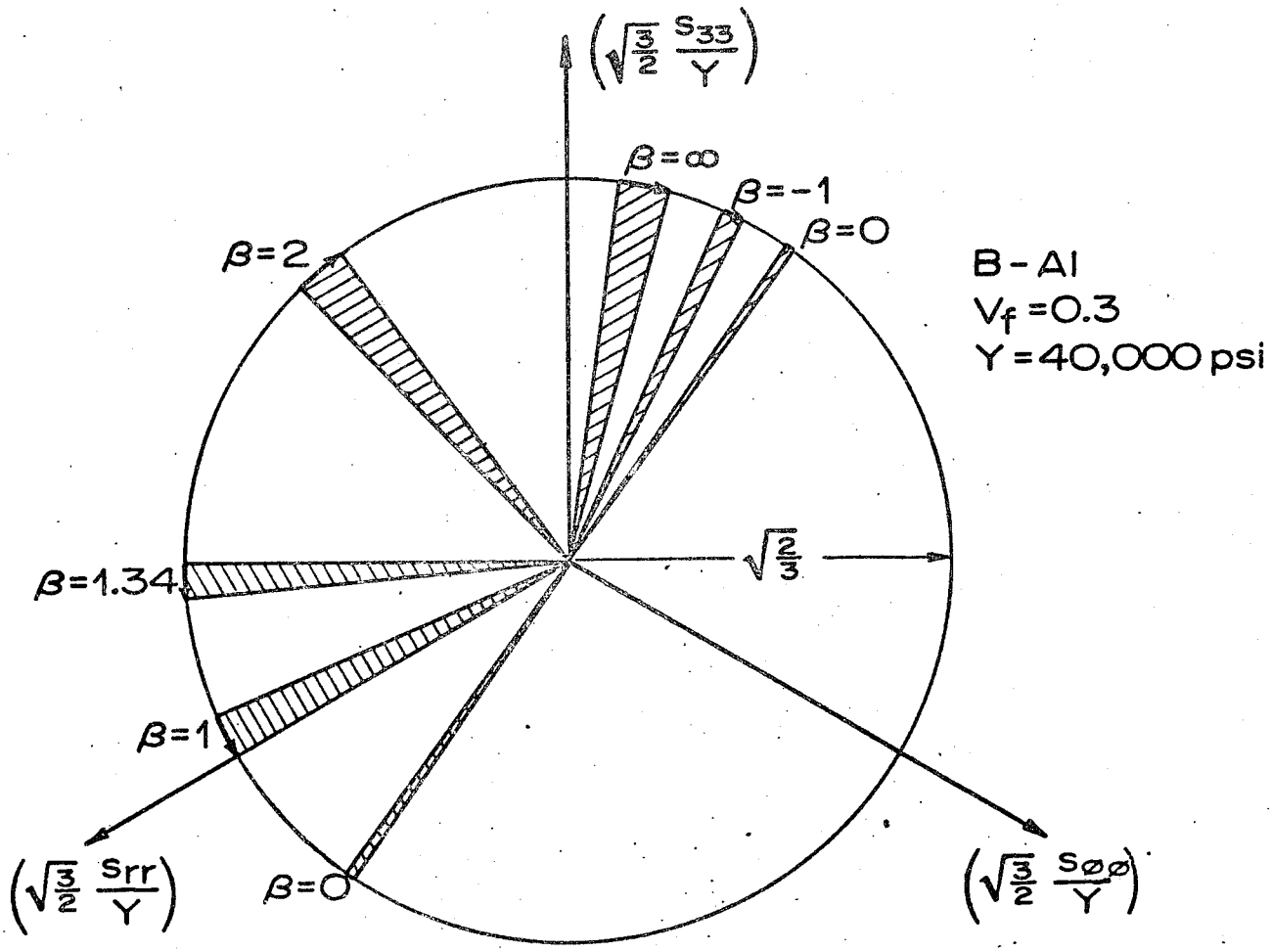

Figure 3-2. Variation of directions of local stress vectors at the interface of a composite cylinder for loading along radial paths $I_2 = \beta I_1$.

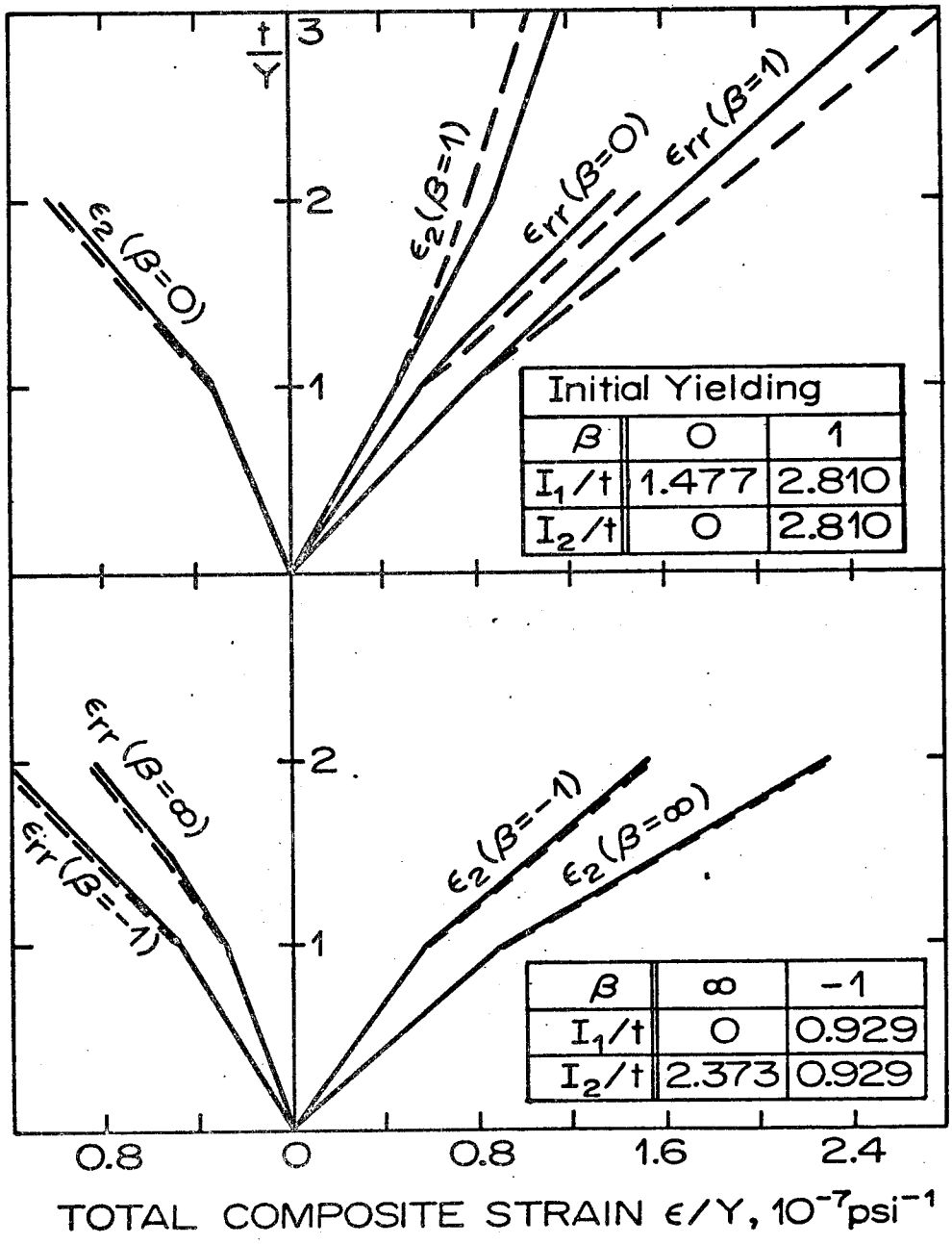

Figure 3-3. Composite Stress-Strain Curves obtained for proportional Loading $I_2 = \beta I_1$ from Hardening Rule I (dashed lines), and from the ELAS65 finite element solution (solid lines). B-Aℓ Composite, $V_f = 0.30$, Y = 40,000 psi.

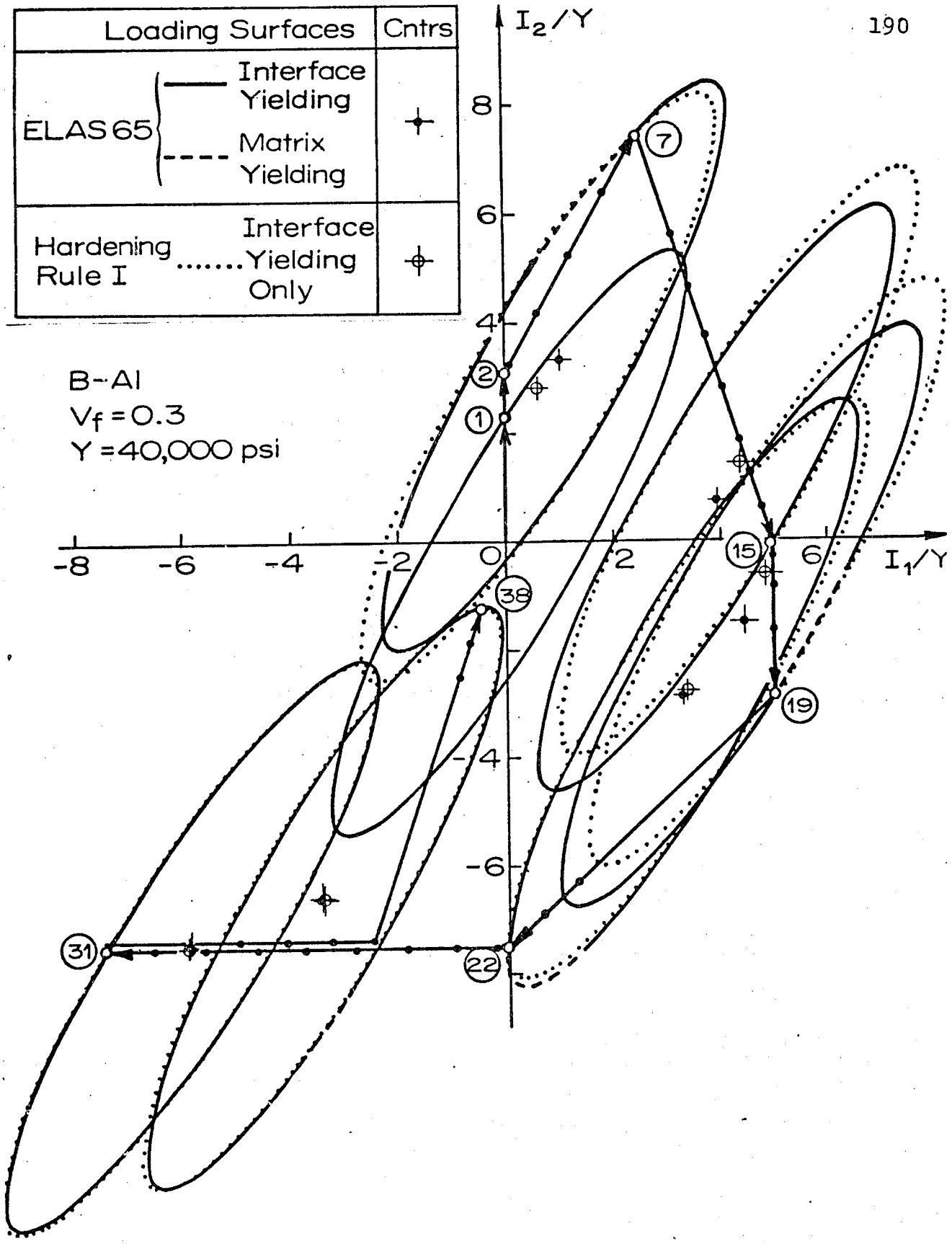

Figure 3-4. Kinematic motion of composite loading surfaces of the B-Aℓ Composite Loaded along Zig-Zag Path I.

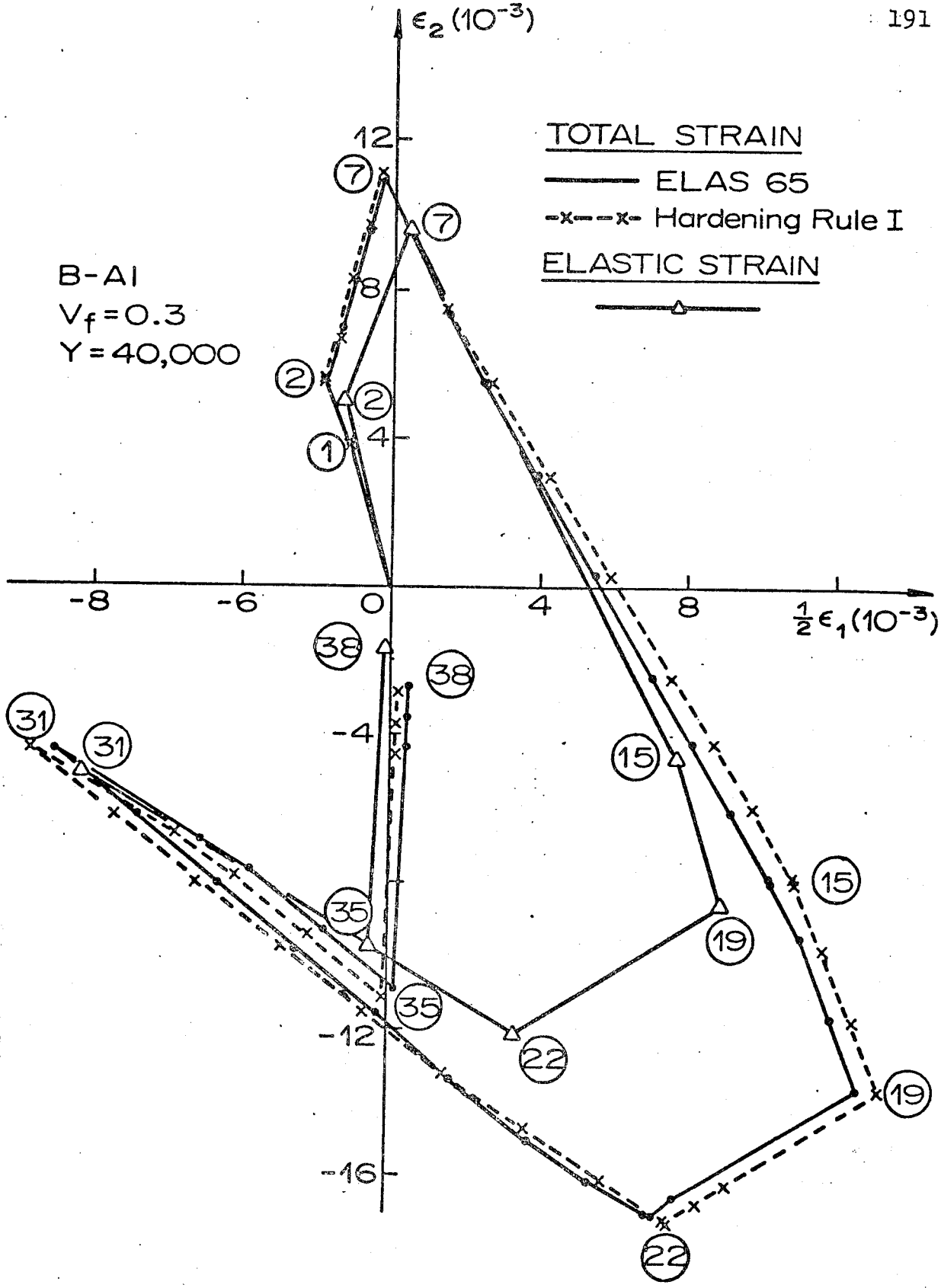

Figure 3-5. Total and Elastic Composite Strains for the B-Aℓ Composite Loaded along Zig-Zag Path I.

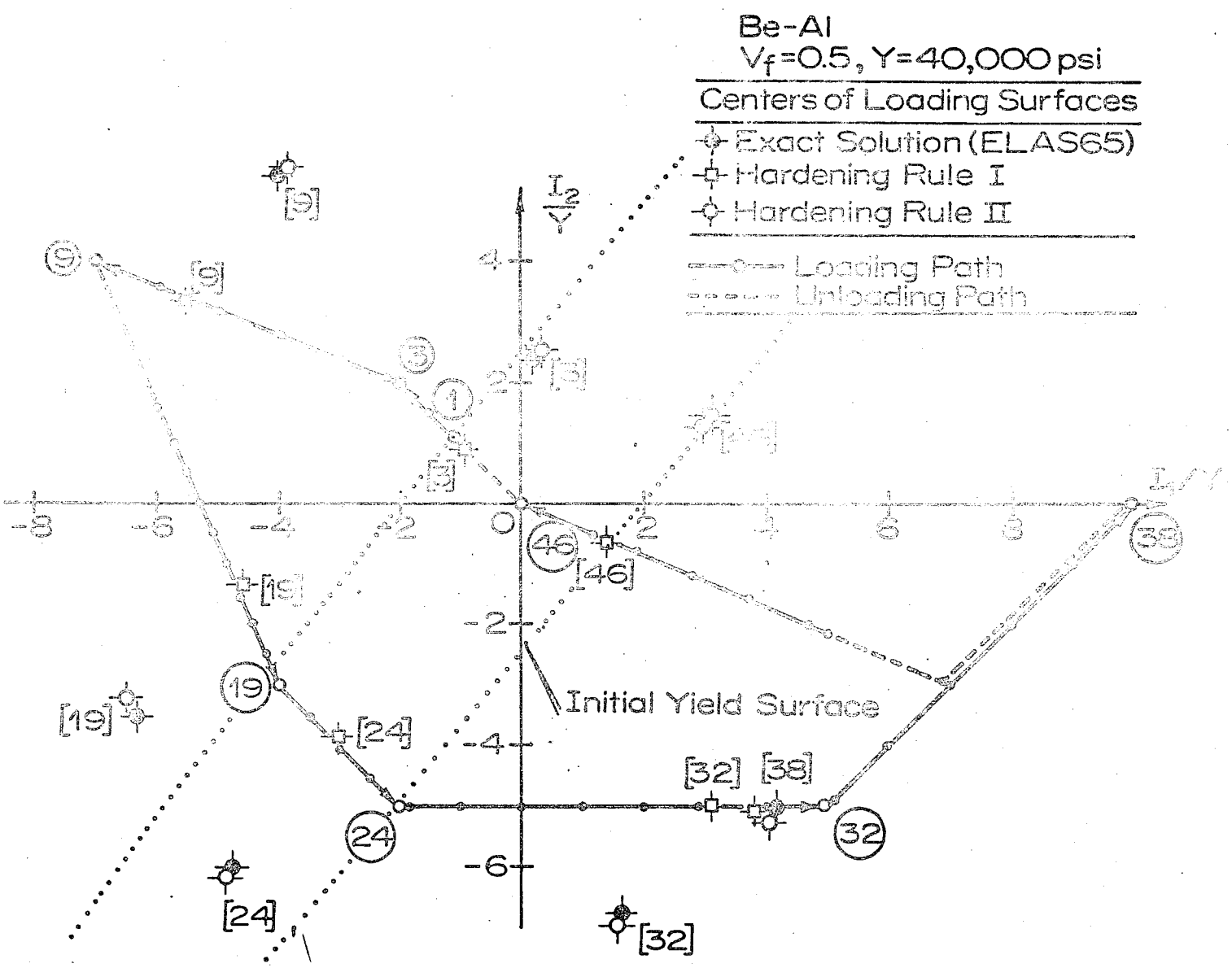

Figure 3-6. Positions of the Centers of Loading Surfaces for the Be-Al Composite at Selected Points of the Zig-Zag Path II.

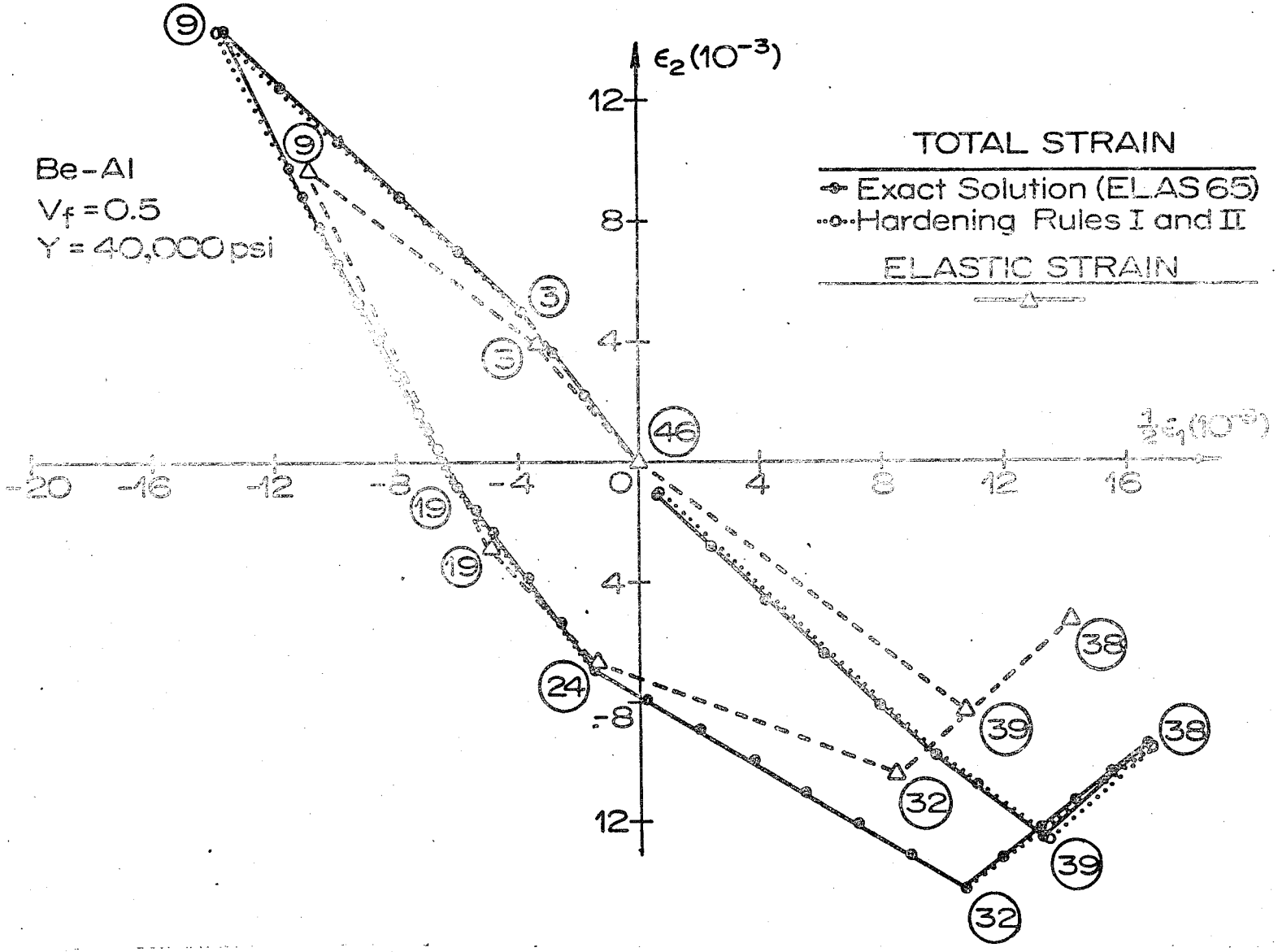

Figure 3-7. Total and Elastic Composite Strains for the Be-Aℓ Composite Loaded along Zig-Zag Path II.

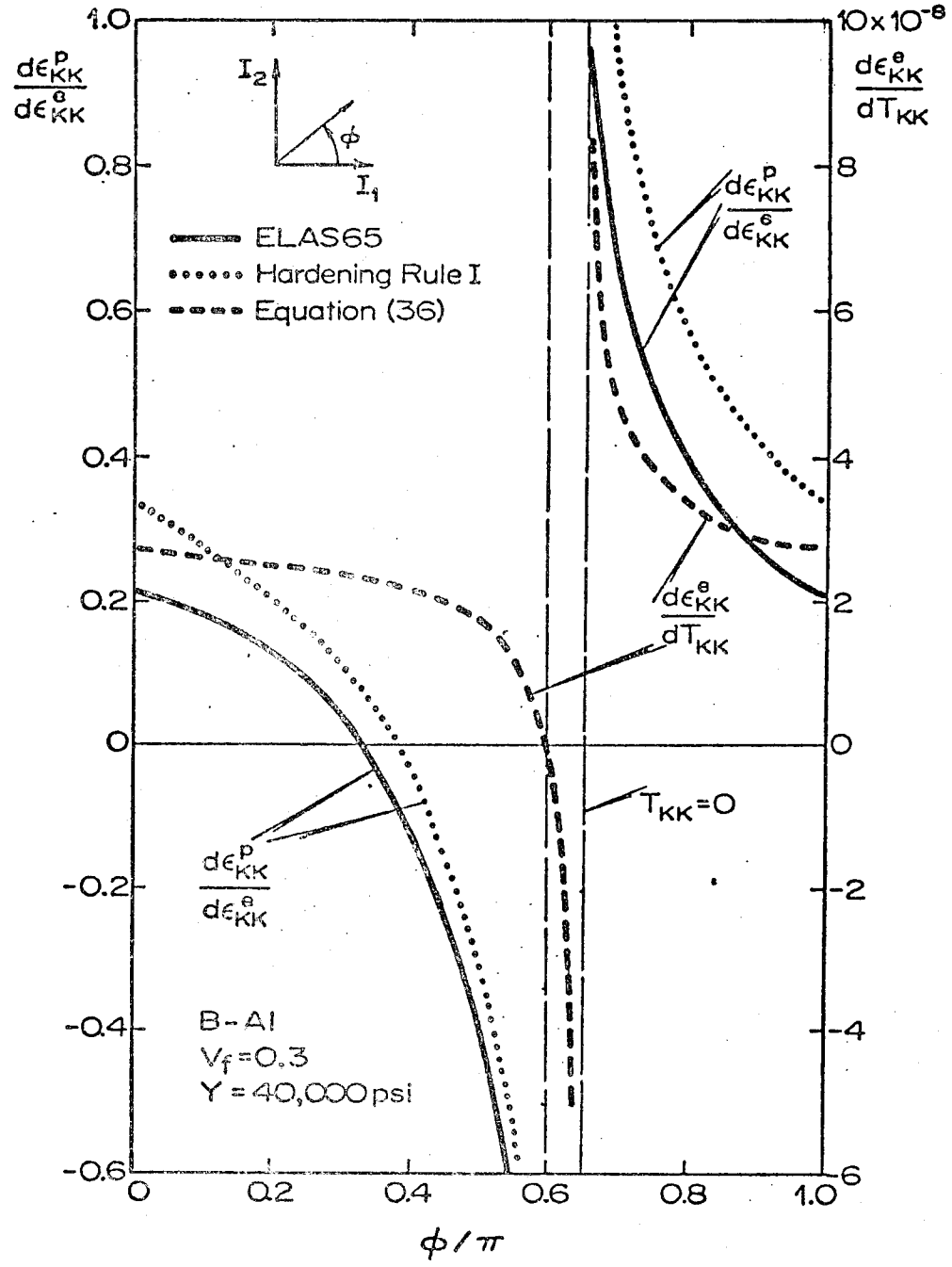

Figure 3-8. The Ratio of Plastic and Elastic Dilatations $d\varepsilon_{kk}^{p}/d\varepsilon_{kk}^{e}$, and the Elastic Bulk Compliance $d\varepsilon_{kk}^{e}/dT_{kk}$ for the B-Aℓ Composite as Functions of the Angle $\phi = \tan^{-1}\beta$, for Proportional Loading $I_2 = \beta I_1$.

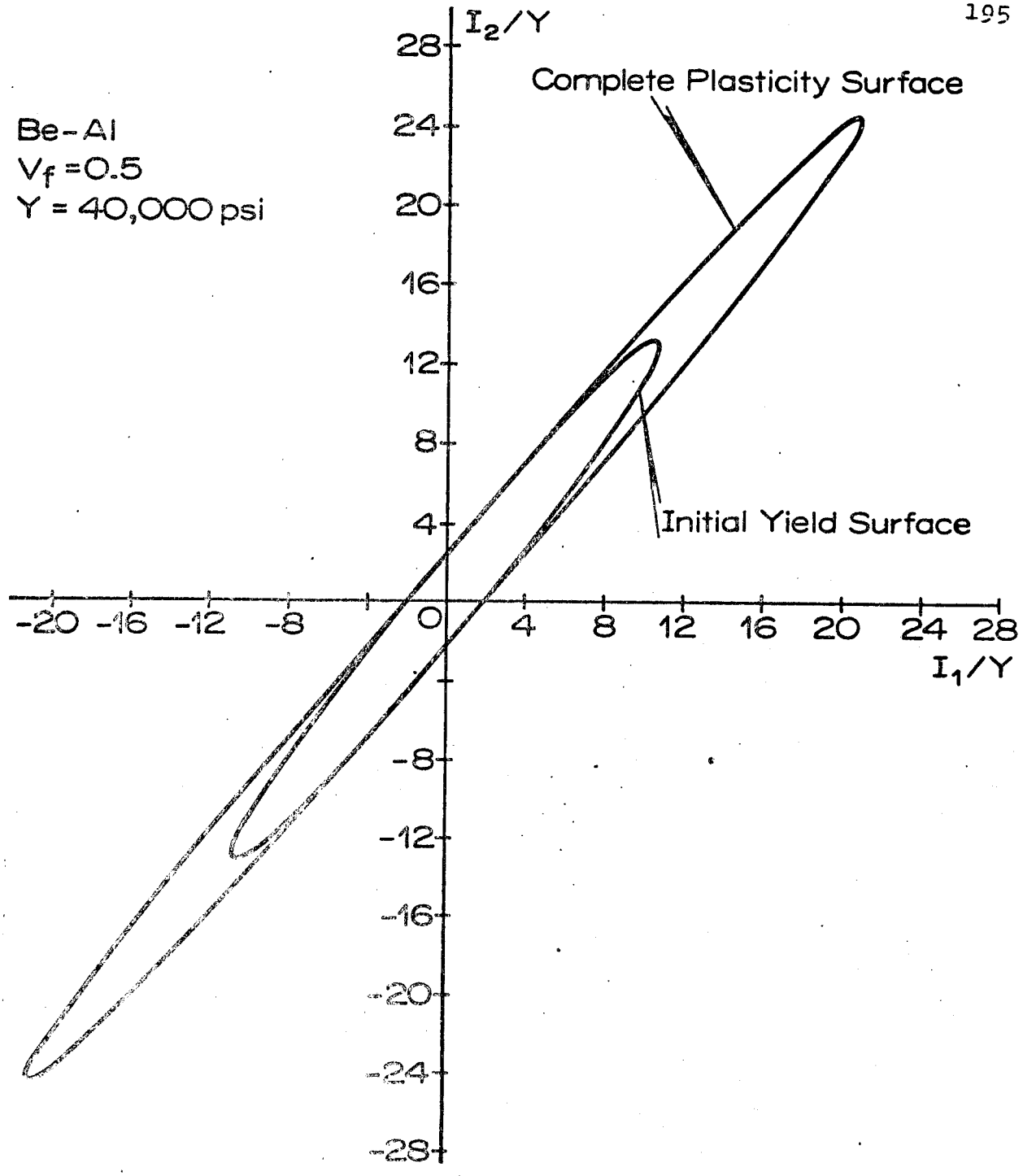

Figure 4-1. The initial Yield Surface, and the Complete Plasticity Surface for Proportional Loading of a Be-Aℓ Composite.

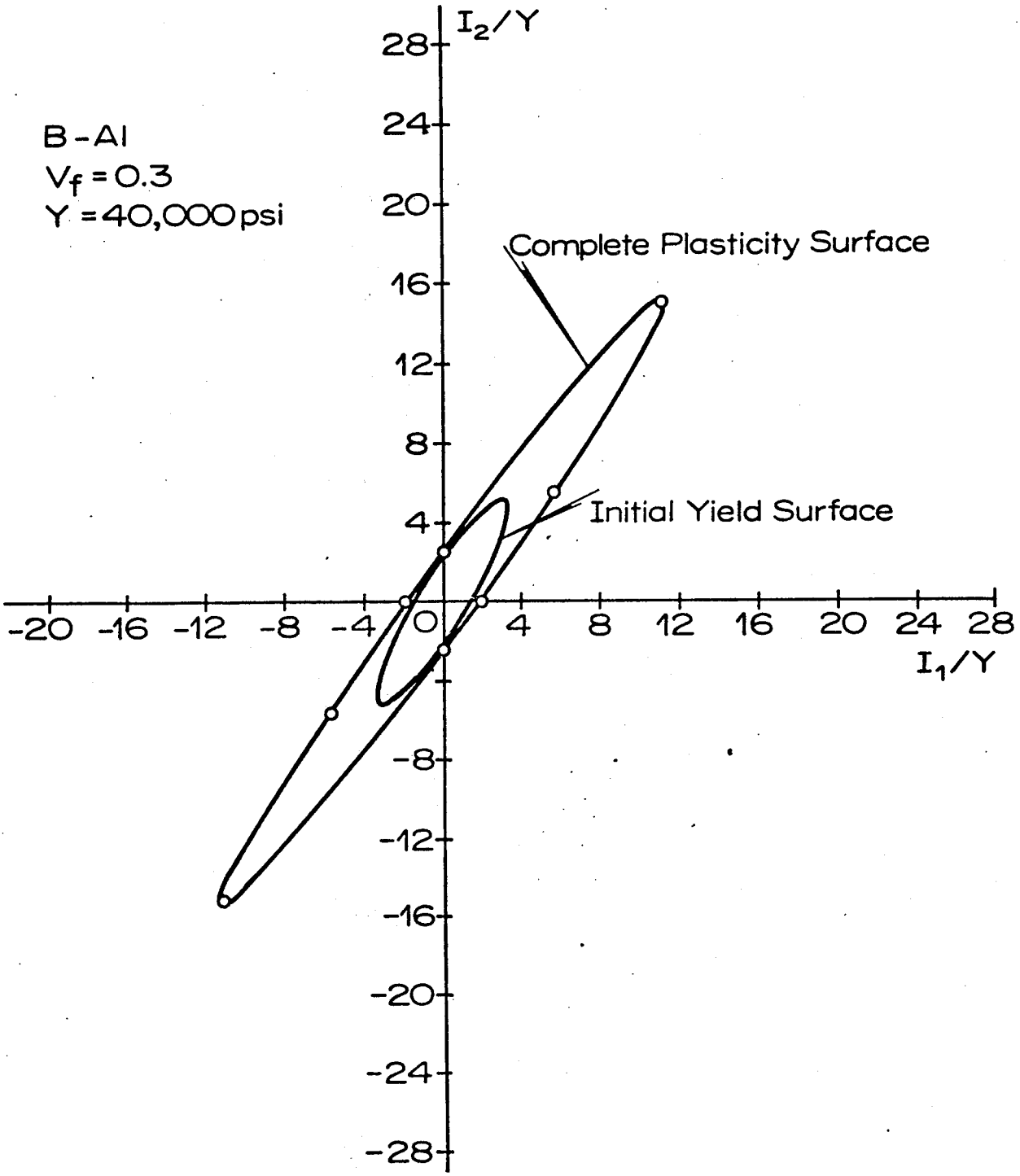

Figure 4-2. The Initial Yield Surface, and the Complete Plasticity Surface for Proportional Loading of a B-Aℓ Composite (0 Indicates Points Calculated by the Finite Element Method).

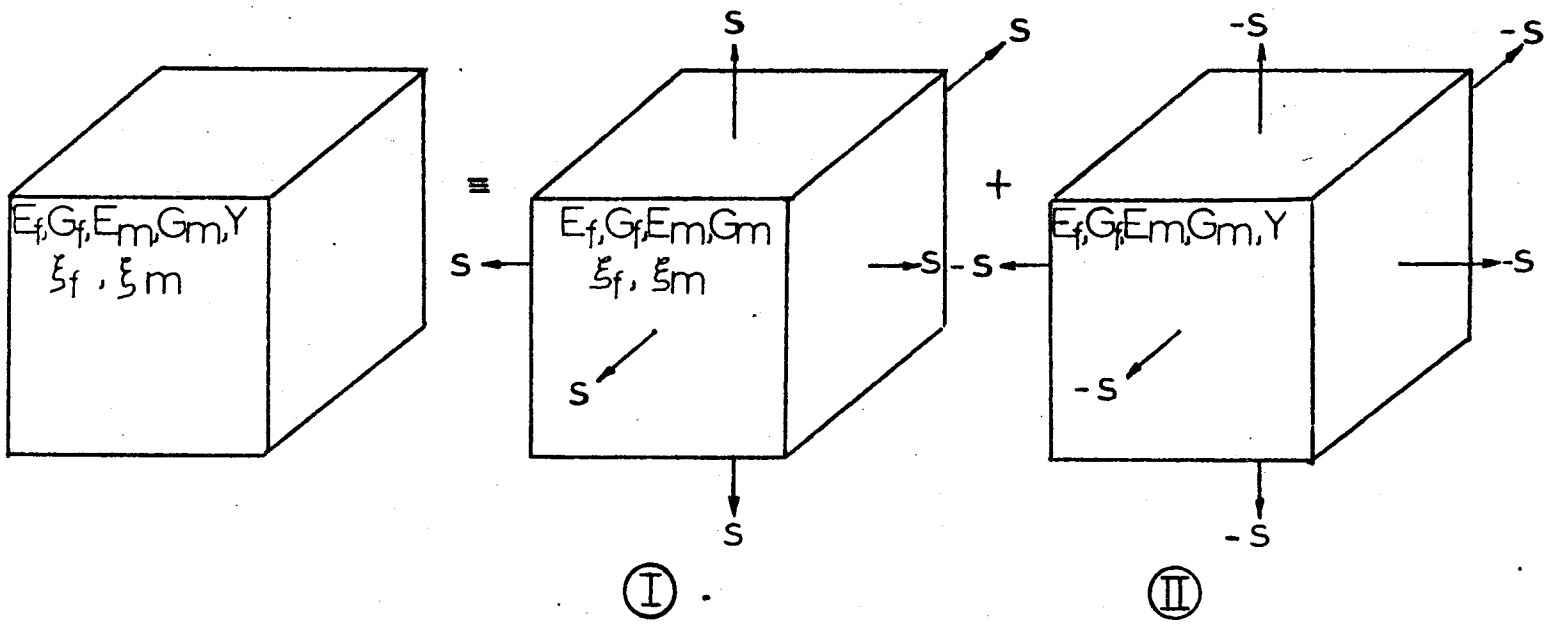

Figure 5-1. Thermo-mechanical Analogy Illustrating the Two-Part Solution for Temperature Change in the Composite and Volume Changes in the Matrix Due to Metallurgical Transformations.

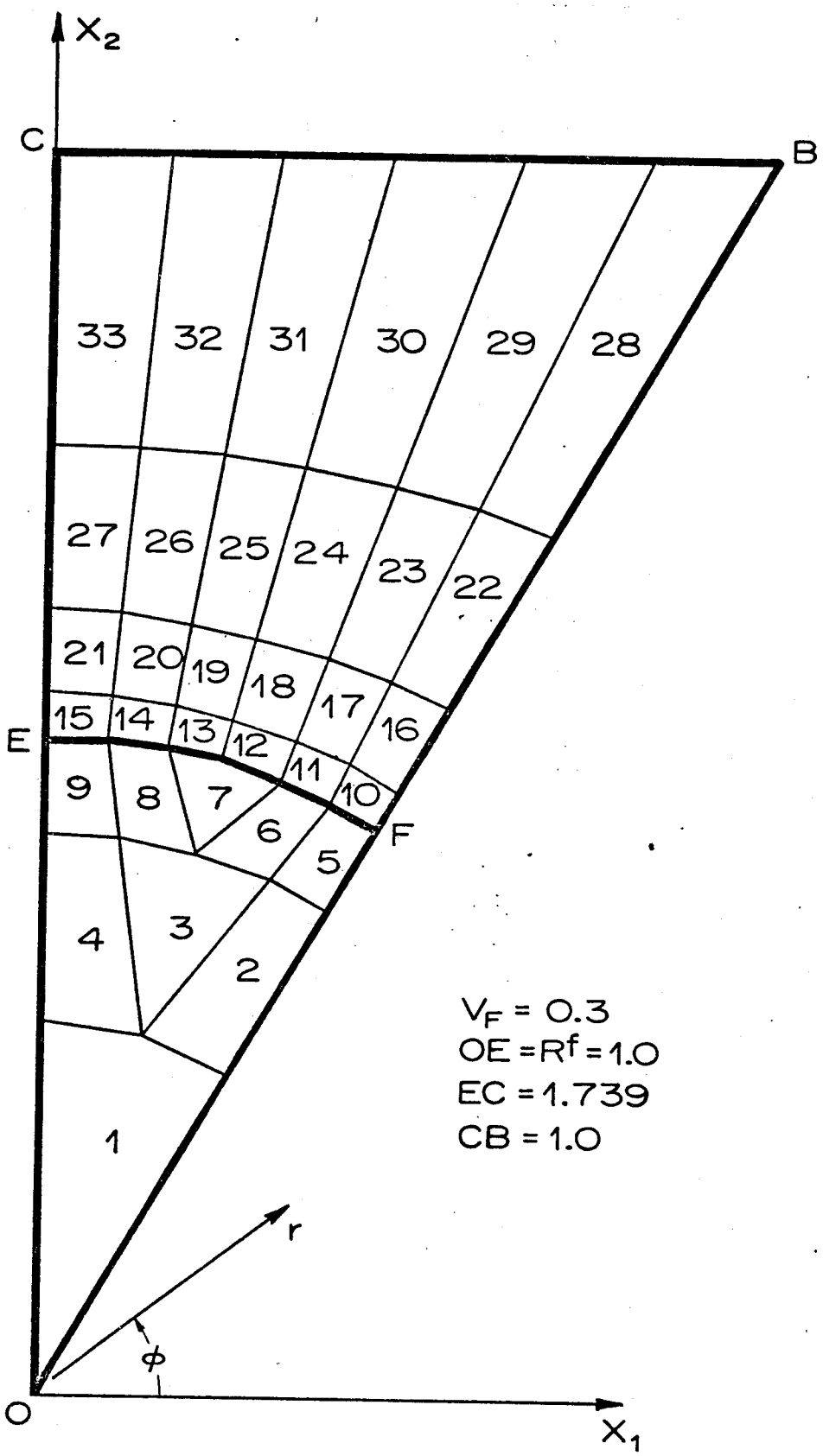

Figure 5-2. The Elementary Composite Domain of the Hexagonal Model in Figure 1-1 for Axisymmetric Problems, and the Finite Element Mesh.

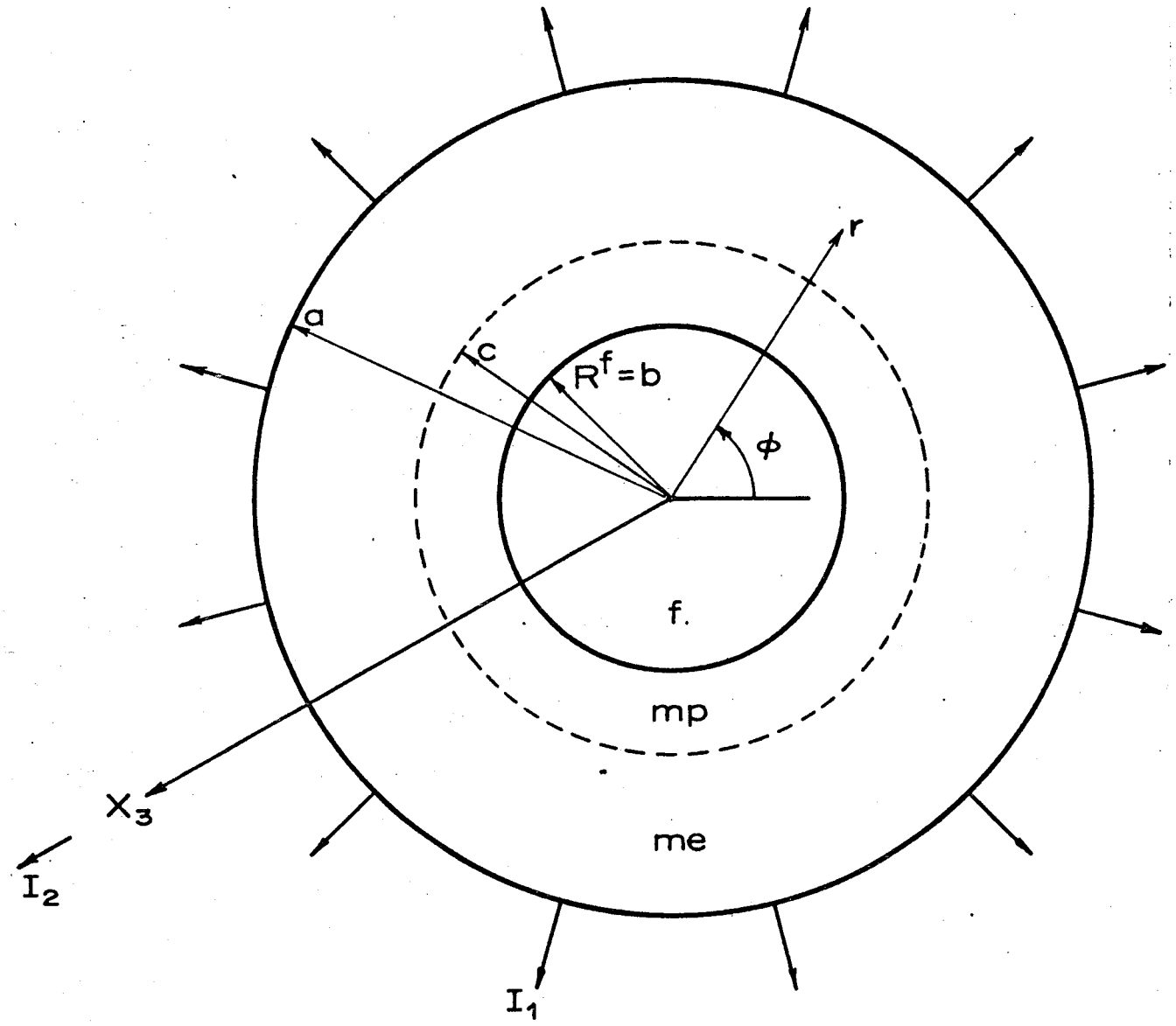

Figure 5-3. Cross Section of an Elastic-Plastic Composite Cylinder Model of a Composite Loaded by Axisymmetric Composite Stresses I_1 and I_2.

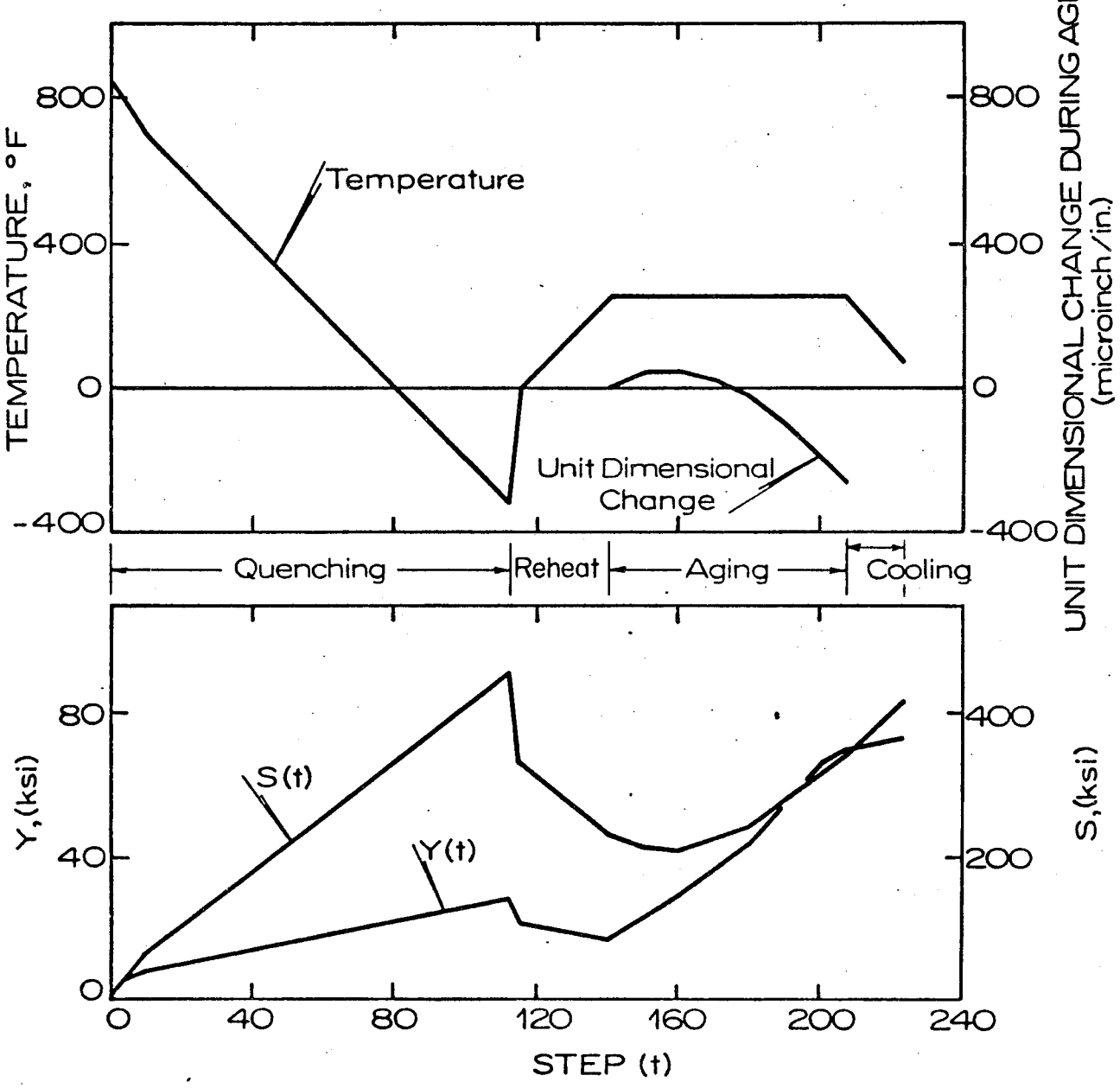

Figure 5-4. Data for the T6M Treatment of 7075 Aℓ-B Composite Required for the Solution of the Heat Treatment Problem.

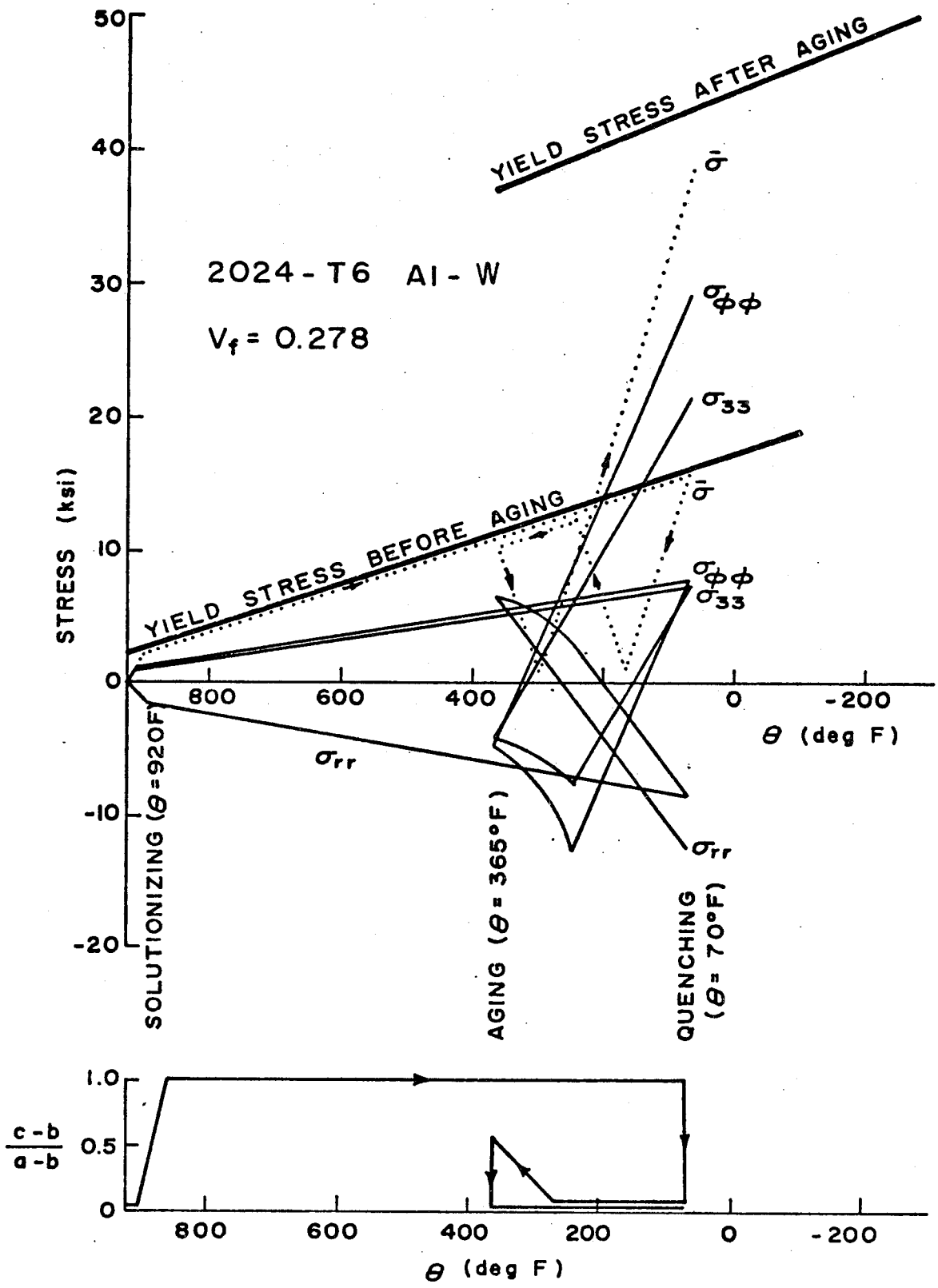

Figure 5-5. Microstresses at the Fiber-Matrix Interface, and the Location of the Elastic-Plastic Boundary (r = c) in the Matrix During Heat Treatment of the 2024-T6 Aℓ-W Composite.

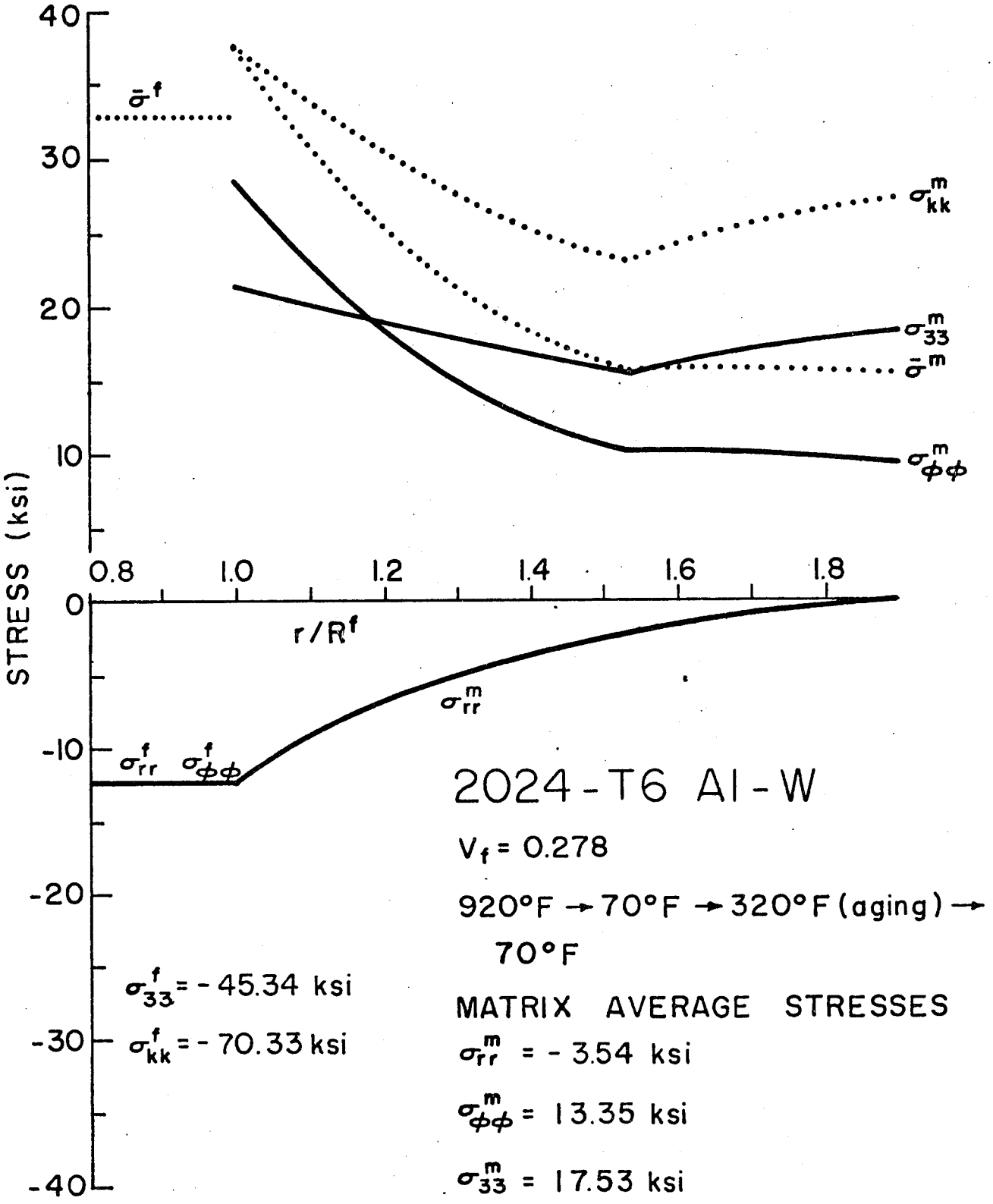

Figure 5-6. Microstress Distribution after Heat Treatment in the Cylinder Model (Figure 5-3) of the 2024-T6 Aℓ-W Composite.

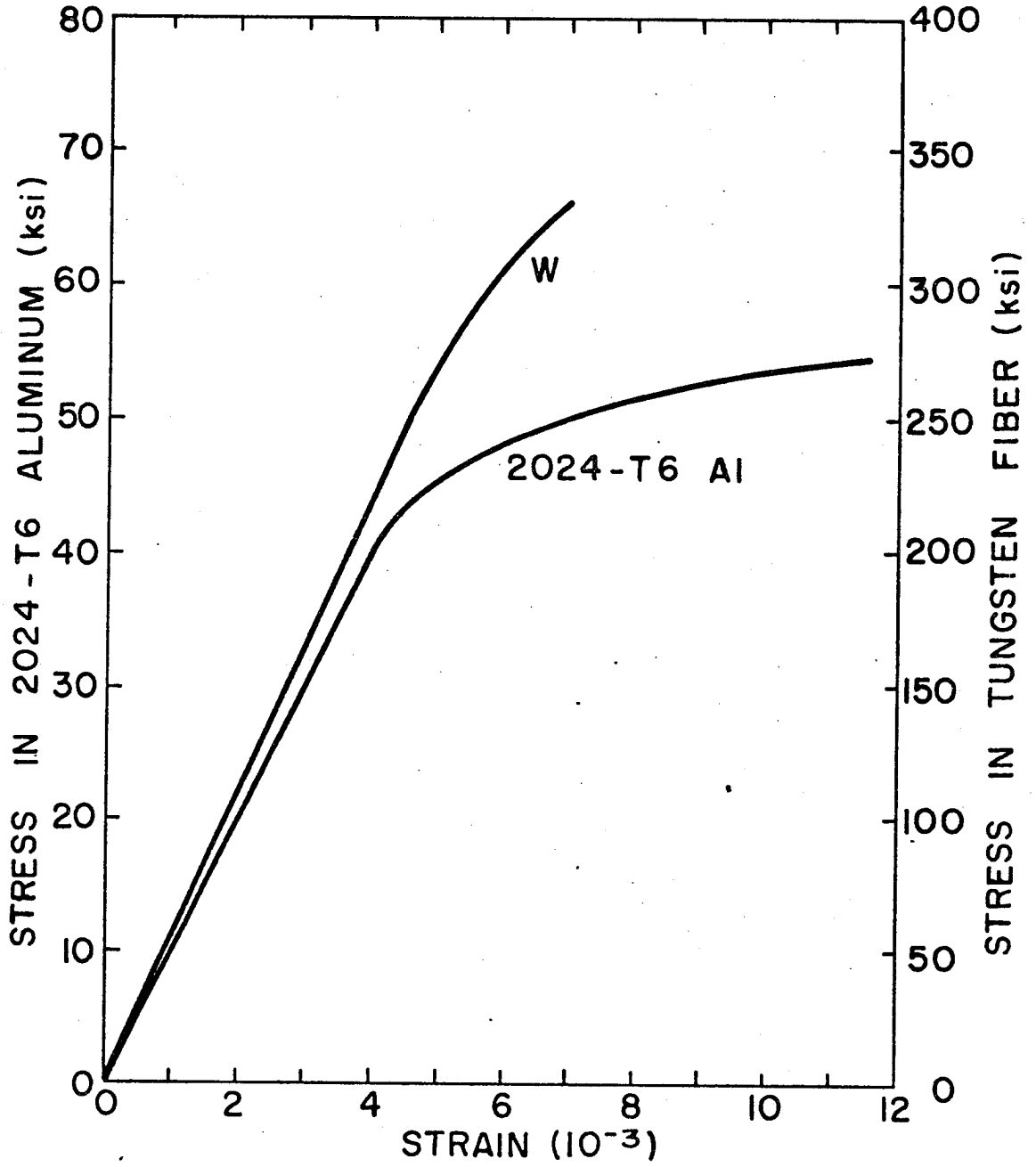

Figure 5-7. Uniaxial Tensile Stress-Strain Curves of the Tungsten Fiber and the Aluminum Matrix.

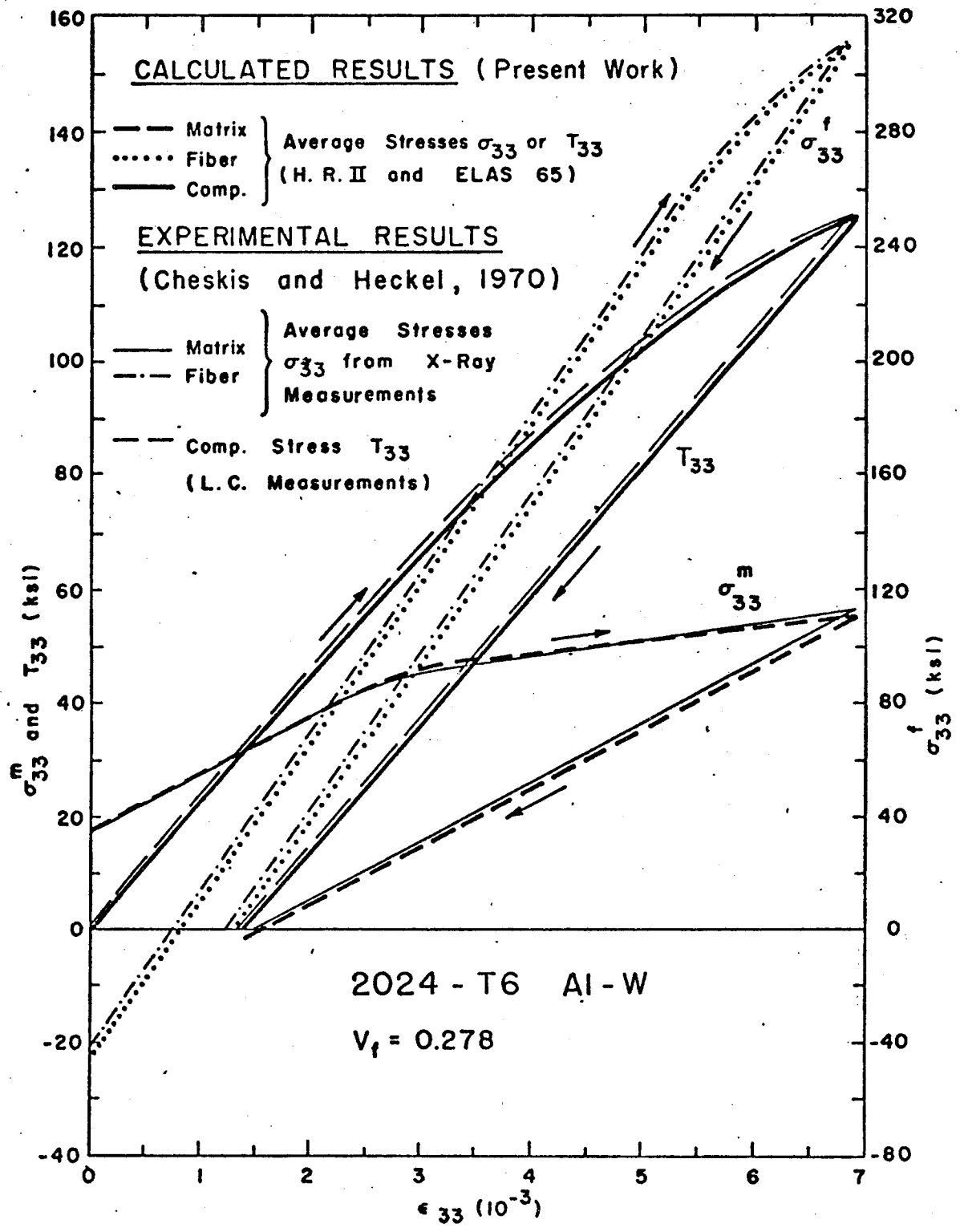

Figure 5-8. Comparison of the Calculated and Experimentally Measured Average Microstresses and Composite Stresses During a Tension Test of a 2024-T6 Aℓ-W Composite. Experimental Data by Cheskis and Heckel, Ref. [46].

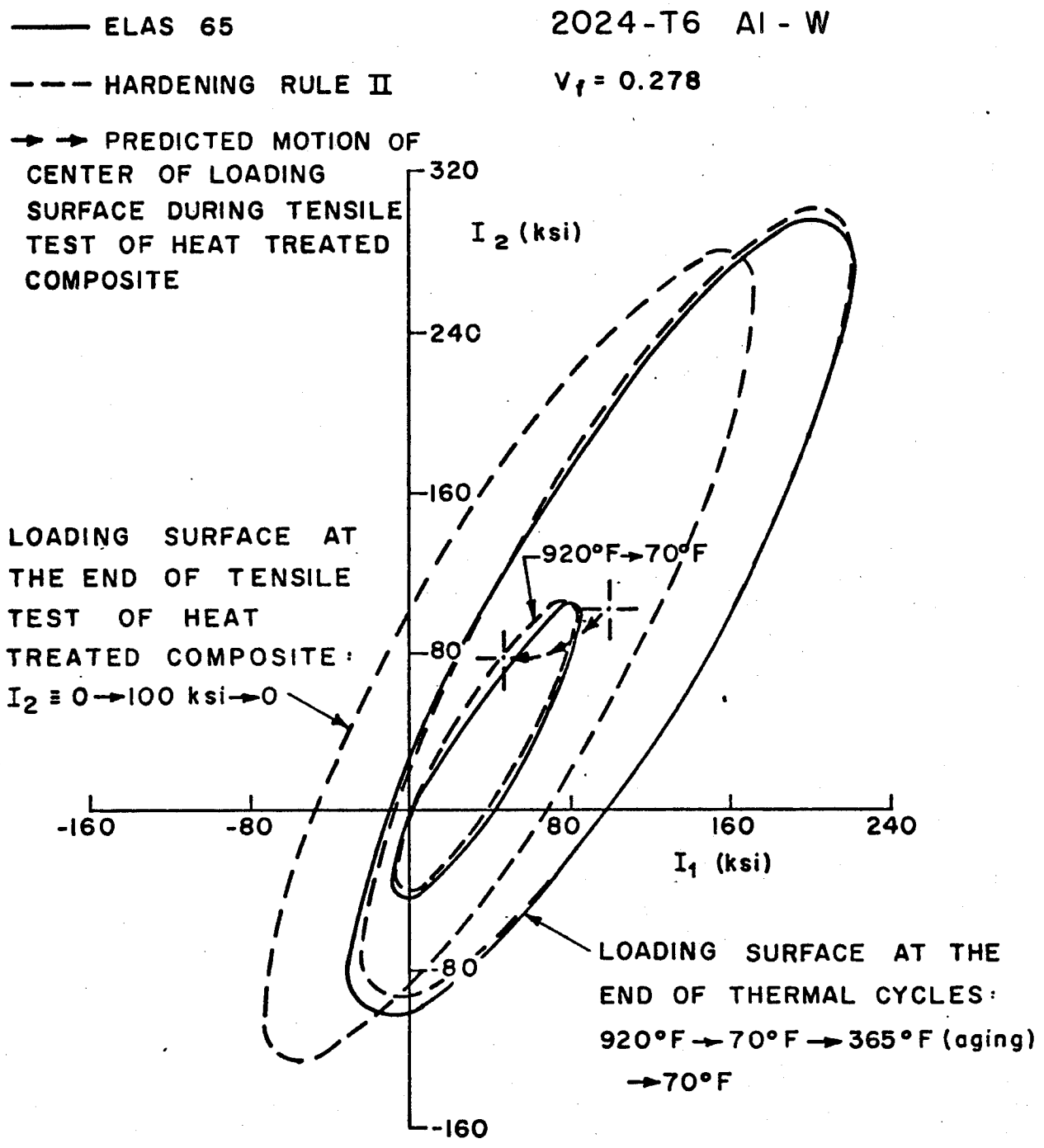

Figure 5-9. Loading Surfaces at Various Stages of Heat Treatment and During a Tension Test of the 2024-T6 Aℓ-W Composite.

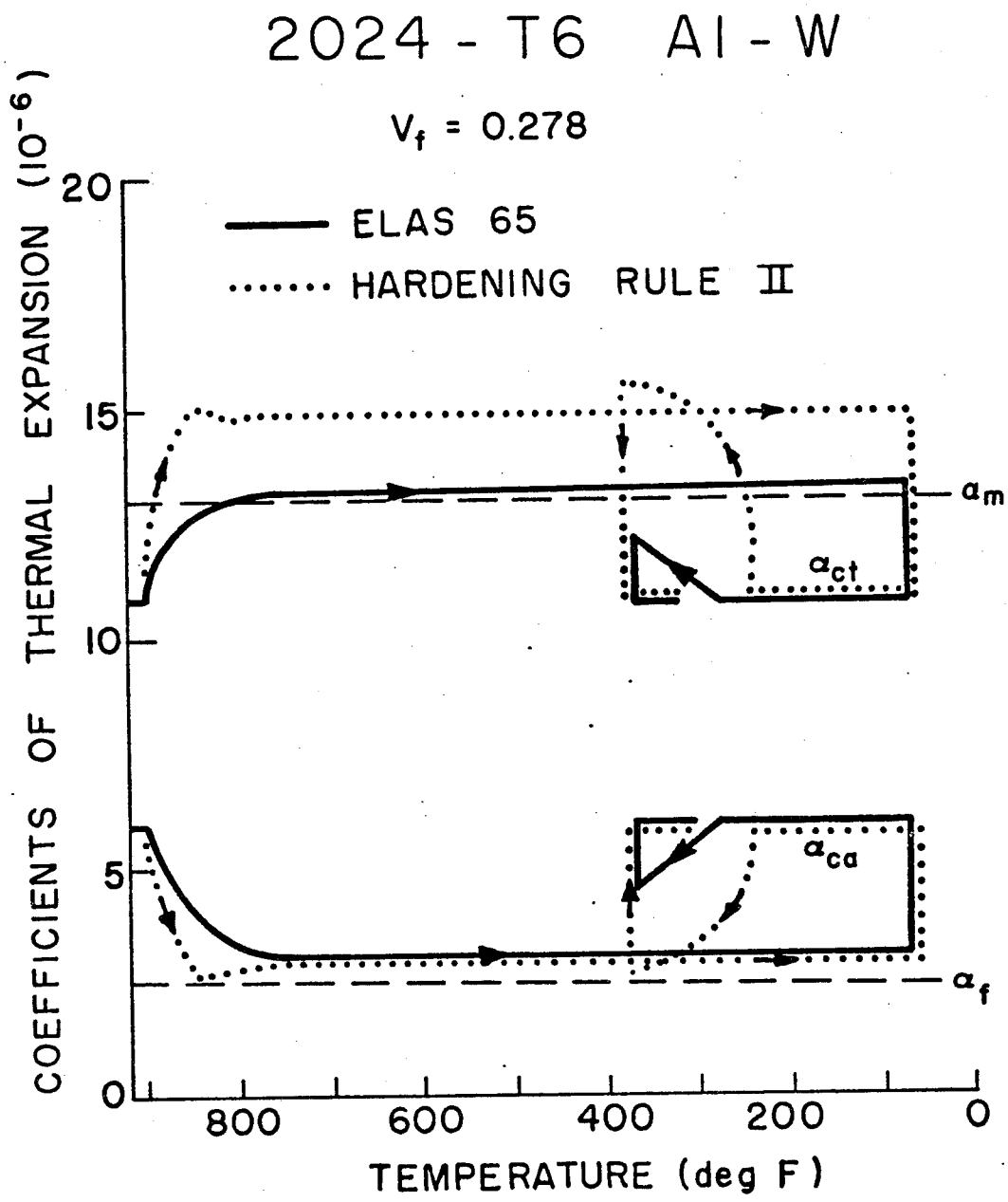

Figure 5-10. Composite Thermal Expansion Coefficients in the Axial (α_{ca}) and Transverse (α_{ct}) Directions During the Heat Treatment of the 2024-T6 Aℓ-W Composite.

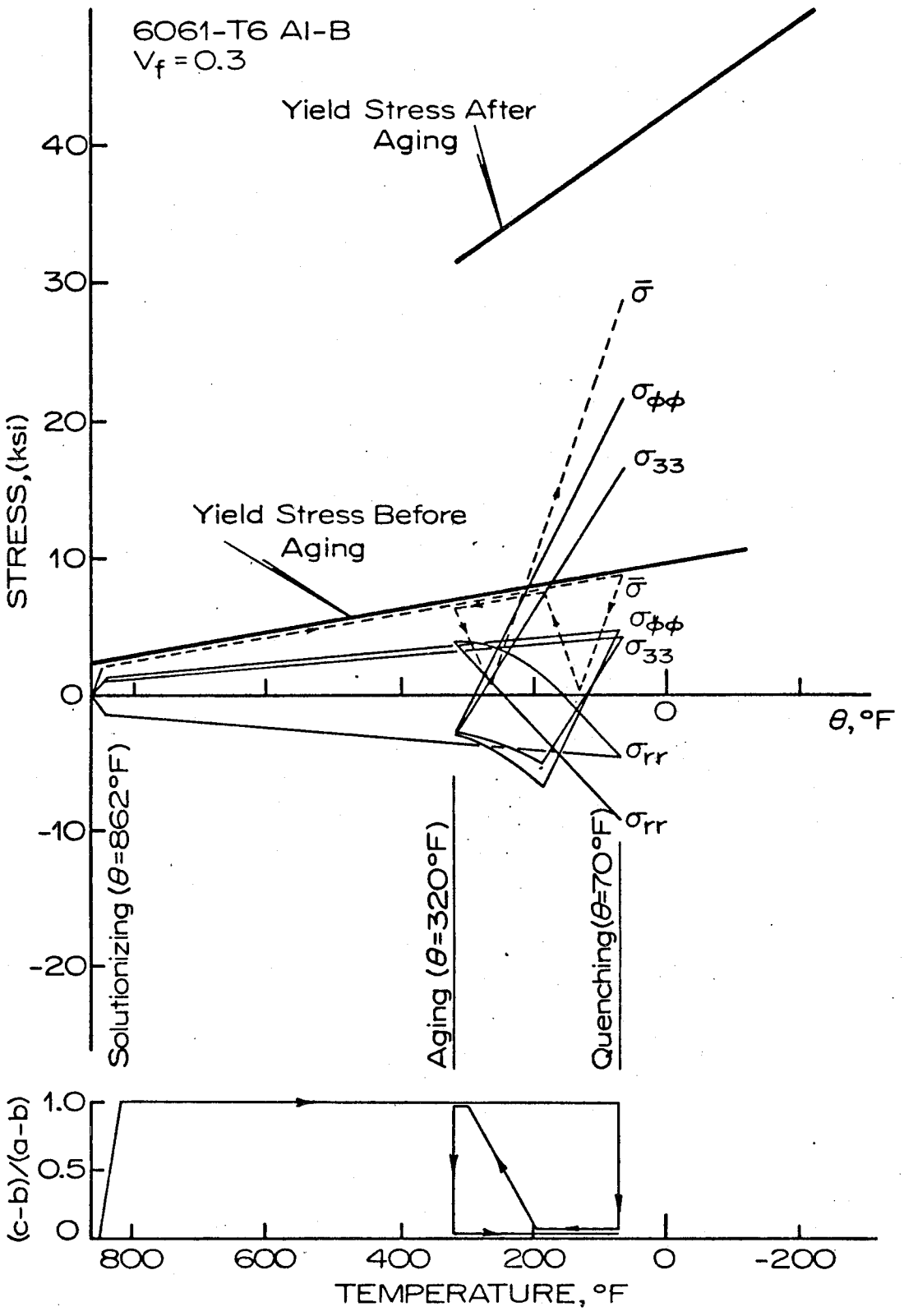

Figure 5-11. Microstresses at the Fiber-Matrix Interface, and the Location of the Elastic-Plastic Boundary (r = c) in the Matrix During Heat Treatment of the 6061-T6 Aℓ-B Composite.

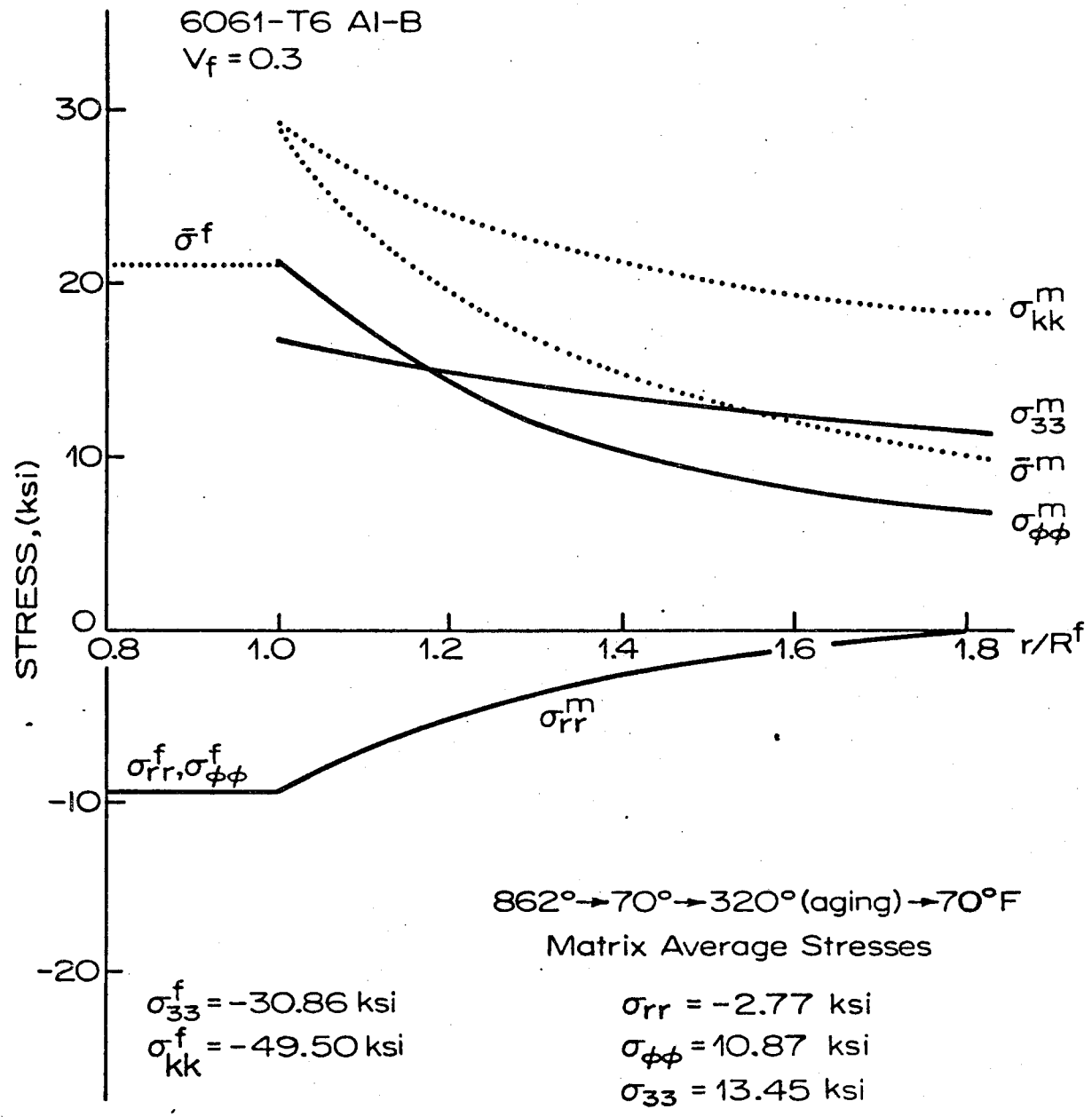

Figure 5-12. Microstress Distribution after Heat Treatment in the Cylinder Model (Figure 5-3) of the 6061-T6 Aℓ-B Composite.

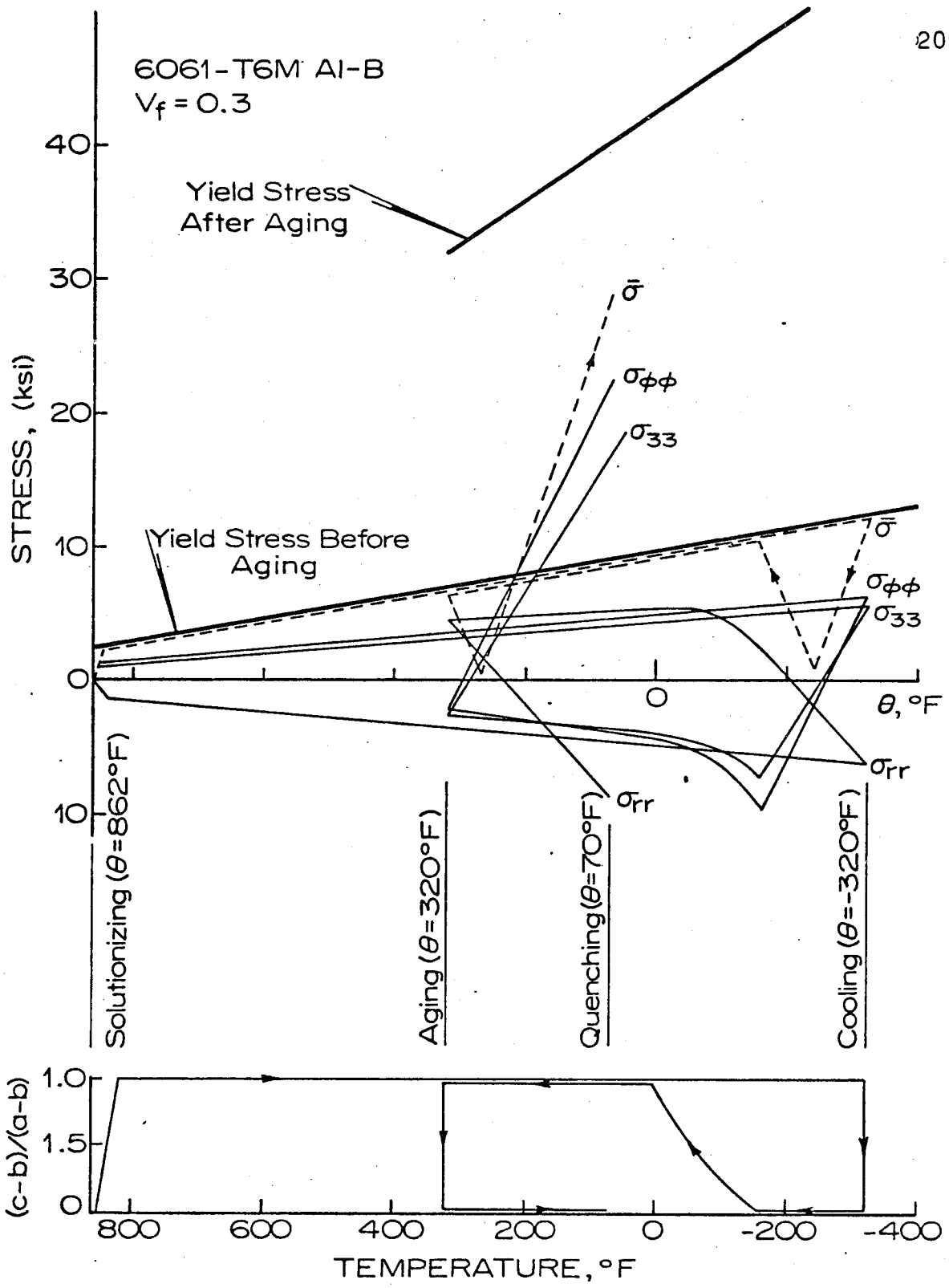

Figure 5-13. Microstresses at the Fiber-Matrix Interface, and the Location of the Elastic-Plastic Boundary (r = c) in the Matrix During the Heat Treatment of the 6061-T6M Aℓ-B Composite.

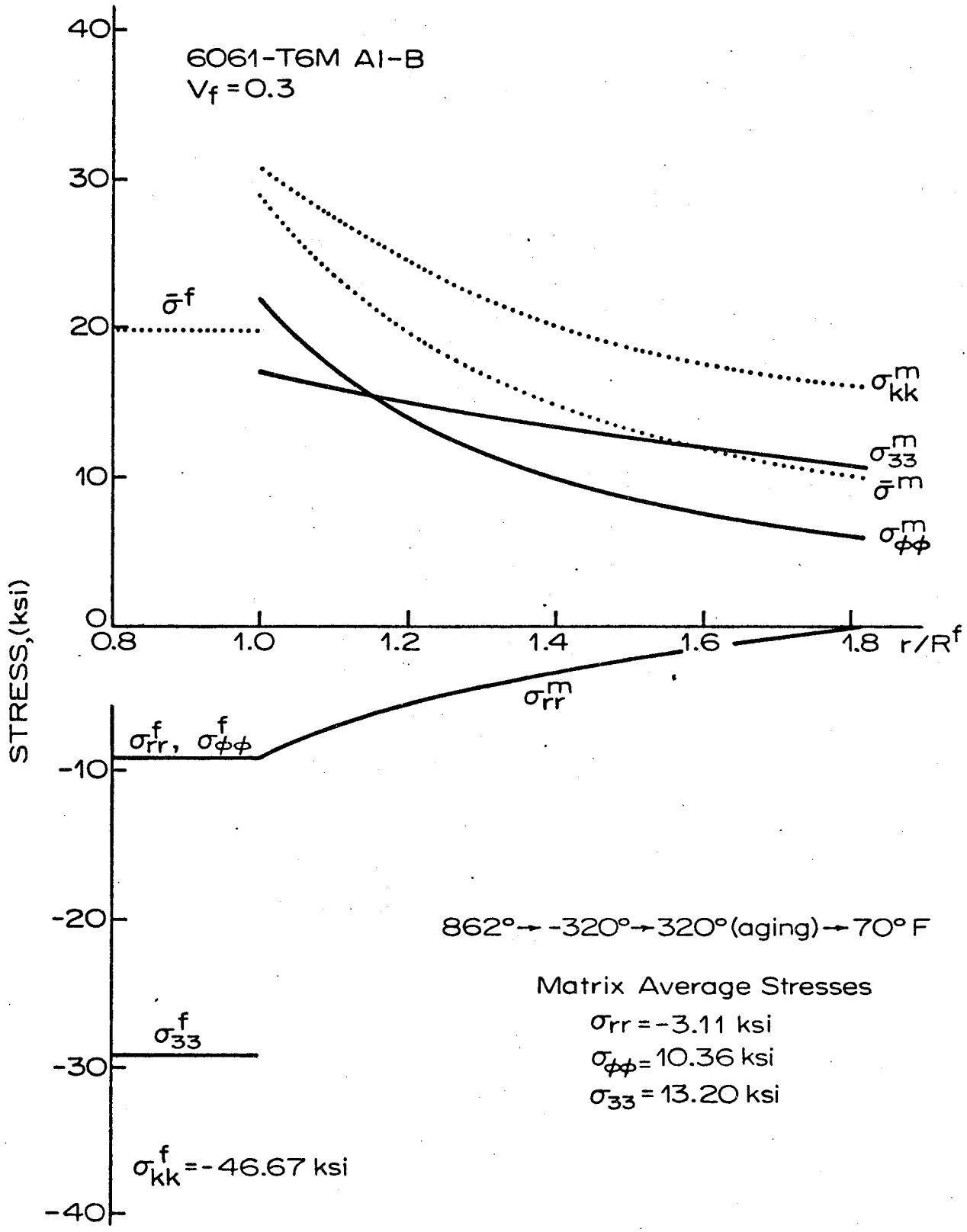

Figure 5-14. Microstress Distribution after Heat Treatment in the Cylinder Model (Figure 5-3) of the 6061-T6M Aℓ-B Composite.

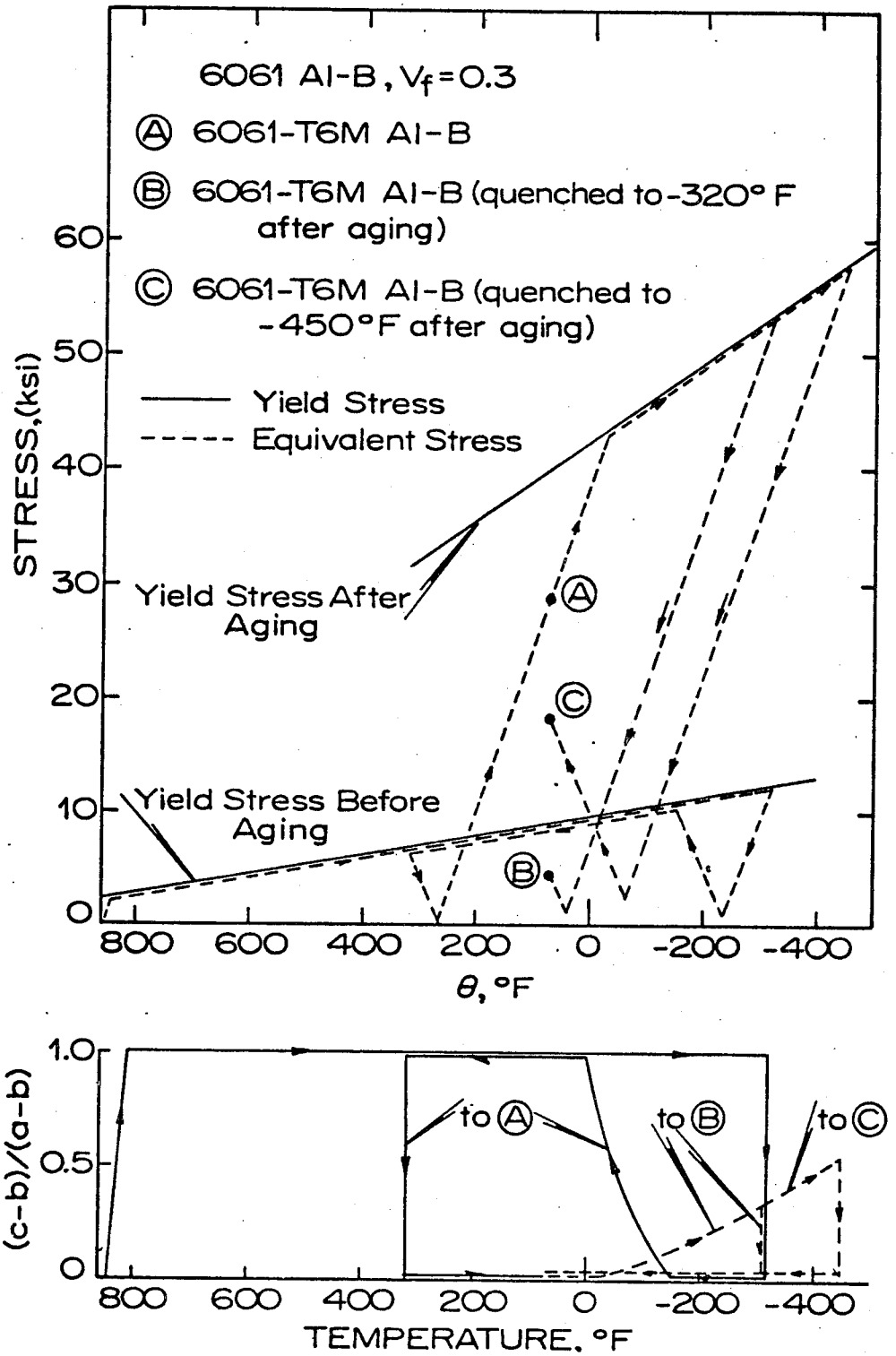

Figure 5-15. Equivalent Stress at the Fiber-Matrix Interface, and the Location of the Elastic-Plastic Boundary in the Matrix During: (A) Heat Treatment of the Matrix to the T6M Temper; (B) a Subsequent Cooling Cycle to -320 deg. F.; (C) a Subsequent Cooling Cycle to -450 deg. F. for a 6061 Aℓ-B Composite.

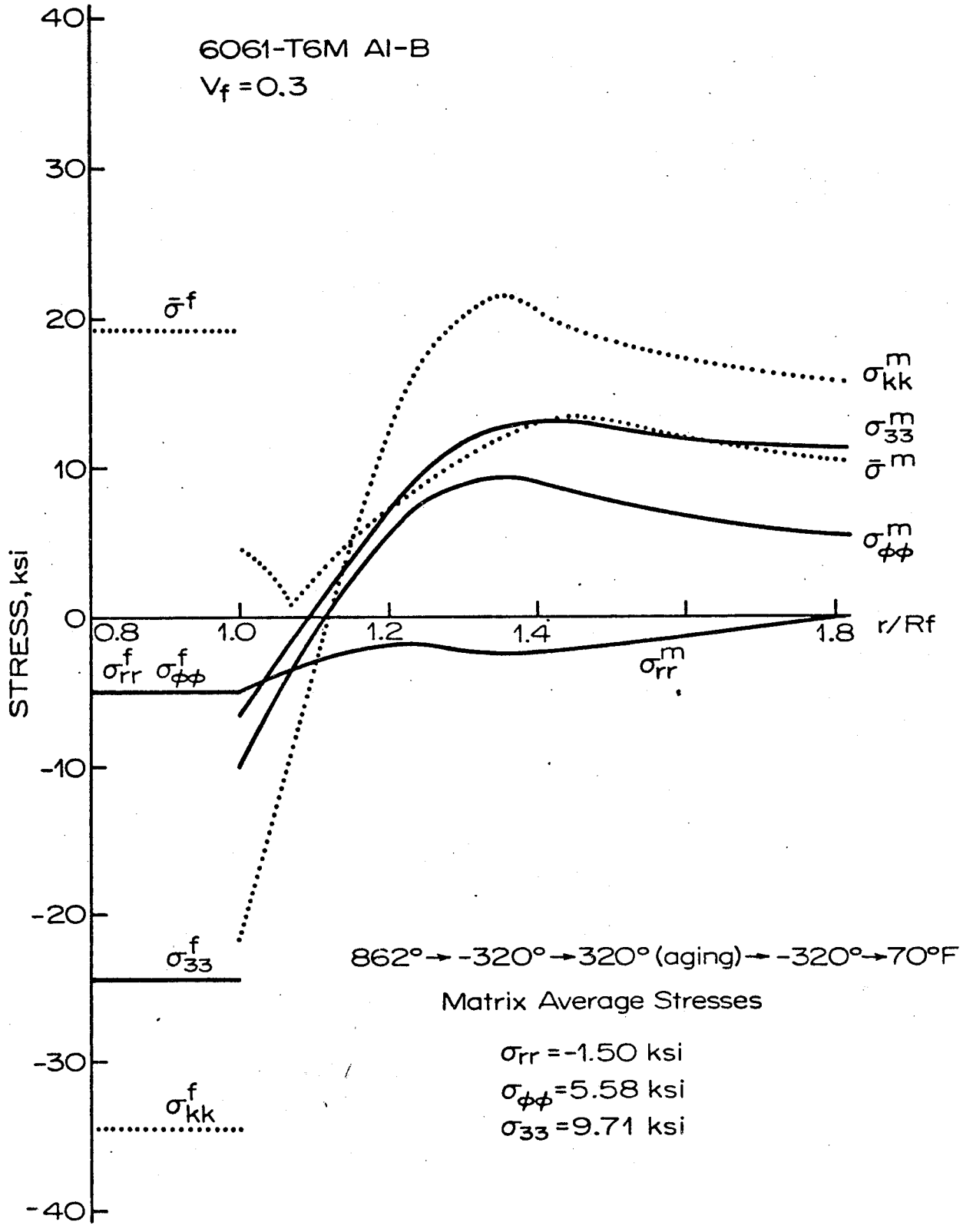

Figure 5-16. Microstress Distribution in the Composite Cylinder Model (Figure 5-3) of the 6061-T6M Aℓ-B Composite, after Completion of a Cooling Cycle to -320 deg. F.

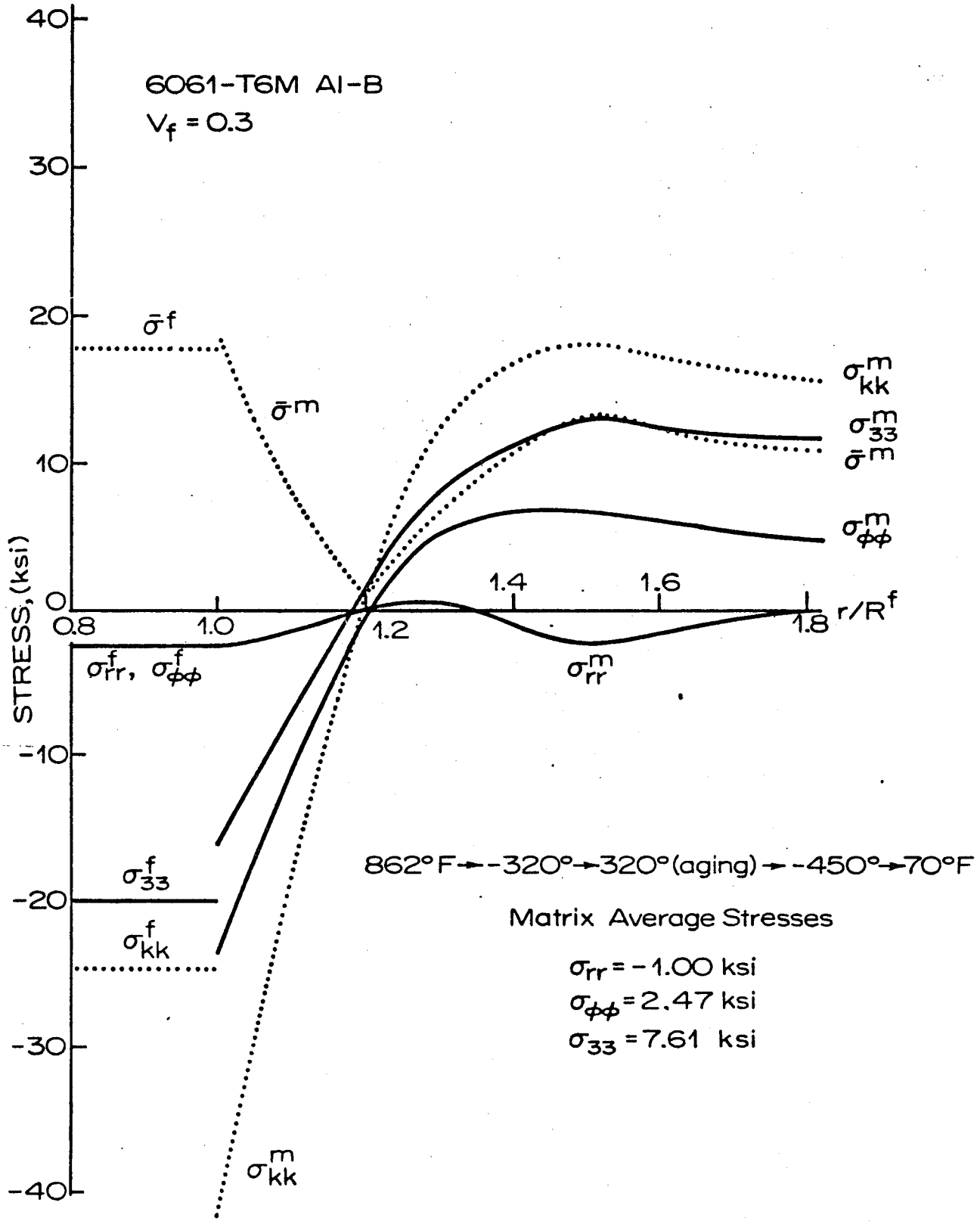

Figure 5-17. Microstress Distribution in the Composite Cylinder Model (Figure 5-3) of the 6061-T6M Aℓ-B Composite, after Completion of a Cooling Cycle to -450 deg. F.

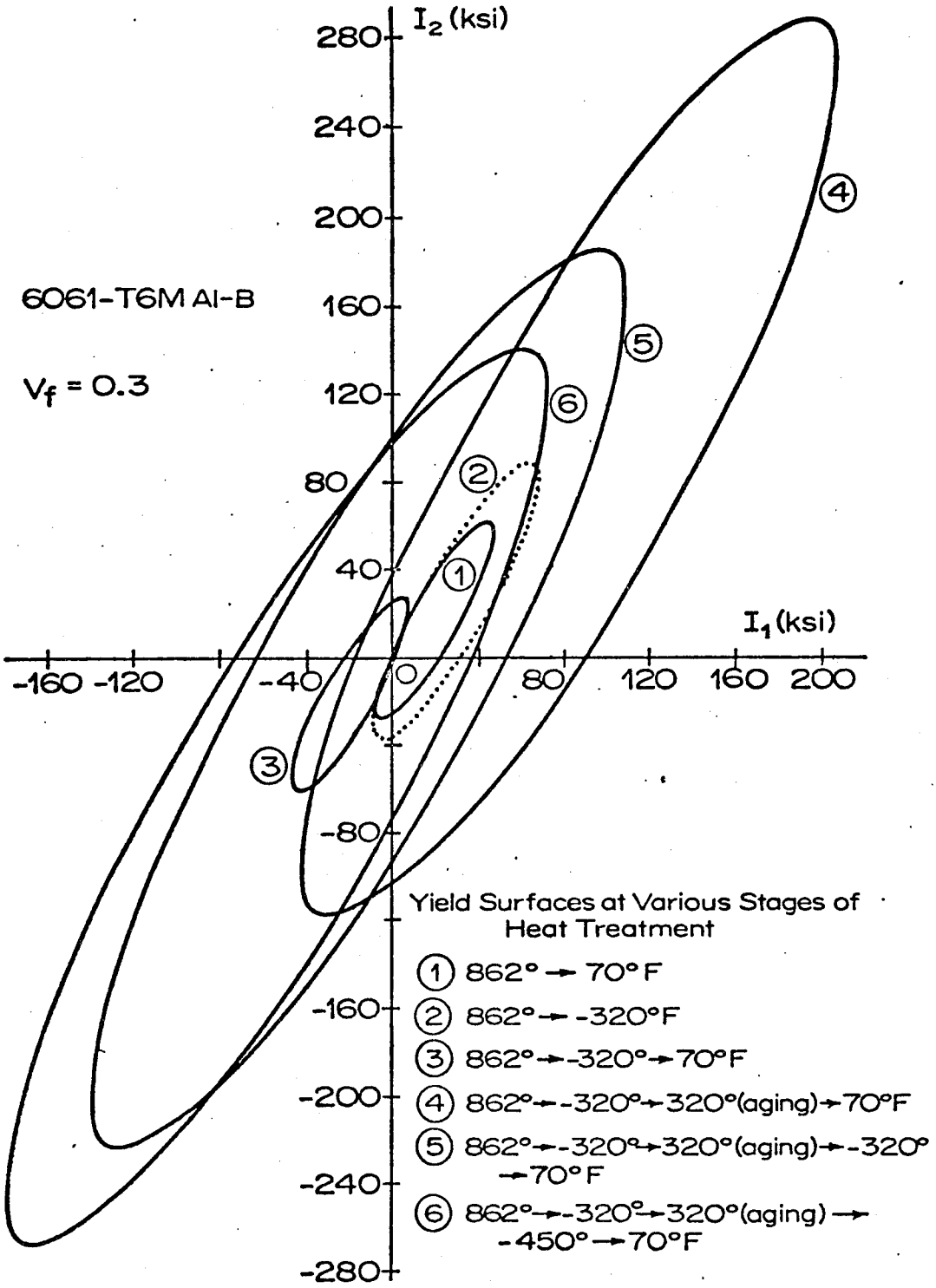

Figure 5-18. Yield (Loading) Surfaces at Various Stages of Heat Treatment of the 6061-T6M Aℓ-B Composite.

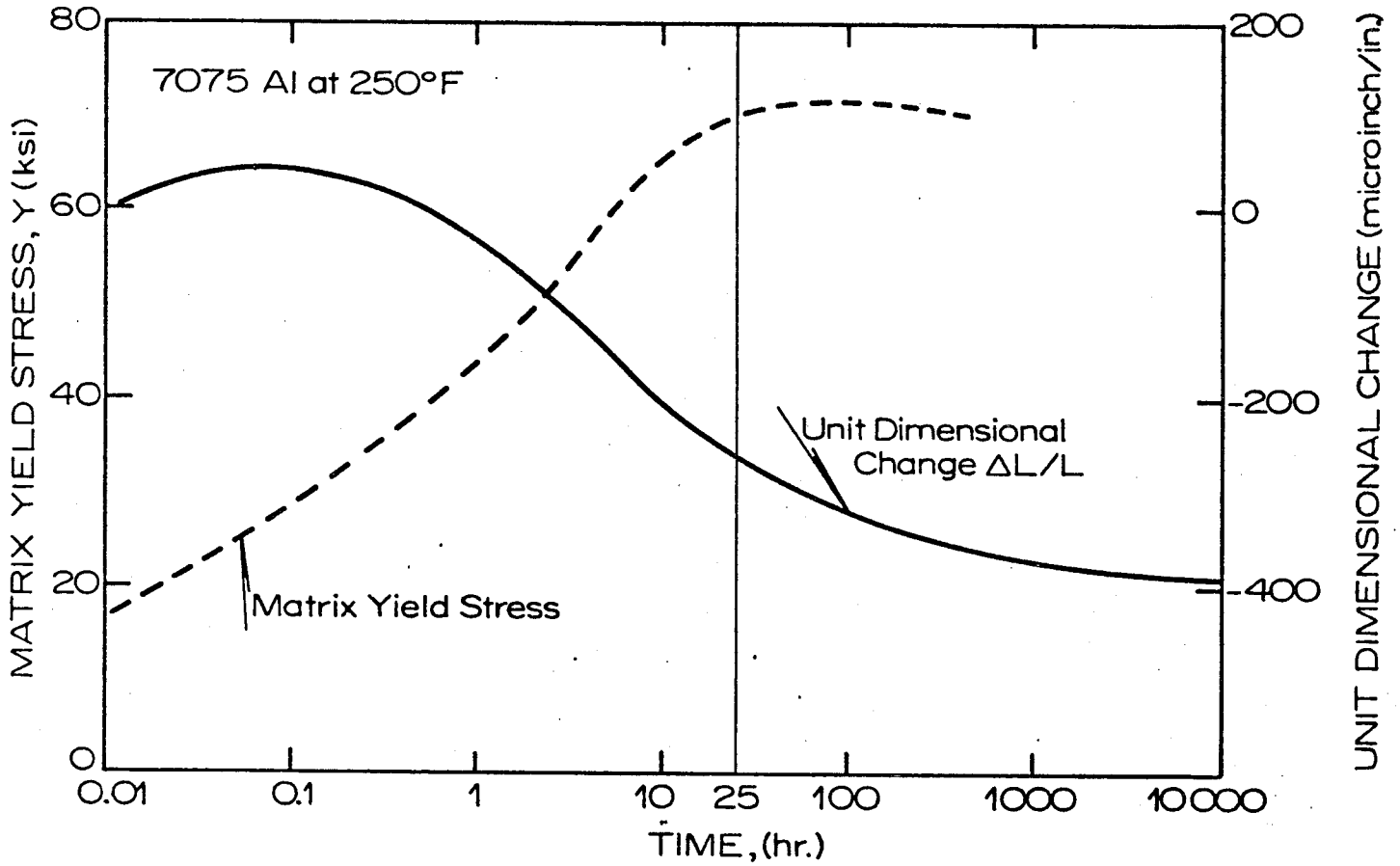

Figure 5-19. The Matrix Yield Stress, and the Unit Dimensional Change in a Quenched 7075-Aℓ Alloy, as Functions of Time at the Aging Temperature of 250 deg. F.

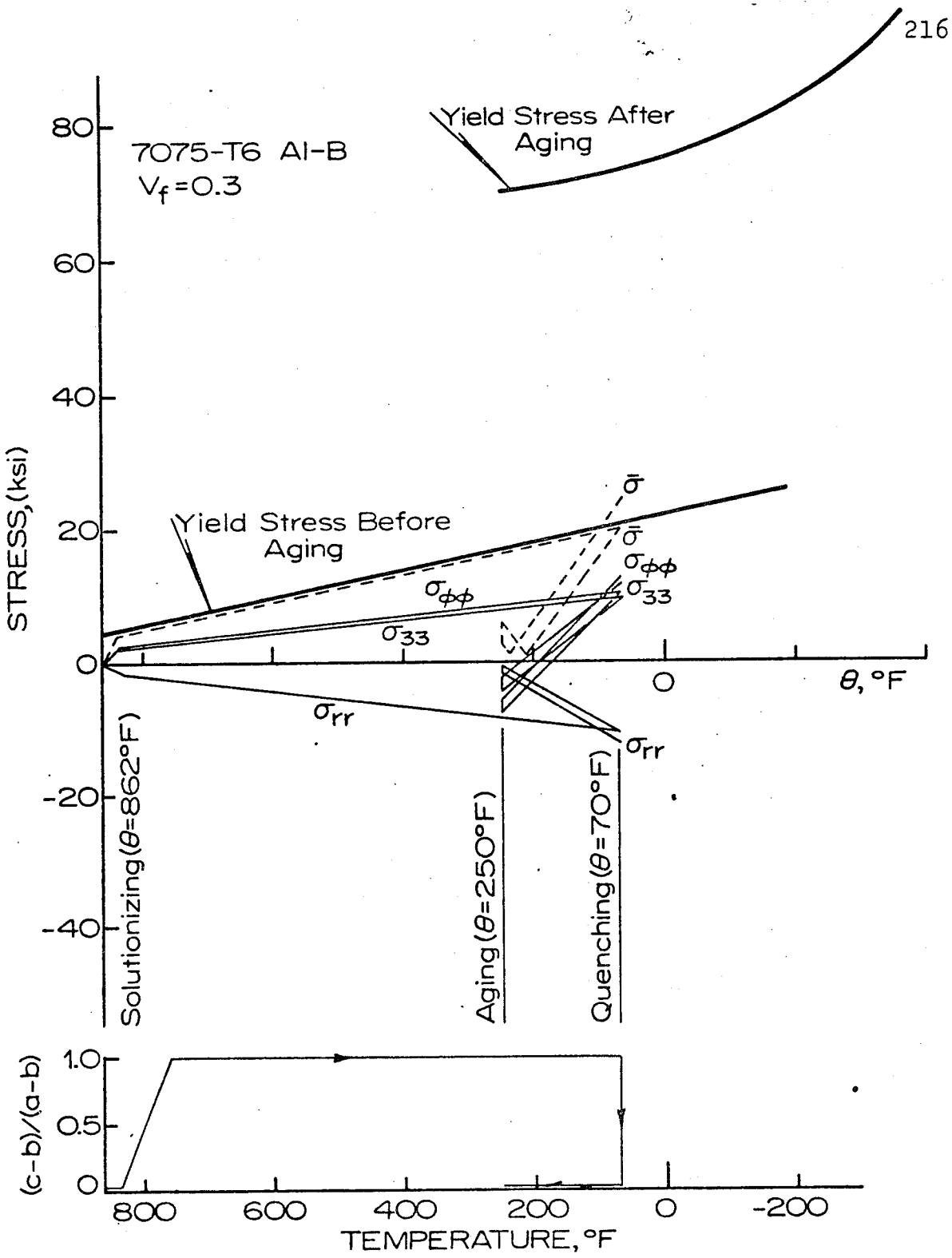

Figure 5-20. Microstresses at the Fiber-Matrix Interface, and the Location of the Elastic-Plastic Boundary (r = c) in the Matrix During Heat Treatment of the 7075-T6 Aℓ-B Composite. Note the Effect of the Dimensional Change at the Aging Temperature.

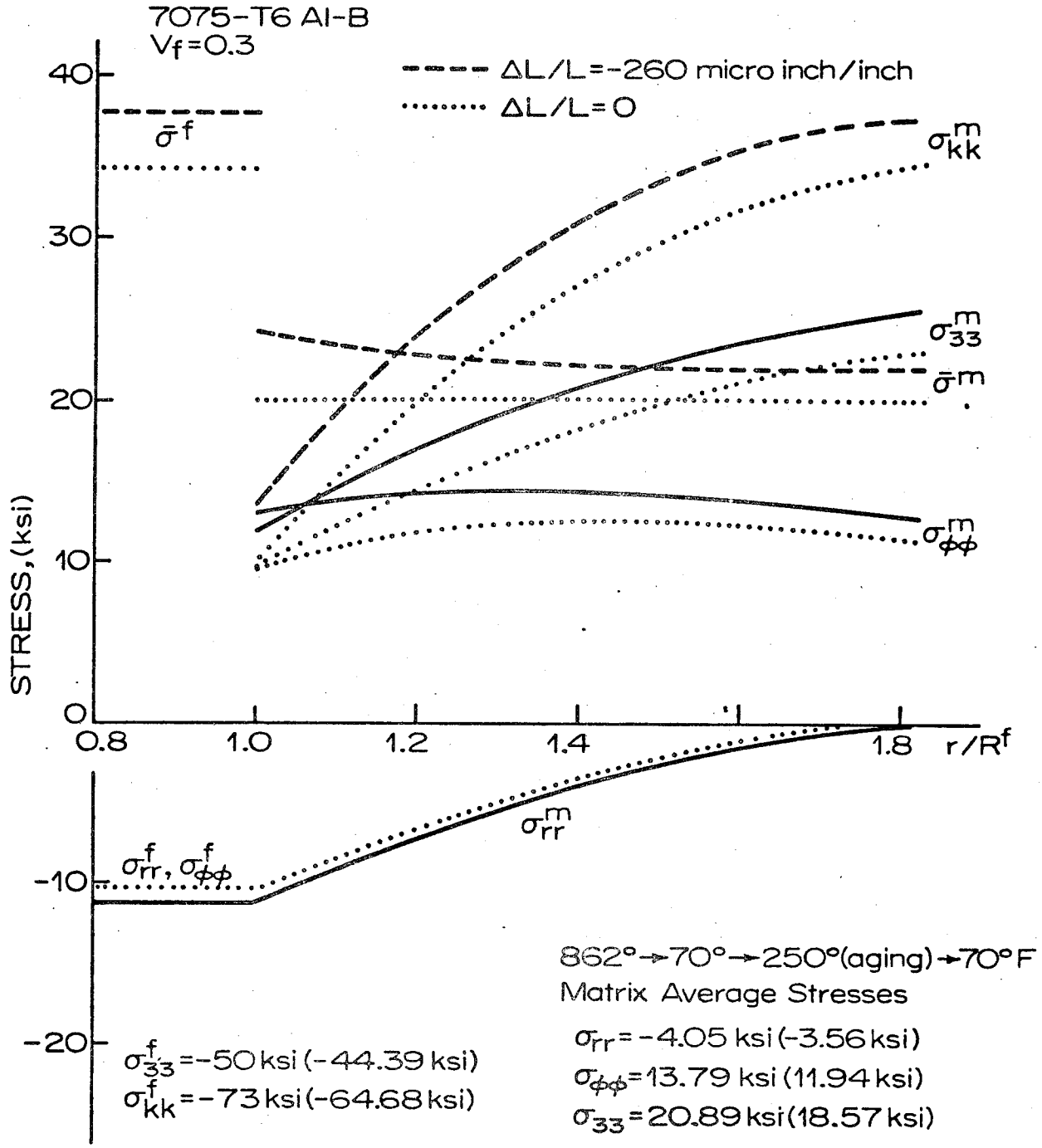

Figure 5-21. Microstress Distribution after Heat Treatment in the Cylinder Model (Figure 5-3) of the 7075-T6 Aℓ-B Composite. Dotted Lines and the Numbers in Parentheses Correspond to $\Delta L/L = 0$.

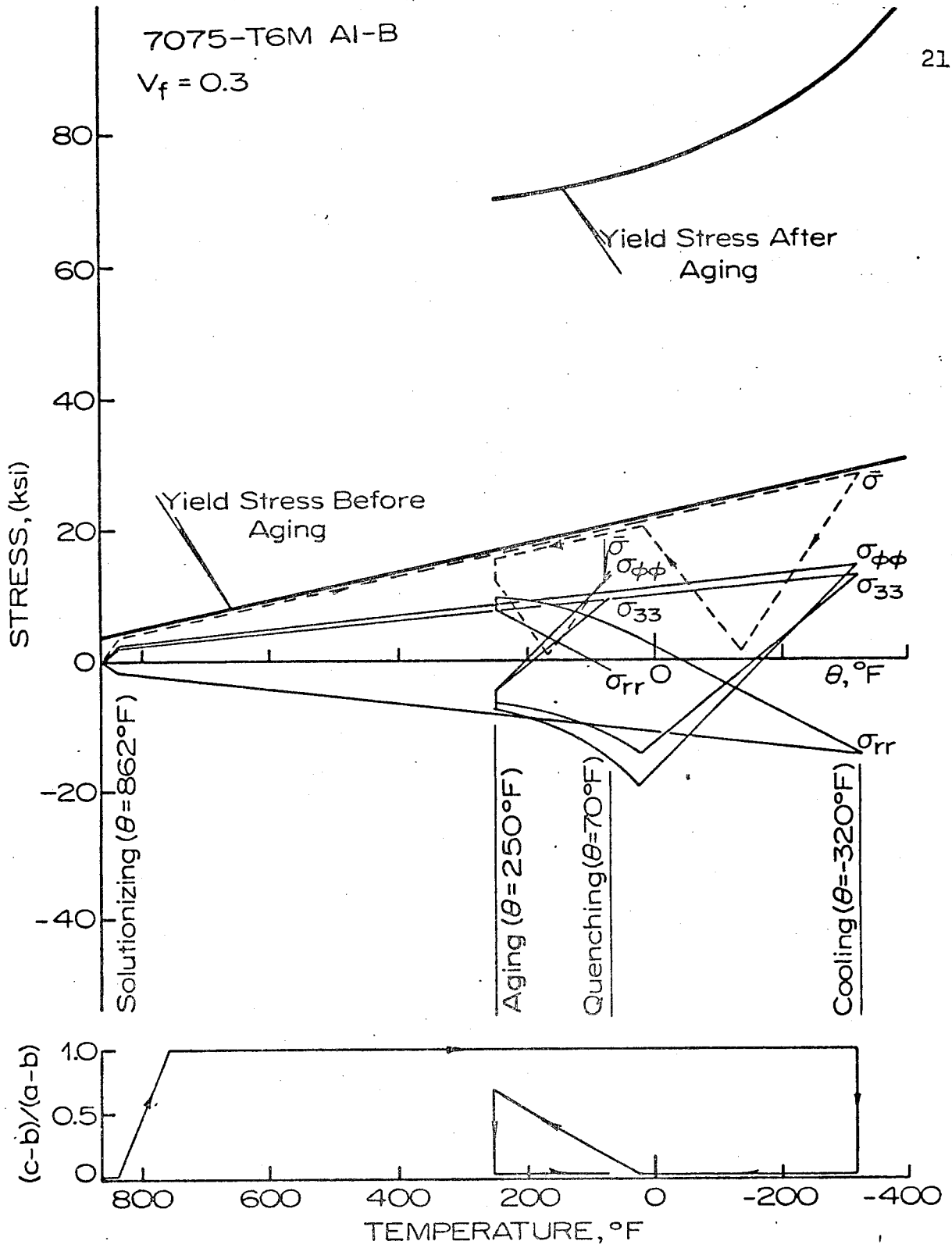

Figure 5-22. Microstresses at the Fiber-Matrix Interface, and the Location of the Elastic-Plastic Boundary (r = c) in the Matrix During Heat Treatment of the 7075-T6M Aℓ-B Composite. Note the Effect of the Dimensional Change at the Aging Temperature.

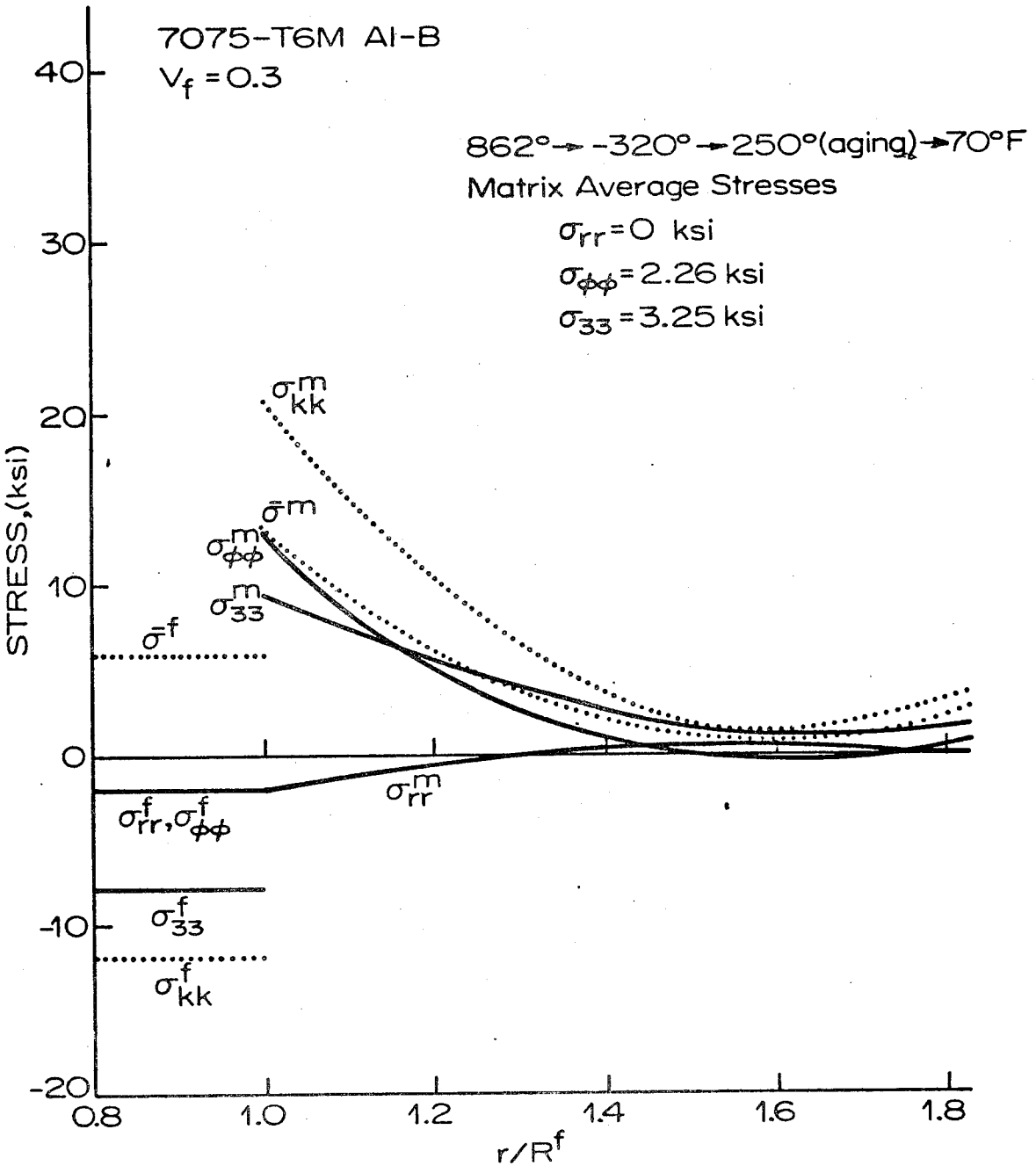

Figure 5-23. Microstress Distribution after Heat Treatment in the Cylinder Model (Figure 5-3) of the 7075-T6M Aℓ-B Composite ($\Delta L/L$ = -260 Microinch/inch).

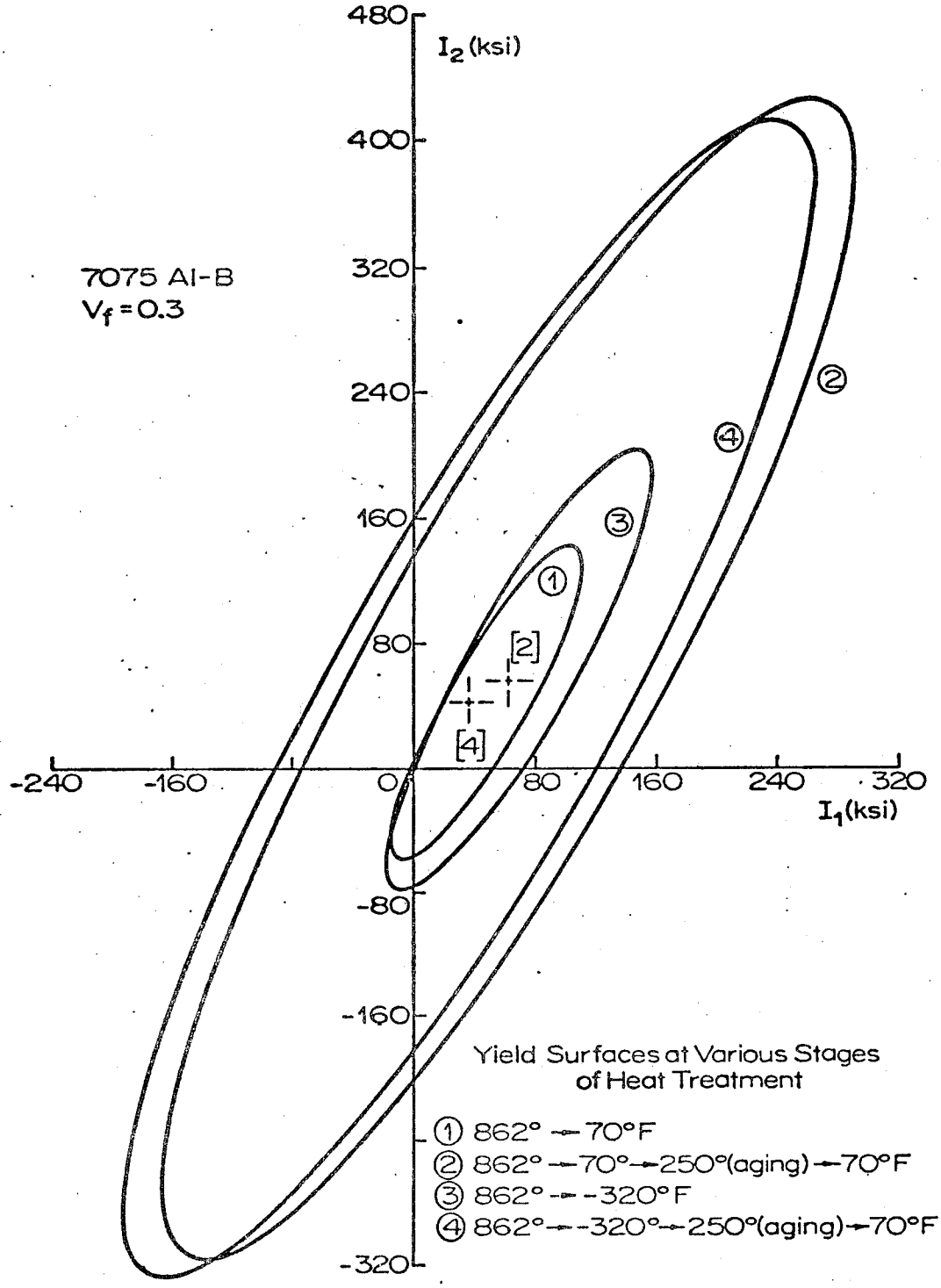

Figure 5-24. Yield (Loading) Surfaces at Various Stages of Heat Treatment of the 7075-T6 Aℓ-B, (2), and 7075-T6M Aℓ-B, (4), Composites.

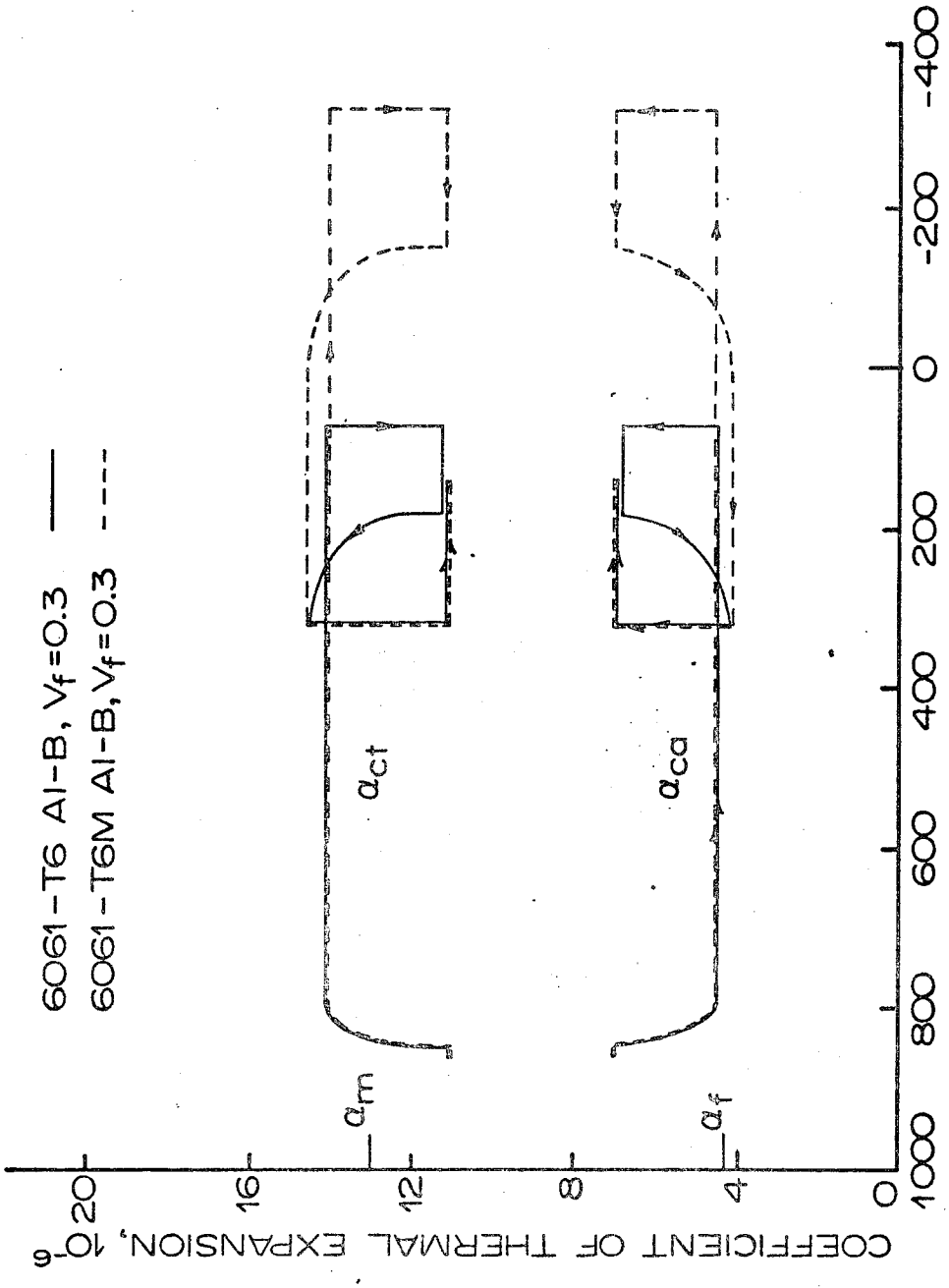

Figure 5-25. Composite Thermal Expansion Coefficients in the Axial (α_{ca}) and Transverse (α_{ct}) Directions During Heat Treatment of the 6061-T6 Al-B, and 6061-T6M Al-B Composites.

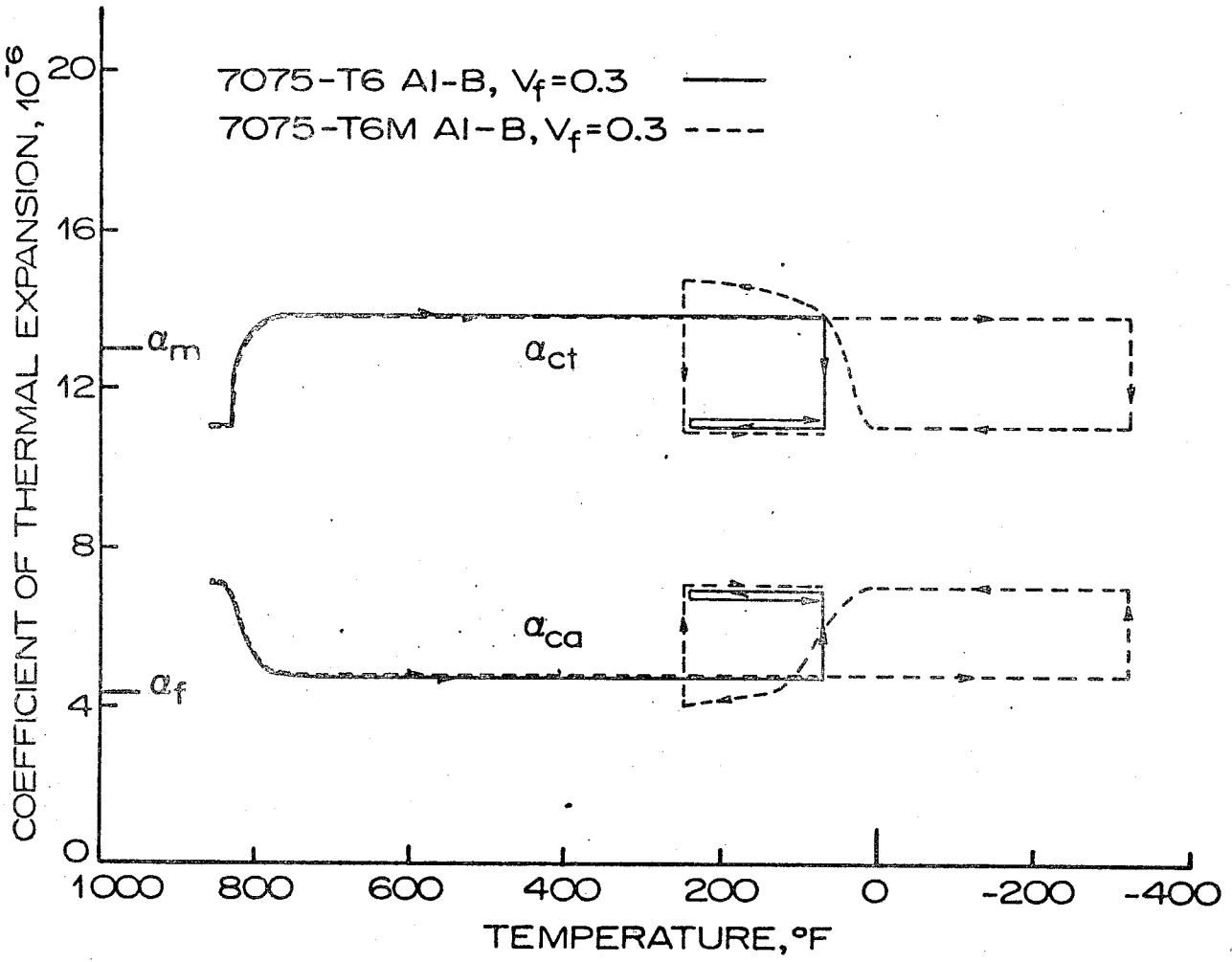

Figure 5-26. Composite Thermal Expansion Coefficients in the Axial (α_{ca}) and Transverse (α_{ct}) Directions During Heat Treatment of the 7075-T6 Aℓ-B, and 7075-T6M Aℓ-B Composites.

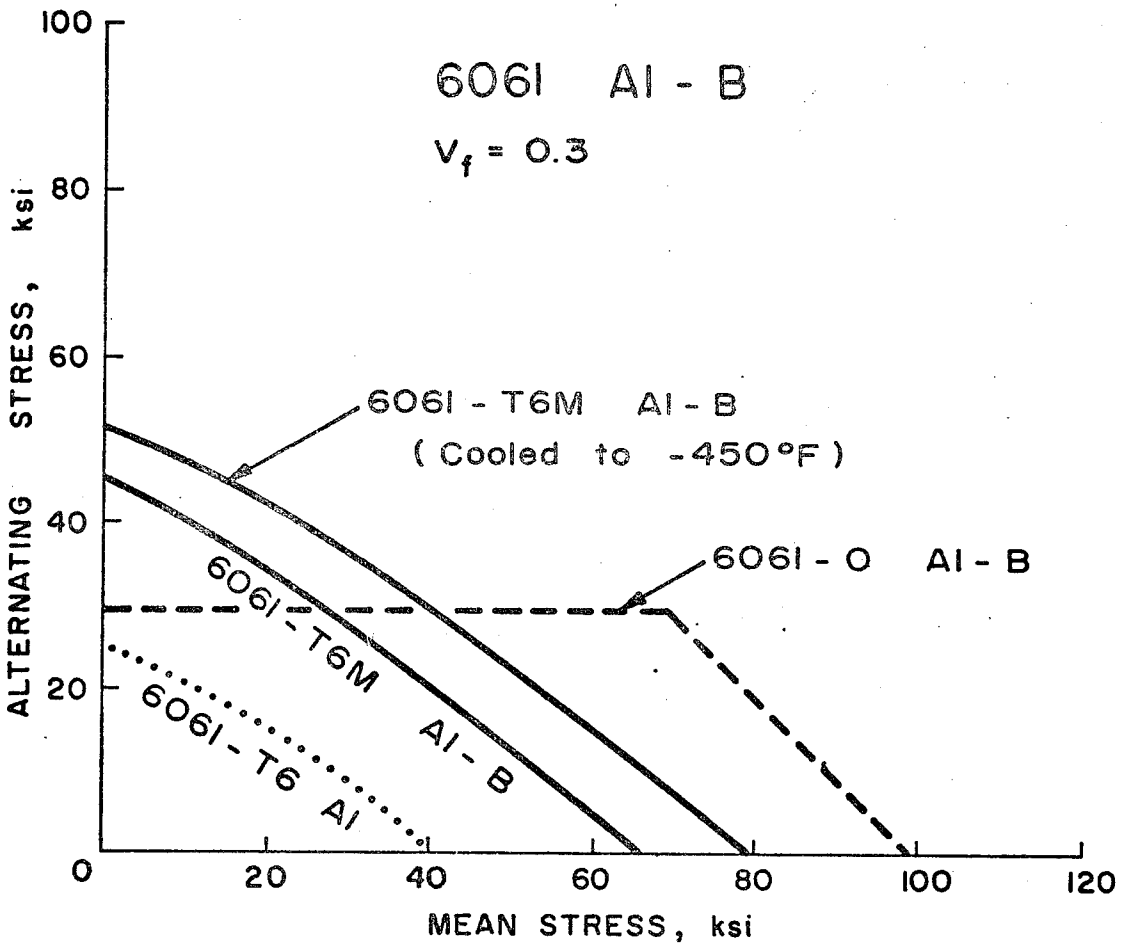

Figure 5-27. Expected Forms of the Goodman Diagram for the 6061 Aℓ-B Composites at 10^6 Cycles of the Uniaxial Loading in the Fiber Direction.

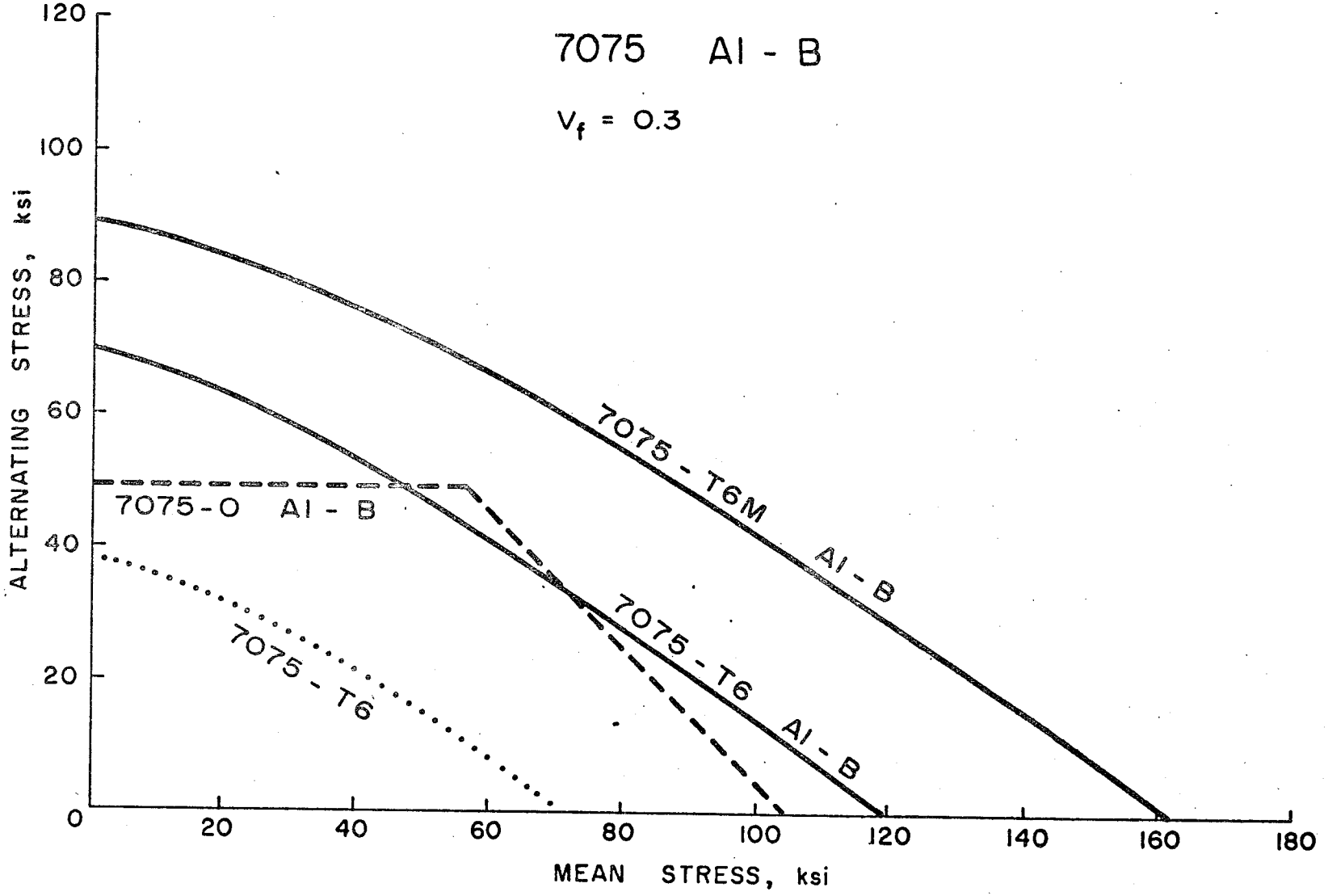

Figure 5-28. Expected Forms of the Goodman Diagrams for the 7075 Aℓ-B Composites at 10^6 Cycles of the Uniaxial Loading in the Fiber Direction.

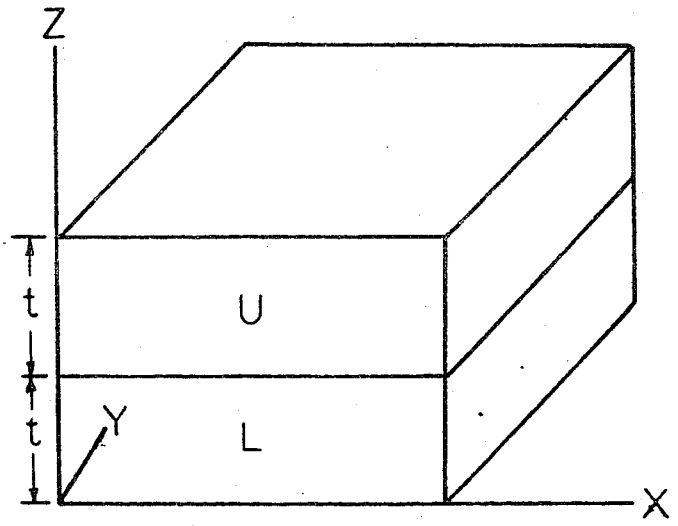

Figure 8-1. One-Half of a Three-Layer Balanced Composite Made of Two Anisotropic Materials U and L.

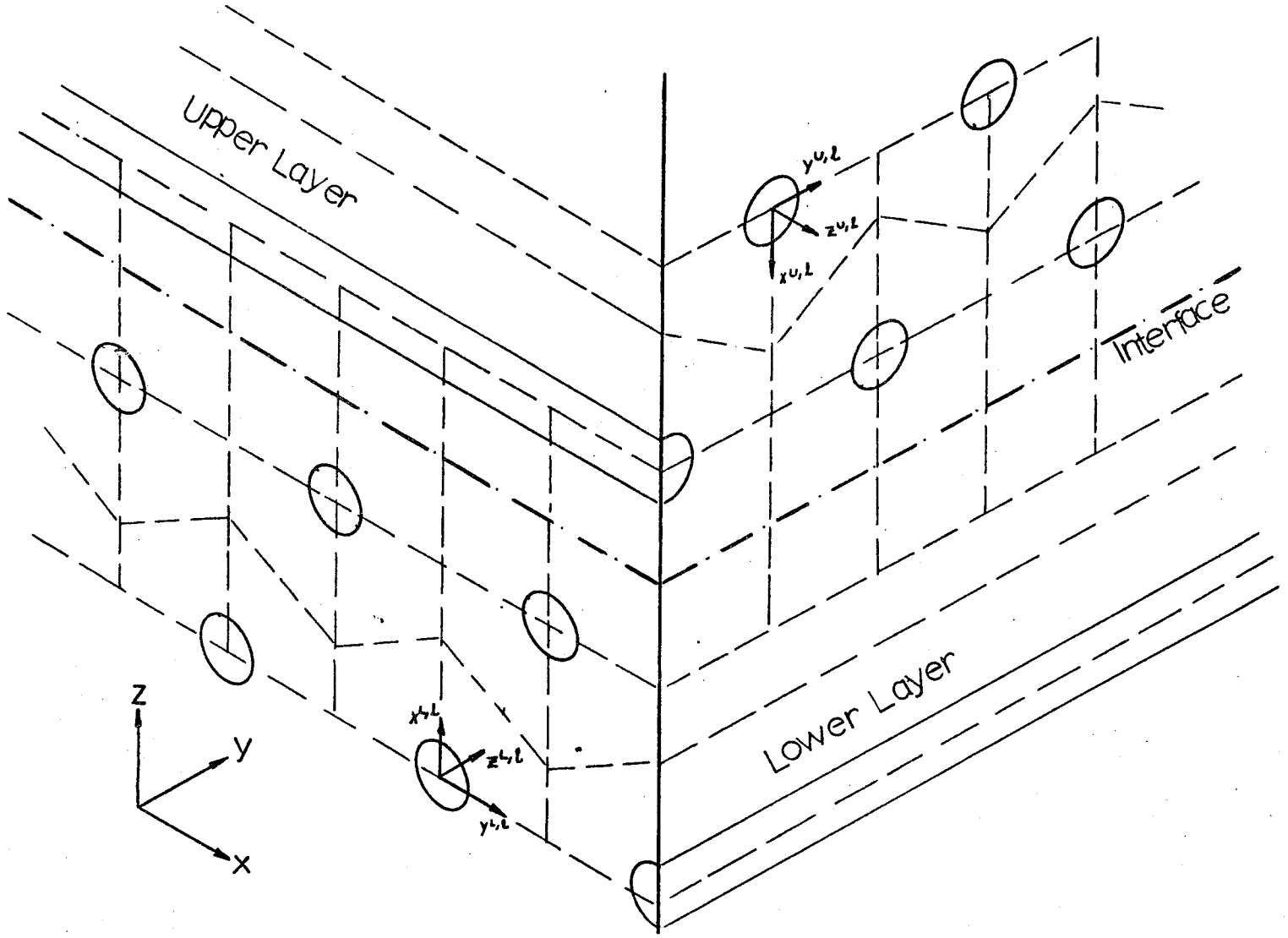

Figure 8-2. Isometric Projection of the Layer-Layer Interface of a 0-90 Multilayered Composite Made of Unidirectional Hexogonal Composites, and the Elementary Volume Domains for the Cross-Over and Regular Solutions.

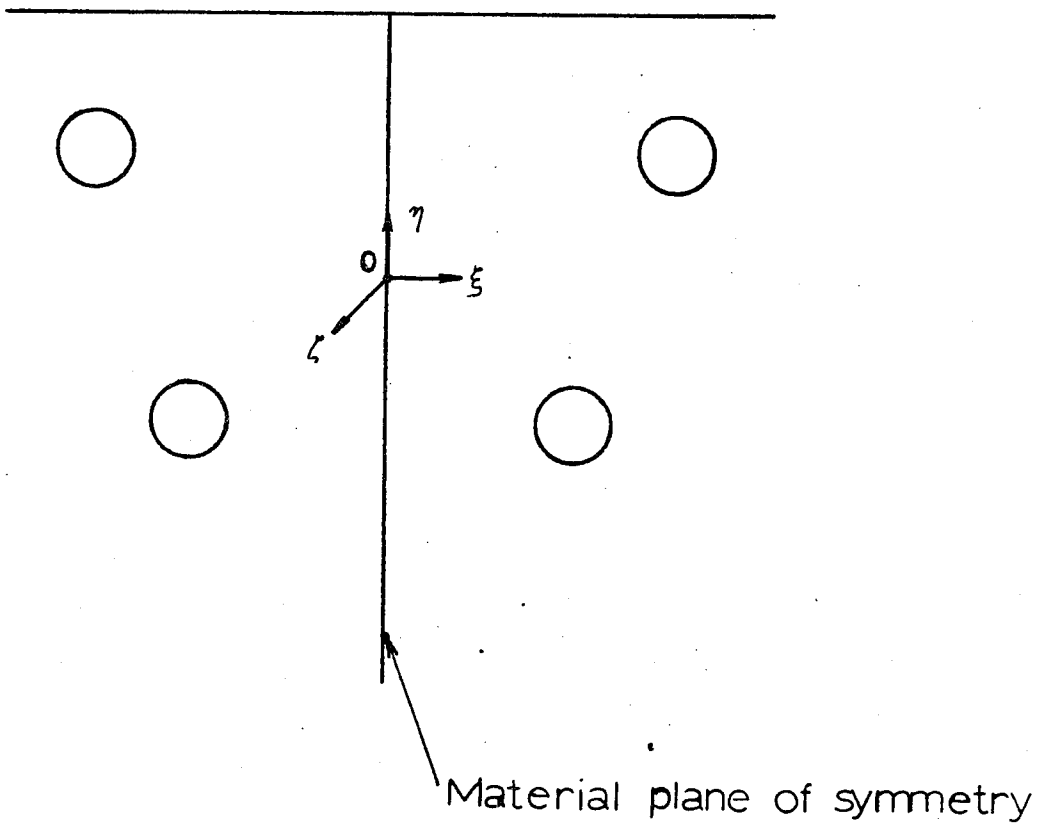

Figure 9-1. Schematic Representation of a Material Plane of Symmetry in a Heterogeneous Solid Made of a Matrix and Cylindrical or Spherical Inclusions.

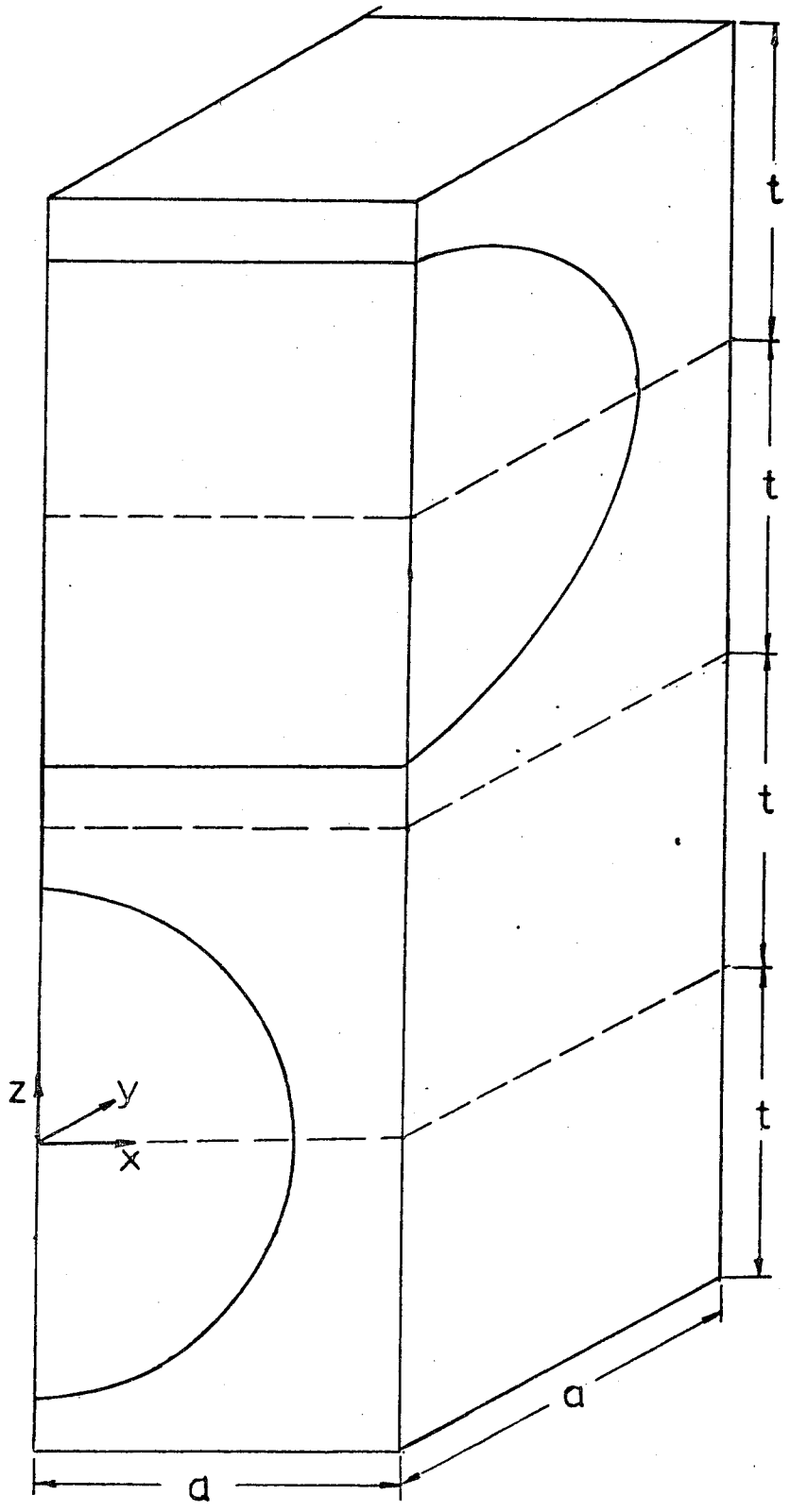

Figure 9-2. An Elementary Model for the Cross-Over Problem of the Multilayered Composite Shown in Figure 8-2.

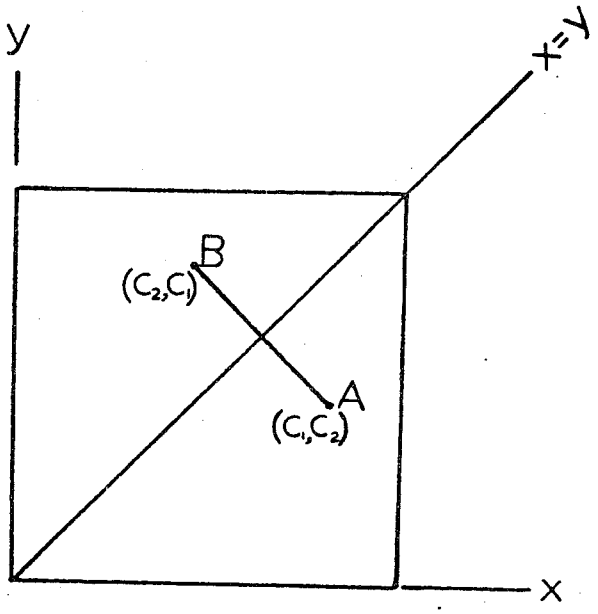

Figure 9-3. Layer-Layer Interface of the Elementary Model Shown in Figure 9-2.

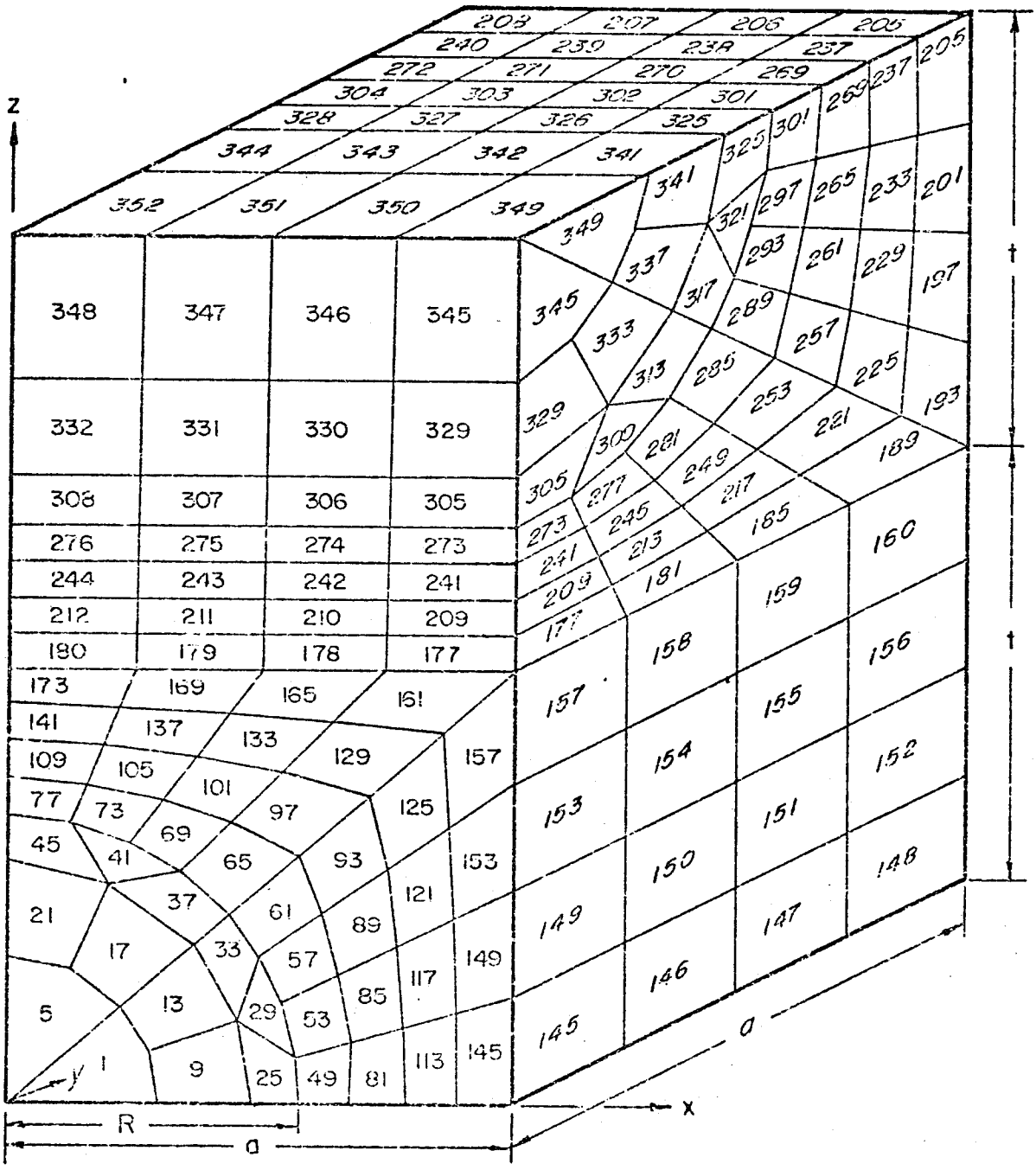

Figure 10-1. Finite Element Mesh for the Cross-Over Solution of the Multilayered Composite by Two-Layer Method.

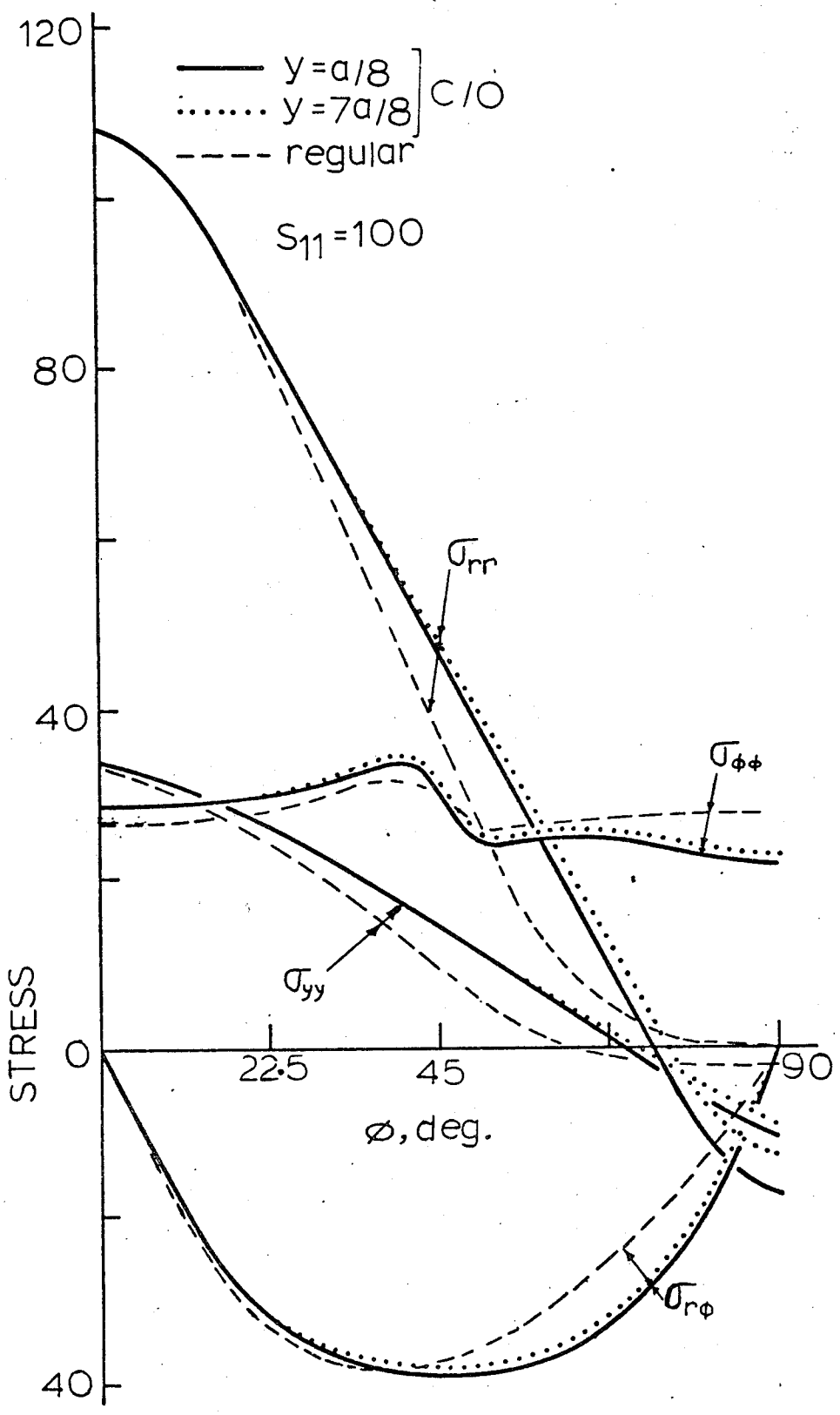

Figure 10-2. Microstress Distribution in the Matrix at the Fiber-Matrix Interface in the Lower Layer of a Multi-Layered B-Aℓ (V_f = 0.3) Composite under S_{11}.

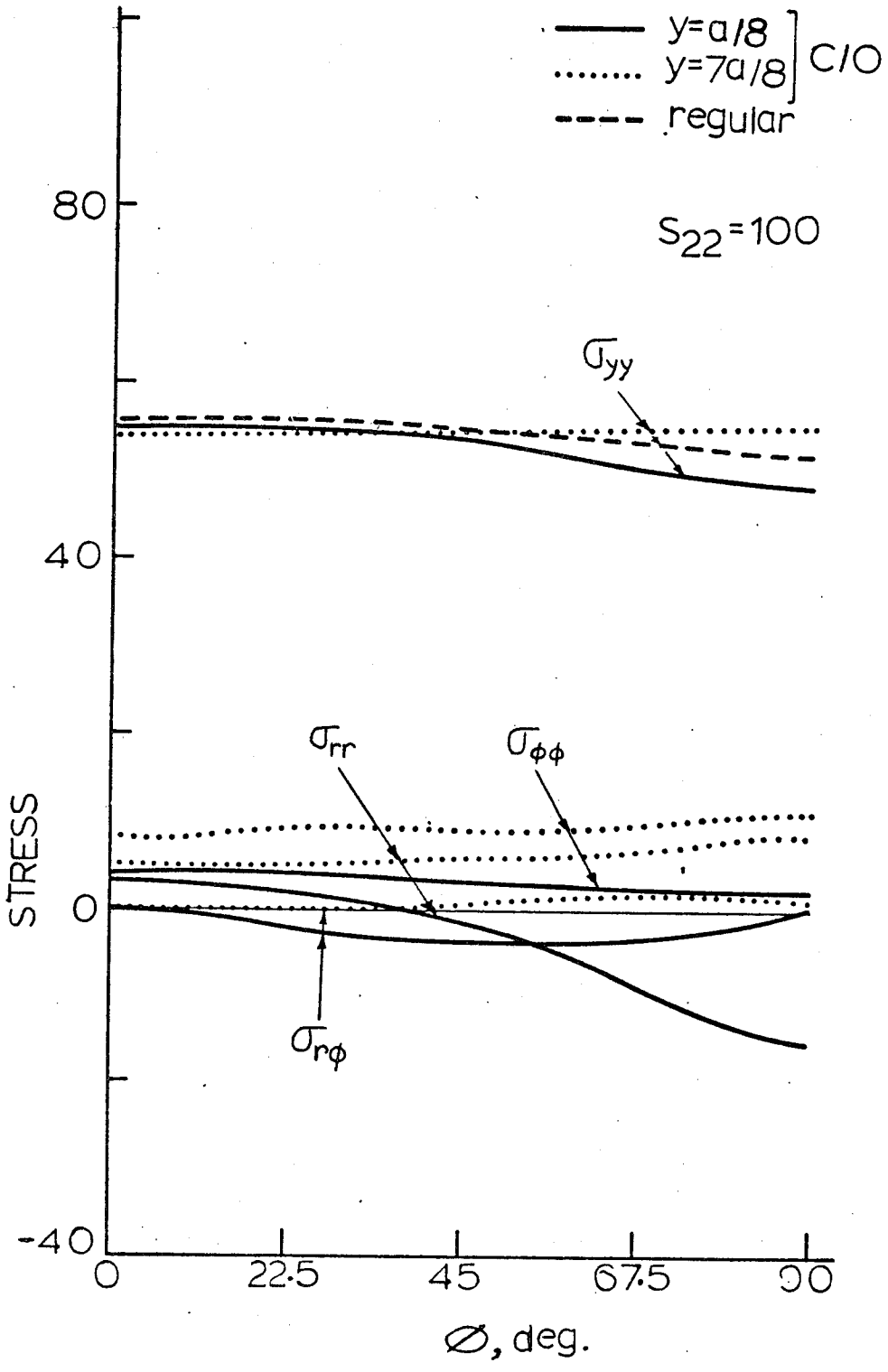

Figure 10-3. Microstress Distribution in the Matrix at the Fiber-Matrix Interface in the Lower Layer of a Multi-Layered B-Aℓ (V_f = 0.3) Composite Under S_{22}.

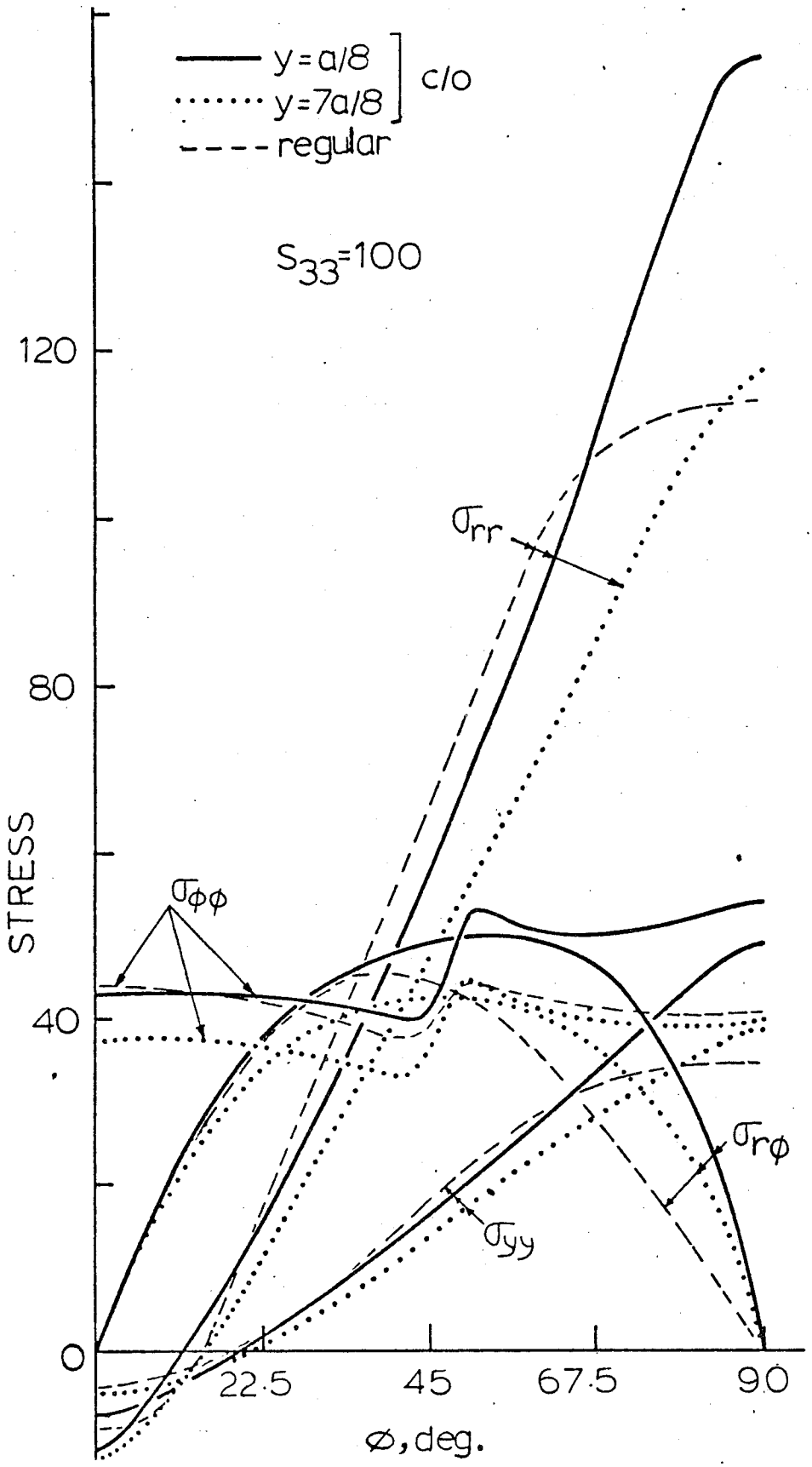

Figure 10-4. Microstress Distribution in the Matrix at the Fiber-Matrix Interface in the Lower Layer of a Multi-Layered B-Aℓ (V_f = 0.3) Composite under S_{33}.

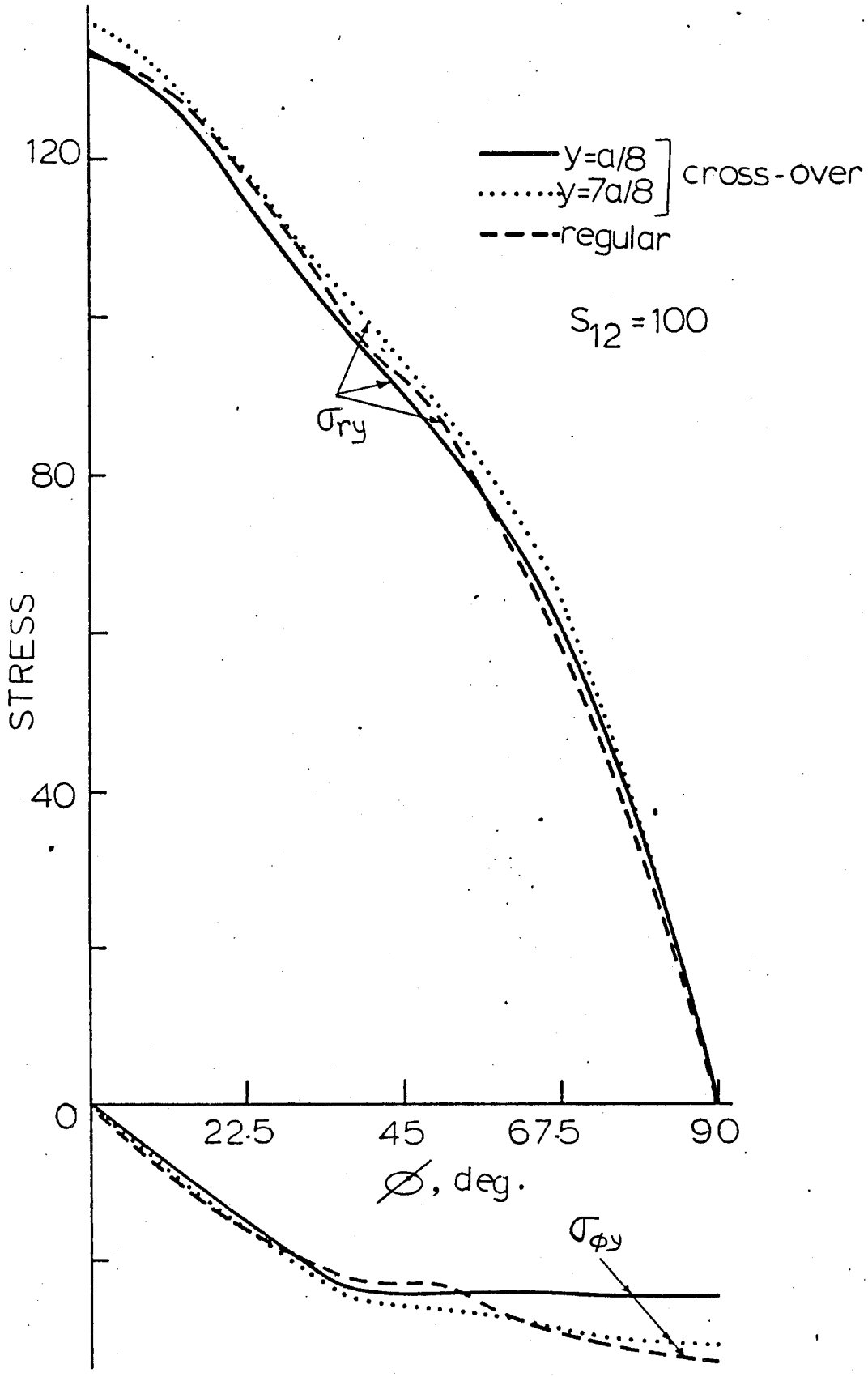

Figure 10-5. Microstress Distribution in the Matrix at the Fiber-Matrix Interface in the Lower Layer of a Multi-Layered B-Aℓ (V_f = 0.3) Composite under S_{12}.

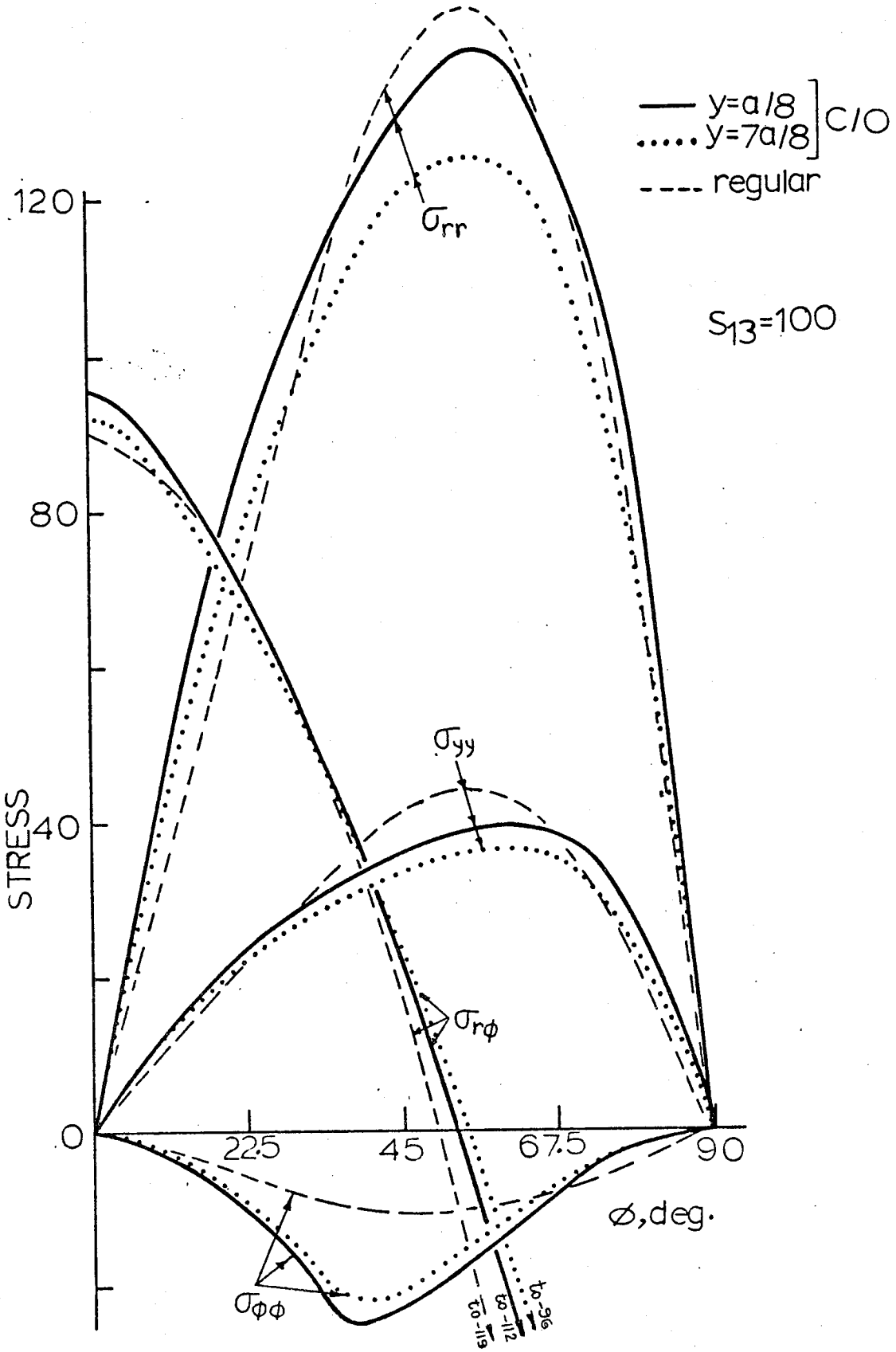

Figure 10-6. Microstress Distribution in the Matrix at the Fiber-Matrix Interface in the Lower Layer of a Multilayered B-Al (V_f = 0.3) Composite under S_{13}.

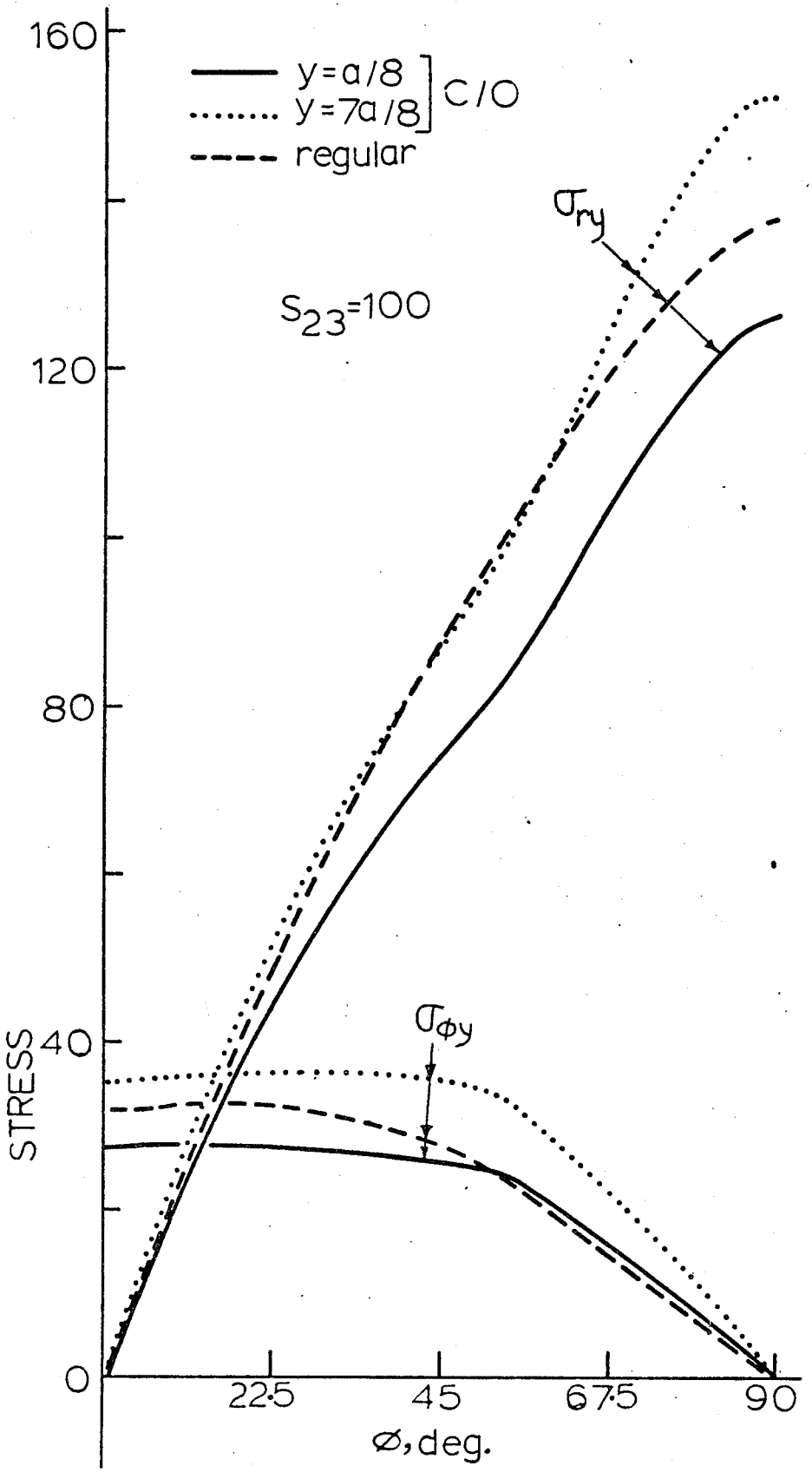

Figure 10-7. Microstress Distribution in the Matrix at the Fiber-Matrix Interface in the Lower Layer of a Multilayered B-Aℓ (V_f = 0.3) Composite under S_{23}.

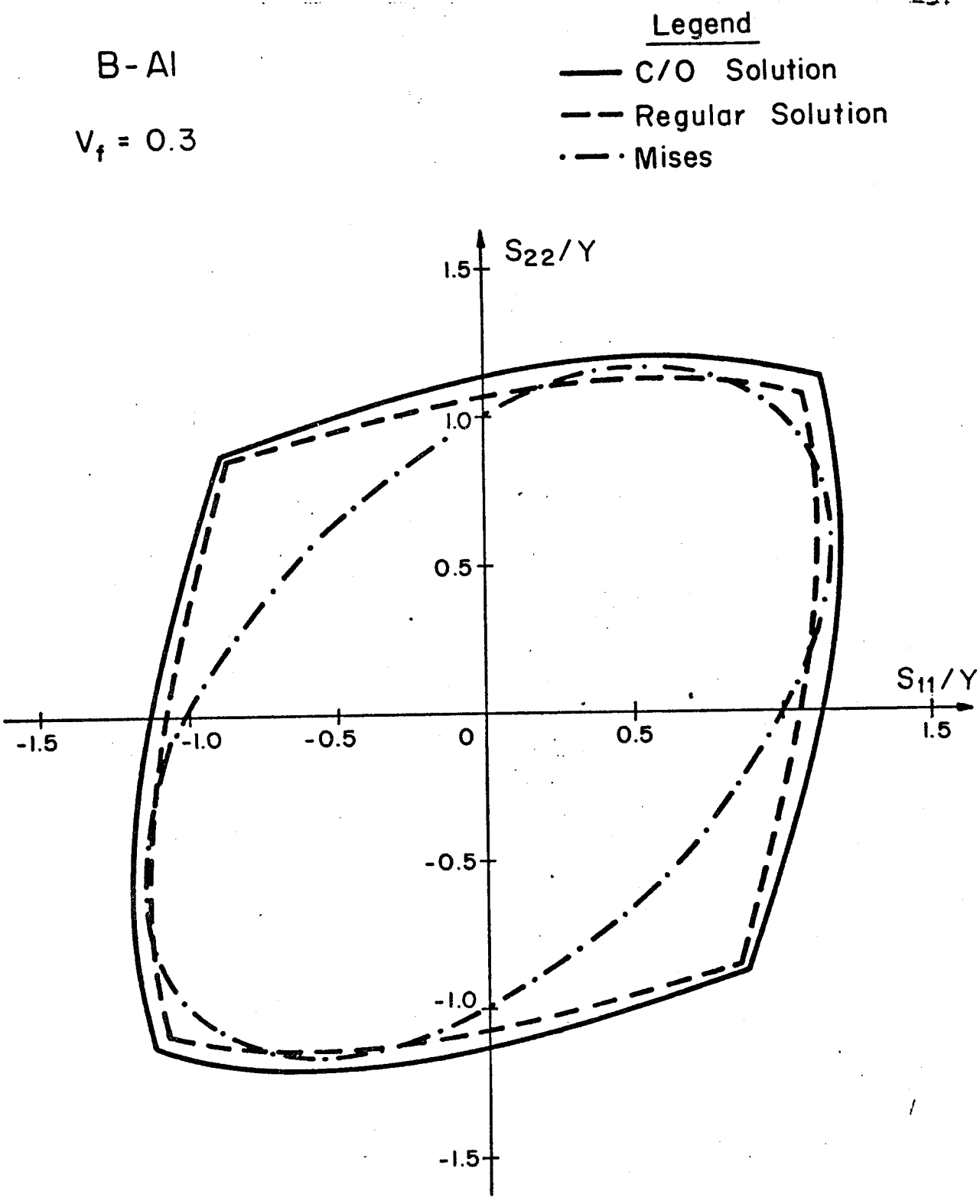

Figure 10-8. Initial Yield Surfaces for a Multilayered B-Aℓ (V_f = 0.3) Composite Loaded in S_{11}-S_{22} Composite Stress Plane. c/o Indicates Cross-Over Solution and Y is the Matrix Yield Stress.

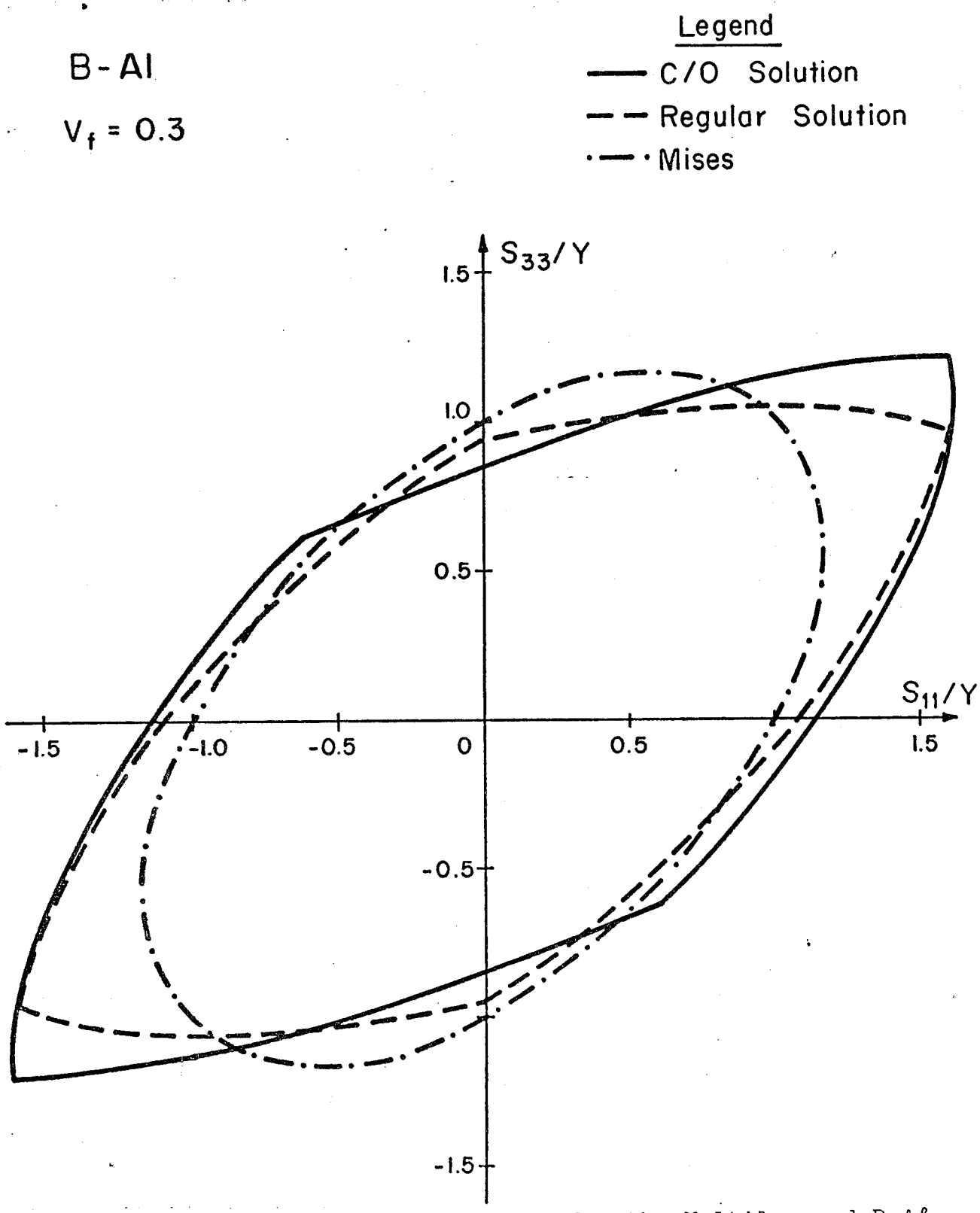

Figure 10-9. Initial Yield Surfaces for the Multilayered B-Aℓ (V_f = 0.3) Composite Loaded in S_{11}-S_{33} Composite Stress Plane.

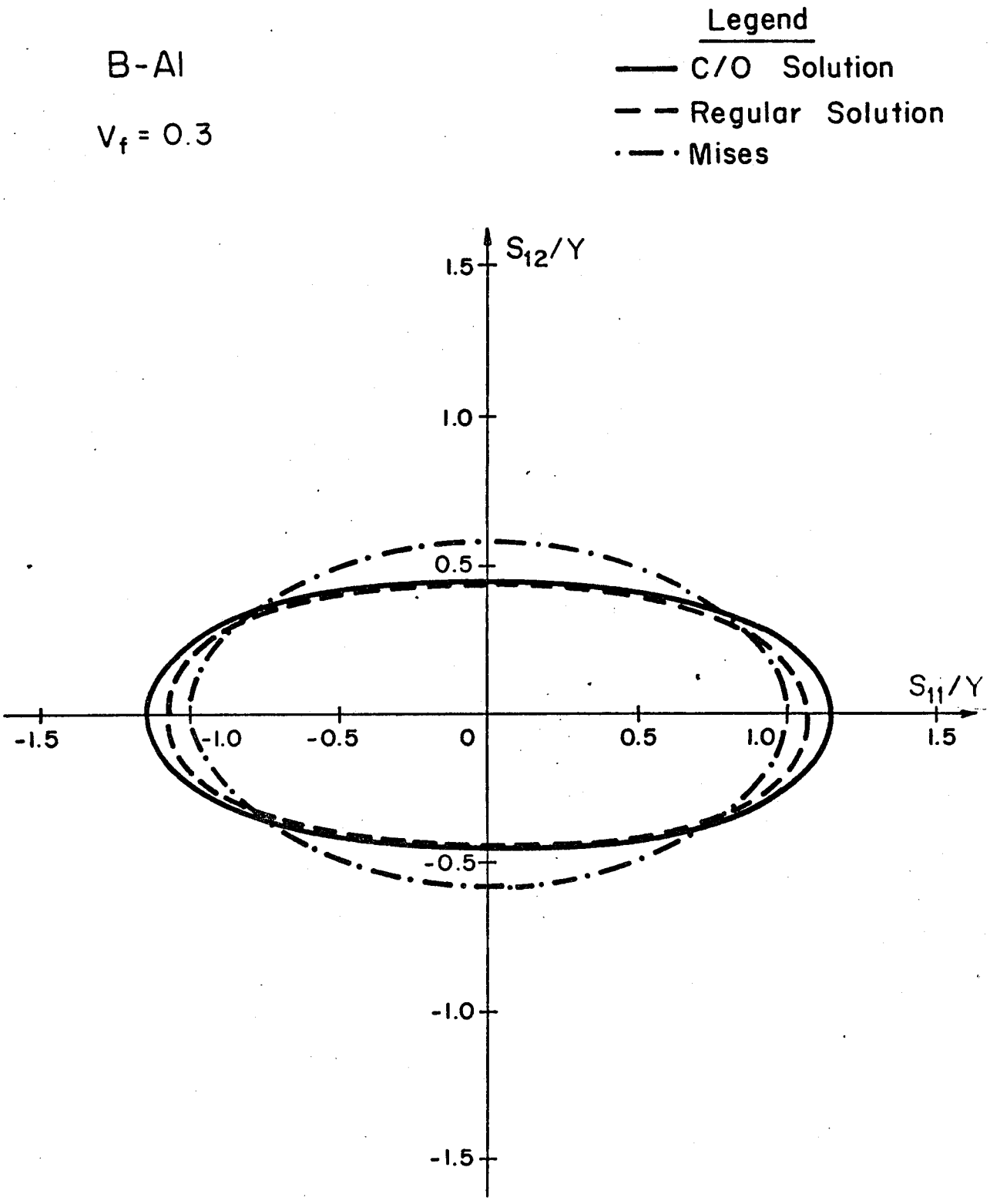

Figure 10-10. Initial Yield Surfaces for the Multilayered B-Aℓ (V_f = 0.3) Composite Loaded in S_{11}-S_{12} Composite Stress Plane.

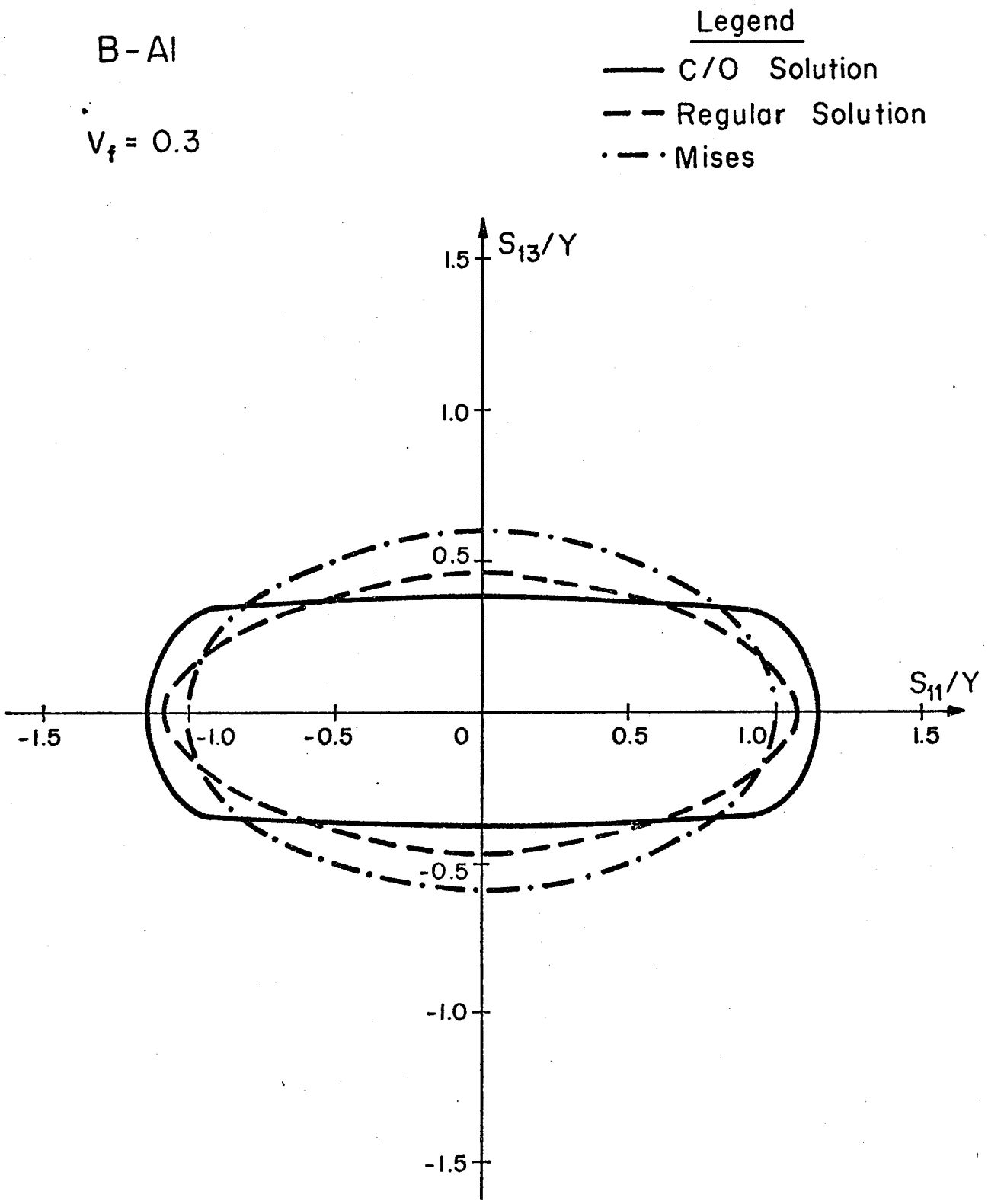

Figure 10-11. Initial Yield Surfaces for the Multilayered B-Aℓ (V_f = 0.3) Composite Loaded in S_{11}-S_{13} Composite Stress Plane.

Unclassified

Security Classification

DOCUMENT CONTROL DATA - R & D

(Security classification of title, body of abstract and indexing annotation must be entered when the overall report is classified)

ORIGINATING ACTIVITY (Corporate author)

Duke University

2a. REPORT SECURITY CLASSIFICATION

Unclassified

2b. GROUP

NA

REPORT TITLE

Microplastic Deformation of Fibrous Composites

DESCRIPTIVE NOTES (Type of report and inclusive dates)

Final Report

AUTHOR(S) (First name, middle initial, last name)

M. S. Madhava Rao and George J. Dvorak

REPORT DATE	7a. TOTAL NO. OF PAGES	7b. NO. OF REFS
September 1974	260	57

8a. CONTRACT OR GRANT NO.	9a. ORIGINATOR'S REPORT NUMBER(S)
DAAG 46-73-C-0228	Solid Mechanics Series No. 11
b. PROJECT NO.	
c.	9b. OTHER REPORT NO(S) (Any other numbers that may be assigned this report)
d.	

10. DISTRIBUTION STATEMENT

Approved for public release; distribution unlimited.

11. SUPPLEMENTARY NOTES	12. SPONSORING MILITARY ACTIVITY
	U.S. Army Materials and Mechanics Research Center Watertown, Massachusetts 02172

13. ABSTRACT

This is a two-part study on the plastic deformation of the fiber-reinforced metal matrix composites.

In the first part of the study, a plasticity theory is formulated to predict analytically the macroscopic and microscopic responses of the unidirectional fiber-reinforced metal matrix composites, loaded by axisymmetric composite stress states. The composites are made of isotropic, linearly elastic fibers, and elastic-plastic, nonhardening matrix of Mises type, and are assumed to be both plastically extensible and compressible. It is shown that the unidirectional composites experience kinematic hardening when loaded by axisymmetric composite stresses. The hardening and flow rules governing the kinematic hardening are formulated. The results obtained by the hardening and flow rules are compared with exact plasticity solutions based on the finite element method. A very good agreement is obtained both for proportional and general loading regimes. An approximate method for the determination of microstresses in the unidirectional composites under axisymmetric loading is described.

The plasticity theory is used to solve micromechanics problems which arise as a result of heat treatment of the composites during fab-

(continued)

DD FORM 1 NOV 68 1473 REPLACES DD FORM 1473, 1 JAN 64, WHICH IS OBSOLETE FOR ARMY USE.

Unclassified

Security Classification

(Abstract continued)

rication. The residual microstresses and the yield surfaces of severa heat-treated unidirectional metal matrix composites are predicted by analytical simulation of the heat treatment sequences. The results ob tained for a heat-treated tungsten-aluminum composite are compared wi existing experimental work to show that the analytical predictions ar very accurate. In addition, new heat treatment sequences that may im prove the properties of unidirectional boron-aluminum composites are scribed.

The second part of the study is concerned with composite laminate Specifically, solution procedures are described for the determination of microstresses in the laminae, and in the fiber crossover regions a the interfaces between the laminae. Particular solutions are present for the 0-90 deg. B-Aℓ laminates. The local microstresses, and the i tial yield surfaces of the laminates are found for the combinations o applied composite stresses which are frequently encountered in practi applications.

14. KEY WORDS	LINK A		LINK B		LINK
	ROLE	WT	ROLE	WT	ROLE
thermoplasticity theory					
kinematic hardening rules					
flow rules					
composite materials					
composite laminates					
microstresses					
heat treatment					
aluminum					
boron					
beryllium					
reinforcement (structures)					